JULIANO MENDONÇA RODRIGUES

TOLERÂNCIA DA SOJA A SECA: RESPOSTAS MOLECULARES DA SUPEREXPRESSÃO DA CHAPERONA BiP E DA INTERAÇÃO COM FUNGO ENDOFÍTICO *Pochonia chlamydosporia*

Tese apresentada à Universidade Federal de Viçosa, como parte das exigências do Programa de Pós-Graduação em Bioquímica Aplicada para obtenção do título de *Doctor Scientiae*.

Orientador: Humberto J. de Oliveira Ramos

Coorientadores: Leandro Grassi de Freitas
Elizabeth Pacheco Batista Fontes
Juliana Rocha Lopes Soares Ramos
Maria Goreti de Almeida Oliveira

VIÇOSA – MINAS GERAIS
2021

Ficha catalográfica elaborada pela Biblioteca Central da Universidade Federal de Viçosa - Campus Viçosa

T

R696t
2021

Rodrigues, Juliano Mendonça, 1991-
Tolerância da soja a seca: respostas moleculares da superexpressão da chaperona BiP e da interação com fungo endofítico *Pochonia Chlamydosporia* / Juliano Mendonça Rodrigues. - Viçosa, MG, 2021.
1 tese eletrônica (209 f.): il. (algumas color.).

Texto em inglês.
Inclui apêndices.
Orientador: Humberto Josué de Oliveira Ramos.
Tese (doutorado) - Universidade Federal de Viçosa, Departamento de Bioquímica e Biologia Molecular, 2021.
Inclui bibliografia.
DOI: https://doi.org/10.47328/ufvbbt.2022.038
Modo de acesso: World Wide Web.

1. Soja - Resistência a doenças e pragas. 2. Stresses (Fisiologia). 3. Fungos. 4. Bactérias fitopatogênicas. I. Ramos, Humberto Josué de Oliveira, 1969-. II. Universidade Federal de Viçosa. Departamento de Bioquímica e Biologia Molecular. Programa de Pós-Graduação em Bioquímica Agrícola. III. Título.

CDD 22. ed. 633.349

Bibliotecário(a) responsável: Renata de Fátima Alves CRB62578

JULIANO MENDONÇA RODRIGUES

TOLERÂNCIA DA SOJA A SECA: RESPOSTAS MOLECULARES DA SUPEREXPRESSÃO DA CHAPERONA BIP E DA INTERAÇÃO COM FUNGO ENDOFÍTICO *Pochonia chlamydosporia*

Tese apresentada à Universidade Federal de Viçosa, como parte das exigências do Programa de Pós-Graduação em Bioquímica Aplicada, para obtenção do título de *Doctor Scientiae*.

APROVADA: 27 de outubro de 2021.

Assentimento:

Juliano Mendonça Rodrigues
Autor

Humberto Josué de Oliveira Ramos
Orientador

A Deus,
Aos meus pais Rita de Cássia e José Jacinto,
À minha avó materna Conceição,
Àqueles que estiveram ao meu lado ao longo de tudo.

AGRADECIMENTOS

Muitos foram os desafios superados desde 2010, quando cheguei em Viçosa para cursar a graduação na UFV. "Grandes realizações não são feitas por impulso, mas por uma soma de pequenas realizações" (Vincent van Gogh). Sozinho, sei que não teria conseguido. Agradeço a todos os que, de alguma forma, colaboraram na minha caminhada até aqui.

A Deus por estar sempre do meu lado nas alegrias e tristezas, me permitindo saber e ser quem eu sou.

Aos meus pais, Rita de Cássia e José Jacinto, pela educação que me deram, honestidade, ensinamento e incentivo para ser uma pessoa boa.

Aos meus irmãos pelo companheirismo e por estarem sempre do meu lado em minhas decisões.

Aos meus familiares pelo apoio e incentivo ao longo dos anos.

Aos meus amigos e madrinhas, em especial a madrinha Judite, pela amizade e por sempre estarem me apoiando e rezando por mim.

À Universidade Federal de Viçosa pelas oportunidades para o crescimento. Aos seus funcionários e servidores pelo gentil convívio e pela ajuda durante minha formação acadêmica.

Aos professores, amigos e colegas de diversos cursos que passaram pela minha graduação em Engenharia Ambiental e pós-graduação pelo aprendizado e pela convivência que trouxe sentido e graça ao longo de minha vida acadêmica.

Às agências de fomento, CAPES (financiadora deste projeto), CNPq e FAPEMIG, pelo apoio à pesquisa e ao desenvolvimento da ciência brasileira; e espero que este apoio não mingue, mas cresça cada vez mais, pois sem ele eu não teria tido esta chance.

Ao professor Humberto Ramos pela orientação, auxílio na condução dos experimentos e análises e por todo ensinamento passado, além da paciência, confiança e amizade.

Aos professores Elizabeth Pacheco Batista Fontes, Leandro Grassi de Freitas e Maria Goreti de Almeida Oliveira por disponibilizarem o material para estudo e permitirem o desenvolvimento dos experimentos planta-bactéria e planta-fungo. Agradeço por oferecerem a estrutura de seus laboratórios para a realização deste trabalho.

Ao Bioagro/INCT-IPP e aos Laboratórios de Biologia Molecular de Plantas; de Enzimologia, Bioquímica de Proteínas e Peptídeos; e de Controle Biológico de Fitonematódeos pelo agradável ambiente de trabalho. Ao Núcleo de Análise de Biomoléculas (Nubiomol) pela estrutura oferecida para espectrometria de massas, conversas e agradável convívio.

Aos professores Max, Marisa, Maria Cristina Baracat, Juliana Ramos, Gustavo Bressan, João Paulo Viana, Luiz Orlando e Renata pelos ensinamentos ao longo da minha formação acadêmica de pós-graduação.

À Flaviane, Jenny, Lucas, Verônica, Angélica, Camilo, Dalila, Neilier, Rafael Barros, Juan Diego, Yaremis, Cecília Fausto, Fernanda Araújo, Thercia, João Carlos, Danilo, Ângelo, Leonardo, Valquíria, Anna Carolina, Jéssica, Thalita, Cássia, Analu e tantos outros pela amizade ao longo dos experimentos, apoio e contribuição em cada momento dessa trajetória.

Por fim, agradeço novamente a cada um que, direta ou indiretamente, me ajudou.

A vida é cheia de surpresas; então, *let there be games begin*! Que venha o futuro e toda a sorte que ele reserva!

If you want your dream to be / Take your time, go slowly / Do few things but do them well / Heartfelt work grows purely.

If you want to live life free / Take your time, go slowly / Do few things but do them well / Heartfelt work grows purely.

Day by day, stone by stone / Build your secret slowly / Day by day, you'll grow too / You'll know heaven's glory.

(Se quiser ver seu sonho se realizar / Não tenha pressa, vá devagar / Faça poucas coisas, mas faça-as bem / O trabalho sincero cresce puro.

Se quiser viver livre / Não tenha pressa, vá devagar / Faça poucas coisas, mas faça-as bem / O trabalho sincero cresce puro.

Dia após dia, pedra sobre pedra / Construa seu segredo devagar / Dia após dia, você também crescerá / E conhecerá a glória celeste.)

IRMÃO SOL, IRMÃ LUA (1972)
Filme de Franco Zeffirelli
sobre S. Francisco de Assis

BIOGRAFIA

JULIANO MENDONÇA RODRIGUES (Vieiras, Minas Gerais, 15 de janeiro de 1991), filho de José Jacinto Rodrigues e Rita de Cássia Mendonça Rodrigues. Frequentou a educação básica e o ensino fundamental e médio em Vieiras, Minas Gerais, estudando a educação infantil no Pré-escolar Municipal Pequeno Polegar, o ensino fundamental na Escola Municipal José Soares de Souza Filho e o ensino médio na Escola Estadual Assis Brasil, tendo concluído o segundo grau em dezembro de 2009. Em março de 2010, ingressou na Universidade Federal de Viçosa (UFV), Minas Gerais, para o curso de Graduação em Engenharia Ambiental, graduando-se em julho de 2015. Em agosto de 2015, ingressou no Programa de Pós-Graduação da UFV, no Mestrado em Bioquímica Aplicada, defendendo em julho de 2017. Em agosto de 2017, ingressou no Programa de Doutorado em Bioquímica Aplicada na UFV, defendendo em outubro de 2021.

RESUMO

RODRIGUES, Juliano Mendonça, D.Sc., Universidade Federal de Viçosa, outubro de 2021**. Tolerância da soja a seca: respostas moleculares da superexpressão da chaperona BiP e da interação com fungo endofítico *Pochonia chlamydosporia*.** Orientador: Humberto Josué de Oliveira Ramos. Coorientadores: Elizabeth Pacheco Batista Fontes, Juliana Rocha Lopes Soares Ramos, Maria Goreti de Almeida Oliveira e Leandro Grassi de Freitas.

Plantas, por estarem inseridas em um ambiente dinâmico e complexo, estão expostas a diversas mudanças das condições ambientais que podem limitar o seu crescimento e produtividade. Estresses abióticos como escassez hídrica e secas prolongadas são um desafio, uma vez que tendem a se tornar cada vez mais frequentes devido a eventos climáticos extremos. Como maior produtor e exportador mundial de soja, a agricultura brasileira tem um interesse especial nos mecanismos de tolerância cruzada a estresses bióticos e abióticos em soja. Por isso, diversos estudos buscam obter mecanismos de adaptação e resistência vegetal a estresses ambientais com o melhoramento da produtividade agrícola e o mínimo de impacto ao meio ambiente. Uma das linhas de pesquisa visa a manipulação da chaperona molecular BiP em plantas transgênicas, cuja resposta ao estresse osmótico e do retículo endoplasmatico podem favorecer a tolerância à seca em soja. Entretanto, são boladas as informações sobre os efeitos da superexpressão de BiP no atraso na ativação da morte celular provocada por reação de hipersensitividade em situações de estresse biótico provocado pela bactéria não compatível *Pseudomonas syringae* pv. tomato. Outra linha de pesquisa, o uso de produtos biológicos baseados em organismos simbiontes da rizosfera vegetal que colonizam como raízes vegetais, dentre os quais o fungo nematófago endofítico *Pochonia chlamydosporia* pode estimular a capacidade da raiz de soja em explorar o solo ao redor favorecendo-a em condições de restrição hídrica. Neste trabalho, foi caracterizado o perfil morfológico, fisiológico e metabólico de genótipos contrastantes de soja quanto à tolerância a seca em resposta a interações bióticas. Foram analisadas a expressão de genes responsivos por RT-PCR, além da regulação diferencial de proteinas e fosfoproteinas responsivas à interação planta-bactéria no genótipo transgênico superexpressando BiP (C9) e (WT), sendo identificado por LC/MS-2DE. Foram também adotados por LC-MS a abundância de fito-hormônios e alguns metabólitos especializados alvos em resposta à interação de soja com *P. syringae* pv. *tomato* e soja com *P. chlamydosporia* para determinar mudanças metabólicas básicas genótipos relacionados com a resposta à seca e/ou a resposta de defesa vegetal sob interações biológicas.

Por sua vez, parâmetros morfofisiológicos de folhas, caule e raiz de genótipos tolerante a seca Embrapa48 e sensível a seca BR16 foram coletados ao longo do experimento planta-fungo. Concluiu-se que a via de síntese de flavonóides e isoflavonóides é uma das principais vias responsivas às inoculações com bactérias e com fungo em plantas, sendo determinante para a presença e contenção do hospedeiro. A resposta hipersensitiva bacteriana provocou uma expressão de genes que modulam a morte celular, sobretudo no genótipo transgênico, uma redução negativa de proteinas da fotossintese e uma regulação positiva de proteinas do metabolismo antioxidativo e do metabolismo dos fenilpropanoides e flavonóides, especialmente O-metiltransferases. Por fim, a interação bacteriana regulou positivamente os níveis de flavonoides e fitoalexinas em genótipos infectados. A presença do fungo, por sua vez, produziu um atraso de um dia na queda do potencial hídrico em ambos os genótipos contrastantes quanto a seca. O aumento do turgor foliar e como mudanças nos níveis de fito-hormônios, poliaminas e compostos fenólicos indicam que uma associação da planta ao fungo nas condições de déficit hídrico é inerente a cada genótipo, sendo que nenhum genótipo é tolerante a seca está ligada às propriedades hidráulicas dos vasos condutores. A presença do fungo promove mudanças morfológicas no sistema radicular e no sistema de vasos condutores da parte aérea em Embrapa48 e, em menor extensão, em BR16. Esses resultados podem ajudar a elucidar os mecanismos predominantes na tolerância cruzada de estresses bioticos e abioticos concomitantes, e como as plantas como utilizam para promover uma maior adaptação ao ambiente.

Palavras-chave: *Glycine max*. *Pseudomonas syringae* patovar *tomato*. *Pochonia chlamydosporia*. Estresses ambientais. Metabolômica. Proteômica.

ABSTRACT

RODRIGUES, Juliano Mendonça, D.Sc., Universidade Federal de Viçosa, October 2021**. Tolerance of the soybean to drought: molecular responses of the overexpression of the chaperone BiP and interaction with endophytic fungus *Pochonia Chlamydosporia*.** Advisor: Humberto Josué de Oliveira Ramos. Co-advisors: Elizabeth Pacheco Batista Fontes, Juliana Rocha Lopes Soares Ramos, Maria Goreti de Almeida Oliveira and Leandro Grassi de Freitas.

Plants, being inserted in a dynamic and complex environment, are exposed to several changes in environmental conditions that can limit their growth and productivity. Abiotic stresses such as water scarcity and prolonged droughts are a challenge as they tend to become more and more frequent due to extreme weather events. As the world's largest producer and exporter of soybeans, Brazilian agriculture has a special interest in the mechanisms of cross-tolerance to biotic and abiotic stresses in soybeans. Therefore, several studies seek to obtain mechanisms for adaptation and plant resistance to environmental stresses with the improvement of agricultural productivity and minimal impact on the environment. One of the lines of research aims at manipulating the molecular chaperone BiP in transgenic plants, whose response to osmotic and endoplasmic reticulum stress can favor drought tolerance in soybean. However, information about the effects of BiP overexpression in the delay in the activation of cell death caused by hypersensitivity reaction in situations of biotic stress caused by the non-compatible bacteria *Pseudomonas syringae* pv. tomato. Another line of research, the use of biological products based on symbiotic organisms from the plant rhizosphere that colonize as plant roots, among which the endophytic nematophagus fungus *Pochonia chlamydosporia* can stimulate the capacity of the soybean root to explore the surrounding soil, favoring it in water restriction conditions. In this work, the morphological, physiological and metabolic profile of contrasting soybean genotypes regarding drought tolerance in response to biotic interactions was characterized. The expression of RT-PCR responsive genes was analyzed, as well as the differential regulation of proteins and phosphoproteins responsive to plant-bacteria interaction in the transgenic genotype overexpressing BiP (C9) and (WT), identified by LC/MS-2DE. The abundance of phytohormones and some specialized target metabolites in response to the interaction of soybean with *P. syringae* pv. tomato and soybean with *P. chlamydosporia* were also adopted by LC-MS to determine basic metabolic changes in genotypes related to drought

response and/or plant defense response under biological interactions. In turn, morphophysiological parameters of leaves, stem and root of drought-tolerant Embrapa48 and drought-sensitive BR16 genotypes were collected during the plant-fungus experiment. It was concluded that the flavonoid and isoflavonoid synthesis pathway is one of the main pathways responsive to inoculations with bacteria and fungus in plants, being crucial for the presence and containment of the host. The bacterial hypersensitive response caused an expression of genes that modulate cell death, especially in the transgenic genotype, a negative reduction of photosynthesis proteins and an upregulation of proteins from the antioxidant metabolism and the metabolism of phenylpropanoids and flavonoids, especially O-methyltransferases. Finally, bacterial interaction positively regulated the levels of flavonoids and phytoalexins in infected genotypes. The presence of the fungus, in turn, produced a one-day delay in the drop in water potential in both contrasting genotypes for drought. The increase in leaf turgor and changes in the levels of phytohormones, polyamines and phenolic compounds indicate that an association of the plant with the fungus under water deficit conditions is inherent to each genotype, and no genotype is drought tolerant is linked to the hydraulics properties of the conducting vessels. The presence of the fungus promotes morphological changes in the root system and in the aerial part vessel system in Embrapa48 and, to a lesser extent, in BR16. These results may help to elucidate the predominant mechanisms in the cross-tolerance of concomitant biotic and abiotic stresses, and how plants use them to promote greater adaptation to the environment.

Keywords: *Glycine max. Pseudomonas syringae* pathovar *tomato. Pochonia chlamydosporia*. Environmental stresses. Metabolomics. Proteomics.

LISTA DE ILUSTRAÇÕES

LISTA DE TABELAS

SUMÁRIO

1 INTRODUÇÃO GERAL

Na civilização humana, a agricultura foi o principal divisor de águas na transição da vida nômade para a sedentária, por meio da qual o cultivo de espécies de animais e plantas domesticadas criou excedentes de alimentos que permitiam às pessoas viver nas cidades. Na história da agricultura, o plantio de grãos se consolidou há cerca de doze mil anos em diferentes regiões do mundo. O cultivo de grãos silvestres ao longo de centenas de gerações selecionou genótipos baseados em características próprias, determinando um conjunto de variedades com propriedades desejáveis pelo homem. Assim, selecionaram-se plantas com rápido crescimento, maior produtividade, grãos maiores e maior tolerância a estresses ambientais. De fato, a produção de grãos atualmente representa um importante setor econômico para o Brasil, haja visto estar entre os maiores produtores mundiais (Oliveira et al. 2016). Entre as *commodities* de origem vegetalmais cultivadas no Brasil estão a soja, milho, arroz, feijão, trigo e algodão.

No Brasil a presença da soja (*Glycine max*, Magnoliophyta: Magnoliopsida: Fabaceae) é reportada desde o fim do século XIX. Entretanto, sua expansão ocorreu nos anos 1970, devido a demanda por farelo de soja para a produção de ração para suínos e aves. Durante duas décadas, o Brasil foi o segundo maior produtor e exportador de soja, tendo alcançado o primeiro lugar em 2020, respondendo por 50% do comércio mundial, com 135.6 milhões de toneladas de soja produzidas (37% da produção mundial). Os EUA passaram a ser o segundo produtor mundial, com 112.5 milhões de toneladas (31% da produção mundial). Cerca de 38.5 milhões de hectares são utilizados para o cultivo de soja, sendo a produtividade correspondente a 3.52 kg/ha. Os Estados brasileiros com maior produção na safra 2020/2021 foram Mato Grosso, Rio Grande do Sul e Paraná (com 35.9, 20.2 e 19.9 milhões de toneladas). O consumo interno da soja em grão em 2020, voltado para a ração animal, indústria e consumo humano, foi de 46.8 milhões de toneladas, enquanto o total exportado de soja em grão, farelo para ração animal e óleo foi de 35.2 milhões de toneladas (Embrapa Soja 2021).

Apesar de sua a importância para a economia brasileira e mundial, a soja é um cultivo inserido no contexto das mudanças climáticas e susceptível a fatores abióticos como secas prolongadas e também a diversas doenças provocadas por micro-organismos. Assim, com o objetivo de superar estes desafios, estudos de engenharia genética e manipulação da expressão de genes e regulação de proteínas vem se desenvolvendo nas últimas décadas.

Estudos sobre a manipulação de genes e de sua expressão, como chaperonas moleculares, proteínas envolvidas no reparo de estruturas proteicas, revelam-se promissores, desenvolvendo características de resistência e tolerância em condições adversas. Se por um lado, a chaperona molecular BiP (*Binding Protein*) se destaca por sua participação na via de proteínas mal dobradas (UPR, *Unfolded Protein Response*), modulando eventos de morte celular programada (PCD, *Programmed Cell Death*), por outro lado, o atraso na percepção da via UPR ocasiona uma perda qualidade no correto dobramento de proteínas no retículo endoplasmático e na percepção de estresses bióticos e abióticos (Costa et al. 2008; Valente et al. 2009; Reis et al. 2011; Carvalho et al. 2014a). Estudos comprovam que a superexpressão de BiP confere tolerância à seca em soja (Alvim et al. 2001; Valente et al. 2009). Outros estudos mostram que BiP também modula uma via de PCD (Carvalho et al. 2014; Reis et al. 2016).

Plantas sofrem influência de múltiplos fatores originados do complexo ambiente em que elas vivem. Denominados fatores ambientais, incluem alterações no índice de luminosidade, qualidade do ar, amplitude de temperatura, precipitações pluviométricas irregulares, ambiente químico do solo e interações bióticas com organismos e micro-organismos, patogênicos ou não-patogênicos, que objetivam o seu próprio desenvolvimento. Esta multiplicidade de interações pode ser favorável ao seu desenvolvimento ou (na maioria dos casos) podem interferir negativamente nos vegetais, prejudicando o crescimento, produtividade e qualidade dos frutos (Boyer 1982; Dresselhaus and Hückelhoven 2018). Estresses ambientais podem ser classificados de acordo com sua intensidade e durabilidade: agudo ou crônico, leve, moderado ou severo; de acordo com a causa: abiótico, causado por fatores ambientais físicos ou químicos, e biótico, causado por seres vivos; por fim, de acordo com sua origem, podendo ser natural, fazendo parte da dinâmica natural do ambiente, ou de origem antropogênica, isto é, relacionado com as atividades humanas (Smirnoff 1998).

Um importante fator ambiental a ser discutido e relevado são os efeitos biológicos potenciais de interações planta-organismo sobre o vegetal. A uma interação biológica próxima e de longo prazo entre duas ou mais espécies diferentes dá-se o nome de simbiose. Desde que surgiu, o conceito de simbiose é alvo de debates acerca de sua amplitude. Os organismos envolvidos, denominados simbiontes, podem estabelecer relações baseadas em mutualismo (ambos os indivíduos se beneficiam), comensalismo (um se beneficia e o outro não é significativamente prejudicado ou beneficiado) ou parasitismo (o parasita se beneficia e o hospedeiro é prejudicado) Steinert et al. 2000). Simbiose pode ainda ser classificada: quanto à

obrigatoriedade para a sobrevivência do simbionte (obrigatória ou facultativa); quanto à localização do simbionte em relação ao hospedeiro (ectossimbiose ou endossimbiose); e quanto ao apego físico, isto é, se ambos formam um corpo único (simbiose conjuntiva) ou outro tipo de arranjo (simbiose disjuntiva).

A maioria das interações simbióticas planta-organismos não implicam em doença, uma vez que o vegetal é um microecossistema onde convivem inúmeras bactérias e fungos de maneira comensal, sem afetar a planta. Porém, um descontrole na colonização do tecido vegetal por estes seres resulta, na maioria dos casos, em efeitos negativos. Os vegetais, por sua vez, reagem de diversos modos ativando respostas de defesa (formação de espécies reativas de carbono, oxigênio e nitrogênio, fitoalexinas, alterações no balanço fito-hormonal e iônico, redução da estabilidade de membrana e reforço da parede celular), visando proteger a planta contra danos que poderiam resultar de um estresse biótico prolongado (Zou et al. 2005; Rojas et al. 2014; Bajaj et al. 2018). O gênero *Pseudomonas syringae,* por exemplo, são fitobactérias que colonizam a superfície dos vegetais e possuem uma especificidade na geração de doenças, de acordo com a espécie vegetal. Uma das doenças na soja provocada por bactéria é o crestamento bacteriano causada por *Pseudomonas syringae* pv. *glycinea;* apesar de não induzir à morte do vegetal, reduz a produtividade e qualidade do grão. Por sua vez, um patovar incompatível, como *Pseudomonas syringae* pv. *tomato*, provoca doença no tomate e ativa os mecanismos de defesa vegetal em soja, produzindo reação hipersensitiva e formação de pequenos halos necróticos de cor castanha ao redor do sítio de invasão que confinam o micro-organismo e detém sua propagação (Gardan, 1999; Preston, 2000; Zou et al. 2005). O aumento da produção de fitoalexinas em consequência de interações planta-organismo é alvo de estudos científicos na área da saúde (Nwachukwu et al. 2013; Egbuonu and Eneogwe 2018 Jeandet et al. 2014).

Mais recentemente, estudos sobre simbiose despertou o interesse de biólogos, na indústria de alimentos e no setor do agronegócio como importante motor na adaptação de espécies e na obtenção de características desejáveis, como no caso de *Pochonia Chlamydosporia* (Goddard) Zare & Gams (2001), um fungo nematófago (Ascomycota: Hypocreales: Clavicipitaceae) que possui ação predatória em ovos de nematoides do gênero *Meloidogyne*, entre outros (Arevalo et al. 2009). Este nematoide ataca e provoca danos às raízes de plantas como cenoura, tomate e soja (Bontempo et al. 2014). Em estudos com tomateiro e alface, a colonização da rizosfera por hifas de *P. chlamydosporia* também promove o crescimento das plantas (Dallemole-Giaretta et al. 2015). Assim, observamos uma

simbiose onde o fungo e a planta são beneficiados (este por obter uma fonte de nematoides como alimento, esta por obter proteção contra nematoides que prejudicariam o crescimento, produção e qualidade do produto). Maiores estudos sobre interações biológicas podem esclarecer os mecanismos relacionados.

Assim, plantas desenvolveram, em resposta a estresses ambientais, respostas rápidas e coordenadas às condições adversas (Smirnoff 1998; Dresselhaus and Hückelhoven 2018). As interações bióticas, como simbioses, e abióticas, como tolerância à seca, estão relacionadas com mudanças no metabolismo primário nas plantas por meio da expressão de genes e síntese de enzimas, fatores de transcrição e modificações pós-traducionais (Smirnoff 1998; Rojas et al. 2014).

Com eventos extremos relacionados com as mudanças climáticas tornando-se mais frequentes, como a elevação da temperatura e períodos irregulares de chuvas e seca (Cunha et al. 2019), os sistemas de defesa da planta tendem a ser mais exigidos. Isto pode resultar em menor crescimento, produtividade e na perda da qualidade do grão. O estudo das alterações na fisiologia e no metabolismo vegetal frente a estresses concomitantes é importante porque reflete o que na realidade ocorre no meio ambiente. Durante um ataque patogênico, a planta pode passar por um período de seca; do mesmo modo, durante o regime de seca, a planta pode ser atacada por outros organismos. Estudos indicam que os estresses biótico e abiótico sofridos pelo vegetal afetam os processos de produção de energia, como respiração, fotossíntese e fotorrespiração, impactando outras vias como metabolismo de aminoácidos, lipídios e carboidratos. Outras vias são up-reguladas para síntese de compostos envolvidos em respostas de defesa e de osmoprotetores como prolina, polióis e açúcares (Rojas et al. 2014; Dresselhaus and Hückelhoven 2018).

Assim sendo, o presente trabalho teve como objetivos principais caracterizar as respostas fisiológicas, fenotípicas e do metabolismo vegetal de soja frente a estresses ambientais. Analisamos o evento de morte celular programada relacionada com reação hipersensitiva provocada pela bactéria não compatível *P. syringae* pv. tomato em genótipos contrastantes quanto à seca, com a isolinha transgênica superexpressando a chaperona molecular BiP e tolerante à seca. Além disso, também se observou os aspectos moleculares da interação biótica do fungo nematófago *P. chlamydosporia* em raízes de soja em um ensaio de restrição hídrica em variedades contrastantes à seca. Dados morfofisiológicos e perfis de proteoma e de metaboloma, determinantes fenotípicos e moleculares das interações planta-bactéria (Capítulos 1 e 2) e planta-fungo (Capítulo 3) foram avaliados, ressaltando a

importância da via dos fenilpropanoides, flavonoides e isoflavonoides nas respostas de proteção da planta frente a estresses ambientais.

REFERÊNCIAS

ALVIM, F. C.; CAROLINO, S. M. B.; CASCARDO, J. C. M.; NUNES, C. C.; MARTINEZ, C. A.; OTONI, W. C.; FONTES, E. P. B. (2001) Enhanced accumulation of BiP in transgenic plants confers tolerance to water stress. Plant Physiol. 126, 1042-1054. https://doi.org/10.1104/ pp.126.3.1042.

AREVALO, J.; HIDALGO-DÍAZ, L.; MARTINS, I.; SOUZA, J. F.; CASTRO, J. M. C.; CARNEIRO, R. M. D. G.; TIGANO, M. S. (2009) Cultural and morphological characterization of *Pochonia chlamydosporia* and *Lecanicillium psalliotae* isolated from *Meloidogyne mayaguensis* eggs in Brazil. Tropical Plant Pathology 34 (3)

BONTEMPO, A. F.; FERNANDES, R. H.; LOPES, J.; FREITAS, L. G.; LOPES, E. A. (2014) *Pochonia chlamydosporia* controls *Meloidogyne incognita* on carrot. Australasian Plant Pathology, 43(4), 421-424. https://doi.org/10.1007/s13313-014-0283-x

BAJAJ, R.; HUANG, Y.; GEBRECHRISTOS, S.; MIKOLAJCZYK, B.; BROWN, H.; PRASAD, R.; VARMA, A.; BUSHLEY, K. E. (2018) Transcriptional responses of soybean roots to colonization with the root endophytic fungus *Piriformospora indica* reveals altered phenylpropanoid and secondary metabolism. Sci. Rep. 8, 10227. https://doi.org/10.1038/s41598-018-26809-3.

BOYER, J. S. (1982) Plant productivity and environment. Science. 29;218(4571):443-8. https://doi.org/10.1126/science.218.4571.443

CARVALHO, H. H.; SILVA, P. A.; MENDES, G. C.; BRUSTOLINI, O. J.; PIMENTA, M. R.; GOUVEIA, B. C. VALENTE, M. A.; RAMOS, H. J. O.; RAMOS, J. R. L.; S.; FONTES, E. P. (2014) The endoplasmic reticulum binding protein BiP displays dual function in modulating cell death events. Plant Physiol. 164(2):654-70. https://https://doi.org/10.1104/pp.113.231928

COSTA, M. D. L.; REIS, P. A. B.; VALENTE, M. A. S.; IRSIGLER, A. S. T.; CARVALHO, C. M.; LOUREIRO, M. E.; ARAGA˜O, F. J. L.; BOSTON, R. S.; FIETTO, L. G.; FONTES, E. P. B. (2008) A new branch of endoplasmic reticulum stress signaling and the osmotic signal converge on plant-specific asparagine-rich proteins to promote cell death. J. Biol. Chem. 283, 20209-20219. https://doi.org/10.1074/jbc.M802654200.

CUNHA, A. P. M. A.; ZERI, M.; LEAL, K. D.; COSTA, L.; CUARTAS, L. A.; MARENGO, A.; TOMASELLA, J.; VIEIRA, R. M.; BARBOSA, A. A.; CUNNINGHAM, C.; GARCIA, J. V. C.; BROEDEL, E.; ALVALÁ, R.; RIBEIRO-NETO, G. (2019) Extreme Drought Events over Brazil from 2011 to 2019. Atmosphere, 10(11), 642. https://doi.org/10.3390/atmos10110642

DALLEMOLE-GIARETTA, R.; FREITAS, L. G.; LOPES E. A.; SILVA, M. C. S.; KASUYA, M. C. M.; FERRAZ, S. (Oct. -Dec 2015) *Pochonia chlamydosporia* promotes the

growth of tomato and lettuce plants. Acta Scientiarum. Agronomy Maringá, 37(4):417-423. https://doi.org/10.4025/actasciagron.v37i4.25042

DRESSELHAUS, T.; HÜCKELHOVEN, R. (2018) Biotic and Abiotic Stress Responses in Crop Plants. Agronomy. 8(11):267. https://doi.org/10.3390/agronomy8110267

EMBRAPA SOJA. (2021) Soja em números (safra 2020/21). Embrapa. https://www.embrapa.br/soja/cultivos/soja1/dados-economicos. Access: Out de 2021.

GARDAN, L.; SHAFIK, H.; BELOUIN, S.; BROCH, R.; GRIMONT, F.; GRIMONT, P. A. D. (1999) DNA relatedness among the pathovars of *Pseudomonas syringae* and description of *Pseudomonas tremae* sp. nov. and *Pseudomonas cannabina* sp. nov (ex Sutic and Dowson 1959). Int. J. Syst. Evol. Microbiol. 49, 469-478. https://doi.org/10.1099/00207713-49-2-469.

JEANDET, P.; HÉBRARD, C.; DEVILLE, M. A.; CORDELIER, S.; DOREY, S.; AZIZ, A.; CROUZET, J. (2014) Deciphering the role of phytoalexins in plant-microorganism interactions and human health. Molecules (Basel, Switzerland), 19(11), 18033-18056. https://doi.org/10.3390/molecules191118033

NWACHUKWU, I. D.; LUCIANO, F. B.; UDENIGWE, C. C. (2013) The inducible soybean glyceollin phytoalexins with multifunctional health-promoting properties. Food Research International, 54(1), 1208-1216. https://doi.org/10.1016/j.foodres.2013.01.024

OLIVEIRA, G. D. L.; SCHNEIDER, M. (2016) The politics of flexing soybeans: China, Brazil and global agroindustrial restructuring. J. Peasant Stud. 43, 167-194.

PRESTON, G. M. (2000) *Pseudomonas syringae* pv. tomato: the right pathogen, of the right plant, at the right time. Mol. Plant Pathology 1 (5), 263-275. https://doi.org/10.1046/ j.1364-3703.2000.00036.x.

REIS, P. A. B.; ROSADO, G. L.; SILVA, L. A.; OLIVEIRA, L. C.; OLIVEIRA, L. B.; COSTA, M. D.; ALVIM, F. C.; FONTES, E. P. B. (2011) The binding protein BiP attenuates stress-induced cell death in soybean via modulation of the N-rich protein-mediated signaling pathway. Plant Physiol. 157, 1853-1865.

REIS, P. A. B.; CARPINETTI, P. A.; FREITAS, P. P. J.; SANTOS, E. G. D.; DE CAMARGOS, L. F.; OLIVEIRA, I. H. T.; SILVA, J. C. F.; CARVALHO, H. H.; COSTA, M. D. L.; RAMOS, J. L. R. S.; FONTES, E. P. B. (2016) Functional and regulatory conservation of the soybean ER stress-induced DCD/NRP-mediated cell death signaling in plants. BMC Plant Biol. 16, 156. https://doi.org/10.1186/s12870-016-0843-z.

ROJAS, C. M.; SENTHIL-KUMAR, M.; TZIN, V.; MYSORE, K. S. (2014) Regulation of primary plant metabolism during plant-pathogen interactions and its contribution to plant defense. Front. Plant Sci. 5, 17. https://doi.org/10.3389/fpls.2014.00017.

SMIRNOFF, N. (1998) Plant resistance to environmental stress. Current Opinion in Biotechnology, 9(2), 214-219. https://doi.org/10.1016/s0958-1669(98)80118-3

STEINERT, M.; HENTSCHEL, U.; HACKER, J. (2000) Symbiosis and pathogenesis: evolution of the microbe-host interaction. Die Naturwissenschaften.87(1):1-11. https://doi.org/10.1007/s001140050001

VALENTE, M. A. S.; FARIA, J. Q. A.; RAMOS, J. R. L. S.; REIS, P. A. B.; PINHEIRO, G. L.; PIOVESAN, N. D.; MORAIS, A. T.; MENEZES, C. C.; CANO, M. A. O.; FIETTO, L. G.; LOUREIRO, M. E.; ARAGAO, F. J. L.; FONTES, E. B. P. (2009) The ER luminal binding protein (BiP) mediates an increase in drought tolerance in soybean and delays drought-induced leaf senescence in soybean and tobacco. J. Exp. Bot. 60, 533-546. https://doi.org/10.1093/jxb/ern296

ZOU, J.; RODRIGUEZ-ZAS, S.; ALDEA, M.; LI, M.; ZHU, J.; GONZALEZ, D. O.; VODKIN, L. O.; DELUCIA, E.; CLOUGH, S. J. (2005) Expression profiling soybean response to *Pseudomonas syringae* reveals new defense-related genes and rapid hr-specific downregulation of photosynthesis. Mol Plant-Microbe Interact 18(11):1161-1174

CAPÍTULO I

BiP-OVEREXPRESSING SOYBEAN PLANTS DISPLAY ACCELERATED HYPERSENSITIVITY RESPONSE (HR) AFFECTING THE SA-DEPENDENT SPHINGOLIPID AND FLAVONOID PATHWAYS

CAPÍTULO I – BiP-OVEREXPRESSING SOYBEAN PLANTS DISPLAY ACCELERATED HYPERSENSITIVITY RESPONSE (HR) AFFECTING THE SA-DEPENDENT SPHINGOLIPID AND FLAVONOID PATHWAYS

ABSTRACT

Biotic and abiotic environmental stresses have limited the increase in soybean productivity. Overexpression of the molecular chaperone BiP in transgenic plants has been associated with the response to osmotic stress and drought tolerance by maintaining cellular homeostasis and delaying hypersensitive cell death. Here, we evaluated the metabolic changes in response to the hypersensitivity response (HR) caused by the non-compatible bacteria *Pseudomonas syringae* pv. *tomato* in BiP-overexpressing plants. The HR-modified metabolic profiles in BiP-overexpressing plants were significantly distinct from the wild-type untransformed. The transgenic plants displayed a lower abundance of HR-responsive metabolites as amino acids, sugars, carboXylic acids and signal molecules, including p-aminobenzoic acid (PABA) and dihydrosphingosine (DHS), when compared to infected wild-type plants. In contrast, salicylic acid (SA) biosynthetic and signaling pathways were more stimulated in transgenic plants, and both pathogenesis-related genes (PRs) and transcriptional factors controlling the SA pathway were more induced in the BiP-overexpressing lines. Furthermore, the long-chain bases (LCBs) and ceramide biosynthetic pathways showed alterations in gene expression and metabolite abundance. Thus, as a protective pathway against pathogens, HR regulation by sphingolipids and SA may account at least in part by the enhanced resistance of transgenic plants. GmNAC32 transcriptional factor was more induced in the transgenic plants and it has also been reported to regulate flavonoid synthesis in response to SA. In fact, the BiP-overexpressing plants showed an increase in flavonoids, mainly prenylated isoflavones, as precursors for phytoalexins. Our results indicate that the BiP-mediated acceleration in the hypersensitive response may be a target for metabolic engineering of plant resistance against pathogens.

Keywords: *Glycine max. Pseudomonas syringae* pathovar *tomato.* Fabaceae. Plant-pathogen interaction. Plant breeding. Environmental stress. Metabolomics. Gene expression.

1 INTRODUCTION

Soybean [*Glycine max* (L.) Merr.)] is a plant of the Fabaceae family and is one of the most important crops worldwide because of its application in the food industry and biodiesel production. Brazil stands out as the second-largest producer and exporter of soybeans. Nevertheless, the potential for expansion has faced constraints due to climatic events such as drought, which is the main limiting factor for soybean growth, development, and productivity (Dai, 2013). Therefore, it is necessary to obtain plants capable of maintaining high productivity under water-limiting conditions (Ku et al. 2013), since the predictions for water scarcity in the world are significantly worrisome.

One of the strategies used to mitigate the damage caused by drought in the plant metabolism involve the modifications of the expressions of genes and transcription factors associated with the biosynthesis of endoplasmic reticulum (ER) proteins. The accumulation of poorly folded proteins triggers an ER stress signaling pathway, designated the unfolded protein response (UPR), which induces ER-associated quality control genes to promote the restoration of ER homeostasis (Leborgne-Castel et al. 1999; Pincus et al. 2010; Williams et al. 2014; Silva et al. 2015; Reis et al. 2016; de Camargos et al. 2018; Melo et al. 2018). The ER-resident molecular chaperone binding protein (BiP), which belongs to the family of 70 kDa heat shock protein (HSP70), has been shown previously to be involved in enhanced tolerance to drought conditions (Alvim et al. 2001; Valente et al. 2009). BiP promotes a delay in the perception of stress symptoms and negatively regulates the expression and activity of the components of the development cell death domain-containing N-rich protein (DCD/NRP)-mediated programmed cell death (PCD), including GmNRP-A, GmNRP-B, GmNAC81 and the vacuolar processing enzymes (VPE) (Costa et al. 2008; Valente et al. 2009; Reis et al. 2011; Carvalho et al. 2014a). In soybean and *Arabidopsis thaliana*, the mechanism for BiP-mediated increase in drought tolerance has been linked to its capacity to modulate the stress-induced DCD/NRP-mediated cell death pathway negatively (Carvalho et al. 2014a; Reis et al. 2016). In contrast, BiP has also been shown to accelerate the hypersensitive response (HR) induced by an incompatible plant-bacterium interaction and stimulate the salicylic acid-mediated signaling pathway positively (Reis et al. 2011; Carvalho et al. 2014a, b; Silva et al. 2015; Reis et al. 2016).

Pseudomonas syringae pathovar (pv.) tomato are phytobacteria of the *Pseudomonas* group (Gram negative, aerobic, flagellated bacilli, and ubiquitous). It colonizes the plant tissue of diverse plants and can cause spots and blight on leaves and fruits, compromising productivity and food security. *P. syringae* pv. tomato has the ability to survive on seeds, exudates, crop residues and soil, constituting a source of inoculum for soybean (Gardan, 1999; Preston, 2000). In addition, pathogen- or microbe-associated molecular patterns (PAMPs or MAMPs), molecules present on the surface of the invading organism, may be recognized by plasma membrane-anchored receptors, designated PAMP-recognition receptors (PRR), to activate the first layer of plant defense (PAMP-triggered immunity) (Baltrus et al. 2012; Ichinose et al. 2013). The second layer of plant defense, designated effector-triggered immunity (ETI), is more specific and is activated by a pathogen effector and a specific plant resistance (R) protein in resistant genotypes. In the latter case, the plant often develops the HR, which triggers the synthesis of specific compounds that lead to PCD of neighboring cells at the site of the invasion, as a mechanism to contain the pathogen at the site of infection and hence prevent its spread (Finkel, 2000; Zou et al. 2005; Coll et al. 2011).

Another plant defense strategy upon bacterial infection involves alterations of the specialized metabolism such as the biosynthesis of phytoalexins, which function as antimicrobial compounds and are produced constitutively or in response to plant damage. Flavonoids are phenolic compounds that accumulate in the plants as core compounds, called aglycones, or combined with chemical groups (methylation, acylation, malonylation, prenylation, glycosylation or polymerization), called flavogenins. In plants, most flavonoids occur in the form of glycoconjugates, harboring saccharide moieties that increase or reduce the phytoalexin activity against the invading organisms (Zabala et al. 2006; Aron and Kennedy, 2008; Ahuja et al. 2012; Ferreyra et al. 2012; Alam et al. 2014). Flavonoids have a wide range of functions, including antioXidant activity, protection against UV radiation, and defense against phytopathogens (Graham, 1998; Hassan and Mathesiu, 2012; Chin et al. 2018).

BiP-overexpressing plants have been characterized at the genetic and molecular levels; however, little information is available about the effect of the BiP-overexpression in the plant metabolism under biotic interactions. Furthermore, how BiP overexpression acts directly in PCD-induced by HR had not yet been evaluated. Thus, as HR is an important process involved in plant-pathogen interactions, the analysis of metabolomic profiles may contribute to elucidate mechanisms of plant defense responses in this transgenic soybean plant showing drought tolerance. Here, we evaluated the metabolic responses triggered by the non-

compatible bacteria *P. syringae* pv. tomato (HR induced) in the drought-tolerant BiP-overexpressing transgenic soybean plants. We determined the differential metabolic profiles by GC/MS, the production of phytohormones and flavonoids by LC/MS, and the gene expression of some target genes by qRT-PCR. These analyses were integrated into the signaling networks of hypersensitive cell death triggered by *P. syringae* pv. tomato in the BiP-overexpressing plants. Overall, the results indicate the importance of the BiP cascades as targets for breeding programs aiming at obtaining tolerant plants to biotic and abiotic stresses.

2 RESULTS

2.1 SYMPTOMS OF HR IN SOYBEAN LEAVES OF BiP-OVEREXPRESSING AND WT LINES

BiP-overexpressing soybean plants (C9 plants) display an accelerated hypersensitive response triggered by *P. syringae* pv. tomato (Carvalho et al. 2014a) and have been characterized at genetic level. To examine whether this phenotype would be associated with alterations in specialized metabolites accumulation, we inoculated the transgenic and wild-type plants with *P. syringae* pv. tomato for metabolomic analysis. At 8 h after inoculation, symptoms of hypersensitivity were not observed, while at 36 h after inoculation. HR symptoms were observed in both WT and C9 genotypes, showing the formation of brown halos, necrosis signs at the site of infection, which were pronounced in the transgenic plant C9 (**Figure 1**). In contrast, the leaves from the control plants had no visible symptoms. The symptoms of PCD became clearer over the course of days. At 15 and 30 days after inoculation (dai), the drought tolerant C9 plants displayed necrotic halos in larger numbers, coalescing and covering a larger area than WT plants.

Figure 1 – Symptoms of the soybean leaves from the transgenic overexpressing BiP (**C9**) and untransformed (**WT**) genotypes submitted to inoculation by *P. syringae* pv. tomato. In **(A)** Leaves from plants after 8 and 36 hai (hour after inoculation) and in **(B)** after 15 and 30 dai (day after inoculation).

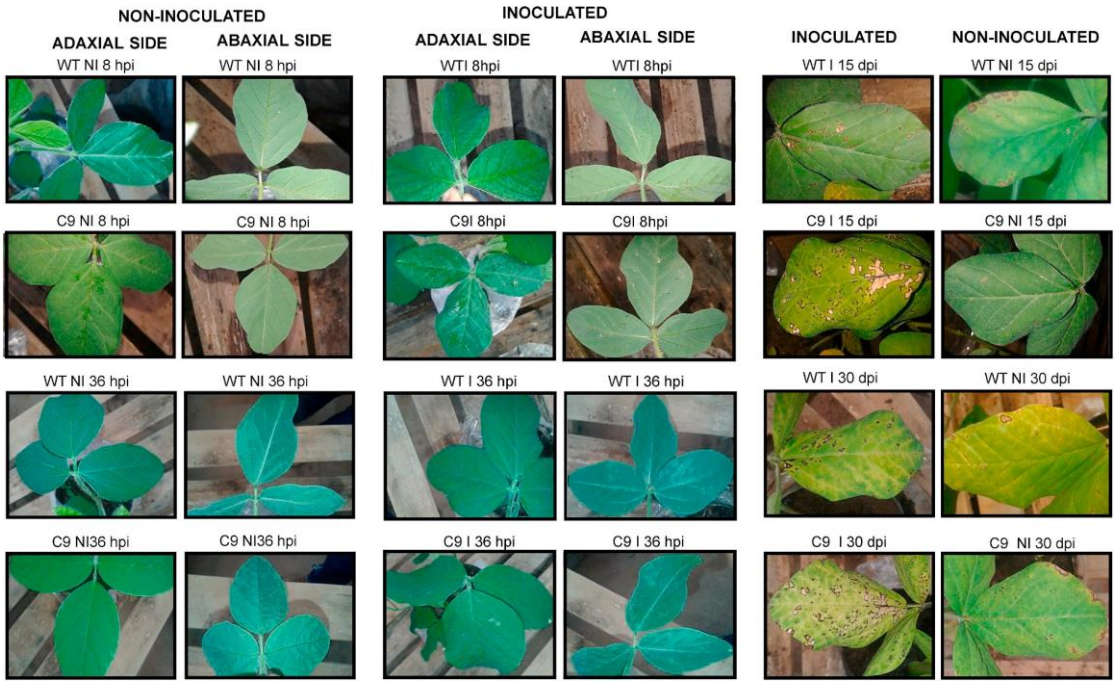

Source: Survey's data.

2.2 BiP-OVEREXPRESSING PLANTS SHOWED DISTINCT METABOLIC PROFILES UNDER BACTERIAL INFECTION

Hypersensitive response (HR) in the plant leaves involve signaling molecules and gene reprograming. Thus, in order to understand the main physiological processes affected by bacterial HR stress in the BiP-overexpressing soybean, we first analyzed the changes in the metabolite profiles by GC/MS. The identified metabolites were analyzed by MetaboAnalyst platform. We identified 241 metabolites and discriminant analyses by PLS-DA and VIP score (**Figure 2**) were used to determine how the differential accumulation of all metabolites correlated with genotypes and treatments. PLS-DA plot of the profile GC/MS (**Figure 2A**) indicated similar patterns between genotypes in absence of the inoculations. In contrast, the BiP-overexpressing transgenic plants showed significant grouping, with a clear separation compared to wild-type plants in absence of bacterial infection. Thus, indicating that general metabolism response was different in the transgenic plants (**Figure 2A**) when triggered by pathogen attack (70.3% of the total variance). These grouping patterns were also visualized by the VIP score plot (Figure 2B) that indicate those compounds that contributed more for the

group separation by PSL-DA as indicated in **Figure 2A**. The compounds showing higher dysregulation were 4-Amino-butanoic acid, Fumaric acid, Dihydrosphingosine and Malonic acid (**Figure 2B**).

Figure 2 – Analysis of the metabolic profiles of the C9 and WT genotypes in soybean leaves from the WT and C9 genotypes infected (I) or noninfected (NI) by *P. syringae* pv. tomato 36 h after inoculation. In **(A)** 2D Scores Plot generated by Partial Least Squares Discriminant Analysis (PLS-DA) of all the metabolites. Points represent analyzed replicates, whereas ellipses indicate 95% confidence region. In **(B)** Major metabolites responsible for discrimination between inoculated and mock inoculated soybean groups identified by VIP score. Green color represents a decrease, and red color an increase**.**

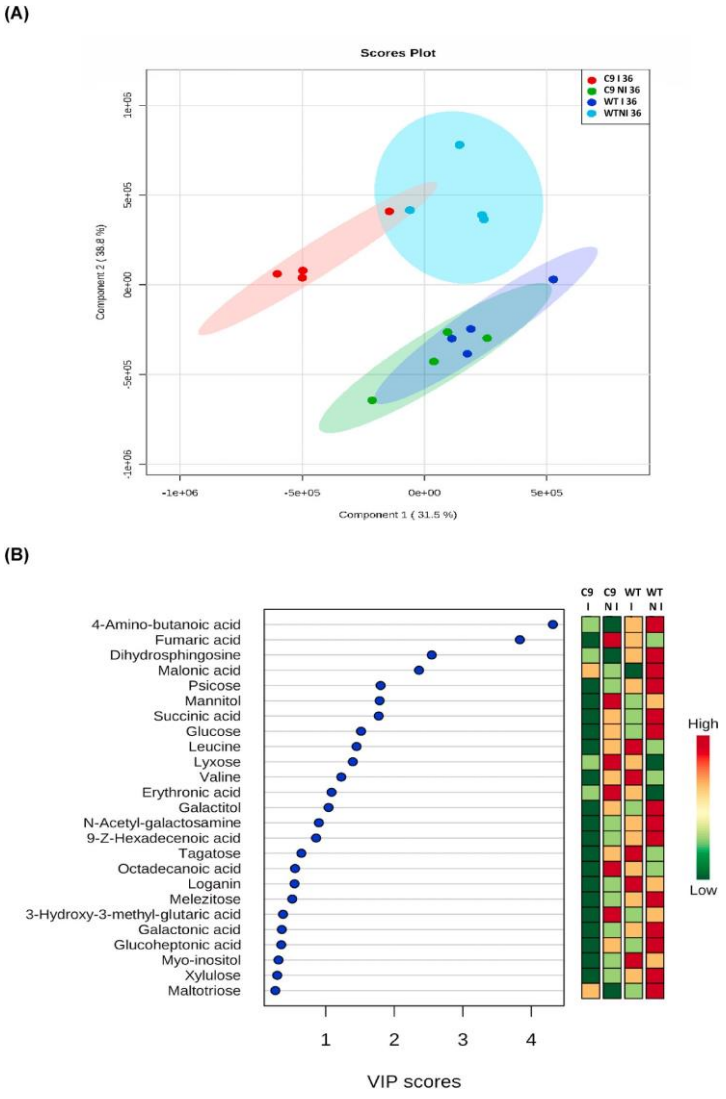

Source: Survey's data.

Hierarchical clustering analysis by Heatmap was also used to determine the behavior of the more responsive metabolites in soybean leaves in response to HR (bacterial infection) and BiP overexpression (**Figure 3**). This analysis also indicated the metabolites 4-

amino benzoic acid (PABA), fumaric acid, dihydrosphingosine, and malonic acid as the main contributors for the separation of GC/MS profiles by PLS-DA. However, the Heatmap also showed that the abundances for some metabolites were completely distinct and antagonistic to the contrast C9 NI vs WT NI. This contrasting metabolic profiles may be a direct result of BiP-overexpression even in absence of bacterial infection in the transgenic plants (**Figure 3**). This separation of the genotype-derived metabolic profiles was more evident at 36 h after bacterial inoculation, when the HR symptoms were visible. A set of metabolites, including branched chain amino acids (BCAA: leucine, isoleucine and valine), alanine, arbutin (hydroquinone 4-O-glycoside) and 2-amino butanoic acid (or α-aminobutyrate; AABA) showed a higher abundance (**Figure 3**) in WT I as compared to WT NI (induced under bacterial infection). In contrast, this same group of HR-induced metabolites in the WT genotype displayed lower abundance in C9 I compared to C9 NI (reduced after bacterial infection).

In the same way, other metabolites were slightly induced during HR process in WT (cluster starting in Loganin to Guanidine) while for C9 were repressed (**Figure 3**). Other contrasting metabolic cluster, starting by Ascorbic acid and ending by Octadecanoic acid, was highly repressed by bacterial infection (HR process) in transgenic plants C9 and just barely altered in WT genotype.

On the other hand, similar changes, to the metabolite profile induced by HR, were also observed in WT and C9, although to a different extent. A group of metabolites, including 4-amino butanoic acid (γ-aminobutyrate; GABA), dihydrosphingosine (DHS), long chain organic acids, erythrose, glucose and other sugars and their derivatives showed lower abundance WT I and C9 I as compared to their respective control WT NI and C9 NI. In C9 genotype under infection (C9 I), the majority of metabolites were downregulated by HR. Only fructose 6-phosphate was upregulated (**Figure 3**).

Overall, the results indicate that the BiP-overexpressing transgenic plants presented a mechanism to trigger the hypersensitive response (HR) distinct from those currently observed for soybean plants under non-compatible bacterial infection.

Figure 3 – Clustering analysis by Heat Map method of the characterized metabolites by GC/MS in soybean leaves from the WT and C9 genotypes, infected (I) or noninfected (NI) by *P. syringae* pv. tomato 36 h after inoculation. Differences in the abundance of the metabolites are indicate in response to treatments.

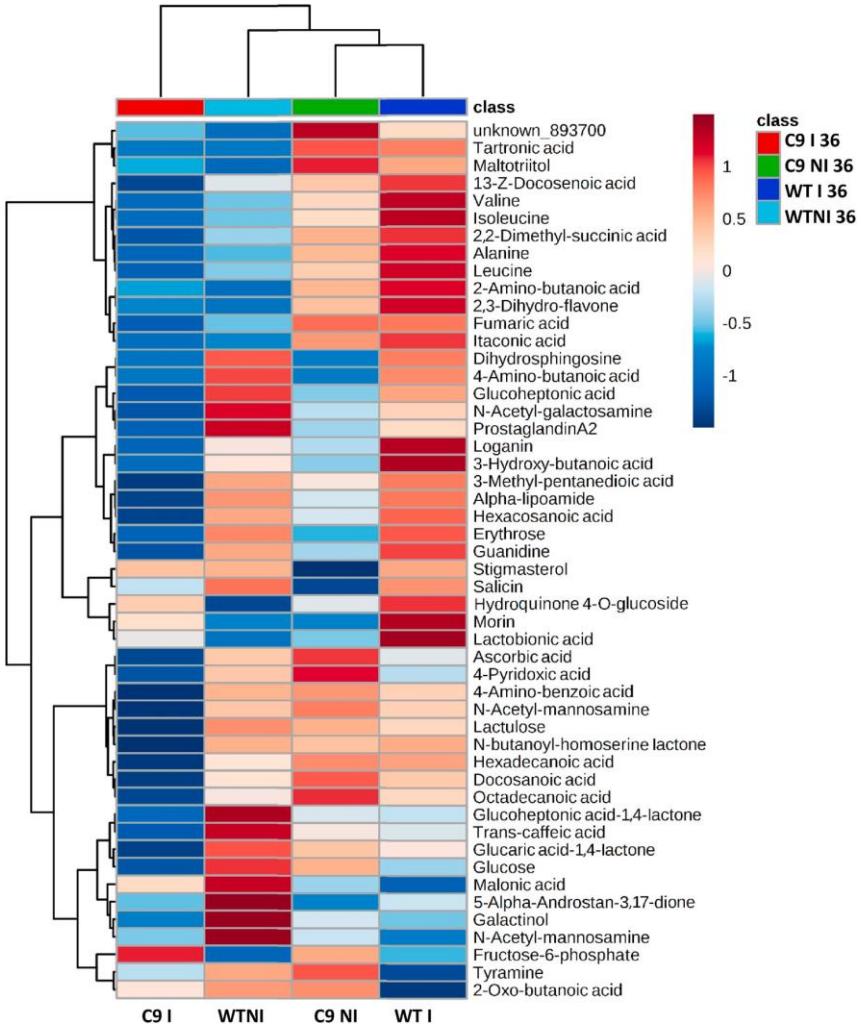

Source: Survey's data.

2.3 SALICYLIC ACID LEVELS WERE HIGHER IN BOTH INFECTED OR NONINFECTED BiP-OVEREXPRESSING TRANSGENIC PLANTS

Phytohormones regulate a large variety of physiological processes in plants. Salicylic acid (SA), jasmonic acid (JA), abscisic acid (ABA), and ethylene (ET) are responsible for primary defense responses against abiotic and biotic stresses, while plant growth regulators, such as auxins, brassinosteroids (BRs), cytokinins (CKs), and gibberellins (GAs), also contribute to plant immunity (Sánchez-Rangel et al. 2015). Thus, the phytohormone profiles of transgenic (C9) and wild-type (WT) plants were also evaluated. The absolute concentrations of the phytohormones were obtained by mass spectrometry coupled to liquid

chromatography (**Figure 4A**). SA is a key signaling molecule that is required for induction of defense-related genes promoting a rapid and localized cell death at the site of bacterial infection (hypersensitive response). Accordingly, the SA levels were increased in both genotypes after bacterial inoculation. However, the SA levels in C9 genotype were higher in both infected or noninfected plants than in the WT counterparts. Under normal conditions, transgenic plants have previously showed higher SA levels than wild-type soybean (Carvalho et al. 2014a; Coutinho et al. 2019). Here, we extended these previous observations and showed that after bacterial inoculation the levels of SA were approximately 1.5-fold higher in the transgenic leaves than in WT leaves (**Figure 4A**).

AIA levels increased significantly in both C9 and WT-infected plants compared to the noninfected plants, although to a more extent in C9 infected leaves. The concentrations of methyljasmonate and zeatin were similar in the genotypes and did not alter in the response to bacterial inoculation. In contrast, JA levels were higher in transgenic plants under infested conditions and the ABA levels were repressed under infection (**Figure 4A**). Overall, the levels of JA and SA were higher in the C9 plants compared to WT plants under HR induced by *Pseudomonas*.

2.4 PRIMARY SOYBEAN ISOFLAVANOIDS ACCUMULATE TO A HIGHER EXTENT IN C9- THAN IN WT-INFECTED LEAVES

Functional categorization of the transcriptome of BiP-overexpressing plant indicated an upregulation of some flavonoid-related genes (Carvalho et al. 2014a), thus we performed LC/MS analysis to verify the abundance of these compounds in soybean leaves. Firstly, a LC/MS-based target method (Gómez et al. 2018) was used to perform the analysis of specific flavonoids. Some of this target compounds showed mass spectrum and chromatographic signals sufficient to perform the quantitative analysis in soybean leaves (**Figure 4B**). For the aglycone flavonoid standards evaluated by this approach, the concentrations of apigenin, dadzein, naringenin, and genistein were higher in inoculated plants when compared to non-inoculated plants, however theincreases were more pronounced in the C9 genotype. In contrast, the content of quercetin remained not altered between genotypes while the kaempferol levels was reduced only in transgenic plants C9 under bacterial infection (**Figure 4B**). Interestingly, the most important isoflavonoids in soybean plants daidzein and genistein, whose aglycone forms are precursors for methylated,

glucoside and malonate derivatives acting against pathogens (Mierziak et al. 2014), were more abundant in transgenic plants C9.

Figure 4 – Absolute concentrations of phytohormones **(A)** and of flavonoid aglycones **(B)** by UHPLC/MS QqQ. The data represent the mean ± standard error. Bars (mean ± SE; n = 4) with the same capital letters indicate no significant difference between control and inoculated treatments and those followed by the same lowercase letters indicate no significant difference among genotypes within the same treatment (Student's test: $P < 0.05$).

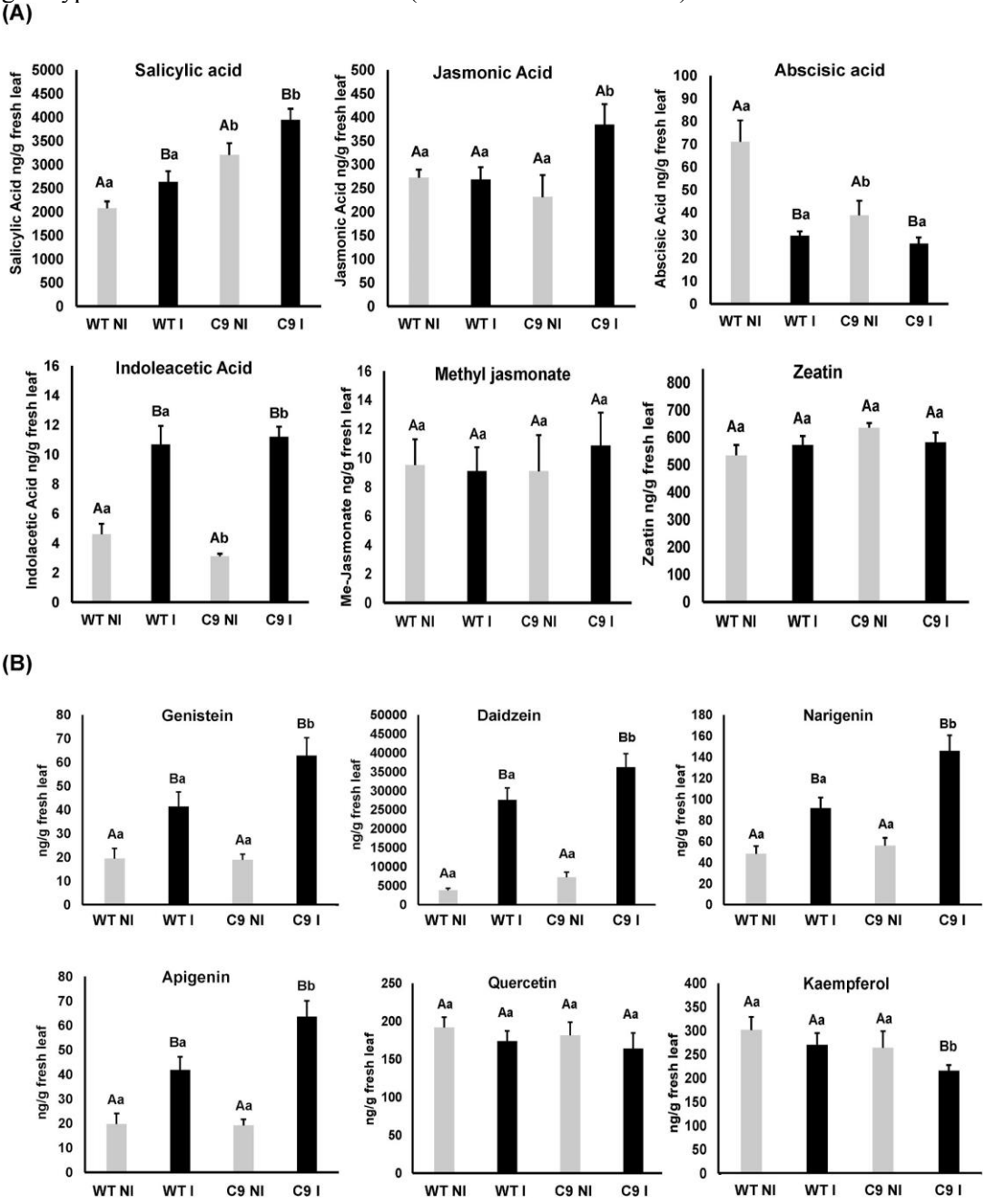

Source: Survey's data.

2.5 PROFILING OF THE NON-TARGET FLAVONOIDS IN WT AND C9 SOYBEAN LEAVES

Flavonoids occur as aglycones, glycosides and methylated derivatives, increasing the structural and functional complexity of this class of phenolic compounds. Thus, we also applied a MS-based approach for broad range profiling to evaluate their glycoconjugate forms. Each commercial standard flavonoid was injected into LC/MS QqQ to generate the pseudo MS3 spectrum of the aglycone cores, as described by Gomez at al. (2018). The fragment relative intensities (FRI) between the ions were measured to determine which m/z values are distinguishable between the aglycone isomers (**Appendix B, C, D and E**). It was not possible to apply the pseudo-MS3/MRM method for the compounds Myricetin, Epicatechin-Catechin, Phloretin and Naringenin, since the mass spectrometry signals were very low and signals of FRI% between the ions were disproportionate as compared to the standards. As the pseudoMS3/MRM method only provides structural information about the aglycone core, another method was needed to elucidate the molecular masses present in the molecular structure of the compounds from the fragmentation pattern. Thus, flavonoids could be characterized from the difference between the total mass of the molecule and the mass of the aglycone core (**Appendix A**). All flavonoids detected by the target and non-target methods were used together for clustering analyses aiming to compare the abundance variations between transgenic and wild-type genotypes and also in response to bacterial inoculations. Analysis of the flavonoid profiles by PLS-DA plot (**Figure 5**) indicated similar patterns between genotypes in absence of the inoculations. However, the BiP-overexpressing transgenic plants showed a clear separation related to wild-type when the plants were under bacterial infection (31.9% of the total variance). Thus, the flavonoid biosynthetic pathways were also affected by the cascades regulated by BiP. A hierarchical Heatmap plot, of the most dysregulated flavonoids from PLS-DA analysis (**Figure 5**), characterized the compounds responsive to genotypes and treatments (**Figure 6**) and confirmed the grouping patterns. The clustering of the flavonoids into three different groups also could be observed in the Heatmap (**Figure 6**) generated from the relative abundance of XIC plots for the individual RTs. Furthermore, these analyses enable a characterization of the responsive compounds specifically in BiP-overexpressing transgenic soybean (**Figure 6**).

Figure 5 – Analysis of 2D Scores Plot by Partial Least Squares Discriminant Analysis (PLS-DA) of characterized flavonoids in soybean leaves from the C9 and WT genotypes, infected (I) or noninfected (NI) by *P. s.* pv. *tomato* 36 h after inoculation. Points represent replicates analyzed, whereas ellipses indicate 95% confidence region.

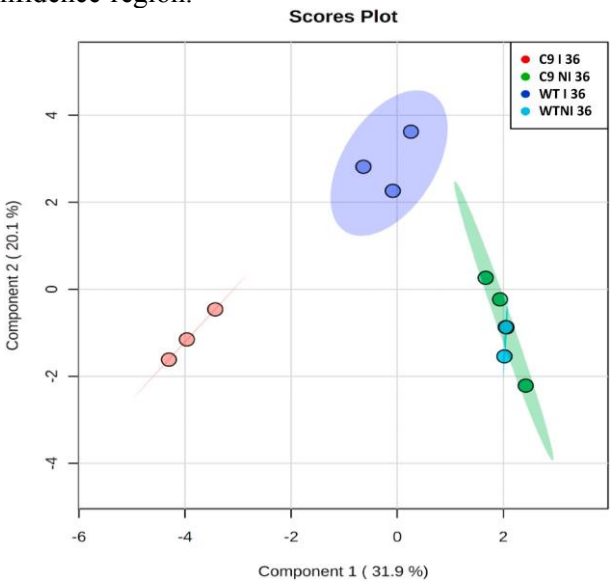

Source: Survey's data.

Using the flavonoid class and m/z values observed for each XIC as filters, it was possible to search, against the mass spectra database Mass Bank (http://www.massbank.jp) or other sources in the literature to verify which flavonoids share the same mass observed in the precursor ion scan (Gómez et al. 2018). When the precursor ion scan was applied to Genistein-Apigenin class (m/z 271 for aglycone), RTs equal to 6.5 and 7.1 indicated RFI% similar to genistein, while the other RTs did not allow the identification of genistein precisely (**Appendix A and B**). Thus, the class of some compounds remained as undefined. Applying this strategy for the Daidzein class (m/z 255 for aglycone), the results indicated the presence of isoflavonoid in all treatments along the RTs (**Appendix A and E**). Interestingly, prenylated isoflavonoids, such as dimethylalllyldaidzein (identified in daidzein-10.1) and dimethylalllylgenistein (identified in genistein-10.7), were observed at RT values next to 10 min (**Appendix A** and **Figure 7**). The presence of dimethylallyldaidzein, which was more abundant in C9-infected leaves, and dimethylallylgenistein more abundant in WT-inoculated leaves may be associated with the HR-induced antibacterial, cytotoXic and antioXidant activities of plant cells. These compounds may be involved in the defense response against invading organisms.

Figure 6 – Clustering analysis by Heat Map method of the characterized flavonoids by LC QqQ in soybean leaves from the WT and C9 genotypes, infected (I) or noninfected (NI) by *P. syringae* pv. tomato 36 h after inoculation. This shows the differences in the abundance of the flavonoids analyzed by LC-MS in response to bacterial infection. Differences in the abundances of the detected flavonoids are indicate in response to treatments. Green color represents a decrease, and red color an increase.

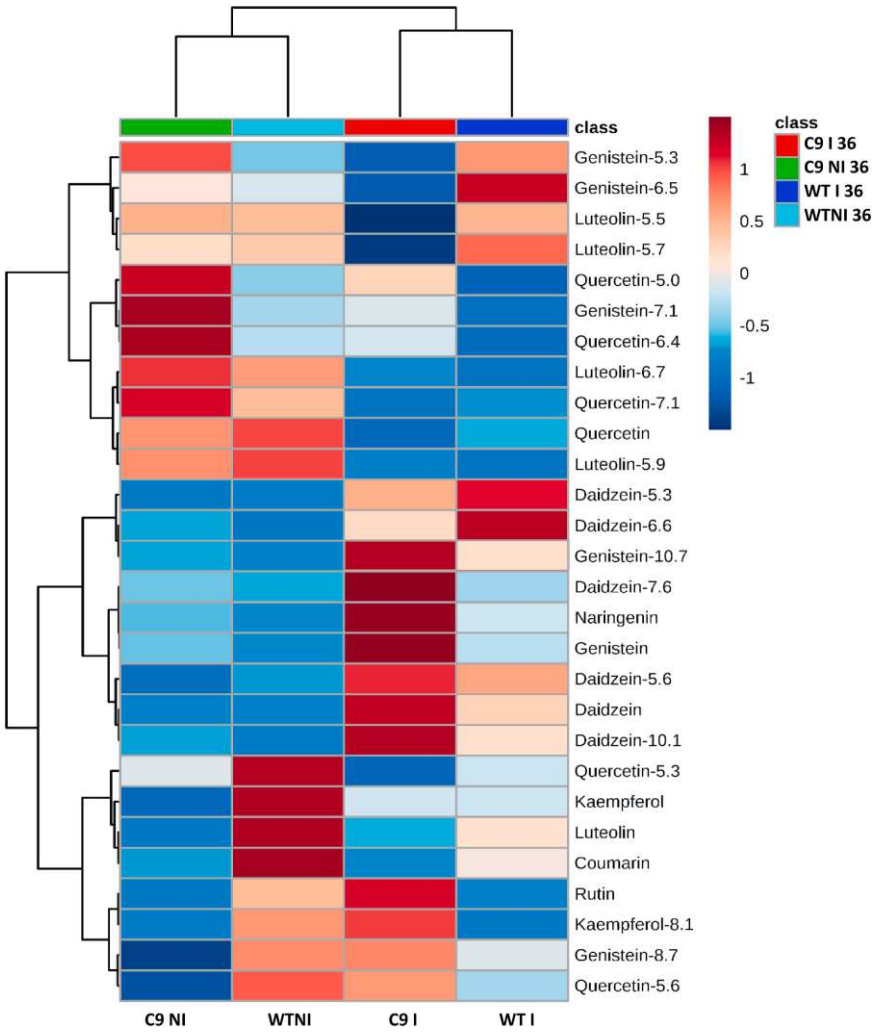

Source: Survey's data.

For the Morin-Hesperetin-Quercetin class (m/z = 303 for aglycone), the patterns of quercetin glicoconjugates were observed at RTs of 5.0, 5.3, 5.6 and 6.4 min. For RTs 7.1 and 8.4 min, the fragmentation patterns differed slightly from those observed for quercetin (**Appendix A and C**). When the precursor ion scan was applied to Luteolin-Kaempferol class (m/z 287 for aglycone), four RTs (5.5, 5.7, 5.9 and 6.7 min) displayed RFI% similar to luteolin, and one RT = (8.4) displayed RFI% similar to kaempferol. However, the identification of kaempferol could not be ascertained, since the proportions of the fragmentation patterns were different from those observed in the aglycone (**Appendix A and D**).

Figure 7 – Schematic overview of flavonoid biosynthesis pathway reconstructed using the characterized compounds from soybean leaves. Each colored square boX is indicative of the abundance levels of the metabolites involved in the flavonoid biosynthesis and identified for each WT and C9 genotypes, infected (I) or noninfected (NI) by *P. syringae* pv. tomato. The main flavonoids of pathway are sketched by continuous line while compounds not detected, but intermediate of the pathway, are sketched by dashed line. Compounds marked by blue asterisk were more abundant in the inoculated C9 genotype while compounds marked by red asterisk were more abundant in the inoculated WT

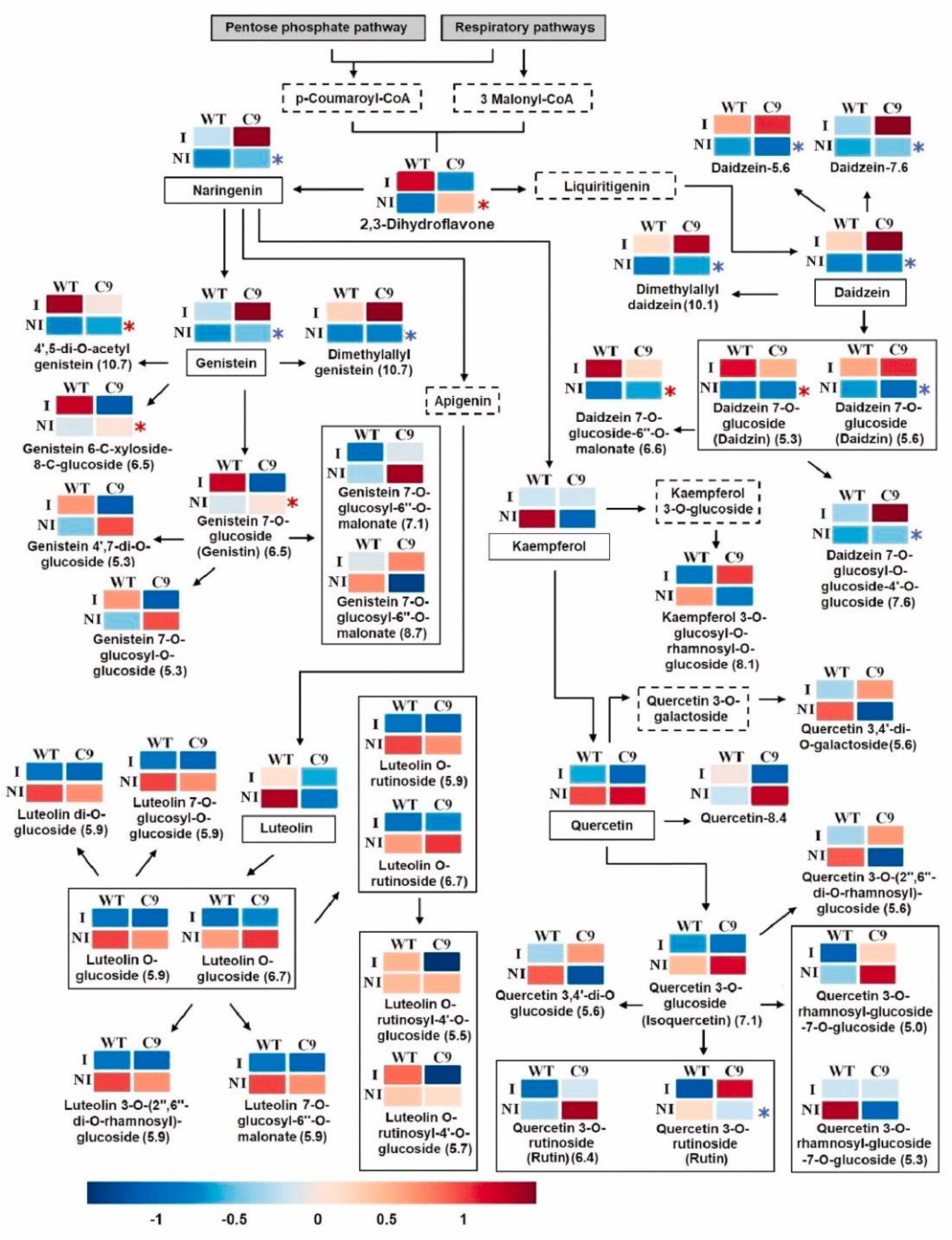

Source: Survey's data.

In some cases, the same RT generated different XICs. For example, for Luteolin-Kaempferol class, m/z 741.1, 611.3, 595.2 and 449.1 ions were detected at RT = 5.9 min and may represent similar compounds that elute at near retention times. In other cases, more than one glycoconjugate was observed for the same XIC. For example, for Genistein-Apigenin class, at RT = 5.3 min and m/z 595.3, two compounds were found, genistein 7,4′-di-O-glucoside and genistein 7-O-glucosyl-O-glucoside. The same XIC was also recorded at different retention times, which may be explained by the co-elution of different molecules (isomers) in the analytical column. Finally, no data were found for some m/z values in the literature or in the spectrum database, and it was not possible to infer the compound (**Appendix A**).

2.6 GLOBAL ANALYSIS OF THE DYSREGULATED FLAVONOIDS

These differences between genotypes and treatments could be better visualized when the relative abundances, of each identified compound, were used to reconstruct the flavonoid biosynthetic pathways. From the data of **Appendix A** and Heatmap plot of the characterized flavonoids (**Figure 6**), the relative abundance (defined by the colors of the heat map) of flavonoids and precursors was integrated into a metabolic map of flavonoid and conjugates biosynthesis (**Figure 7**). Therefore, it was possible to analyze the correlation of the levels of abundance of flavonoids and infer its increase or decrease by differences in the plant metabolism in response to genotypes and treatments. Five main biosynthetic routes were identified in the flavonoid biosynthetic pathway mainly for glycoconjugates of daidzein, genistein, luteolin, kaempferol and quercetin. When analyzing individually the values of relative abundance of RTs, in terms of XICs, of some flavonoid compounds characterized (**Appendix B, C, D and E**), the HeatMap analysis (**Figure 6**) and metabolic pathway map of flavonoid biosynthesis (**Figure 7**), some compounds were grouped into similar patterns. Four main compounds formed the first cluster: genistein-6.5, genistein-10.7, daidzein-5.3 and daidzein-6.6, which showed higher concentrations for both inoculated genotypes, but higher in WT inoculated plants (**Figure 8**). On the other hand, seven compounds, naringenin, genistein, daidzein, daidzein-5.6, daidzein-7.6 and daizein-10.1, and rutin, forming the second cluster that exhibit high levels of relative abundance in both inoculated genotypes, but greater in C9 inoculated plants.

Figure 8 – Relative abundance of the flavonoid derivatives from BiP-overexpressing (C9) and wild-type (WT) soybean plants infected (I) or noninfected (NI) with *P. syringae* pv. tomato. Bars (mean ± SE; n = 4) with the same capital letters indicate no significant difference between control and inoculated treatments and those followed by the same lowercase letters indicate no significant difference among genotypes within the same treatment (Student's test: $P < 0.05$).

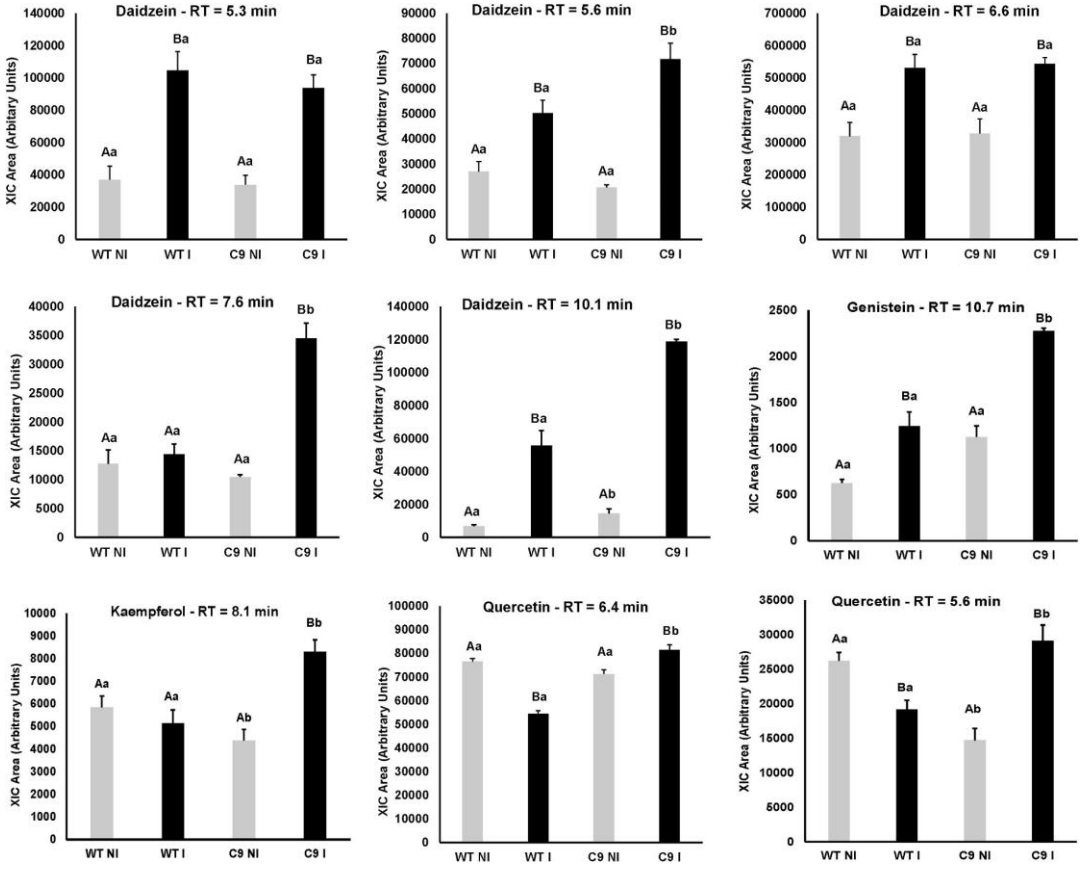

Source: Survey's data.

In addition, we identified some glycoconjugates (**Figure 7**), which have been confirmed in soybean leaves (Yazaki et al. 2011; Cheng et al. 2011; Bajaj et al. 2018), but have not been described in the soybean KEGG database (http://www.genome.ad.jp/kegg), which was used as reference to construct biosynthetic routes. These compounds were inserted in the biosynthesis pathway, including the prenylated isoflavonoids (identified in daidzein-10.1 and genistein-10.7), present in high abundance in the infected treatments, and rutinosides of luteolin (identified in luteolin-5.5, 5.7, 5.9 and 6.7) (**Appendix B, C, D and E; Figure 6 and 7**).

2.7 GENE EXPRESSION ANALYSIS BY QRT-PCR CONFIRM CASCADES ACTIVATING HR IN TRANSGENIC PLANTS

The transgenic soybean plants analyzed in this study have been previously demonstrated to overexpress a functional BiP and to accumulate different levels of BiP in the microsomal fractions (Valente et al. 2009). The transcriptome in soybean leaves grown under normal conditions indicated a predominance of upregulated defense and immune system-related genes in BiP-overexpressing plants (Carvalho et al. 2014a). These include genes involved in HR elicited in nonhost or incompatible interactions upon pathogen infection. Thus, we evaluated the expression profile of BiP-induced defense-related genes in soybean leaves showing a nonhost-HR process induced by *P. syringae* pv. tomato. Pathogenesis-related proteins (PR proteins) play crucial roles in the plant defense system. *PR-3* encodes a basic chitinase involved in ethylene/jasmonic acid mediated signaling pathway and has been used as a marker gene for jasmonic acid (JA)-dependent SAR. The *GmPR-3* gene encoding for a chitinase was induced by BiP overexpression under

Figure 9 – Expression analysis of target genes performed by qRT-PCR involved in plant bacterial interactions from BiP-overexpressing (C9) and wild-type (WT) soybean plants infected (I) or noninfected (NI) with *P. syringae* pv. tomato. The expression levels were obtained using the $2^{-\Delta CT}$ method. Bars (mean ± SE; n = 4) with the same capital letters indicate no significant difference between control and inoculated treatments and those followed by the same lowercase letters indicate no significant difference among genotypes within the same treatment (Student's test: $P < 0.05$).

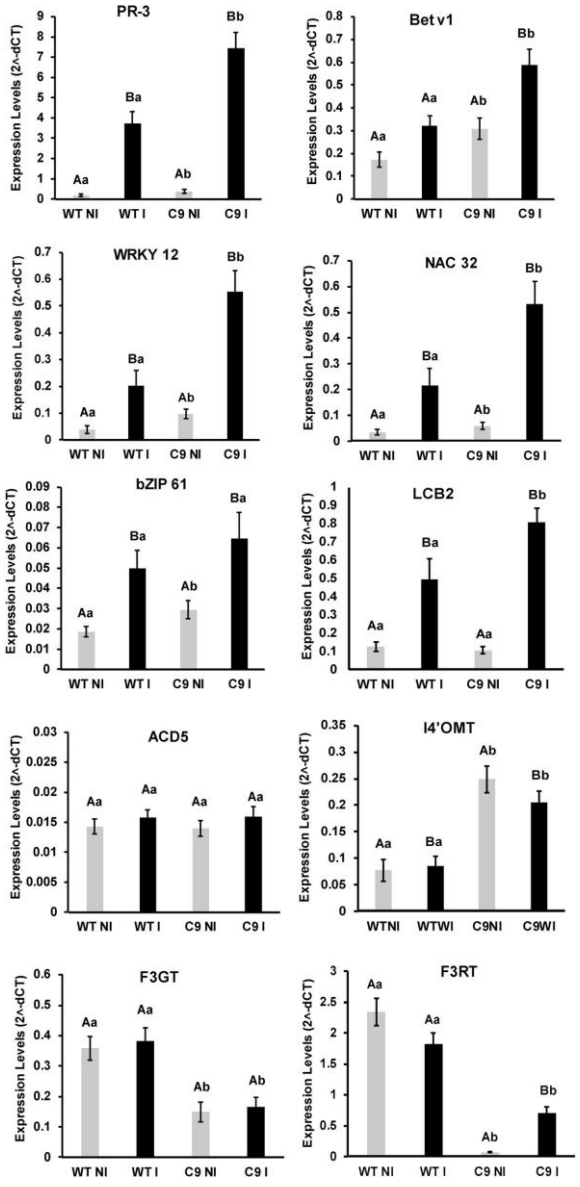

Source: Survey's data.

normal conditions and further induced under nonhost-HR process in WT, as expected. However, this induction was observed in a higher extent in C9 leaves (**Figure 9**). The major allergen of birch tree pollen is Bet v 1 protein, which shows significant sequence homology to a group of pathogenesis-related plant proteins. This gene has also been classified as a PR-10 like protein. PR-10 proteins have ribonuclease activity and are differentially expressed in the presence of different signaling molecules and biotic stress. *GmBetv1* was also upregulated by BiP overexpression under normal conditions. Furthermore, The HR-mediated induction of *GmBetv1* expression was higher in C9 leaves than in WT leaves (**Figure 9**).

Some transcriptional factors (TF) showing differential expression in soybean genotypes under normal conditions (Carvalho et al. 2014a) were also evaluated for expression in response to bacterial infection. WRKY TFs are a large family of regulatory proteins involved in various plant processes but most notably in response to biotic and abiotic stresses (Pandey and Somssich, 2009). Kim et al. (2014) observed that WRKY12 gene confers enhanced resistance to *Pseudomonas* through transcriptional activation of defense-related genes. The expression patterns of the soybean *GmWRKY12* gene were similar to PR genes described above, being also more responsive in the C9 transgenic plants (**Figure 9**) when compared to WT.

The NAC genes also encode transcription factors involved with the control of plant stress responses, such as cell death signaling, as verified for GmNAC81, which was effectively induced by *Pseudomonas* spp. infiltration (Carvalho et al. 2014a). Interestingly, the expression responses of the GmNAC32 TF were similar to that observed for WRKY12 TF, which again were more induced in the C9 transgenic plants (**Figure 9**). Other TF showing differential expression between C9 and WT genotypes in the absence of bacterial infection (Carvalho et al. 2014a,b) belonging to the bZIP family was *GmbZIP61*. Despite presenting a response to bacterial expression, the levels were similar between genotypes (**Figure 9**). Several studies revealed that ceramides and sphingoids long-chain base (LCBs) are also potent inducers of PCD in plants (Sánchez-Rangel et al. 2015). Our metabolic profiles by GC/MS (**Figure 3**) revealed different abundances of the metabolite dihydrosphingosine (d18:0), which is an intermediary of the ceramide biosynthetic pathway. Thus, we also evaluated the expression levels of the LCB2 and accelerated cell death 5 (ACD5) genes. Serine palmitoyl transferase (SPT), a heterodimer formed by LCB1 and LCB2 subunits, catalyzes the first reaction in sphingolipid biosynthesis to form LCBs. Interestingly, the expression patterns of LCB2 were similar to WRKY12 and NAC32 TFs, which was strongly

induced in BiP-overexpressing transgenic plants (**Figure 9**). *ACD5* encodes a 608-amino acid protein with ceramide kinase activity, which did not show change in its expression levels in response to bacterial infection (**Figure 9**) for both genotypes.

The O-methyltransferases, which participate in the biosynthesis of flavonoids and lignin, have been implicated in disease resistance in plants (Lam et al. 2007) and two isoforms were upregulated in the transgenic BiP-overepression plants (Carvalho et al. 2014a). The isoflavone-4′-O-methyltransferase (I4′ OMT), catalyzing specifically the 4′-O-methylation of isoflavones is considered to be the last enzymatic step in 4-methoxyisoflavone biosynthesis, displayed higher expression levels in transgenic plant than wild-type under bacterial infection (**Figure 9**). Flavonoids are synthesized by a very complex metabolic pathway and the diversity of these molecules can be further increased under the action of UDP-glycosyltransferases and UDP-rhamnosyltransferase. Futhermore, these are composed by a very complex multigene family (Roy et al. 2016) showing regiospecificity. The expression of the gene encoding for a Flavonol 3-O-glucosyltransferase 1 (F3GT) showed higher expression levels in the WT plant, being not ponsive to bacterial infection (**Figure 9**). On the other hand, the gene encoding a Flavonol-3-O-glucoside L-rhamnosyltransferase (F3RT) was induced in BiP-overexpressing plants in response to bacterial elicitation. Flavonol 3-O-rhamnosyltransferase can catalyze the transfer of rhamnose from UDP-rhamnose to the 3-OH position of kaempferol and quercetin (Roy et al. 2016). In fact, the flavonoids profiles (**Figure 8**) showed the compounds Quercetin 3-O-rutinoside (Rutin), Quercetin 3-O-rhamnosyl)-glucoside and Kaempferol 3-O-glucoside-O-rhamnosyl-O-glucoside in higher abundances in the transgenic plants.

3 DISCUSSION

Soybean plants showing BiP-mediated drought tolerance have been related to a delayed drought-induced leaf senescence by a NRP-mediated cell death signaling and attenuated ER and osmotic stress-induced cell death (PCD) phenotypes (Reis et al. 2011; Carvalho et al. 2014a, b). BiP-overexpressing plants also displayed leaf senescence under normal conditions and accelerated hypersensitive response (HR) triggered by *P. syringae* pv. tomato in soybean (Carvalho et al. 2014a). During the hypersensitive PCD, BiP positively regulates the NRP cell death signaling through a yet undefined mechanism that is activated by SA signaling and related to ER functioning. Therefore, it was of interest to evaluate the physiological responses

of these transgenic plants by comparing the metabolic profiles of the leaves under the infection of an incompatible bacterial pathogen.

As expected, the inoculation of *P. syringae* pv. tomato caused a phenotypic response of hypersensitive cell death, visible at 36 hai. The formation of brown necrosis halos in larger numbers in BiP-overexpressing plants indicated enhanced or accelerated PCD induced by HR as described by Carvalho et al. (2014a). Even during the early stages of infection (8 and 36 hai), the halos were more evident than in the susceptible infected WT genotype. These results are in accordance with previous studies showing the induction of PDC in tobacco and Arabidopsis leaves, indicating that during the hypersensitive PCD, BiP positively regulates the NRP cell death signaling (Alvim et al. 2001; Valente et al. 2009; Reis et al. 2011, 2016).

As the plant undergoes stress conditions, it responds by inducing the mobilization of nutrients, such as amino acids, sugars, lipids and derivatives, in order to guarantee energy supply and protection under stress conditions. Several compounds that showed increase in inoculated soybean plants are amino acids, sugars and short chain organic acids belonging to respiratory pathway's tricarboXylic acid cycle (TCA). The increase in the relative concentration of some sugars and derivatives (sugar alcohols and acid sugars) in leaf tissue may be related to the need to protect damaged cells, in the formation of structural barriers or as antioXidants (Rojas 2014). Studies relate the accumulation of isoleucine, leucine and valine with the control of damage caused by biotic or osmotic stress in plants, by the biosynthesis of specific specialized metabolites (glycosinolates), synthesis of leucine rich proteins that participate in senescence and PCD, cellular respiration or participation in the restructuring of the osmotic equilibrium (Mikkelsen and Halkier 2003; Choi et al. 2011; Kochevenko et al. 2012; Rojas 2014; Pires et al. 2016; Huang et al. 2017). The increase in the relative concentration of BCAA amino acids (branched-chain amino acids) were also observed by Coutinho et al. (2019) for BiP-overexpressing drought tolerant plants, therefore indicating an adaptive response also to biotic stress such as pathogen attack (Rojas et al. 2014). The metabolic profiles also indicated that these metabolic reprogramming was also observed for wild-type (WT) soybean under bacterial infection. GABA is a non-protein amino acid that accumulates rapidly in plant tissues in response to biotic and abiotic stress and it can be involved in regulatory process of the plant defense and be critical to contain HR spread (Tarkowisk et al. 2020). BiP-overexpression accelerated hypersensitive response triggered by *P. syringae* pv. tomato in soybean (Carvalho et al. 2014a), however our metabolomic profiles showed reduced levels of GABA in the presence and absence of bacterial infection. Thus,

GABA may not be an important metabolite, acting as a signaling molecule in the plant bacterial interactions, for regulation of the HR and PCD response in transgenic plants.

A successful innate immune response often includes the so-called hypersensitive response (HR), a form of rapid programmed cell death (PCD) occurring in a limited area at the site of infection. This suicide of the infected cells is to limit the spread of biotrophic pathogens. Recent studies have shown that in plants, sphingolipids such as dihydrosphingosine (DHS) trigger PCD events by the formation of reactive oxygen species (ROS). In fact, the application of DHS in tobacco resulted in the increase of cytosolic Ca^{2+}, related to the production of ROS and activation of plant defense, and nuclear Ca^{2+}, which triggers the PCD pathway. Thus, ROS and Ca^{2+} would play an important role in the control of sphingolipid-induced PCD (Lachaud et al. 2010; Pata et al. 2010). Moreover, the DHS levels were higher in wild-type soybean genotype under bacterial infection, as expected. However, for C9 transgenic soybean plants the levels were not altered in response to infection and these were lower than in wild-type. In addition to DHS, other ceramides and long-chain bases (LCBs) are also potent inducers of PCD in plants. On the other hand, Peer et al. (2010) suggested that t18:0 (phytosphingosine) rather than d18:0 (dihydrosphigosine) is a positive regulator of HR. Thus, other LCBs not detected by the GC/MS metabolite profiles can be acting in the signaling pathway of the hypersensitive response (HR) of the transgenic plant. In fact, the LCBs biosynthetic pathway was more induced in BiP-overexpressing transgenic plants as revealed by qRT-PCR analysis of the expression levels for the gene LCB2, a subunit of the SPT complex. The activity of enzymes of elongation and desaturation of fatty acids and serine-palmitoyl transferases (SPT), important in the synthesis of ceramides and sphingolipids, participate in the induction of defense responses, such as the synthesis of PR-proteins and ROS (Yaeno et al. 2004). Salicylic acid (SA) is a phytohormone involved in local and systemic resistance, as well as in the response to abiotic stress. Interestingly, SA production is controlled by multiple positive and negative regulators including several sphingolipid intermediates which induce SA accumulation and affect the disease resistance. In fact, the levels of SA were increased after non-compatible bacterial infection and the transgenic plants presented higher abundance than wild-type, as also verified by Carvalho et al. (2014a), that verified also higher levels of expression for genes responsive to SA. Thus, higher activation of LCBs pathway may contribute for activation of the biosynthesis of SA in the transgenic soybean plants despite not being detected in our GC/MS profiles.

Carvalho et al. (2014a) verified that during the hypersensitive PCD, BiP positively regulates the NRP cell death activated by SA signaling. Likewise, in the present study we also observed pronounced induction of defense and immune system related genes in BiP-overexpressing plants, which were characterized by the rapid death of plant cells at the site of pathogen infection. One possible mode of action of SA during pathogen attack is to promote defense reactions leading to a faster response of the plant after pathogen attack (Zimmerli et al. 2000). In addition, LCBs, ceramides, reactive oXygen species (ROS) are also positive regulators of SA biosynthesis (Sanches-Rangel et al. 2015), being H_2O_2 from oXidative bursts known to drive PCD at challenged sites. In fact, a significantly enhanced oXidative burst was induced in WT inoculated leaves; however, a higher amount of H_2O_2 accumulated in the BiP-overexpressing inoculated plants (Carvalho et al. 2014a). Some studies demonstrated that jasmonic acid (JA), another phytohormone known to be mutually antagonistic to SA in many cases, is also accumulated in and required for defense response (Kenton et al. 1999; Magnin-Robert et al. 2015). Betsuyaku et al. (2018), using intravital time-lapse imaging, observed that the JA signaling pathway is activated in the cells surrounding the central SA-active cells around the infection sites in *A. thaliana*. JA levels were higher only in the transgenic plant leaves under bacterial infection. Interestingly, Magnin-Robert et al. (2015) highlighted that disturbance of sphingolipid metabolism could impact not only the cell death program but also the JA signaling pathway. In fact, gmNAC32, which showed higher expressions in BiP-overexpressing plants activates SA signaling by repressing NIMIN1, a key negative regulator of SA-dependent defense (Allu et al. 2016). However, in contrast with our results for soybean transgenic plants, it was also observed that ANAC032 TF decreased JA signaling (Allu et al. 2016).

Phenolic compounds, which derive from phenylalanine, are among the most widespread groups of plant specialized metabolites, and display a wide range of biological properties. The synthesis and accumulation of many plant phenolics are induced by biotic and abiotic stresses. Many pathogen-induced phenolic compounds, including various coumarins and flavonoids, are considered phytoalexins given their accumulation in plant tissues upon infection and their antimicrobial activity *in vitro* (Mierziak et al. 2014). In the present study, we observed a remarkable difference in the flavonoid profiles in transgenic plants overexpressing BiP related to WT. Abundance differences were detected for aglycone as well as for glycoconjugates and these were responsive to noncompatible bacterial infections triggering hypersensitive response (HR). The levels of the aglycones naringenin, apigenin, daidzein and genistein were

higher in transgenic plants. In fact, flavonoids are very important in plant resistance against pathogenic bacteria and fungi and can be non-specific and result, in part, from their antioXidative properties. Flavonoid compounds are transported to the site of infection and induce the hypersensitivity reaction, which is the earliest defense mechanism employed by the infected plants, and programmed cell death (Mierziak et al. 2014). Flavonoid biosynthesis is very complex and the plant genomes present several isoforms, which hinder the selection of genes for expression analysis. However, a gene encoding for an isoflavone methyl transferase (I4'OMT) showed higher expression in transgenic plants. Interestingly, a methylated form of aglycone daizein (dimethylalllyldaidzein) and genistein (dimethylalllylgenistein), showed higher abundance in transgenic plants under infection. Flavonoids undergo further modifications, for example methylation by methyltransferases and glycosylation by specific glycosyltransferases. These modifications often alter their solubility, reactivity and stability. The majority of flavonoids are present in the form of glycosides under natural conditions (Mierziak et al. 2014). The flavonoid profiles revealed that some glyconjugates were more abundant in BiP-overexpressing transgenic plants, such as Daidzein 7-O-glucosyl-O-glucoside-4'-O-glucoside (daidzein-7.6) and rutin (quercetin 3-O-rutinoside) and Quercetin 3-O-rutinoside-7-O-glucoside (quercetin-5.0). It has also been reported that ANAC032 regulates flavonoid synthesis (Allu et al. 2016) despite some genes associated to this biosynthetic pathway were significantly downregulated (Maki et al. 2019). In accordance with these results, we also observed that this transcriptional factor was more induced in transgenic C9 plants when compared to the WT. Interestingly, Sayed et al. (2017) observed that SA is the best elicitor of flavonoid accumulation in *Rumex vesicarius* callus cultured on fructose and could be linked with the best management of H_2O_2 as signaling molecule in mediating SA-induced flavonoids. Furthermore, increase of phenolic and flavonoid compound levels in leaves of saffron (Tajik et al. 2019) and of myricetin and rutin were activated by applying exogenous SA in the leaves under hydroponic conditions (Gondor et al. 2016).

4 CONCLUDING REMARKS

Molecular characterization of the regulatory pathways controlling plant tolerance to biotic and abiotic stresses is important for breeding programs for the development of plant genotypes showing sustainable production under multiple environmental constrains. BiP-overexpressing soybean plants have shown increase in the drought stress tolerance by

affecting the PCD process, which also promotes a hypersensitive response of the leaves inoculated with *P. syringae* pv. tomato. Thus, these responses of the transgenic plants indicate that a crosstalk between pathways controlling biotic and abiotic stresses could be used as target for genetic manipulation aiming at a broad range tolerance.

The metabolic profiles of transgenic plants C9 related to WT genotype were distinct showing that some typical signal molecules cannot be involved directly as signals in the accelerated HR, such as PABA, GABA and dyhidrosphingosine. However, the SA biosynthetic pathway was more stimulated in the leaves of the transgenic plants as indicated by LC/MS profiles. Both pathogenesis-related genes (PRs), involved in resistance to bacterial attack, and transcriptional factor controlling the SA pathway were more induced in the BiP-overexpressing soybean plants. Furthermore, the LCBs and ceramide biosynthetic pathways showed alterations in gene expression and metabolite abundances when comparing these genotypes. As, HR can be an effective strategy of plants to protect against (hemi)biotrophic microorganisms and PCD processes promote the spread of necrotrophic pathogens, the regulation of sphingolipid pathway via JA/SA phytohormone cascades could be important in the transgenic C9 plants to promote pathogen tolerance. In fact, the BiP-overexpressing plants showed increase in the levels of some flavonoids, mainly isoflavones, which have shown antimicrobial activity against plant pathogens.

An additional evidence linking BiP-overexpressing and plant-bacterial interactions were the alterations observed in the flavonoid biosynthetic pathways. Soybean (*Glycine max*) accumulates several prenylated isoflavonoid phytoalexins, collectively referred to as glyceollins. The bioactive isoflavonoids of the Leguminosae often are methylated on the 4′-position of their B-rings and isoflavone *O*-methyltransferase (IOMT) from alfalfa is involved in the biosynthesis of 4′-*O*-methylated isoflavonoids such as the phytoalexin medicarpin. In fact, as in alfalfa many other legumes, including clover, pea, and chickpea, methylation of the 4′-hydroxyl is a prerequisite for further substitutions of the isoflavonoid nucleus that can lead to the pterocarpan phytoalexins such as medicarpin. We observed for transgenic soybean plants an induction of transcription of the gmI′4OMT gene and a higher abundance of methylated daidzein and genistein. Furthermore, overexpression of IOMT results in increased induction of phenylpropanoid/isoflavonoid pathway gene transcripts after infection and these plants display resistance to *Phoma medicaginis*.

Overall, the gene expression and metabolic reprograming in the BiP-overexpressing transgenic plants indicate that the genetic manipulation of soybean could be directed by

breeding programs to attain tolerance to multiple stresses. Thus, plant growth and productivity under environmental constraints, such as drought and pathogen attack, could be improved.

5 EXPERIMENTAL

5.1 GREENHOUSE EXPERIMENT

The plant-bacteria interaction experiments were carried out in a greenhouse at Universidade Federal de Viçosa (UFV), Viçosa, Minas Gerais. The transgenic lines 35S:BiP-2 and 35S:BiP-4 were previously obtained by transforming soybean (Fabaceae) plants (*Glycine max* cv. Conquista) with a soyBiPD gene (GeneBank accession AF031241) under the control of a cauliflower mosaic virus 35S promoter (Cascardo et al. 2001; Valente et al. 2009). As the transgenic lines showed similar physiological and genetic behaviors, the experiments were conducted using the 35S:BiP-4 (C9 plants). Trangenic plants overexpressing BiP have been characterized as drought tolerant compared to the wild-type cultivar Conquista (Coutinho et al. 2019) by mechanisms involving osmoprotection and has also been shown to accelerate the hypersensitive response (HR) induced by an incompatible plant-bacterium interaction (Carvalho et al. 2014a)

Transformed soybean plants, designated C9, and untransformed ones, designated WT, were germinated and maintained in 1 L pots containing previously autoclaved mixture of soil, sand, and dung (3:1:1).

5.2 INOCULATION ASSAYS

P. syringae pv. tomato was provided by the Phytopathogen Populations Laboratory of Universidade Federal de Viçosa/UFV. The inoculum was prepared in three 500 mL Erlenmeyer flasks containing liquid medium King B growing at 28 °C until A_{600nm} = 0.700. Then, the cells were washed and the pellet was homogeneously dissolved in 2 L of 10 mM $MgCl_2$ previously sterilized. This suspension was used for the inoculation experiment. The infiltration of *P. syringae* pv. tomato in soybean was carried out according to Zou et al. (2005) with some modifications. Leaves were inoculated when the third trifoliate leaves were completely expanded. Inoculations were performed at 30 days after sowing, by inverting the

vessel containing the soybean plants into a Becker filled with inoculum (I, infected plants). The entire system was closed within a vacuum chamber, and mock-inoculated leaves were vacuum-infiltrated with 10 mM $MgCl_2$ and used as controls (NI, noninfected plants). A drawn vacuum (500 mmHg) was applied for about 90 s and then was released quickly, compelling the inoculum in through the open stomata and taking up full apoplastic space. Immediately after infiltration, the plants were maintained under greenhouse conditions.

The leaf symptoms of bacterial infection and hypersensitive response (HR) were monitored by daily inspections when the symptoms turning more evident by the presence of cell death. Then, the leaves were collected after 8 and 36 hai (hour after inoculation) and immediately frozen in liquid nitrogen and stored at - 80 °C. Thus, the gene expression and physiological evaluations were performed at first stages of the plant-bacteria interactions. In order to compare the response. The same plants were also photographed at 15 and 30 dai (days after inoculation) when the differences of response between transgenic plants and wild-type (necrotic halos) were more visible. For each treatment we used 4 pots each containing 3 plants, thus 4 independent biological replicates.

5.3 METABOLITE EXTRACTION, CHEMICAL DERIVATIZATION AND METABOLITE ANALYSIS BY GC/MS

The leaf samples were ground in liquid nitrogen and 50 mg of powder was used for metabolite extractions added to 700 µL of methanol containing 60 µL of ribitol (0.2 mg/mL stock in water) as an internal quantitative standard. Samples were homogenized and derivatized as described by Coutinho et al. (2019) and Lima et al. (2019). FAMEs (fatty acids methyl esters) were used as internal standard for correction of the retention times (Lisec et al. 2006).

The samples were analyzed using a GC/MS system TruTOF GC-TOF (Agilent Chromatograph, 7890a) and TruTOF® HT TOFMS Spectrometer (LECO), equipped with a 30 m capillary column (MDN-35). A temperature gradient was used and the mass spectrum obtained by the full-scan method ranging from 33 to 600 m/z. A series of n-alkanes were used along with samples to calculate the retention indexes (Lima et al. 2019; Coutinho et al. 2019). Raw GC/MS data were processed and converted to the CDF format (NetCDF) using the ChromaTof package (LECO) and automatically analyzed by TargetSearch algorithms (bioconductor.org). We used a script for identification and quantification of metabolites

designed to run on R (Cuadros-Inostroza et al. 2009), the processing parameters and the alignment were optimized for our GC/TOF platform. The parameters used were: massRange of 85–500 Da, In Threshold 50, TopMasses 10, r thresh of 0.05. The compounds present in the samples were identified using a spectral mass library of trimethylsilyl compounds derived from the Max Planck Institute for Plant Molecular Physiology (http://csbdb. mpimp-golm. mpg. de/csbdb). The intensities of the identified metabolites were normalized by the area of the peak corresponding to the ribitol through *MetaboAnalyst* and adjusted by the foliar mass of each sample. A quality factor over 600 was used for generate a filtered identification table containing the identified compounds and their intensities for each treatment (Lima et al. 2019; Coutinho et al. 2019). This table was used as input for statistical processing and statistical analysis by MetaboAnalyst platform (http://www.metaboanalyst.ca/).

5.4 PHYTOHORMONES ANALYSIS

The phytohormone extractions were performed from soybean leaves according to the procedure described by Muller and Munné-Bosch (2011) with some modifications (Lima et al. 2019; Coutinho et al. 2019; Vital et al. 2019a). Leaves extracts were prepared by powdering approximately 110 mg fresh weight in liquid nitrogen and 400 µl of extraction solution [methanol, isopropanol and acetic acid 20:79:1 (v/v/v)]. Then, the samples were shaken in a vortex four times for 20 s (on ice), subjected to ultrasound treatment for 5 min, placed on ice for 30 min and then centrifuged at 14000 × *g* for 30 min at 4 °C. The supernatant was removed and transferred to a new tube. A new extraction cycle was carried out with the resulting pellet from the previous extraction to increase the extraction efficiency, and then the supernatants were pooled. Finally, the total supernatant was filtered through 0.45 mm filters. About 400 µL of the extracts were placed in vials, and 5.0 µL were injected into the LC/MS system (Agilent Eclipse Plus, RRHD, 1.8 µm, 2.1 × 50 mm) from NuBioMol (Center for Biomolecules Analysis-UFV, Brazil), with the continuous flow (Φ = 0.3 mL/min), coupled online to a mass spectrometer QqQ triple quadrupole (Agilent). Phytohormones were separated by ultra-high performance chromatography (UHPLC, Agilent) using chromatography column C18 (50 mm × 1.0 mm ID, 1.7 µm particle and 300 *A*) coupled to the mass spectrometer (QqQ Agilent) at negative/positive modes, alternating according to the retention time for each hormone. The samples were scanned by MRM (multiple reaction monitoring) for detecting the phy tohormones. The tests were carried out

with four biological replicates for each treatment. The mass spectrometry was processed using the Skyline software (MacCoss Lab Software) according to the methods described by Coutinho et al. (2019) and Vital et al. (2019b). A standard curve of each hormone, in a concentration ranging from 0.1 to 800 ng/mL, was used to convert the area values from XIC in ng/g of plant tissue. Area values were converted using the Excel program into ng/g (plant hormone/fresh plant tissue).

5.5 TARGET AND NON-TARGET LC/MS-BASED METHODS FOR THE FLAVONOID PROFILING

The flavonoids were extracted from soybean leaves using the same procedure described for phytohormone extraction (Gómez et al. 2018). In the target LC/MS-based method, eighteen flavonoids (hesperidin, rutin, naringin, isoorientin, isovitexin, myricetin, morin, hesperetin, quercitin, kaempferol, luteolin, phloretin, epicatechin, catechin, narigenin, genistein, apigenin, and daidzein) were analyzed. In contrast, for the non-target LC/MS-based method, eight classes of flavonoids (Daidzein, Genistein-Apigenin, Luteolin-Kaempferol, Morin-Hesperen tin-Quercetin, Myricetin, Epicatechin-Catechin, Phloretin, and Naringenin) were analyzed. The non-target LC/MS-based method for analysis of flavonoid profiles was performed according to the procedure described by Gómez et al. (2018) and Vital et al. (2019b). The abundance of each characterized flavonoid from each genotype and treatment with *P. syringae* pv. tomato was combined in a table and analyzed in the MetaboAnalyst platform (http://www.metaboanalyst.ca). In the MetaboAnalyst platform, quality filters based on the standard deviation method were used to remove low-quality data, and then the intensity values were normalized by sum for flavonoids by LC/MS and were not normalized for metabolites by GC/MS (all data were previously normalized by weight).

Data were analyzed using the Partial Least Squares Discriminant Analysis (PLS-DA) to generate 2D Score Plots displaying genotypes and treatment effects on data grouping. The cluster analysis by the Heatmap method was also performed for each flavonoid group by their relative abundances in genotypes and treatments, using the following parameters: Distance Measure: Euclidean; Clustering Algorithm: Ward; Data Source: Normalized Data; Standardized Data: Autoscale features; T-test/ANOVA; Options: Show only group average; and View Mode: Overview. For quantitative analysis of characterized compounds, the one-

way analysis of variance (ANOVA) was used with the following parameters: Adjusted p-value (FDR) cutoff: 0.05; Post-hoc analysis: Fisher's LSD.

Lastly, the identified compounds were organized according to the metabolic pathways for flavonoid biosynthesis using as reference the relative intensity data from Heatmap and the *Glycine max* maps from the KEGG (Kyoto Encyclopedia of Genes and Genomes) repository (Kanehisa, 2000).

5.6 RNA EXTRACTION, cDNA SYNTHESIS AND EXPRESSION ANALYSIS BY QRT-PCR

The leaves were pulverized with liquid nitrogen and macerated. Total RNA was extracted from leaf tissues using Trizol reagent (Invitrogen) according to the manufacturer's instructions. RNA quality was examined in agarose gel that was stained with 0.1 µg/mL ethidium bromide (EtBr) and quantified using a Thermo Scientific NanoDrop 2000c. A total of 4 µg of RNA was used for cDNA synthesis with the SuperScript III kit (Invitrogen) following the manufacturer's instructions. Gene expression was evaluated using an ABI 7500 fast thermal cycler (Applied Biosystems, Foster City, CA, USA) and Fast Master SYBR Green Master Mix (Thermo Fisher Scientific). The amplification reactions were performed with the cycling conditions: 15 s at 95 °C, 40 cycles at 95 °C for 3s and 30 s at 60 °C and final denaturation at 95 °C for 20s, followed by a melting curve. RT-qPCR-specific primers were designed using the Primer-BLAST software (https://www.ncbi.nlm.nih.gov/tools/primer-blast/), with a melt temperature (T) of 59–61 °C, a length of 18–23 bp, an amplifier product size of 120–150 bp, and a 40–60% GC content. Three technical replicates were performed for each one of the three biological replicates. Gene expression was quantified using the ΔCT method and the absolute expression levels were calculated as $2^{-\Delta CT}$ (Pfaffl, 2001).

Target genes were chosen as responsive to bacterial infection and phytohormonal pathways such as PR-3 and Bet V1 (PR-10 like). Others shown to be dysregulated in the transgenic plants (Carvalho et al. 2014b) as WRKY12 and NAC 32, which have also been involved in plant resistance to bacterial infection. The LCB2 gene was monitored because it encoded to a key-enzyme in the sphingolipid biosynthesis pathway, while the genes I4′ OMT, F3GT and F3RT have been observed as important to flavonoid biosynthetic pathways.

5.7 EXPERIMENTAL DESIGN AND STATISTICAL ANALYSIS

The experimental design was completely randomized using three plants per pot. For each treatment we used 4 pots and the samples consisted of a pool containing one trifoliate leaf of each plant (3 leaves per replicate). Thus, the biochemical analyses were performed using the 4 independent pools, as 4 biological replicates. Pair-wise analyzes (Student's test: $P < 0.05$) were performed to evaluate significant differences between control and inoculated treatments and among genotypes within the same treatment (Student's test: $P < 0.05$). Clustering analysis of the metabolite intensities were performed by Partial Least Squares Discriminant Analysis (PLS-DA) by *MetaboAnalyst* platform using 95% confidence interval.

DECLARATION OF COMPETING INTEREST

The authors declare that they have no known competing financial interests or personal relationships that could have appeared to influence the work reported in this paper.

ACKNOWLEDGMENTS

This study was supported by the National Institute of Science and Technology in Plant-Pest Interaction (MCT/INCT-IPP), Núcleo de Análises de Biomoléculas (NuBioMol, UFV), Fundação de Amparo à Pesquisa de Minas Gerais (FAPEMIG), Empresa Brasileira de Pesquisa Agropecuária (EMPRAPA), Coordenação de Aperfeiçoamento de Pessoal de Nível Superior (CAPES) and Conselho Nacional de Desenvolvimento Cientifico e Tecnológico (CNPq).

SUPPLEMENTARY DATA

Supplementary data to this article can be found in the appendix and online at https://doi.org/10.1016/j. phytochem. 2021.112704.

REFERENCES

AHUJA, I.; KISSEN, R.; BONES, A. M. (2012) Phytoalexins in defense against pathogens. Trends Plant Sci. 17 (2), 73-90. https://doi.org/10.1016/j.tplants.2011.11.002.

ALAM, M. A.; SUBHAN, N.; RAHMAN, M. M.; UDDIN, S. J.; REZA, H. M.; SARKER, S. D. (2014) Effect of citrus flavonoids, naringin and naringenin, on metabolic syndrome and their mechanisms of action. Adv. Nutr. 5 (4), 404-417. https://doi.org/10.3945/an.113.005603.

ALLU, A. D.; BROTMAN, Y.; XUE, G. P.; BALAZADEH, S. (2016) Transcription factor ANAC032 modulates JA/SA signalling in response to *Pseudomonas syringae* infectionEMBO. For. Rep. 17 (11), 1578-1589. https://doi.org/10.15252/embr.201642197.

ALVIM, F. C.; CAROLINO, S. M. B.; CASCARDO, J. C. M.; NUNES, C. C.; MARTINEZ, C. A.; OTONI, W. C.; FONTES, E. P. B. (2001) Enhanced accumulation of BiP in transgenic plants confers tolerance to water stress. Plant Physiol. 126, 1042-1054. https://doi.org/10.1104/pp.126.3.1042.

ARON, P. M.; KENNEDY, J. A. (2008) Flavan-3-ols: nature, occurrence and biological activity. Adv. Food Nutr. Res. 52, 79-104. https://doi.org/10.1002/mnfr.200700137.

BAJAJ, R.; HUANG, Y.; GEBRECHRISTOS, S.; MIKOLAJCZYK, B.; BROWN, H.; PRASAD, R.; VARMA, A.; BUSHLEY, K. E. (2018) Transcriptional responses of soybean roots to colonization with the root endophytic fungus *Piriformospora indica* reveals altered phenylpropanoid and secondary metabolism. Sci. Rep. 8, 10227. https://doi.org/10.1038/s41598-018-26809-3.

BALTRUS, D.; NISHIMURA, M.; DOUGHERTY, K.; BISWAS, S.; MUKHTAR, M. S.; VICENTE, J.; HOLUB, E.; JEFFERY, D. (2012) The molecular basis of host specialization in bean pathovars of *Pseudomonas syringae*. Mol. Plant Microbe Interact. 25 (7), 877-888. https://doi.org/10.1094/MPMI-08-11-0218.

BETSUYAKU, S.; KATOU, S.; TAKEBAYASHI, Y.; SAKAKIBARA, H.; NOMURA, N.; FUKUDA, H. (2018) Salicylic acid and jasmonic acid pathways are activated in spatially different domains around the infection site during effector-triggered immunity in *Arabidopsis thaliana*. Plant Cell Physiol. 59 (1), 8-16. https://doi.org/10.1093/pcp/pcx181.

CARVALHO, H. H.; BRUSTOLINI, O. J.; PIMENTA, M. R.; MENDES, G. C.; GOUVEIA, B. C.; SILVA, P. A.; SILVA, J. C.; MOTA, C. S.; RAMOS, J. R. L.; S.; FONTES, E. P. B. (2014) The molecular chaperone binding protein BiP prevents leaf dehydration-induced cellular homeostasis disruption. PLoS One. 2014 Jan; 9(1):e86661. https://https://doi.org/10.1371/journal.pone.0086661

CARVALHO, H. H.; SILVA, P. A.; MENDES, G. C.; BRUSTOLINI, O. J.; PIMENTA, M. R.; GOUVEIA, B. C. VALENTE, M. A.; RAMOS, H. J. O.; RAMOS, J. R. L.; S.; FONTES, E. P. (2014) The endoplasmic reticulum binding protein BiP displays dual function in modulating cell death events. Plant Physiol. 164(2):654-70. https://https://doi.org/10.1104/pp.113.231928

CASCARDO, J. C. M.; BUZELI, R. A. A.; ALMEIDA, R. S.; OTONI, W. C.; FONTES, E. P. B. (2001) Differential expression of the soybean BiP gene family. Plant Sci. 160, 273-281. https://doi.org/10.1016/S0168-9452(00)00384-8.

CHENG, J.; YUAN, C.; GRAHAM, T. L. (2011) Potential defense-related prenylated isoflavones in lactofen-induced soybean. Phytochemistry (Oxf) 72 (9), 875-881. https://doi.org/10.1016/j.phytochem.2011.03.010.

CHIN, S.; BEHM, C.; MATHESIUS, U. (2018) Functions of flavonoids in plant-nematode interactions. Plants 7 (4), 85. https://doi.org/10.3390/plants7040085.

CHOI, H. W.; KIM, Y. J.; HWANG, B. K. (2011) The hypersensitive induced reaction and leucine-rich repeat proteins regulate plant cell death associated with disease and plant immunity. Mol. Plant Microbe Interact. 24 (1), 68-78. https://doi.org/10.1094/MPMI-02-10-0030.

COLL, N. S.; EPPLE, P.; DANGL, J. L. (2011) Programmed cell death in the plant immune system. Cell Death Differ. 18, 1247-1256. https://doi.org/10.1038/cdd.2011.37.

COSTA, M. D. L.; REIS, P. A. B.; VALENTE, M. A. S.; IRSIGLER, A. S. T.; CARVALHO, C. M.; LOUREIRO, M. E.; ARAGA˜O, F. J. L.; BOSTON, R. S.; FIETTO, L. G.; FONTES, E. P. B. (2008) A new branch of endoplasmic reticulum stress signaling and the osmotic signal converge on plant-specific asparagine-rich proteins to promote cell death. J. Biol. Chem. 283, 20209-20219. https://doi.org/10.1074/jbc.M802654200.

COUTINHO, F. S.; SANTOS, D. S.; LIMA, L. L.; VITAL, C. E.; SANTOS, L. A.; PIMENTA, M. R.; SILVA, J. C.; RAMOS, J. R. L.; S.; METHA, A.; FONTES, E. P. B.; RAMOS, H. J. O. (2019) Mechanism of the drought tolerance of a transgenic soybean overexpressing the molecular chaperone. BiP Physiol. Mol. Biol. Plants. 1, 1-16. https://doi.org/10.1007/s12298-019-00643-x.

CUADROS-INOSTROZA, A´.; CALDANA, C.; REDESTIG, H.; KUSANO, M.; LISEC, J.; PEN˜A-CORTE´S, H.; WILLMITZER, L.; HANNAH, M. A. (2009) TargetSearch - a bioconductor package for the efficient preprocessing of GC-MS metabolite profiling data. BMC Bioinf. 10, 428-435. https://doi.org/10.1186/1471-2105-10-428.

DAI, A. (2013) Increasing drought under global warming in observations and models. Nat. Clim. Change 3, 52-58. https://doi.org/10.1038/nclimate1811.

DE CAMARGOS, L. F.; FRAGA, O. T.; OLIVEIRA, C. C.; SILVA, J. C. F.; FONTES, E. P. B.; REIS, P. A. B. (2018) Development and cell death domain-containing asparagine-rich protein (DCD/ NRP):an essential protein in plant development and stress responses. Theor. Exp. Plant Physiol. 31, 59-70. https://doi.org/10.1007/s40626-018-0128-z.

FERREYRA, M. L. F.; RIUS, S. P.; CASATI, P. (2012) Flavonoids: biosynthesis, biological functions and biotechnological applications. Front. Plant Sci. (3), 222. https://doi.org/10.3389/fpls.2012.00222.

FINKEL, T. (2000) Redox-dependent signal transduction. FEBS Lett. 476 (1-2), 52-54. https://doi.org/10.1016/s0014-5793(00)01669-0.

GARDAN, L.; SHAFIK, H.; BELOUIN, S.; BROCH, R.; GRIMONT, F.; GRIMONT, P. A. D. (1999) DNA relatedness among the pathovars of *Pseudomonas syringae* and description of *Pseudomonas tremae* sp. nov. and *Pseudomonas cannabina* sp. nov (ex Sutic and Dowson 1959). Int. J. Syst. Evol. Microbiol. 49, 469-478. https://doi.org/10.1099/00207713-49-2-469.

GOMEZ, J. D.; VITAL, C. E.; OLIVEIRA, M. G. A.; RAMOS, H. J. O. (2018) Broad range flavonoid profiling by LC/MS of soybean genotypes contrasting for resistance to Anticarsia gemmatalis (Lepidoptera: Noctuidae). PloS One 13 (10), e0205010. https://doi.org/101371/journalpone0205010

GONDOR, O. K.; JANDA, T.; SOÓS, V.; PÁL, M.; MAJLÁTH, I.; ADAK, M. K.; BALÁZS, E.; SZALAI, G. (2016) Salicylic acid induction of flavonoid biosynthesis pathways in wheat varies by treatment. Front. Plant Sci. 7, 1447. https://doi.org/10.3389/fpls.2016.01447.

GRAHAM, T. L. (1998) Flavonoid and flavonol glycoside metabolism in Arabidopsis. Plant Physiol. Biochem. 36 (1-2), 135-144. https://doi.org/10.1016/s0981-9428(98)80098-3.

HASSAN, S.; MATHESIU, U. (2012) The role of flavonoids in root-rhizosphere signalling: opportunities and challenges for improving plant-microbe interactions. J. Exp. Bot. 63 (9), 3429-3444. https://doi.org/10.1093/jxb/err430.

HUANG, T.; JANDER, G. (2017) Abscisic acid-regulated protein degradation causes osmotic stress-induced accumulation of branched-chain amino acids in *Arabidopsis thaliana*. Planta 246 (4), 737-747. https://doi.org/10.1007/s00425-017-2727-3.

ICHINOSE, Y.; TAGUCHI, F.; MUKAIHARA, T. (2013) Pathogenicity and virulence factors of *Pseudomonas syringae*. Plant Pathology J. 79, 285-296. https://doi.org/10.1007/s10327-013-0452-8.

KANEHISA, M. (2000) KEGG: Kyoto Encyclopedia of genes and genomes. Nucleic Acids Res. 28 (1), 27-30. https://doi.org/10.1093/nar/28.1.27.

KENTON, P.; MUR, L. A. J.; ATZORN, R.; WASTERNACK, C.; DRAPER, J. (1999) (2) (—)-Jasmonic acid accumulation in tobacco hypersensitive response lesions. Mol. Plant Microbe Interact. 12, 74-78. https://doi.org/10.1094/MPMI.1999.12.1.74.

KIM, H. S.; PARK, Y. H.; NAM, H.; LEE, Y. M.; SONG, K.; CHOI, C.; AHN, I.; PARK, S. R.; LEE, Y. H.; HWANG, D. J. (2014) Overexpression of the *Brassica rapa* transcription factor WRKY12 results in reduced soft rot symptoms caused by *Pectobacterium carotovorum* in Arabidopsis and Chinese cabbage. Plant Biol. 16 (5), 973-981. https://doi.org/10.1111/plb.12149.

KOCHEVENKO, A.; ARAÚJO, W. L.; MALONEY, G. S.; TIEMAN, D. M.; DO, P. T.; TAYLOR, M. G.; KLEE, H. J.; FERNIE, A. R. (2012) Catabolism of branched chain amino acids supports respiration but not volatile synthesis in tomato fruits. Mol. Plant 5 (2), 366-375. https://doi.org/10.1093/mp/ssr108.

KU, Y. S.; AU-YEUNG, W. K.; YUNG, Y. L.; LI, M. W.; WEN, C. Q.; LIU, X.; LAM, H. M. (2013) Drought stress and tolerance in soybean. In: Board, J. E. (Ed.), A Comprehensive Survey of International Soybean Research - Genetics, Physiology, Agronomy and Nitrogen Relationships. InTech, New York, pp. 209-237.

LACHAUD, C.; DA SILVA, D.; COTELLE, V.; THULEAU, P.; XIONG, T. C.; JAUNEAU, A.; BRIERE, C.; GRAZIANA, A.; BELLEC, Y.; FAURE, J. -D.; RANJEVA, R.; MAZARS, C. (2010) Nuclear calcium controls the apoptotic-like cell death induced by d-erythro-sphinganine in tobacco cells. Cell Calcium 47 (1), 92-100. https://doi.org/10.1016/j.ceca.2009.11.011.

LAM, K. C.; IBRAHIM, R. K.; BEHDAD, B.; DAYANANDAN, S. (2007) Structure, function, and evolution of plant O-methyltransferases. Genome 50 (11), 1001-1013. https://doi.org/10.1139/g07-077.

LEBORGNE-CASTEL, N.; JELITTO-VAN DOOREN, E. P. W. M.; CROFTS, A. J.; DENECKE, J. (1999) Overexpression of BiP in tobacco alleviates endoplasmic reticulum stress. Plant Cell 11, 459-470. https://doi.org/10.1105/tpc.11.3.459.

LIMA, L. L.; MESQUITA, R.; BALBI, B. P.; COUTINHO, F. S.; SILVA, C.; CARMO, F. M. S.; VITAL, C. E.; MEHTA, A.; LOUREIRO, M. E.; FONTES, E. P. B.; BARROS, E. G.; RAMOS, H. J. O. (2019) Proteomic and metabolomic analysis of a drought tolerant soybean cultivar from Brazilian savanna. Crop. Breed. Genet. Genom 1, e190022. https://doi.org/10.20900/cbgg20190022.

LISEC, J.; SCHAUER, N.; KOPKA, J.; WILLMITZER, L.; FERNIE, A. R. (2006) Gas chromatography mass spectrometry-based metabolite profiling in plants. Nat. Protoc. 1, 387-396. https://doi.org/10.1038/nprot.2006.59.

MAGNIN-ROBERT, M.; LE BOURSE, D.; MARKHAM, J.; DOREY, S.; CLEMENT, C.; BAILLIEUL, F.; DHONDT-CORDELIE, S. (2015) Modifications of sphingolipid content affect tolerance to hemibiotrophic and necrotrophic pathogens by modulating plant defense responses in Arabidopsis. Plant Physiol. 169 (3), 2255-2274. https://doi.org/10.1104/pp.15.01126.

MAKI, H.; SAKAOKA, S.; ITAYA, T.; SUZUKI, T.; MABUCHI, K.; AMABE, T.; SUZUKI, N.; HIGASHIYAMA, T.; TADA, Y.; NAKAGAWA, T.; MORIKAMI, A.; TSUKAGOSHI, H. (2019) ANAC032 regulates root growth through the MYB30 gene regulatory network. Sci. Rep. 9 (1), 11358. https://doi.org/10.1038/s41598-019-47822-0.

MELO, B. P.; FRAGA, O. T.; SILVA, J. C. F.; FERREIRA, D. O.; BRUSTOLINI, O. J. B.; CARPINETTI, P. A.; MACHADO, J. P. B.; REIS, P. A. B.; FONTES, E. B. P. (2018) Revisiting the soybean GmNAC superfamily. Front. Plant Sci. 9, 1864. https://doi.org/10.3389/fpls.2018.01864.

MIERZIAK, J.; KOSTYN, K.; KULMA, A. (2014) Flavonoids as important molecules of plant interactions with the environment. Molecules 19 (10), 16240-16265. https://doi.org/10.3390/molecules191016240.

MIKKELSEN, M. D.; HALKIER, B. A. (2003) Metabolic engineering of valine- and isoleucine-derived glucosinolates in Arabidopsis expressing CYP79D2 from Cassava. Plant Physiol. 131 (2), 773-779. https://doi.org/10.1104/pp.013425.

PANDEY, S. P.; SOMSSICH, I. E. (2009) The role of WRKY transcription factors in plant immunity. Plant Physiol. 150 (4), 1648-1655. https://doi.org/10.1104/pp.109.138990.

PATA, M. O.; HANNUN, Y. A.; NG, C. K. (2010) Plant sphingolipids: decoding the enigma of the Sphinx. New Phytol. 185 (3), 611-630. https://doi.org/10.1111/j.1469-8137.2009.03123.x.

PEER, M.; STEGMANN, M.; MUELLER, M. J.; WALLER, F. (2010) *Pseudomonas syringae* infection triggers de novo synthesis of phytosphingosine from sphinganine in Arabidopsis thaliana. FEBS Lett. 594, 4053-4056. https://doi.org/10.1016/j.febslet.2010.08.027.

PFAFFL, M. W. (2001) A new mathematical model for relative quantification in real-time RT-PCR. Nucleic Acids Res. 29 (9), e45. https://doi.org/10.1093/nar/29.9.e45.

PINCUS, D.; CHEVALIER, M. W.; ARAGON, T.; VAN ANKEN, E.; VIDAL, S. E.; EL-SAMAD, H. (2010) BiP Binding to the ER-stress sensor ire1 tunes the homeostatic behavior of the unfolded protein response. PLoS Biol. 8 (7) https://doi.org/10.1371/journal.pbio.1000415e1000415.

PIRES, M. V.; PEREIRA JÚNIOR, A. A.; MEDEIROS, D. B.; DALOSO, D. M.; PHAM, P. A.; BARROS, K. A.; ENGGVIST, M. K. M.; FLORIAN, A.; KRAHNERT, I.; MAURINO, V. G.; ARAÚJO, W. L.; FERNIE, A. R. (2016) The influence of alternative pathways of respiration that utilize branched-chain amino acids following water shortage in Arabidopsis. Plant Cell Environ. 39 (6), 1304-1319. https://doi.org/10.1111/pce.12682.

PRESTON, G. M. (2000) *Pseudomonas syringae* pv. tomato: the right pathogen, of the right plant, at the right time. Mol. Plant Pathol. 1 (5), 263-275. https://doi.org/10.1046/j.1364-3703.2000.00036.x.

REIS, P. A. B.; CARPINETTI, P. A.; FREITAS, P. P. J.; SANTOS, E. G. D.; DE CAMARGOS, L. F.; OLIVEIRA, I. H. T.; SILVA, J. C. F.; CARVALHO, H. H.; COSTA, M. D. L.; RAMOS, J. L. R. S.; FONTES, E. P. B. (2016) Functional and regulatory conservation of the soybean ER stress-induced DCD/NRP-mediated cell death signaling in plants. BMC Plant Biol. 16, 156. https://doi.org/10.1186/s12870-016-0843-z.

REIS, P. A. B.; ROSADO, G. L.; SILVA, L. A.; OLIVEIRA, L. C.; OLIVEIRA, L. B.; COSTA, M. D.; ALVIM, F. C.; FONTES, E. P. B. (2011) The binding protein BiP attenuates stress-induced cell death in soybean via modulation of the N-rich protein-mediated signaling pathway. Plant Physiol. 157, 1853-1865.

ROJAS, C. M.; SENTHIL-KUMAR, M.; TZIN, V.; MYSORE, K. S. (2014) Regulation of primary plant metabolism during plant-pathogen interactions and its contribution to plant defense. Front. Plant Sci. 5, 17. https://doi.org/10.3389/fpls.2014.00017.

ROY, J.; HUSS, B.; CREACH, A.; HAWKINS, S.; NEUTELINGS, G. (2016) Glycosylation is a major regulator of phenylpropanoid availability and biological activity in plants. Front. Plant Sci. 7, 735. https://doi.org/10.3389/fpls.2016.00735.

SÁNCHEZ-RANGEL, D.; RIVAS-SAN VICENTE, M.; DE LA TORRE-HERNA´NDEZ, M. E. (2015) Nájera-Martínez, M. Plasencia, J. Deciphering the link between salicylic acid signaling and sphingolipid metabolism. Front. Plant Sci. 6, 125. https://doi.org/10.3389/fpls.2015.00125.

SAYED, M.; KHODARY, S. E. A.; AHMED, E. S.; HAMMOUDA, O.; HASSAN, H. M.; EL-SHAFEY, N. M. (2017) Elicitation of flavonoids by chitosan and salicylic acid in callus of *Rumex vesicarius* L. Acta Hortic. 1187, 165-176. https://doi.org/10.17660/actahortic.2017.1187.18.

SILVA, P. A.; SILVA, J. C. F.; CAETANO, H. A. D. N.; MACHADO, J. P. B.; MENDES, G. C.; REIS, P. A. B.; BRUSTOLINI, O. J. B.; DAL-BIANCO, M.; FONTES, E. P. B. (2015) Comprehensive analysis of the endoplasmic reticulum stress response in the soybean genome: conserved and plant specific features. BCM Genomics 16, 783. https://doi.org/10.1186/s12864-015-1952-z

TAJIK, S.; ZARINKAMAR, F.; SOLTANI, B. M.; NAZARI, M. (2019) Induction of phenolic and flavonoid compounds in leaves of saffron (*Crocus sativus* L.) by salicylic acid. Sci. Hortic. 257, 108751. https://doi.org/10.1016/j.scienta.2019.108751.

TARKOWSKI, Ł. P.; SIGNORELLI, S.; HÖFTE, M. (2020) γ-Aminobutyric acid and related amino acids in plant immune responses: emerging mechanisms of action. Plant Cell Environ. 43 (5), 1103-1116. https://doi.org/10.1111/pce.13734.

VALENTE, M. A. S.; FARIA, J. Q. A.; RAMOS, J. R. L. S.; REIS, P. A. B.; PINHEIRO, G. L.; PIOVESAN, N. D.; MORAIS, A. T.; MENEZES, C. C.; CANO, M. A. O.; FIETTO, L. G.; LOUREIRO, M. E.; ARAGAO, F. J. L.; FONTES, E. B. P. (2009) The ER luminal binding protein (BiP) mediates an increase in drought tolerance in soybean and delays drought-induced leaf senescence in soybean and tobacco. J. Exp. Bot. 60, 533-546. https://doi.org/10.1093/jxb/ern296

VITAL, C. E.; GÓMEZ, J. D.; VIDIGAL, P. M.; BARROS, E.; PONTES, C. S. L.; VIEIRA, N. M.; RAMOS, H. J. O. (2019) Phytohormone profiling by liquid chromatography coupled to mass spectrometry (LC/MS). Protocols. io. https://doi.org/10.17504/protocols.io.zgff3tn

VITAL, C. E.; GÓMEZ, J. D.; VIDIGAL, P. M.; BARROS, E. G.; PONTES, C. S. L.; VIEIRA, N. M.; OLIVEIRA, M. G. A.; RAMOS, H. J. O. (2019) Flavonoid profiling by liquid chromatography coupled to mass spectrometry (LC/MS). Protocols. io. https://doi.org/10.17504/protocols.io.zggf3tw

WILLIAMS, B.; VERCHOT, J.; DICKMAN, M. B. (2014) When supply does not meet demand-ER stress and plant programmed cell death. Front. Plant Sci. 5, 1-9. https://doi.org/10.3389/fpls.2014.00211.

YAENO, T.; MATSUDA, O.; IBA, K. (2004) Role of chloroplast trienoic fatty acids in plant disease defense responses. Plant J. 40 (6), 931-941. https://doi.org/10.1111/j.1365-313X.2004.02260.x.

YAZAKI, K.; SASAKI, K.; TSURUMARU, Y. (2009) Prenylation of aromatic compounds, a key diversification of plant secondary metabolites. Phytochemistry (Oxf.) 70 (15-16), 1739-1745. https://doi.org/10.1016/j.phytochem.2009.08.023.

ZABALA, G.; ZOU, J.; TUTEJA, J.; GONZALEZ, D. O.; CLOUGH, S. J.; VODKIN, L. O. (2006) Transcriptome changes in the phenylpropanoid pathway of *Glycine max* in response to *Pseudomonas syringae* infection. BMC Plant Biol. 6 (1), 26. https://doi.org/10.1186/1471-2229-6-26.

ZIMMERLI, L.; JAKAB, G.; METRAUX, J. P.; MAUCH-MANI, B. (2000) Potentiation of pathogen-specific defense mechanisms in Arabidopsis by beta-aminobutyric acid. Proc. Natl. Acad. Sci. U. S. A. 97 (23), 12920-12925. https://doi.org/10.1073/pnas.230416897.

ZOU, J.; RODRIGUEZ-ZAS, S.; ALDEA, M.; LI, M.; ZHU, J.; GONZALEZ, D. O.; VODKIN, L. O.; DELUCIA, E.; CLOUGH, S. J. (2005) Expression profiling soybean response to *Pseudomonas syringae* reveals new defense-related genes and rapid hr-specific downregulation of photosynthesis. Mol Plant-Microbe Interact 18(11):1161-1174

APPENDIX

Appendix A – Flavonoid derivatives identified by *precursor ion scan* method from soybean leaves.

Flavonoid class	Precursor (m/ z)	RT (min)	Conjugate (m/ z)	Sugar Moiety (mass)	Relative Abundance in XIC (%)				FRI% Match	Flavonoid name	Mass Bank (Database/ Literature)
					C9 I	C9 NI	WT I	WT NI			
Daidzein	255	5.3	417.1	162.1	100	100	100	100	+/-	Daidzein 7-O-glucoside	Wu et al. 2004
	255	5.6	757.3	502.3	100	100	100	100	+/-	NH	-
	255	5.6	417.1	162.1	39.9	65.76	-	63.36	+/-	Daidzein 7-O-glucoside	Wu et al. 2004
	255	6.6	503	248	100	100	100	100	+/-	Daidzein 7-O-glucoside-O-6"-malonate	Wu et al. 2004
	255	7.6	741.1	486.1	37.2	60.3	100	-	+/-	Daidzein 7-O-glucosyl-O-glucoside-4'-O-glucoside	PubChem Massbank
	255	7.6	545.2	290.2	100	100	-	100	+/-	NH	PubChem Massb
	255	10.1	322.9	67.9	100	100	100	100	+/-	Dimethylallyl daidzein	Yoneyama et al. 2016
Genistein-Apigenin	271	5.3	595.3	324.3	62.4	71.2	59.4	68	+/-	Genistein 4',7-di-O-glucoside	Boue et al. 2003
	271	5.3	595.3	324.3	62.4	71.2	59.4	68	+/-	Genistein 7-O-glucosyl-O-glucoside	Massbank; PubChem
	271	6.5	565.3	294.3	61.9	20.3	16.34	35.6	+/-	Genistein 6-C-xyloside-8-C-glucoside	Massbank; PubChem
	271	6.5	433.1	162.1	100	100	100	100	+/-	Genistein 7-O-glucoside	Massbank; PubChem
	271	7.1	519.3	248.3	100	100	100	100	+/-	Genistein 7-O-glucoside-O-6"-malonate	Boue et al. 2003
	271	8.7	518.8	247.8	-	100	-	100	+/-	Genistein 7-O-glucoside-O-6"-malonate	Boue et al. 2003
	271	10.7	355.4	84.4	-	100	-	100	+/-	4',5-di-O-acetylgenistein	Massbank; PubChem
	271	10.7	339.2	68.2	100	-	100	42.7	+/-	Dimethylallyl genistein	Yoneyama et al. 2016;
Luteolin-Kaempferol	287	5.5	757.3	470.3	100	100	100	100	+/-	Luteolin 3-O-rutinoside-4'-O-glucoside	Massbank; PubChem
	287	5.7	757.3	470.3	100	100	100	100	+/-	Luteolin 3-O-rutinoside-4'-O-glucoside	Massbank; PubChem
	287	5.9	741.1	454.1	100	100	100	100	+/-	Luteolin 3-O-(2",6"-di-O-rhamnosyl)-glucoside	Massbank; PubChem
	287	5.9	611.3	324.3	79.1	42.9	43.8	74.7	+/-	Luteolin 7-O-glucosyl-O-glucoside	Massbank; PubChem
	287	5.9	611.3	324.3	79.1	42.9	43.8	74.7	+/-	Luteolin di-O-glucoside	Massbank; PubChem
	287	5.9	595.2	308.2	84.8	82.6	56.9	82.5	+/-	Luteolin O-rutinoside	Massbank; PubChem
		5.9	449.1	162.1	78.7	81.4	75.2	74.1	+/-	Luteolin O-glucoside	Massbank; PubChem
	287	6.7	595	308	100	100	100	100	+/-	Luteolin O-rutinoside	Massbank; PubChem
	287	6.7	535	248	-	17	18.4	20.9	+/-	Luteolin 7-O-glucoside-6"-O-malonate	Massbank; PubChem

	287	6.7	449	162	19.02	32.14	15.1	12.7	+/-	Luteolin O-glucoside	Massbank; PubChem
	287	8.1	757.4	454.4	37.6	100	18.3	100	SI	Kaempferol 3-O-glucoside-O-rhamnosyl-O-glucoside	Ho et al. 2002
Morin-Hesperentin-Quercetin	303	5	773.6	470.6	100	100	100	100	+/-	Quercetin 3-O-rutinoside-7-O-glucoside	Lin et al. 2008
	303	5.3	773.6	470.6	100	100	100	100		Quercetin 3-O-rutinoside-7-O-glucoside	Lin et al. 2008
	303	5.6	757	454	98	90.3	100	52.7	+/-	Quercetin 3-O-(2",6"-di-O-rhamnosyl)-glucoside	Lin et al. 2008
	303	5.6	627.2	324.2	100	100	70	61.2	+/-	Quercetin 3,4'-diglucoside	Lin et al. 2008
	303	5.6	627.2	324.2	100	100	70	61.2	+/-	Quercetin 3,4'-digalactoside	Lin et al. 2008
	303	6.4	611.1	308.1	100	100	100	100	+/-	Rutin	MassBank; Olsen et al. 2012
	303	7.1	465.4	162.4	100	100	100	100	+/-	Isoquercetin	MassBank; Olsen et al. 2012
	303	8.4	633.5	330.5	100	100	100	100	+/-	NH	

Source: Survey's data.

Note: NH: no hit (in database or literature); **Relative Abundance in XIC (%)**: percentage of the relative intensity in mass spectrum (values below 15% were not reported); **+/-:** when FRI% match in both genotypes and treatments.

Appendix B – Non-target analysis of flavonoids from Genistein-Apigenin classes in soybean leaves from the WT and C9 genotypes in the inoculation or mockinoculation by *P. syringae* pv. tomato at 36 hours after inoculation. In **(A)** Compounds detected for each genotype, the retention times (RT) observed and their RFI% calculated as in Gómez et al. (2018). The compounds that share the same RFI% patterns related to standard were considered as belonging to a glycoconjugate for those classes. In **(B)** the relative abundances, in terms of XICs and in accordance with RT, of some flavonoid compounds characterized as genistein conjugates in (A) in the presence or absence of *P. syringae* pv. tomato. The data represent the mean ± standard error. Bars (mean ± SE; n = 4) with the same capital letters indicate no significant difference between control and inoculated treatments and those followed by the same lowercase letters indicate no significant difference among genotypes within the same treatment (Student's test: $P < 0.05$).

A)

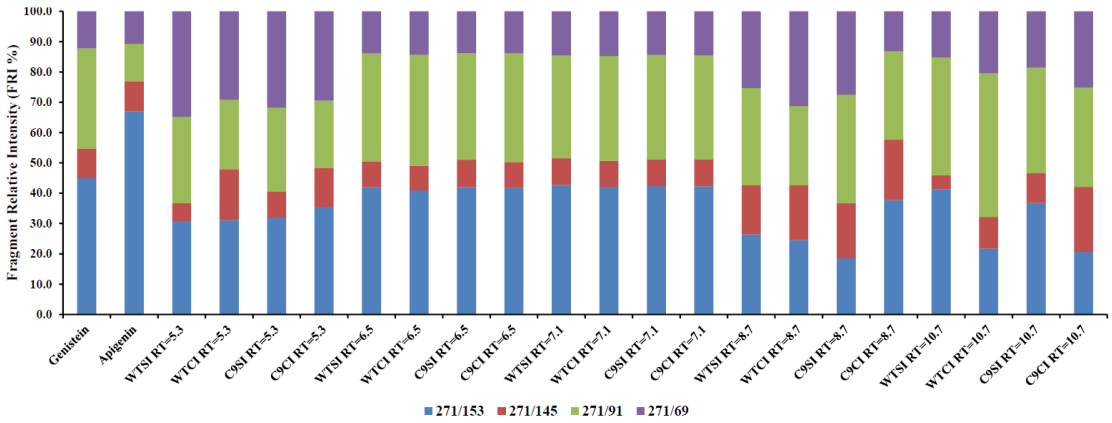

B)

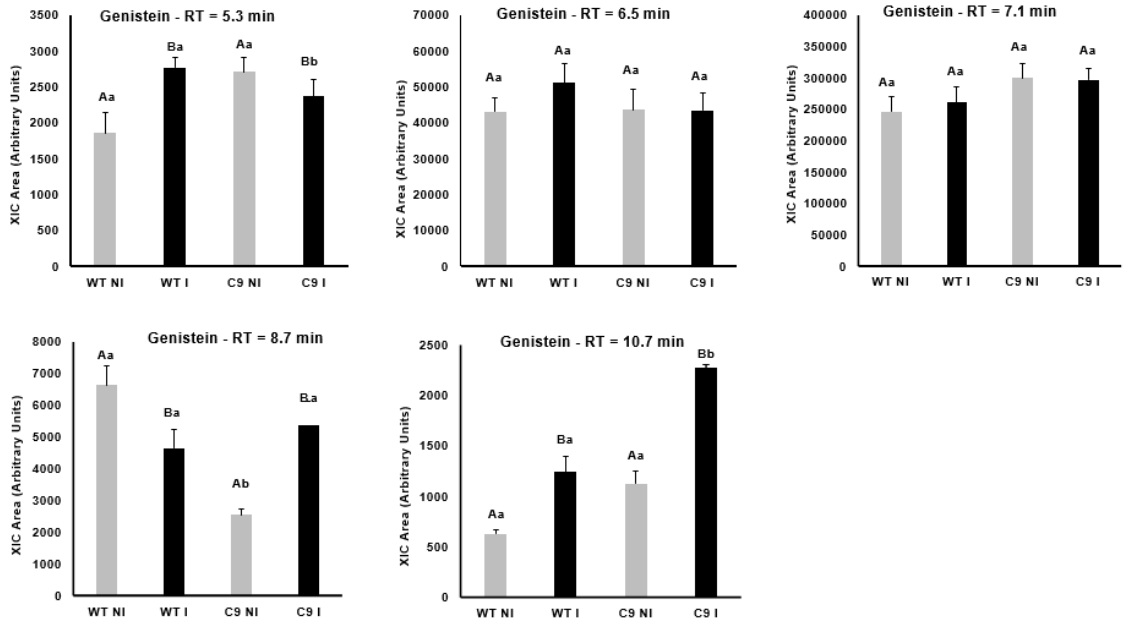

Source: Survey's data.

Appendix C – Nontarget analysis of flavonoids from Morin-Hesperetin-Quercetin classes in soybean leaves from the WT and C9 genotypes in the inoculationor mock inoculation by *P. syringae* pv. tomato at 36 hours after inoculation. In **(A)** compounds detected for each genotype, the retention times (RT) observed and their RFI% calculated as in Gómez et al. (2018). The compounds that share the same RFI% patterns related to standard were considered as belonging to a glycoconjugate for those classes. In **(B)** the relative abundances, in terms of XICs and in accordance with RT, of some flavonoid compounds characterizedas quercetin conjugates in (A) in the presence or absence of *P. syringae* pv. tomato. The data represent the mean ± standard error. Bars (mean ± SE; n = 4) with the same capital letters indicate no significant difference between control and inoculated treatments and those followed by the same lowercase letters indicate no significant difference among genotypes within the same treatment (Student's test: $P < 0.05$).

A)

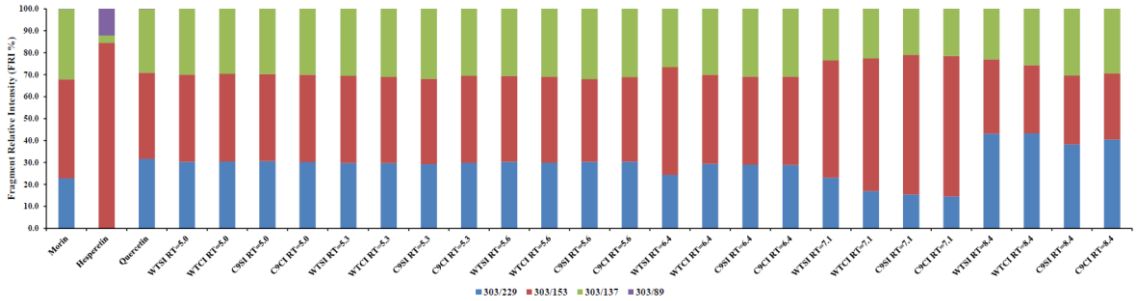

B)

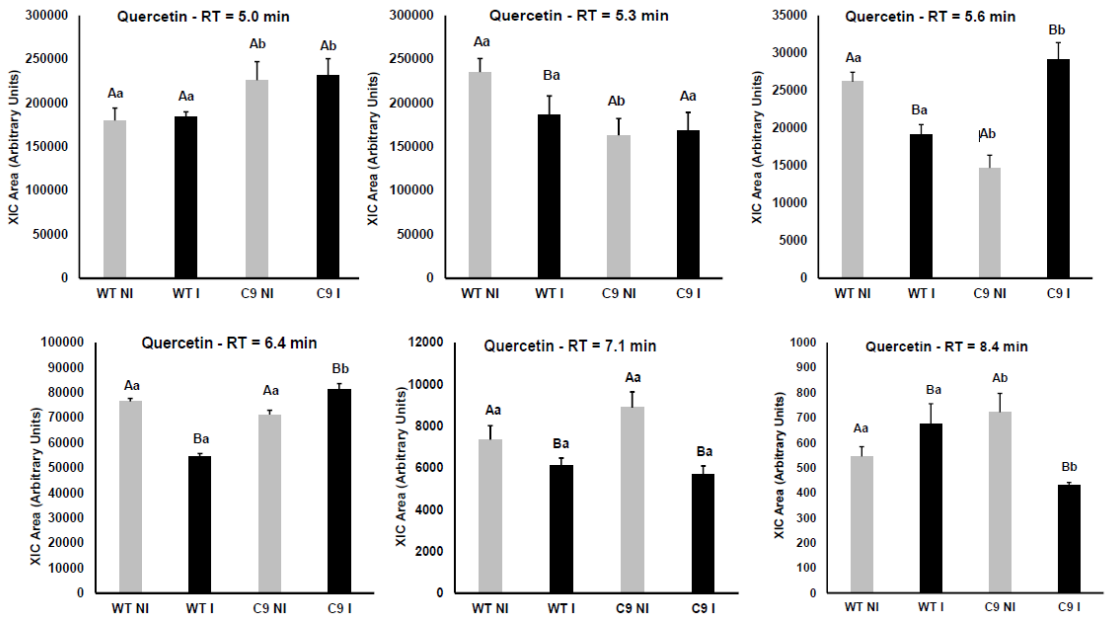

Source: Survey's data.

Appendix D – Nontarget analysis of flavonoids from Luteolin-Kaempferol classes in soybean leaves from the WT and C9 genotypes in the inoculation or mockinoculation by *P. syringae* pv. tomato at 36 hours after inoculation. In **(A)** compounds detected for each genotype, the retention times (RT) observed and their RFI% calculated as in Gómez et al. (2018). The compounds that share the same RFI% patterns related to standard were considered as belonging to a glycoconjugate for those classes. In **(B)** The relative abundances, in terms of XICs and in accordance with RT, of some flavonoid compounds characterized as luteolin or kaempferol conjugates in **(A)** in the presence or absence of *P. syringae* pv. tomato. The data represent the mean ± standard error. Bars(mean ± SE; n = 4) with the same capital letters indicate no significant difference between control and inoculated treatments and those followed by the same lowercase letters indicate no significant difference among genotypes within the same treatment (Student's test: $P < 0.05$).

A)

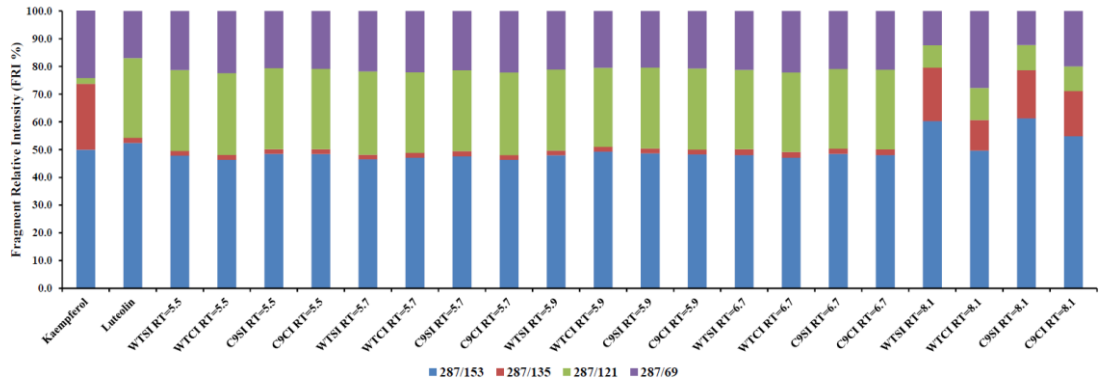

B)

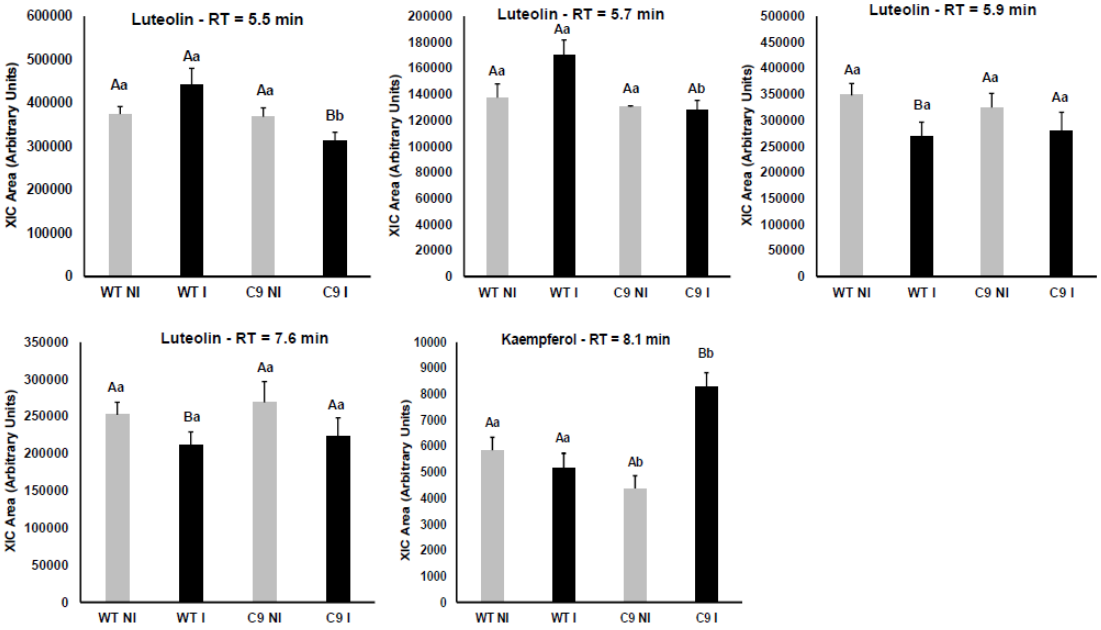

Source: Survey's data.

Appendix E – Nontarget analysis of flavonoids from Daidzein classe in soybean leaves from the WT and C9 genotypes in the inoculation or mock inoculationby *P. syringae* pv. tomato at 36 hours after inoculation. In **(A)** compounds detected for each genotype, the retention times (RT) observed and their RFI% calculated as in Gómez et al. (2018). The compounds that share the same RFI% patterns related to standard were considered as belonging to a glycoconjugate for those classes. In **(B)** The relative abundances, in terms of XICs and in accordance with RT, of some flavonoid compounds characterizedas luteolin or kaempferol conjugates in **(A)** in the presence or absence of *P. syringae* pv. tomato. The data represent the mean ± standard error. Bars (mean ± SE;n = 4) with the same capital letters indicate no significant difference between control and inoculated treatments and those followed by the same lowercase letters indicate no significant difference among genotypes within the same treatment (Student's test: $P < 0.05$).

A)

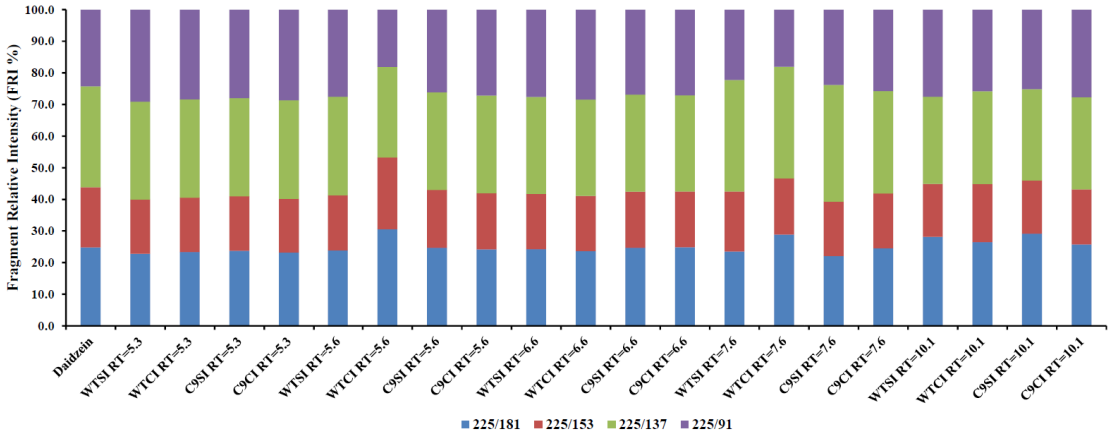

B)

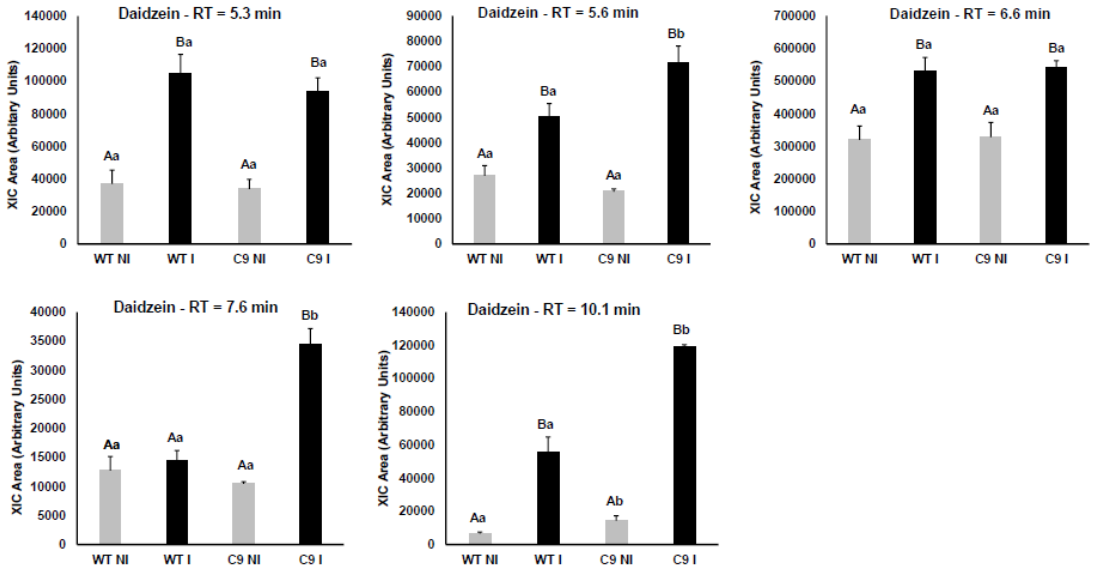

Source: Survey's data.

CAPÍTULO II

PROTEOMIC AND METABOLOMIC ANALYSIS OF BiP-OVEREXPRESSING SOYBEAN PLANTS DISPLAYING AN ACCELERATED HYPERSENSITIVITY RESPONSE (HR)

CAPÍTULO II – PROTEOMIC AND METABOLOMIC ANALYSIS OF BIP-OVEREXPRESSING SOYBEAN PLANTS DISPLAYING AN ACCELERATED HYPERSENSITIVITY RESPONSE (HR)

ABSTRACT

Soybean plants overexpression of the molecular chaperone BiP in transgenic plants has showed enhance in the tolerance to drought and delaying hypersensitive cell death in response to bacterial infection. In this study, we evaluated the proteomic and metabolomic profiles in BiP-overexpressing soybean plants in response to the hypersensitivity response (HR) caused by the non-compatible bacteria *Pseudomonas syringae* pv. tomato. The induction of HR-related plant defense mechanisms in plants overexpressing BiP by *P. syringae* pv. tomato exhibited down-regulation of photosynthetic proteins and an upregulation of antioxidative metabolism proteins in response to inoculation with *P. syringae* pv. tomato, in addition to causing an increase in the expression of O-methyltransferases (OMTs) in the infected transgenic genotype. It was also observed, related to OMTs, a greater presence of flavonoids and methylated isoflavonoids. Furthermore, there has been an increase in the levels of phytoalexins such as coumestrol, pterocarpans and glyceollins in genotypes infected with the incompatible bacteria. These results can be used to clarify the mechanisms of resistance to plant tissue induced by colonization by non-pathogenic pathovars of *P. syringae* in contrasting genotypes regarding drought tolerance.

1 INTRODUCTION

Plants are exposed to various environmental factors such as atmospheric gases, light, temperature, excess or lack of water, action of injuries and attacks by organisms and microorganisms. Such environmental factors can exert a certain level of stress on plants, which can act concomitantly or not. Plants, in turn, promote mechanisms to protect themselves from possible unfavorable situations for their development (Vierling and Kimpel 1992). Plant defense involves the induction of stress-responsive genes or involved in signal transduction, increased protein synthesis and degradation, post-translational protein modifications and specialized metabolite biosynthesis (Kim et al. 2008; De Wit 2007; Hahn et al. 2013; Ahanger et al. 2017), with the aim of regulating and maintain plant cell homeostasis.

As protein function may also be affected by environmental stresses, the role of plant proteins acting in protein remodeling has been studied as determinant of the tolerance. One of these proteins is the ER-resident molecular chaperone binding protein (BiP), belonging to the 70 kDa heat shock protein (HSP70) family and involved in increasing tolerance to drought conditions by promoting delayed stress perception (Alvim et al. 2001; Valente et al. 2009). Furthermore, the BiP-mediated drought tolerance mechanism has been associated with its ability to negatively modulate N-rich protein (DCD/NRP)-mediated programmed cell death (PCD) when induced by drought (Carvalho et al. 2014a, Reis et al. 2016; De Camargos et al. 2018; Melo et al. 2018). However, when subjected to biotic stresses induced by incompatible plant-bacterium interaction, BiP was shown to anticipate the hypersensitivity (HR) response mediated by salicylic acid (Reis et al. 2011; Carvalho et al. 2014a,b; Silva et al. 2015; Reis et al. 2016; Rodrigues et al. 2021).

Since plants are exposed to a wide variety of microorganisms present in the environment, they have developed intrinsic mechanisms to recognize, tolerate, resist and defend against possible damage. One of these mechanisms is the down-regulation of genes related to processes linked to photosynthesis and primary metabolism, while genes that regulate the plant defense responses against pathogens tend to be up-regulated (Berger et al. 2004; Bilgin et al. 2010; Ahuja et al. 2012). However, several studies report that primary metabolism proteins may acting in the mediation of plant defense mechanisms against microorganisms. Thus, some proteins from primary metabolism may be up-regulated and related not only to plant growth, but also to protection against pathogens (Rojas 2014).

Several compounds are involved in the plant-microorganism interaction, such as fatty acids (FA), phytosterols, lipids and membrane proteins, glycoproteins, among others (Welti et al. 2007; Takahashi et al. 2009; Zhao et al. 2013). A priori, many play the role of maintaining structural integrity in cell membranes, but many also participate as mediators of signal transduction at various levels, from cross-tolerance, warning of pathogenic invasion, to detection of pathogen-associated molecular protein (PAMPs), until it activates plant resistance mechanism for pattern-triggered immunity (PTI) or effector-triggered immunity (ETI) (Wang 2004; Kim et al. 2008; Walley et al. 2013; Zhang and Xiao 2015; Siebers et al. 2016). Several products of enzymatic activities participate as secondary messengers of HR-related bacterial attacks, such as in the modulation of transcription factors involved in defense response. Low mass molecules, such as phenolic compounds can act as photoprotectors, antioxidant agents or in defense against phytopathogenic agents (Graham, 1998; Chin et al. 2018). Enzymes such

as Lipoxygenases (LOX) can act in this environment, through the production of oxylipins and JA (Feussner and Wastenack 2002; Ferreira et al. 2005). Thus, LOX may also be important acting in changes in unsaturated FA, changing the fluidity and permeability of membranes (Upchurch 2008).

Pseudomonas syringae pathovar (pv.) tomato are ubiquitous phytobacterium that colonize the plant tissue of several plants and, despite not causing disease in soybeans, they cause brown spots on leaves and fruits, impairing productivity and grain quality. Furthermore, the ability to persist in seeds, exudates, crop residues and soil makes *P. syringae* pv. tomato a bacterium that is difficult to control in the field (Gardan, 1999; Preston, 2000). As soybean did not a host susceptible to this species, infection by *P. syringae* pv. tomato have been used study the HR response in soybean plants overexpressing BiP (Carvalho et al. 2014a,b). In previous studies, Rodrigues et al. (2021) characterized the metabolic alterations in these transgenic plants related to its wild-type. Thus, in this study, the proteomic and phosphoproteomic profiles of transgenic soybean plants overexpressing the molecular chaperone BiP are also evaluated. Furthermore, some specific phenolic compounds and phytoalexins were analyzed by a LC/MS to verified if the biosynthesis of defense molecules were activated in response to bacterial infection differentially in the transgenic plants. In general, the results show an integration between the expression of antioxidant metabolism proteins and those related to the synthesis of phenylpropanoids, flavonoids and phytoalexin isoflavonoids.

2 EXPERIMENTAL

2.1 INOCULATION ASSAYS AND OBTAINING OF PLANT MATERIAL

The plant-pathogen interaction experiment was set up and conducted in the greenhouse at the Federal University of Viçosa (UFV), Viçosa, Minas Gerais. Transgenic lines 35S::BiP-2 and 35S::BiP-4 were previously obtained by transforming soybean plants (*Glycine max* cv. Conquista) with the soyBiPD gene (GeneBank accession AF031241) under the control of a cauliflower mosaic virus 35S promoter (Cascardo et al. 2001; Valente et al. 2009). Soybean seeds untransformed, wild-type Conquest genotype (WT), and transgenic, line 35S::BiP-4 (C9 genotype), were grown in 1 L pots containing previously autoclaved mixture of soil, sand and dung (3:1:1).

Colonies of P. s. pv. tomato was obtained by Phytopathogen Populations Laboratory of Plant Pathology Department of Universidade Federal de Viçosa The inoculum was prepared in three 500 mL Erlenmeyer flasks containing liquid medium King B growing at 28 °C until A_{600nm} = 0.700. Then, the cells were washed and the pellet was homogeneously dissolved in 2 L of 10 mM $MgCl_2$ previously sterilized. This suspension was used for the inoculation experiment.

The infiltration of *P. syringae* pv. tomato in soybean was carried out according to Zou et al (2005) with some modifications. Leaves were inoculated when the third trifoliate leaves were completely expanded, and the fourth trifoliate leaves were beginning to emerge. Inoculations were performed at 30 days after sowing, about 3 to 6 h after the day cycle began by inverting the vessel containing the soybean plants into a Becker filled with inoculum (I, infected plants). The entire system was closed within a vacuum chamber, and mock-inoculated leaves were vacuum-infiltrated with 10 mM $MgCl_2$ and used as controls (NI, noninfected plants). A drawn vacuum (500 mmHg) was applied for about 90 s and then was released quickly, compelling the inoculum in through the open stomata and taking up full apoplastic space. Immediately after infiltration, the plastic bag was removed, and the plants were maintained under greenhouse conditions. Leaves were collected and immediately frozen in liquid nitrogen and stored at -80 ºC.

2.2 PROTEIN AND PHOSPHOPROTEIN EXTRACTION AND DETECTION

2.2.1 PROTEIN EXTRACTION

The soybean inoculated with *P. syringae* pv. tomato leaf proteins were extracted following the method described by Aryal et al. (2012) and Lima et al (2019), with some modifications. The leaves were macerated in liquid nitrogen and 2 g of dust were weighed for each aliquot and resuspended in 6 mL extraction buffer [Nuclei Isolation Buffer (NIB) (Sigma Aldrich) four-fold dilution, 1 mM DTT, 0.2% (v/v)] protease inhibitor cocktail (P-9599, Sigma Aldrich) and 1% (v/v) phosphatase inhibitor cocktail (P-0044, Sigma Aldrich)] and 0.5% (w/w) polyvinylpolypyrrolidone (PVPP).

The samples were vortexed for 30s, then the solution was filtered in a Mesh 100 filter and the filtered collected in a new tube. Subsequently, the filtrate was centrifuged at 1260 × g for 10 min, and supernatant was collected. To this supernatant was added one volume of extraction solution [four-fold dilute NIB, 2% (v/v) Triton X-100, β-mercaptoethanol 2% (v/v),

0.2% (v/v) protease inhibitor cocktail (P-9599, Sigma Aldrich) and 1% (v/v) phosphatase inhibitor cocktail (P-0044, Sigma Aldrich) and 30% (w /v) of polyethylene glycol 4000 (PEG 4000)]. This solution was vortexed for 30s, kept on ice for 30 min and centrifuged 3200 × g for 20 min at 4°C. After, the supernatant obtained, containing low abundance proteins, was collected and added a volume of 20% (w/v) trichloroacetic acid in acetone and 16 h at -20°C, in order to cause protein precipitation. The solution was centrifuged again at 6000 × g for 30 min at 4°C and the precipitate was washed three times in 80% (v/v) acetone, once in 70% (v/v) ethanol, in resuspension and centrifugation cycles at 6000 × g for 10 min at 4°C, and dried at room temperature.

Finally, pellets were resuspended in 7 M urea, 2 M thiourea and 4% (w/v) CHAPS, with the solution being solubilized using the UltraSonic Processor (Model GE 50). The samples remained on ice during the process and the potency used was 10%, for cycles of 5 to 10 s until complete pellet solubilization and the samples were stored at -80°C. Protein quantification was performed by the Bradford method with a bovine serum albumin standard to ensure a protein concentration between 1 and 15 mg/mL (Bradford 1976).

2.2.2 TWO-DIMENSIONAL ELECTROPHORESIS (2D-PAGE)

The isoelectric focusing (IEF) was performed in a 13 cm IPG strip pH 4-7 (GE Healthcare). Initially, the strips were rehydrated for 20 h in 250 μL of rehydration buffer [7 M urea, 2 M thiourea, 2% (w/v) CHAPS, 0.002% (w/v) bromophenol blue, 2% IPG-buffer and 0.2% (w/v) DTT] containing 1.0 mg protein for each sample. The protein extracts were separated in the first dimension at 20°C using an IPGphor3 isoelectric focusing system (GE Healthcare). The voltage settings for IEF was 200 V for 1 h, 500 V for 2 h, 1000 V for 4 h, 8000 V for 4 h, and 8000 V into a total of 46.9 kVh.

The strips were subjected to reduction with equilibrium solution [50 mM Tris-HCl pH 8.8, 6 M urea, 30% (v/v) glycerol, 4% (w/v) SDS, 0.002% (w/v) bromophenol blue] and 1% (w/v) DTT and then alkylated with an equilibrium solution containing 2.5% (w/v) iodoacetamide for 30 min at room temperature and in the absence of light. The second-dimensional electrophoresis was performed on a 12.5% polyacrylamide gel using the Hoefer SE 600 Ruby electrophoresis unit (GE Healthcare) and according to the methodology described by Laemmli (1970). At the end of the electrophoresis, the phosphorilated proteins staining procedure was performed for detection. The gels were stained with Pro-Q® Diamond Phosphoprotein Stain kit – Pro-Q DPS (Invitrogen, Carlsbad, CA), used to detect phosphate

groups bound to serine, tyrosine or threonine residues in phosphoproteins, according to the method described by Agrawal and Thelen (2009). This procedure consists of five steps (which occurred with constant shaking on an orbital shaker at low speed): i) submersion of the gels in fixation solution [50% (v/v) methanol and 10% (v/v) acetic acid in deionized water] for 30 min, procedure performed twice; ii) submersion in deionized water for 15 min, procedure performed twice; iii) incubation in staining solution [three-fold dilution Pro-Q DPS (v/v) in deionized water] for 2 h in the dark; iv) immersion destaining solution [50 mM sodium acetate-acetic acid pH 4.0 and 20% (v/v) acetonitrile in deionized water] for 30 min in the dark, procedure performed four times; v) washing with deionized water in the dark for 5 min, procedure performed twice.

The gels were then scanned in a FLA 5100 laser scanner using the 532 laser source for electron excitation and 580 nm emission filters for light emission. The images containing the spots stained for phosphorylated proteins were calibrated using the Image Gauge Analysis software (Fujifilm, Stanford, CT). Soon after the gel images were captured by fluorescence, the gels were stained for protein detection, being submerged in Coomassie Blue G-250 solution [8% (w/v) ammonium sulfate, 0.8% (v/v) phosphoric acid, 0.08% (w/v) Coomassie Blue G-250 and 20% (v/v) methanol] for 48 h, according to (Neuhoff et al. 1985), and washed with 1% (v/v) acetic acid solution until complete elimination of excess dye and kept in 10% (v/v) acetic acid solution. Lastly, the gels were scanned using ImageScanner III scanner (Amersham Biosciences) and LabScan software (GE Healthcare, Piscataway, NJ). The images of the gels stained with Pro-Q DPS were overlaid with Colloidal Comassie and the spots marked as phosphoproteins were located for later removal of the gels for identification.

The phosphoprotein and protein profiles of the infected and noninfected treatments for both genotypes were compared using ImageMaster2D Platinum 7 software (GE Healthcare) for the detection of differentially abundant protein spots. As threshold, the proteins were considered as differentially expressed, if they fitted the criteria: (i) a measured overlay variation above 1.0 (ratio normalization), (ii) ANOVA with p value less than 0.05 and (iii) presence in the three gels (biological replicates).

The spots stained with Pro-Q® Diamond with ratio values greater than 1.5 were considered to be differentially expressed phosphorylated proteins ($p < 0.05$). The three replicates were selected for identification by mass spectrometry for each treatment. The abundances (%V) of the phosphoprotein and protein spots differentially expressed using the above criteria were converted to fold-change and classified as up- or down-regulated, with

fold-change higher than 1.3 were plotted, according to Lima et al. (2019). A Venn diagram explaining the number of spots arranged for each treatment was generated with Venny 2.1.0 (https://bioinfogp. cnb. csic. es/tools/venny/), according to Oliveros (2015).

2.2.3. TRYPSINIZATION OF THE PROTEIN SPOTS AND LC/MS

The protein spots of the gels were cut and subjected to in-gel trypsin digestion according to Shevchenko et al. (2007). The protein spots were previously discolored in 50mM ammonia bicarbonate in 50% (v/v) methanol solution, followed by dehydration with acetonitrile. Proteins were then reduced with 200 mM DTT solution prepared in 100 mM ammonium bicarbonate for 30 min at 56°C and alkylation with 200 mM iodoacetamide solution in 100 mM ammonium bicarbonate for 30 min at room temperature. The pieces of gels were washed with 100 mM ammonium bicarbonate solution, dehydrated with acetonitrile and dried by vacuum centrifuging. For proteolytic digestion, the spots were rehydrated with 20 ng/μL trypsin solution for 20 h at 37°C. Digested peptides were extracted for three cycles using the extraction buffer [50% (v/v) acetonitrile and 5% (v/v) formic acid] and dried by vacuum centrifugation.

The digested peptides of phosphoproteins and proteins were dissolved in 0.1% (v/v) formic acid and analyzed by LC-MS using a nanoUPLC (nanoACQUITY-Waters) system containing a capillary column C18 BEH130 1.7 uM -100 nm × 100 mm, operating at a flow rate of 0.5 μL/min. The eluted peptides were automatically injected into an ION TRAP mass spectrometer (Amazon-Bruker), online using the nanoESI ionization needle. The scanning of the ions from the mass spectrometer was performed at between 300 and 1500 m/z in positive mode and data were acquired for 70 min in each LC-MS/MS analysis. The mass spectrometer was operated in the auto-MSn mode. Data acquisition of the LC-MS instrument was managed by Hystar software (Bruker) and the spectra were processed with the Data Analysis software (Bruker) using the default settings for proteomics.

2.2.4 IDENTIFICATION OF PROTEINS

The spectra were analyzed by PEAKS 7.0 program with a local client license, connected to a remote server to identify proteins (Ma et al. 2003). The parameters used in the program were: a protein list obtained from Phytozome, containing all the proteins described for soybean as database, methionine oxidation as a variable modification of cysteine

carbamidomethylation as a fixed modification, one missed cleavage, charge states of 2+, 3+, 4+, trypsin-like cleavage enzyme and mass error of 0.15 Da. For protein identification, we considered a false discovery rate (FDR) less than 1.0% along with at least three unique peptides. The databank Phytozome contains the sequences obtained by sequencing the soybean genome (*Glycine max*) (Goodstein et al. 2012). A database of genes for *Arabidopsis thaliana* (TAIR) was used to corroborate the identification of proteins.

2.2.5. PREDICTION OF THE PUTATIVE PHOSPHORYLATED SITES

The FASTA sequences of the proteins stained as phosphorylated were analyzed for possible phosphorylation sites. The prediction of the number of phosphorylation sites was performed online through the MUSITE website (http://www.musite.net), designed for plant protein and which allows variation in the occurrence of phosphorylation sites (Gao et al. 2010). For this approach, the general phosphorylation on serine and threonine was chosen and all the green plants were considered for group analysis. In order to have differentiated levels of requirement, the number of phosphorylation sites was determined to be 70% (low requirement) and 95%. The presence of homologous proteins or phosphorylated sites was confirmed using the Plant Protein Phosphorilation Data Base (P^3DB) site (http://www.p3db.org) (Yao et al. 2012; Gao et al. 2009) in order to verify whether the protein has already been identified as a target for phosphorylation. It is noteworthy that the non-identification of phosphorylation sites of a protein by the P^3DB site this does not necessarily imply that this protein is not phosphorylated.

2.3 METABOLIC PROFILING BY UNTARGET LC/MS

Metabolite extraction from plant tissue was performed according to the procedure described by Rogachev and Aharoni (2007) with some modifications (Gomez et al 2018). Leaves extract were prepared by powdering approximately 200 mg fresh weight in liquid nitrogen and 500 µl of extraction solvent [75% (v/v) methanol and 0.1% (v/v) formic acid] were added. After that, samples were shaken in vortex by four times for 20 s (on ice), subjected to ultrasound treatment for 5 min, placed on ice for 30 min and then centrifuged at 14000 × g for 30 min at 4 ºC. Then the supernatant was removed and transferred to a new tube. The new extraction cycle was carried out with the resulting pellet from the previous extraction in order to increase the extraction efficiency and then the supernatants were pooled.

After, the supernatant was centrifuged at 18000 × g for 20 min at 4°C and filtered using a PVDF membrane of pore size 0.22 µm. and 100 µL of the solution were then transferred into a vial. The analysis was carried out by injecting an aliquot of 10 µL in a Nano Liquid Chromatography - Mass Spectrometry (nanoLC/MS) using the nanoACQUITY UPLC system (Waters, Milford, MA, USA), containing a trap column and a capillary column ProteCol GHQ303 C18 3.0 µm – 300 µm × 150 mm, operating at a flow rate of 5.0 µL. min-1. The eluted metabolites were injected automatically into the microOTOF QII mass spectrometer (Bruker Daltonics, Bremen, Germany), working in online mode with the microESI ionization needle. A detailed description of all the steps and phase solutions used in gradient programs by LC/MS is shown by Gouveia et al (2019a) and presented by Gómez et al (2020).

The raw mass spectrometry data were converted into the mzML format using the Proteoizard convert tool, through the peak-picking algorithm (Tautenhahn et al. 2012), according to the procedure described by Gouveia et al. (2019b). From this, two approaches were used: i) obtaining the quantitative data of the metabolites using the XCMS platform and ii) identifying the putative metabolites using the Data Analysis software program and NIST library. The list peaks in mzML format were generated in the generic mascot format (mgf) by the Data Analysis software program, and the putative metabolites were identified using NIST library, containing the MS2 spectra for standard compounds downloaded from MassBank of North America, and converted for the NIST format (the tutorial and download can be seen in Gouveia et al. 2019) The raw data converted into mzML were also used to compare the LC/MS metabolite profiles from root extracts by XCMS platform (https://xcmsonline. scripps. edu). The alignments were performed using the default parameters for the UPLC/Qtof system, with 20 ppm accuracy for MS1 and a metabolite database for *A. thaliana*. The multigroup method was used to contrast the treatments.

The Multi-Omic module was used for pathway inference against the metabolite database from *A. thaliana*. A table metabolite containing the intensity of all ions detected in the runs. Lastly, it was exported from the XCMS platform and used as an input for statistical analysis which was carried out by the MetaboAnalyst web-based platform (http://www.metaboanalyst.ca/), using the modules "Statistical analysis" for analysis of individual metabolites and "Functional Analysis" for pathway analysis. Previously, low quality data (maxint ≤ 2000 and/or p-value ≥ 0.05) was removed from table. The quality filters based on standard deviation methods were used to automatically remove low-quality data. The intensity values were then normalized by the weight of the samples and the data

were converted using the Pareto Scaling method. Partial Least Squares - Discriminant Analysis (PLS-DA) and classify the ions (VIP score) were used to determine how the differential accumulation of metabolites in the group of treatments by order of importance, while box-plot graphics and Heatmap based on One-way analysis of variance (ANOVA) were used to visualize the compounds with differential abundance (**Appendix N and O**).

2.4 METABOLIC PROFILING BY TARGET LC/MS

Metabolites were extracted from soybean leaves according to the procedure described by Muller and Munné-Bosch (2011) with some modifications (Lima et al. 2019; Coutinho et al. 2019; Vital et al. 2019). Leaves extract were prepared by powdering approximately 110 mg fresh weight in liquid nitrogen and 400 µL of extractive solution [methanol, isopropanol and acetic acid 20:79:1 (v/v/v)] were added. After that, samples were shaken in vortex by four times for 20 s (on ice), subjected to ultrasound treatment for 5 min, placed on ice for 30 min and then centrifuged at 14000 × g for 30 min at 4 ºC. Then the supernatant was removed and transferred to a new tube. The new extraction cycle was carried out with the resulting pellet from the previous extraction in order to increase the extraction efficiency and then the supernatants were pooled. Finally, the total supernatant was filtered through 0.45 mm filters, and about 400 µL of the extracts were placed in vials and 5.0 µL were injected into the LC/MS system (Agilent Eclipse Plus, RRHD, 1.8 µm, 2.1 × 50 mm), with continuous flow (Φ = 0.3 mL/min), joined online with a QQQ triple quadrupole mass spectrometer (Agilent).

The compounds were separated by ultrahigh performance chromatography (UHPLC, Agilent) using column chromatography C18 (50 mm × 1.0 mm ID, 1.7 µm particle and 300 A) coupled with the mass spectrometer (QqQ Agilent) at negative/positive modes, alternating according to the retention time for each one hormone. The samples were scanned by MRM (multiple reaction monitoring) for detecting each hormone. The tests were carried out for four biological replicates for each treatment. The mass spectrometry was processed using the Skyline software according to the methods describe by Coutinho et al. (2019) and Vital et al. (2019).

Analyzing area values were converted using Excel program into extracted ion chromatogram (XIC) area/g (fresh plant compound/plant tissue). Cluster analysis was also performed using the heatmap method by the Metaboanalyst 5.0 web platform (https://www.metaboanalyst.ca/) in terms of relative abundances (XIC areas) in the genotypes and treatments. the data were normalized by the median and the heatmap was obtained using

the following parameters: Distance Measure: Euclidean; Clustering algorithm: Ward; Data source: Normalized data; Standardized data: automatic scaling capabilities; Test t/ANOVA; Options: Show only the group average; and Display Mode: Overview. For the quantitative analysis of the characterized compounds, one-way analysis of variance (ANOVA) was used with the following parameters: Adjusted p-value (FDR) cut-off point: 0.05; Post-hoc analysis: Fisher's LSD. The identified compounds were organized into an isoflavonoid synthesis metabolic pathway provided by KEGG (https://www.genome.jp/pathway/map00943) and referenced for the relative abundance of heatmap colors for each treatment.

3 RESULTS

3.1 SYMPTOMS OF HYPERSENSITIVE RESPONSE

Infection of soybean plants with *P. syringae* pv. tomato triggered a hypersensitive response (HR), however the evolution of the symptoms was distinct (**Figure 1**) when the transgenic plants (C9) were compared with wild-type (WT), as also observed by Carvalho et al. (2014) and Rodrigues et al. (2021).

Figure 1 – Soybean leaves overexpressing BiP (C9) and untransformed (WT) submitted to inoculation by *P. syringae* pv. tomato at 36 hours after inoculation.

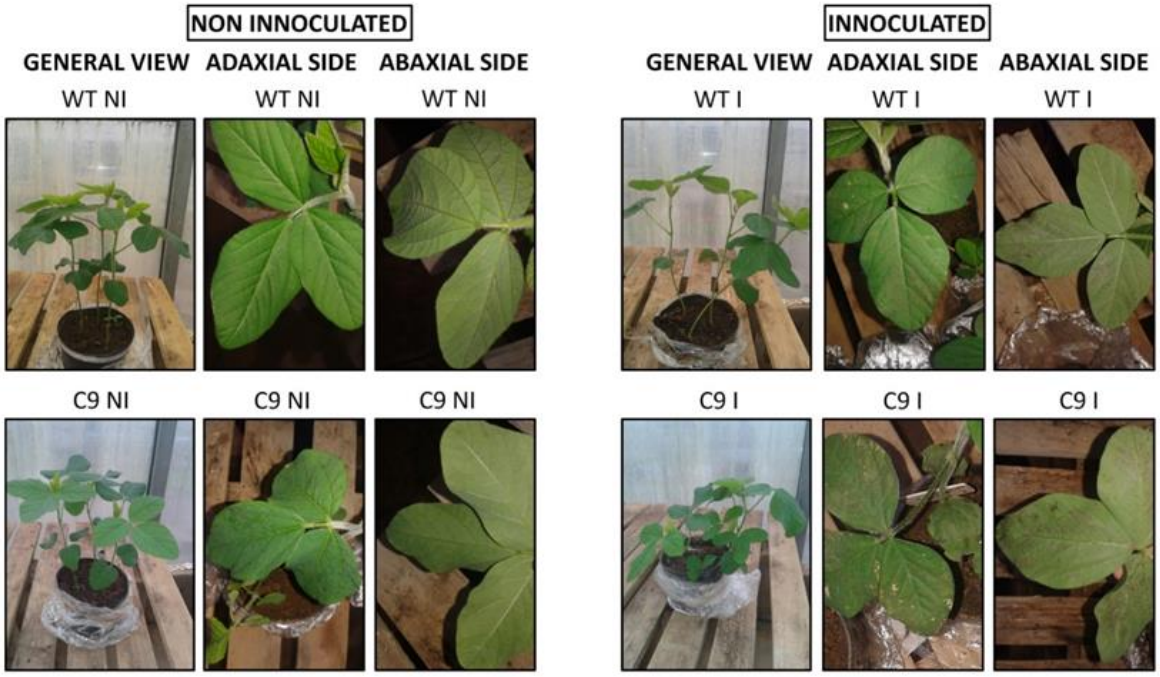

Source: Survey's data.

It was possible to observed the presence of brown halos, corresponding to groups of cells whose programmed cell death (PCD), forming a region of necrotic cells around the site of infection, which may be act to contain the bacterial spread. Symptoms were noticeable in both the adaxial and abaxial regions of the inoculated leaves, these being more pronounced in the C9 genotype (**Figure 1**). In turn, no visible symptoms were observed in leaves of plants not infected with the bacteria.

3.2 PROTEIN

Through LC/MS-2-DE/SDS-PAGE analysis, changes in the protein profile of soybean genotypes in response to infection by non-compatible phytobacterium *P. syringae* pv. tomato was investigated. Comparisons were performed by contrasting treatments for the same genotypes (WT: I x NI, C9: I x NI) and genotypes for the same treatment noninfected (NI: WT x C9), totaling three contrasts. Data referring to the identification of protein spots on the gels can be verified in **Appendix A, B and C**, and data referring to the identification number of protein spots (Spot ID) can be verified in **Appendix D, E and F.** Overall analysis based on functional classes of the dysregulated proteins in response to infection bacterial indicated different behavior related to genotypes. By the Venn diagram (**Figure 2A)**, from a total of 87 proteins, 37 were detected only at least one WT genotype treatment, at least one treatment of genotype C9 and 15 in both genotypes. In the WT genotype, 29 proteins were detected in the NI treatment, three proteins in treatment I and 19 proteins in both treatments, while in the genotype C9, six proteins were observed for the NI treatment, ten proteins for treatment I and 34 proteins for both. Four proteins were responsive in the treatments: Lactate/malate dehydrogenase family protein (mitochondrial); Esponsive to dehydration 21B; Fe Superoxide dysmutase 1; and Aspartate aminotransferase, chloroplastic (spots 129, 97, 3 and 4, respectively). It was possible to verified differences in the variation of the protein abundances which the WT genotype showed the majority as down-regulated (**Figure 2B**). Proteins belongs of the photosynthetic and primary metabolism were the major class negatively affected in their abundances in response to infection for both genotypes (**Figure 2C and D**). One another way, antioxidant metabolism enzymes were the most up-regulated in number in both genotypes. The up-regulation proteins were distinct between genotypes, being verified a higher number in C9 related to antioxidant stress (**Figure 2C and D**).

Figure 2 – In **(A)** Venn Diagram showing the comparison of the number of proteinas differentially expressed. In **(B)** percentual of up-regulated or down-regulated proteins in response to bacterial infection in the leaves from WT and C9 genotypes. In **(C)** and **(D)** functional categorizations of diferentially expressed proteins responsive to infection.

A

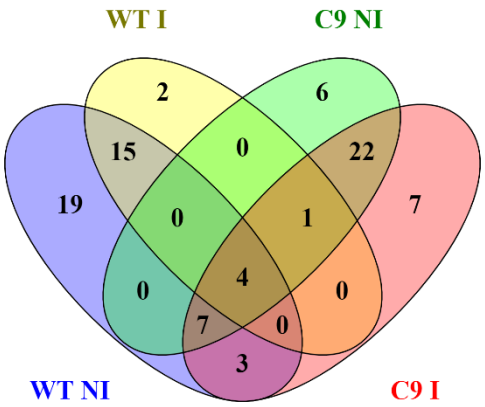

B

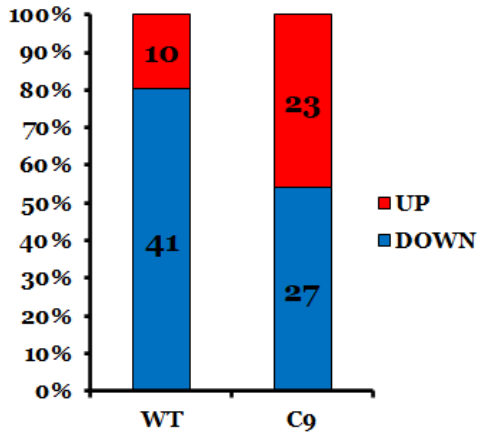

C

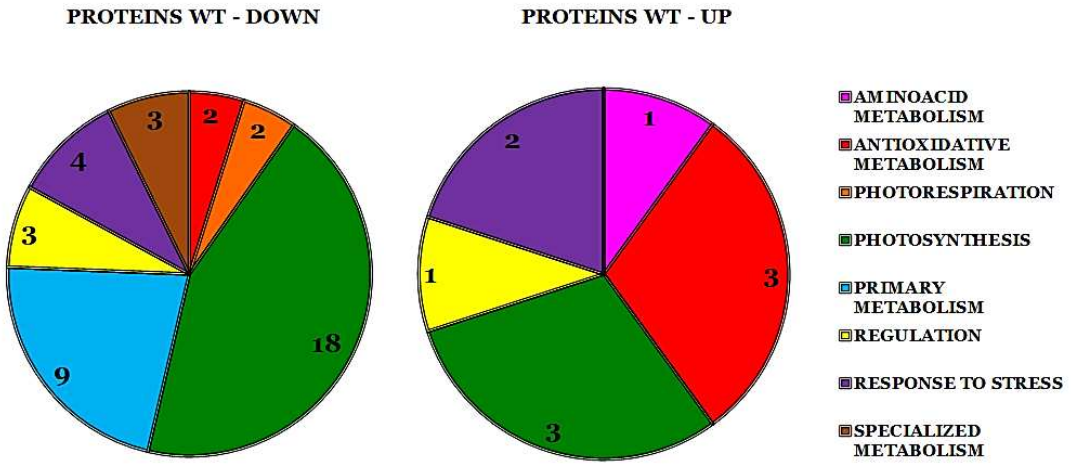

D

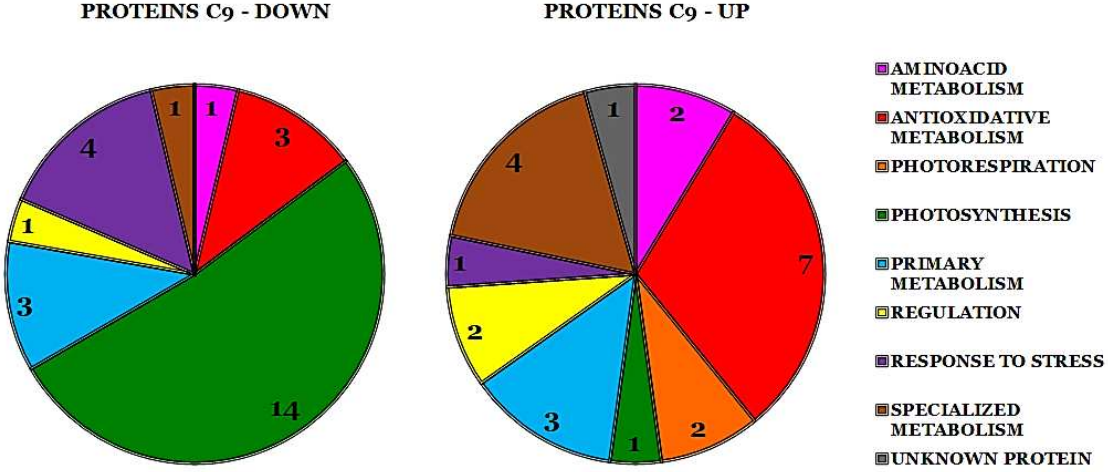

Source: Survey's data.

Of the proteins spots responsive in the contrasts WT I x WT NI, 51 were identified by LC/MS, corresponding to 39 different proteins (**Figure 3**). The remaining (12 spots) possibly correspond to isoforms or post-translational modifications with different spots for a protein in the same gel. Those 51 identified spots, ten proteins had your relative abundance increased or were found exclusively in NI treatments, and 41 had their relative abundance decreased in response to bacterial infection or were found only in treatments I. (**Figure 2B and 3**). for contrast C9 I x C9 NI, 50 dysregulated proteins were identified by LC/MS, corresponding to 41 different proteins and 9 isoforms or post-translational modifications. Those, 23 proteins were down-regulated or found exclusively in NI, and 27 treatments were up-regulated or found only in Treatments I (**Figure 2B and 4**).

Some proteins responsive to infection were observed as up-regulated in the WT genotype (**Figure 3**) and may be involved in the plant defense, such as DNA mismatch repair protein MSH3 (spot 130), Vegetative storage protein 1 (spot 37), Chaperonin 20 kDa, chloroplastic (spot 186), an isoform of Fe superoxide dismutase 1 (spot 3) and Aspartate aminotransferase, chloroplastic (spot 4). Most of the dysregulated proteins in the C9 genotype infected were more up-regulated in response to bacterial infection than WT genotype infected (**Figure 4**). Proteins involved in several processes were differentially expressed, such as antioxidative metabolism [NADPH-dependent alkenal/one oxidoreductase, Fe superoxide dismutase 1, two isoforms of Glyoxalase I homolog and Brassinosteroid-6-oxidase 2 (spots 80, 3, 199, 46 and 108)]; aminoacid metabolism [Cysteine synthase B/O-acetylserine (thiol) lyase B and 2-Keto-3-deoxyarabinoheptulosonate-7-phosphate synthase (spots 196 and 104)]; response to stress [GDSL-like esterase/acyltransferase/lipase superfamily protein (spot 41)] (**Figure 4**).

Figure 3 – Differences in the protein abundances expressed as fold change between the volume (%) of each protein spot of the leaves from wild-type genotype (WT) under infection (I) or mock inoculation (NI) by *P. syringae* pv. tomato. Positive and negative fold change values indicate up- and down-regulation, respectively. Values of fold change for protein spots when present only in a genotype or treatment are shown as 10.00 or -10.00, respectively.

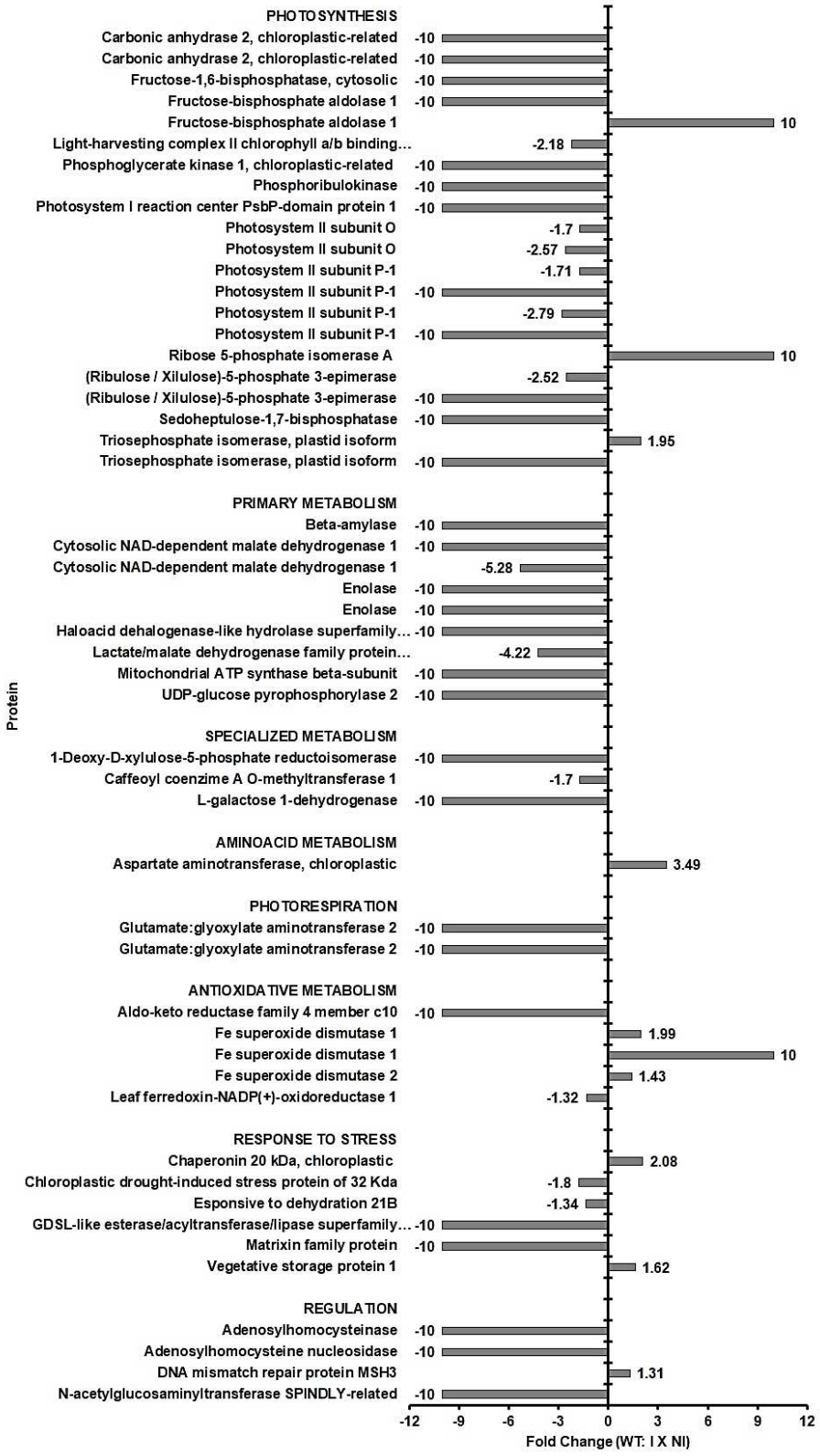

Source: Survey's data.

Figure 4 – Differences in the protein abundances expressed as fold change between the volume (%) of each protein spot of the leaves from overexpressing BiP genotype C9 under infection (I) or mock inoculation (NI) by *P. syringae* pv. tomato. Positive and negative fold change values indicate up- and down-regulation, respectively. Values of fold change for protein spots when present only in a genotype or treatment are shown as 10.00 or -10.00, respectively.

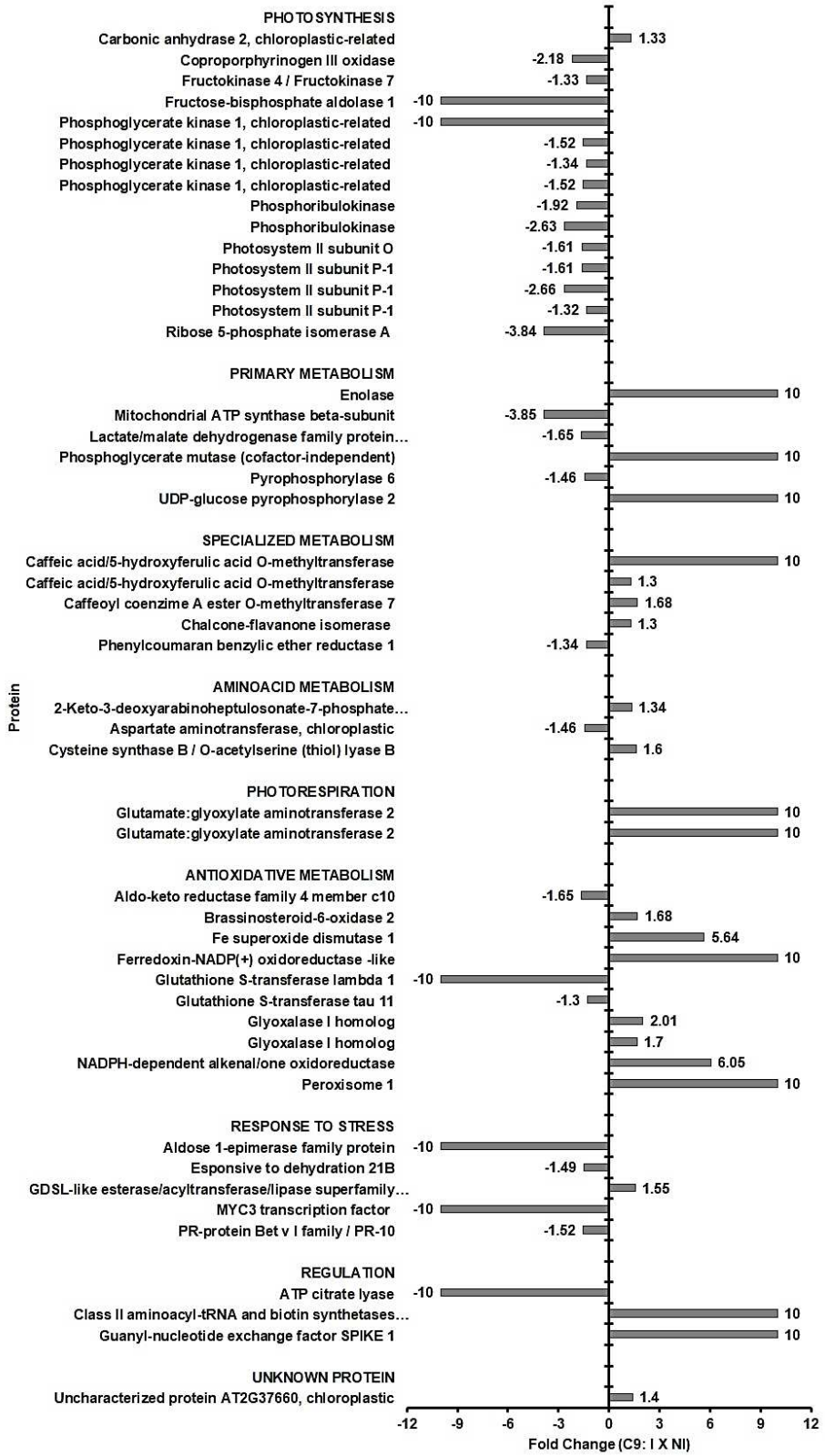

Source: Survey's data.

Some enzymes from specialized metabolism showed isoforms, highlighting the Caffeic acid/5-hydroxyferulic acid O-methyltransferase, found in the C9 genotype, exclusively in treatment infected (spot 108) or being up-regulated (spot 114). It acts mainly in the methylation of hydroxycinnamic acids, essential in the synthesis of lignans and phenolic compounds. The spot 94 was identified as distinct genes, one for each genotype, encoding distinct proteins with caffeoyl coenzyme A O-methyltransferase function. For the WT genotype, a Caffeoyl coenzyme A O-methyltransferase 1 (Glyma.07g214700.1.p) was detected and was down-regulated, while for the C9 genotype, a Caffeoyl coenzyme A ester O-methyltransferase 7 (Glyma.01g004200.1.p) was detected and was up-regulated. Another protein up-regulated in the C9 genotype in response to bacterial infection was identified as UDP-glucose pyrophosphorylase, which is involved in the primary synthesis of UDP-sugars. Nucleotide sugars are the key precursors for all glycosylation reactions and it has been involved in plant defense pathways (Chivasa et al. 2012; Decker and Kleczkowski 2019).

Finally, for evaluate the effect of the transgene, the C9 genotype overexpressing BiP were compared with its isoline WT in absence (**Figure 5**, C9NI x WTNI). In general, low number of protein spots showed differences of abundances when leaf profiles of both genotypes were compared in absence of infestation, as also observed by Coutinho et al. 2018, highlighting most as up-regulated in response to overstressing of BiP.

3.3 PHOSPHOPROTEIN

We used the Pro-Q® Diamond dye to generate 2DE/SDS-PAGE profiles of phosphorylated proteins that are responsive to bacterial infection (**Figure 6, 7** and **8**). The spots that showed differential abundances in the phosphorylation of proteins in the two-dimensional gels for each treatment are represented. Data referring to the identification of phosphorylated protein spots on the gels can be verified in **Appendix G, H and I**, and data referring to the identification number of phosphorylated protein spots (Spot ID) can be verified in **Appendix K, L and M**.

Figure 5 – Differences in protein abundances expressed as fold change between the volume (%) of each protein spot of the leaves from both genotypes in absence of bacterial infection (**C9NI x WTNI**). Positive and negative fold change values indicate up- and down-regulation, respectively.

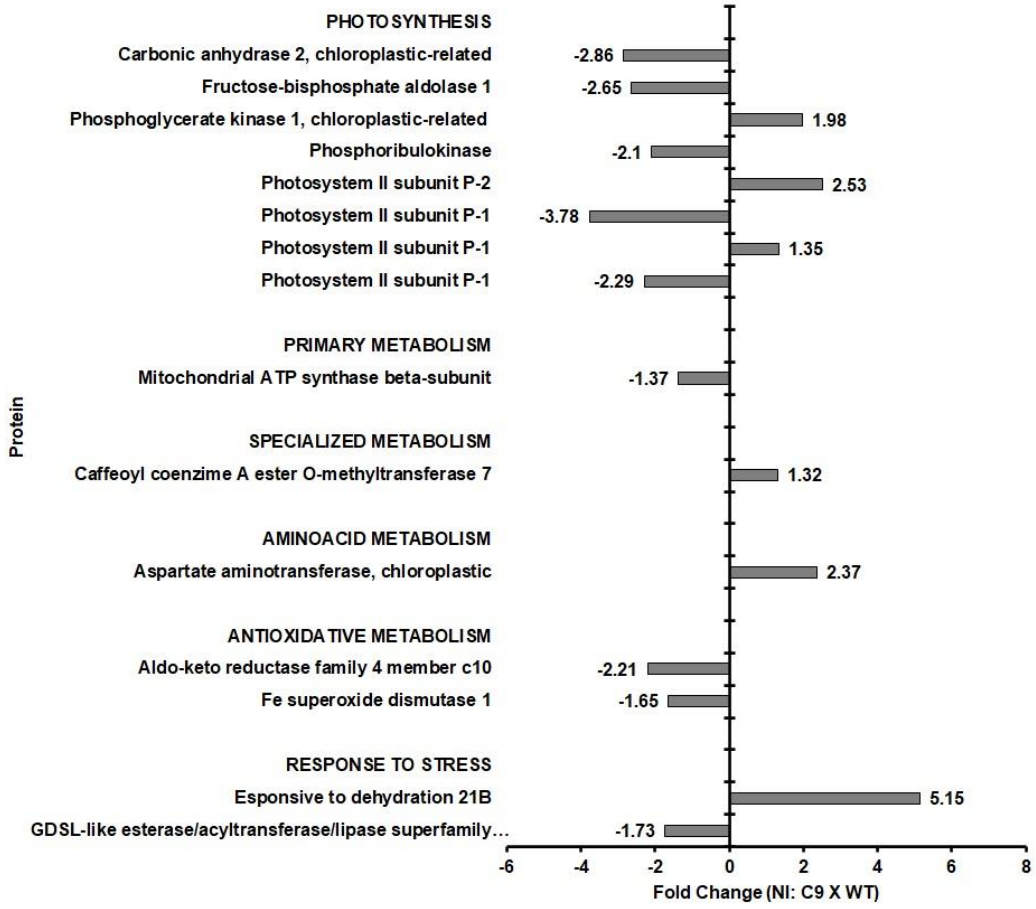

Source: Survey's data.

Analysis of the functional distribution of phosphorylated proteins indicates that those that showed differential expression are mostly from the photosynthetic apparatus (**Appendix J**). While in the WT genotype, 13 phosphoproteins were were up-regulated or and 11 were down-regulated, in the C9 genotype more than 70% of the identified phosphoproteins were up-regulated. By the Venn diagram, two phosphoproteins were detected in the four treatments, corresponding to two proteins of the Photosystem II subunit P-1 (spots 51 and 143) (**Appendix J and Figure 6, 7 and 8**). In the WT genotype, ten phosphoproteins were detected in the NI treatment, one phosphoprotein in treatment I and 13 phosphoproteins in both treatments (accounting for 24 phosphoproteins), while in the C9 genotype, one was observed one phosphoprotein for treatment NI, Ten phosphoproteins for treatment I and four phosphoproteins for both (accounting for 15 phosphorylated proteins). In another hand, 14 phosphoproteins were detected in at least one treatment of the WT genotype, at least one

treatment of the genotype C9 and ten in both genotypes, totaling 29 phosphorylated proteins expressed.

Figure 6 – Differences in the protein abundances expressed as fold change between the volume (%) of each phosphoprotein spot stained by Pro-Q® Diamond of the leaves from overexpressing BiP genotype WT under infection (**WTI x WTNI**). Positive and negative fold change values indicate up- and down-regulation, respectively. Values of fold change for protein spots when present only in a genotype or treatment are shown as 10.00 or -10.00, respectively.

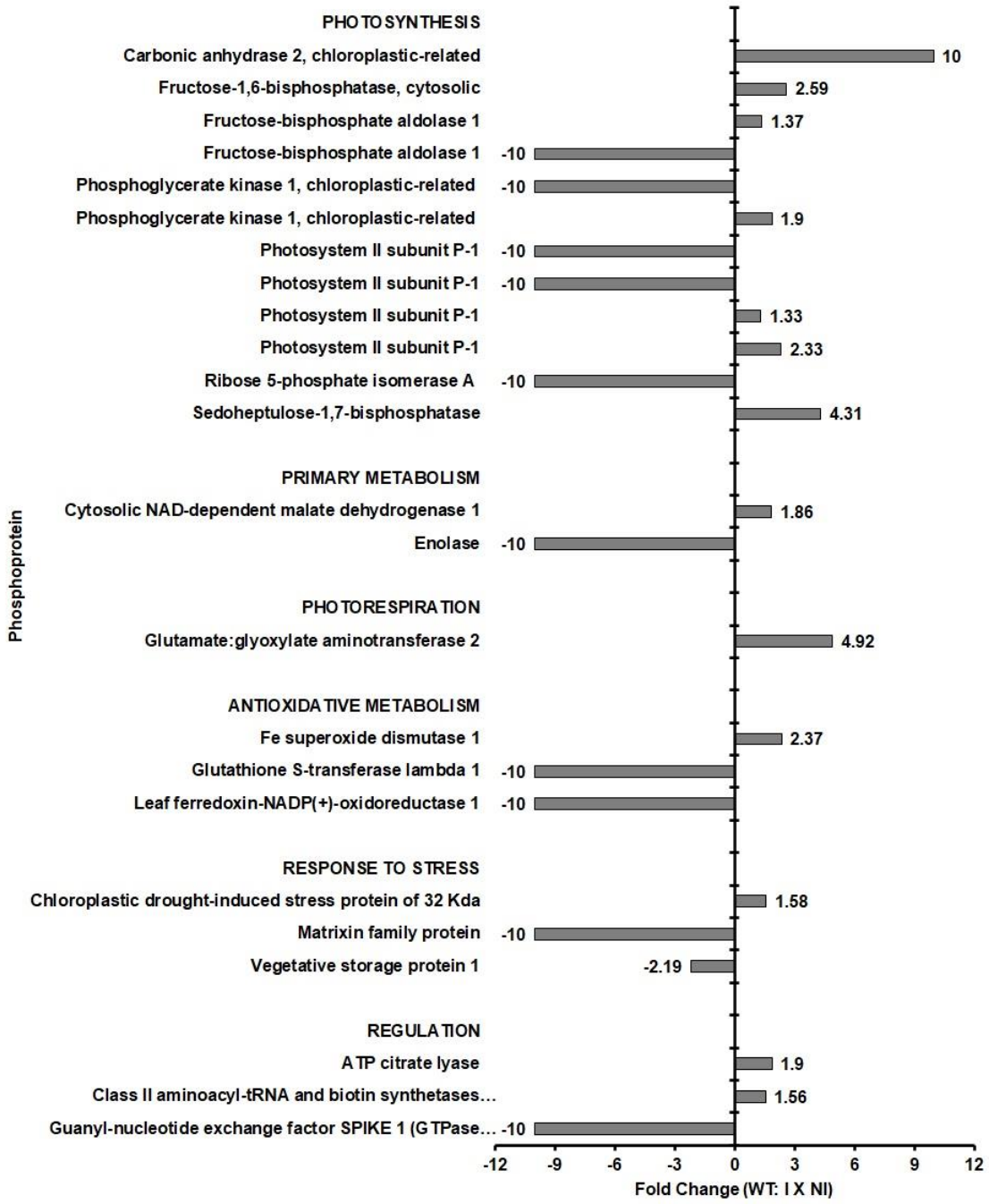

Source: Survey's data.

Of the proteins labeled as phosphorylated in which upregulation was observed for the infected WT genotype (**Figure 6**), there was greater differential expression in proteins related to photorespiratory, antioxidative and carbohydrates [Glutamate: glyoxylate aminotransferase 2 (spot 57, FC = 4.92), Sedoheptulose-1, 7-bisphosphatase (spot 16, FC = 4.31), Fructose-1,6-bisphosphatase cytosolic (spot 17, FC = 2.59), Fe superoxide dismutase 1 (spot 3, FC = 2.37) and one isoform of Photosystem II subunit P-1 (spot 143, FC = 2.33)]. In turn, four proteins had decreased expression, and among them, Vegetative storage protein 1 (spot 37) had lower expression (FC = -2.2).

Figure 7 – Differences in the protein abundances expressed as fold change between the volume (%) of each phosphoprotein spot stained by Pro-Q® Diamond of the leaves from overexpressing BiP genotype C9 under infection (**C9I x C9NI**). Positive and negative fold change values indicate up- and down-regulation, respectively. Values of fold change for protein spots when present only in a genotype or treatment are shown as 10.00 or -10.00, respectively.

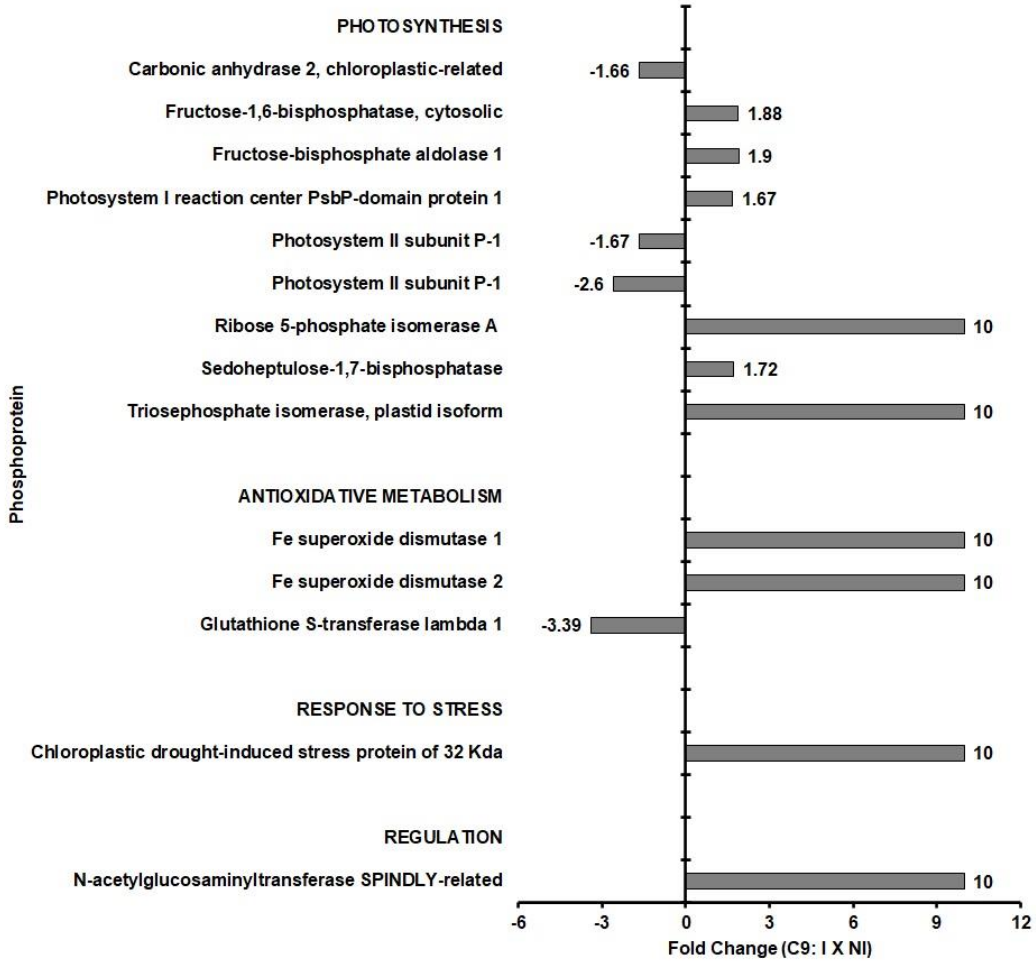

Source: Survey's data.

Four phosphoproteins had their expression significantly increased in C9 (**Figure 7**): Photosystem I reaction center PsbP-domain protein 1, Sedoheptulose-1,7-bisphosphatase, Fructose-1,6-bisphosphatase, cytosolic and Fructose-bisphosphate aldolase 1 (spots 181, 16, 17 and 131), with Fructose-bisphosphate aldolase 1 having the greatest increase in expression (1.9-fold). Another four proteins were down-regulated in the C9 genotype, mostly proteins related to photosynthesis and antioxidant metabolism [Glutathione S-transferase lambda 1 (-3.39-fold), two isoforms of Photosystem II subunit P-1 and Carbonic anhydrase 2 chloroplastic-related (spots 219, 51, 143 and 101)]. In phosphoproteins expressed in non-inoculated plants with HR-causing bacteria (NI; **Figure 8**), the greatest increase in expression of Carbonic anhydrase 2 chloroplastic-related in the C9 genotype (7.22-fold) is highlighted.

Figure 8 – Differences in protein abundances expressed as fold change between the volume (%) of each phosphoprotein spot stained by Pro-Q® Diamond of the leaves from both genotypes in absence of bacterial infection (**C9NI x WTNI**). Positive and negative fold change values indicate up- and down-regulation, respectively.

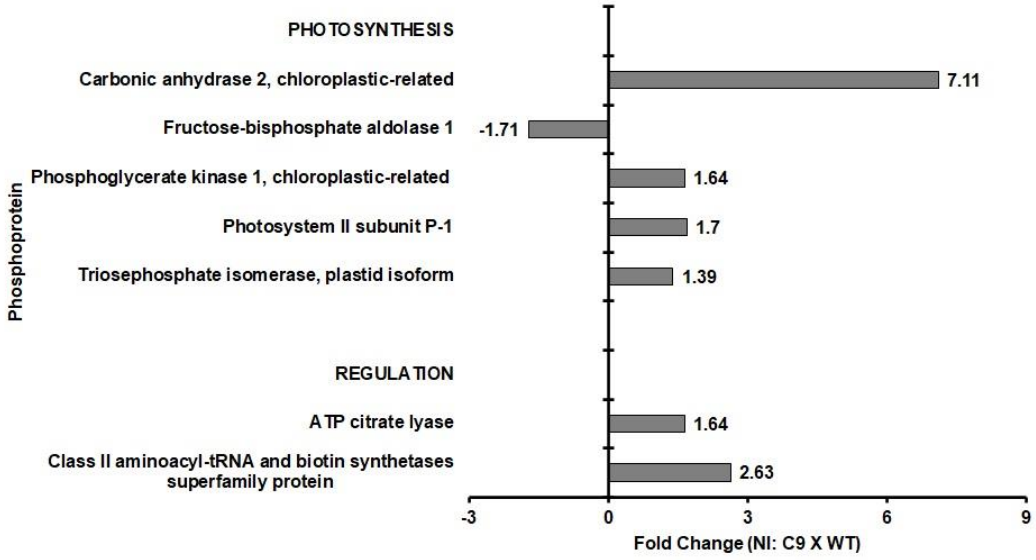

Source: Survey's data.

3.4 UNTARGETED METABOLITES PROFILING BY LC/MS

Since the LC/MS-2DE results indicated changes in the differential expression of proteins and phosphoproteins related to the synthesis and methylation of phenolic compounds and involved in oxidative stress in response to inoculation with *P. syringae* pv. tomato, the metabolic profile in soybean roots by LC/MS was also performed (**Figure 9**). The chromatograms were aligned (**Figure 9C**) to identify compounds and pathways significantly

altered in response to the treatment (**Figure 9A** and **B**) using the MetaboAnalyst platform. All detected ions were contrasted against an Arabidopsis metabolite library (KEGG) to identify which metabolic pathways were most affected by the biotic treatment (**Figure 9B**) The main altered pathways belonging to the synthesis of phenolic compounds such as flavonoids and phenylpropanoids (green, blue, yellow, purple and orange), in addition to pathways of metabolism of cyanoamino acids (precursors to glucosinolates) and biosynthesis terpenoids (precursors of photosynthetic pigments and important specialized metabolites; indigo). The biosynthesis of flavonoids (green) and phenylpropanoids (orange) were the pathways that had the highest number of altered ions involved (24 and seven, respectively). In the heatmap plot (**Figure 9A**), these ions formed clusters, indicating higher abundances of one cluster for the infected C9 genotype and another for the infected WT. The fragmentation spectra of some altered ions were used to identify them using the DataAnalysis software and the NIST library.

Figure 9: Analysis of the metabolite profiles from soybean leaves by LC/MS Q-TOF. All runs were aligned using XCMS algorithm in **(C)** and the intensities of the fifty principal ions were compared in **(A)** and the metabolic pathway analysis were performed using MetaboAnalyst platform in **(B)**. Colored boxes by red, green, yellow, indigo, orange, purple and blue in **(A)** correspond to the ions belongings to the pathways assigned in the (B). The m/z of the ions showed in (B) are the medium values of 4 replicates.

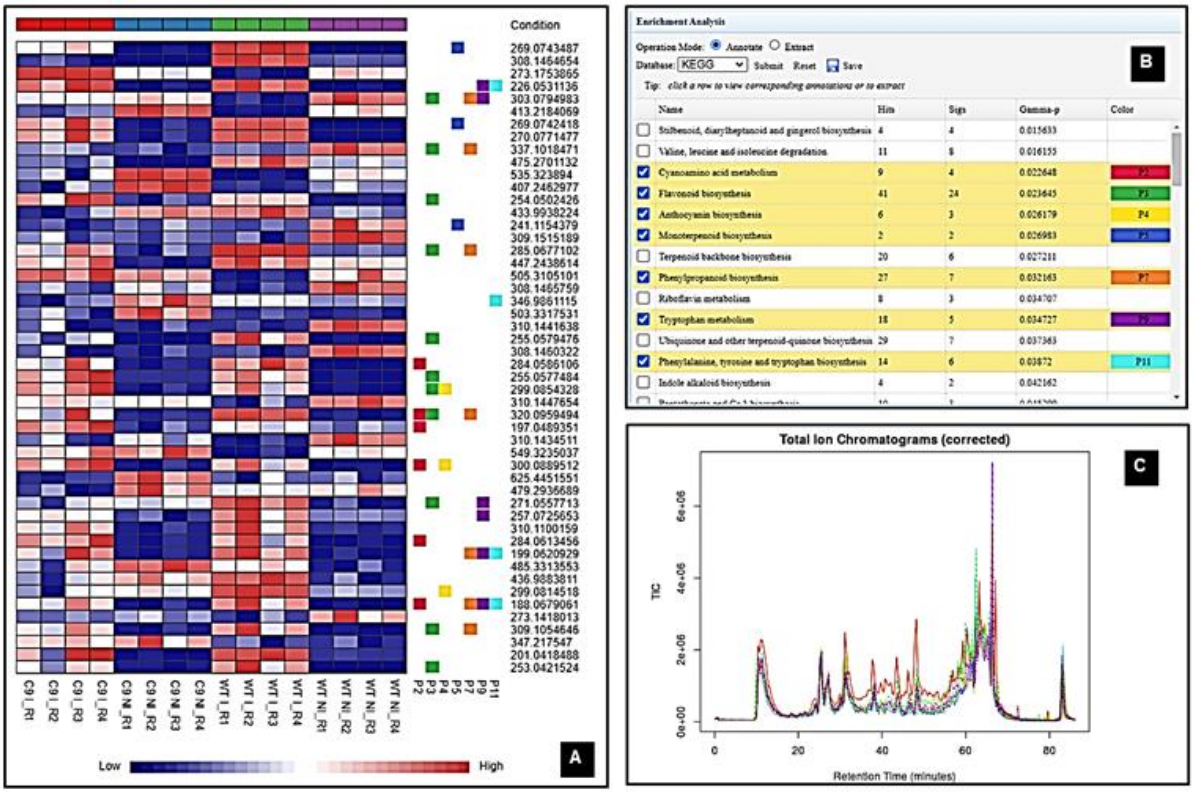

Source: Survey's data.

Putative identifications were possible for some ions present in higher abundances in plants under infection. The peak intensity data of the chromatograms of these compounds from XCMS alignments were analyzed in the MetaboAnalyst web-platform, where box-plot graphs of the treatments were obtained (**Figure 10**). In six of the putative metabolites identified by the NIST platform there was a greater increase for the WT I genotype: m/z=285,0697 (M285T44_1): 4',7-Dihydroxy-6-methoxyisoflavone (glycitein); m/z = 299,0914 (M299T41): 7,4'-dimethoxy-5-hydroxyisoflavone (4',7-dimethoxygenistein); m/z = 323.1278 (M323T63): 3'-prenyl-4',7-dihydroxyisoflavone (neobavaisoflavone) (the levels in WT I being similar to the levels observed in the C9 genotype treatments); m/z = 479.1189 (M479T27): 3-O-glucosyl-3'-methylquercetin (isorhamnetin-3-O-glucoside); m/z = 533,129 (M533T32): 7-(7-O-(6"-O-malonyl)-β-D-glucosyl)-4'-hydroxy-6-methoxyisoflavone (6"-O-malonylglycitin); m/z = 547.1369 (M547T46): 7-O-(6"-O-malonyl)glucosyl-6,4'-dimethoxyisoflavone (afrormosin-7-O-glucoside-6"-O-malonate). In two compounds, an increase in the relative abundance of the C9 I treatment was observed: m/z = 275,201 (M275T57): 9-oxo-10E,12Z,15Z-octadecatrienoic acid (9-OxoOTrE), similarity, neutral loss of 17 kDa; and m/z = 299,1796 (M301T56): 4'-methyl-luteolin (diosmetin) or 4'-methylkaempferol (kaempferide).

Three compounds showed a significant increase in relative abundance for both infected genotypes: m/z = 269,0444 (M267T63): coumestrol (increase in C9 plants greater than in WT); m/z = 269,0808 (M269T59): 3-Hydroxy-7-methoxyflavone; and m/z = 299,0914 (M299T60): 7-hydroxy-2',4'-dimethoxyisoflavone (2'-methoxyformononetin) (**Figure 10**). Levels were higher in the C9 genotype than in the WT genotype in the compound m/z = 275. 2006 (M275T63): 9-oxo-10E,12Z,15Z-octadecatrienoic acid (9-OxoOTrE), similarity, neutral loss 17 kDa; and a decrease in abundance was observed in infected plants of compounds m/z = 269,0808 (M269T61): formononetin (7-hydroxy-4′-methoxyisoflavone) and m/z = 317.0590 (M317T27): 3-methylquercetin (isorhamnetin). Therefore, the metabolic profiles corroborate the LC/MS-2DE results that the biosynthesis pathways of phenolic compounds such as isoflavones, flavones and flavonols were responsive to the stress caused by bacterial inoculation in soybean leaves, showing increased levels in infected plants.

3.5 METABOLITES PROFILING BY LC/MS

Specialized metabolites have been observed as responsive to cross-tolerance to biotic and abiotic environmental stresses, especially phenolic compounds, including flavonoids. Thus, a LC/MS-based method was applied to analysis some target compounds (**Figure 11**). Alterations in the abundance of ferulic acid, coniferyl aldehyde and coumarin for the C9 transgenic genotype were observed after infection, with a lower relative abundance than in the control treatment and compared to its WT infected isoline. The greatest decrease in the relative concentration of C9 I was observed for ferulic acid, with a reduction of 60.9%). The presence of two putative Gossypin compounds, for two retention times (3.3 and 7.0 minutes), a polyhydroxyflavonol [gossypetin (3,5,7,8,3',4'-hexahydroxyflavone) 8-O-beta-D-glucoside] was observed with a significant response in C9-infected leaves, and, for RT = 7.0, the levels were higher when compared to the noninfected C9 genotype, and lower when compared to the infected WT genotype for RT = 3.3 (**Figure 11**).

Phytoalexins are a structural and functional complexity of this class of phenolic compounds. This presence in infected cells may limit the spread of biotrophic and necrotrophic pathogens. Thus, we also analyzed the presence of phytoalexin isoflavonoids by LC/MS-based approach to evaluate their relative abundance in soybean infected leaves (**Figure 11**). In the chromatograms, more than one intensity peak was detected in some compounds containing the same transitions from the MRM. They are possibly structural isomers of the same aglycone. As they have side groups in different positions from the aglycone nucleus, their cleavage produces fragments with different m/z ratio, retention time, molecular weight and relative intensity. In order to clarify whether the compound shown in the peak is the aglycone, the Fragment Relative Intensity (FRI%) graph was sketched (**Appendix P**). The proportion and relative abundance of ion fragments are directly related to the abundance of the compound as a whole and, therefore, disproportions in the relative intensities of fragments in compounds with low abundance must be considered, especially in treatments without inoculation.

Figure 10 – Normalized relative abundances of some ions showing alterations in the C9 and WT genotypes under infection (I) and mock innoculation (NI) by *P. syringae* pv. tomato. Putative identifications were obtained for the metabolites listed below. M267T63: Coumestrol; M269T59: 3-Hydroxy-7-methoxyflavone; M275T57: 9-oxo-10E,12Z,15Z-octadecatrienoic acid (9-OxoOTrE); M285T44_1: 4',7-Dihydroxy-6-methoxyisoflavone (glycitein); M299T60: 7-hydroxy-2',4'-dimethoxyisoflavone (2'-methoxyformononetin); M479T27: 3-O-glucosyl-3'-methylquercetin (isorhamnetin-3-O-glucoside); M533T32: 7-(7-O-(6"-O-malonyl)-β-D-glucosyl)-4′-hydroxy-6-methoxyisoflavone (6"-O-malonylglycitin); M547T46: 7-O-(6"-O-malonyl)glucosyl-6,4'-dimethoxyisoflavone (afrormosin-7-O-glucoside-6"-O-malonate); M323T63: 3'-prenyl- 4',7-dihydroxyisoflavone (neobavaisoflavone); M275T63: 9-oxo-10E,12Z,15Z-octadecatrienoic acid (9-OxoOTrE); M269T61: formononetin (7-hydroxy-4′-methoxyisoflavone); M299T41: 7,4'-dimethoxy-5-hydroxyisoflavone (4',7-dimethoxygenistein); M317T27: 3-methylquercetin (isoramnetin); M301T56: 4′-O-methyl-luteolin (diosmetin) or 4′-O-Methylkaempferol (kaempferide).

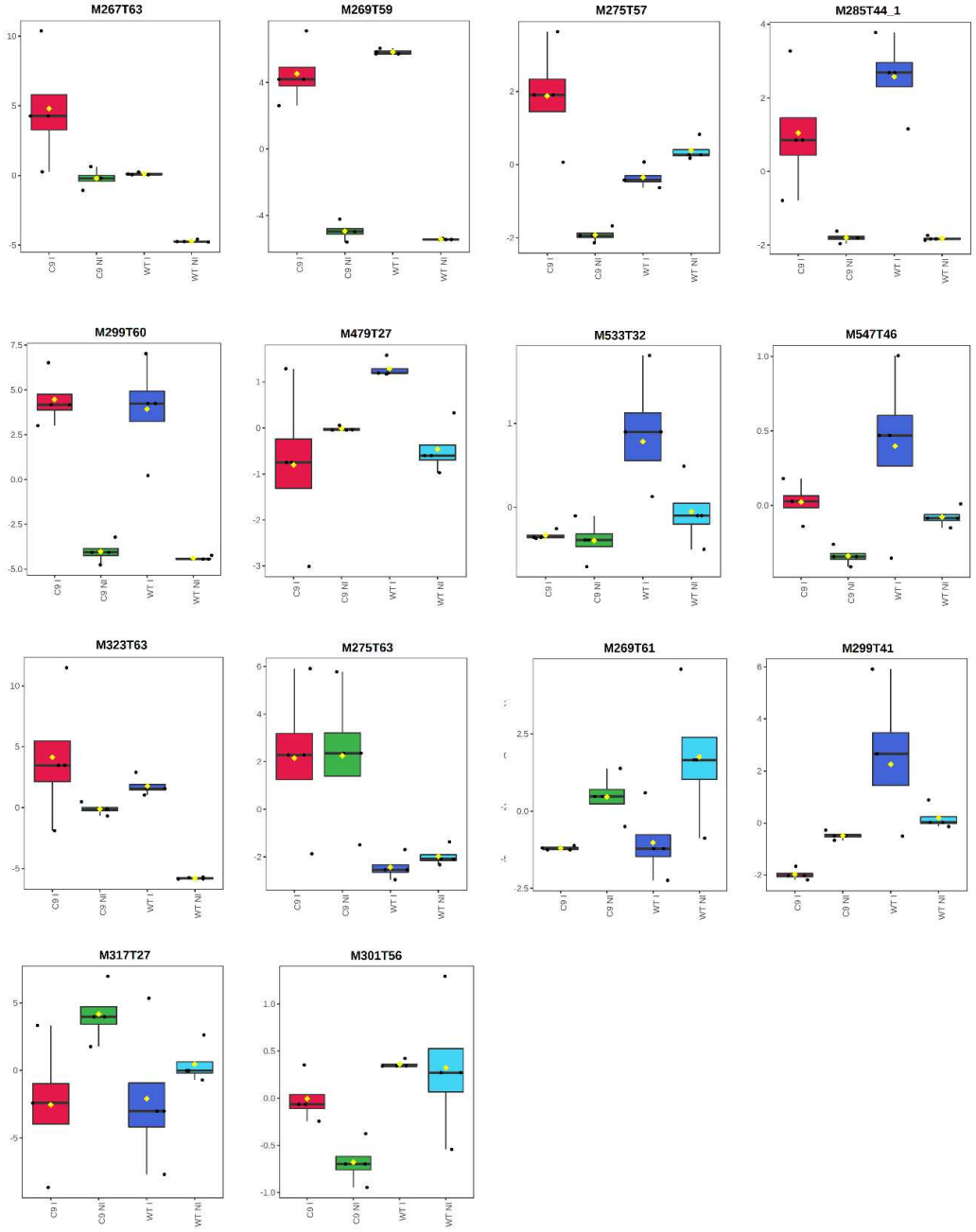

Source: Survey's data.

Figure 11 – Relative abundances in terms of XIC area of phenolics compounds and phytoalexins in soybean leaves from the WT and C9 genotypes in response to infection by *P. syringae* pv. tomato. Each bar represents the mean ± SE (n = 4, where n represents the number of plants, t test $p < 0.05$). Different lower case letters indicate significant differences between averages of the same treatment in different genotypes, and capital letters show significant differences between averages within the same genotype under different treatments

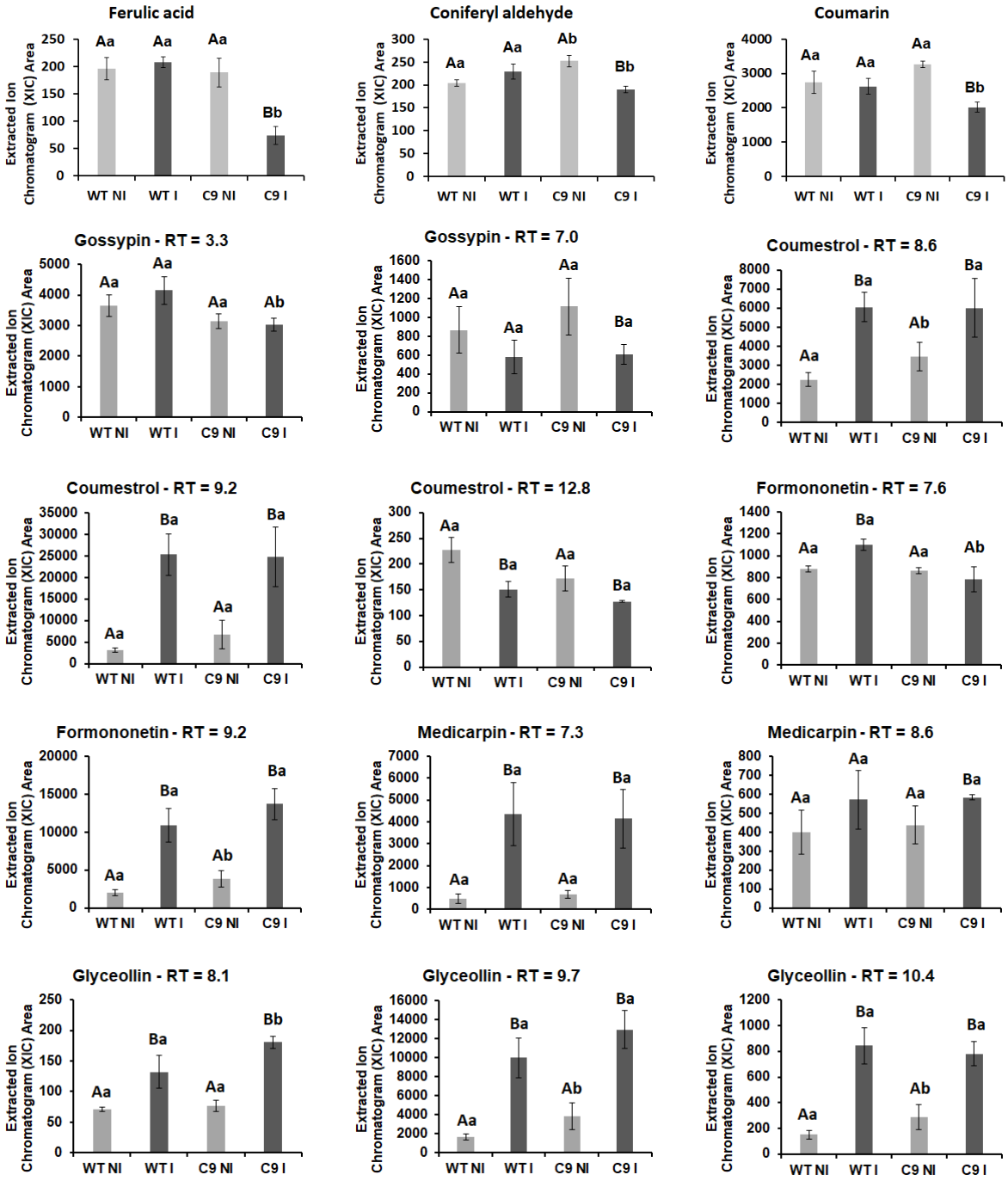

Source: Survey's data.

Peaks with considerable intensity of the compound coumestrol were detected in at least three different retention times, 8.6, 9.2 and 12.8 min (**Figure 11**), whose percentages of

fragmentation of the ions were, respectively, 12.2%, 13.2% and 4.0% (for 269/241); 49.7%, 73.1% and 45.3% (for 269/197) and 38.1%, 13.7% and 50.1% (for 269/157) (**Appendix P**). The standard compound coumestrol corresponds to a retention time of 8.6 min, with the other compounds possibly being structural isomers that may or may not be related to coumestrol. Similarly, two peaks of maximum intensity for formononetin were detected, at retention times of 7.6 min (63.8%, 26.4% and 9.8% for fragmentation patterns 269/105, 269/237 and 269/254, respectively) and 9.2 min (17.8%, 14.3% and 67.8% for the fragmentation patterns 269/105, 269/237 and 269/254, respectively). They probably correspond to the two main forms, formononetin (a daidzein methylated at the C-4' hydroxyl) and isoformononetin (a daidzein methylated at the C-7 hydroxyl), however, it was not possible to distinguish them. Medicarpin was found in two retention points with very different fragmentation patterns: on average, 1.36%, 97.9% and 0.70% for RT = 7.3 min and 37.9%, 12.5% and 49.6% for RT = 8.6 min, respectively, with the percentages corresponding to fragments 271/123.1, 271/137.1 and 271/161.1. Lastly, for glyceollin, pseudo MS3/MRM produced fragmentations whose relative intensities (FRI%), on average, were (I) 57.9%, 16.2% and 25.9% for RT = 8.1 min; (II) 15.75%, 15.0% and 69.3% for RT = 9.7 min; and (III) 36.6%, 12.1% and 51.3% for RT = 10.4 min; percentages corresponding to the fragmentation patterns 337/319, 337/149 and 337/148, respectively. Salvo et al. (2016) identified, for the chromatogram corresponding to glyceollin, as glyceollin I for the first peak, glyceollin II for the second peak and glyceollin III for the third peak. These compounds differ from each other by the cyclization of a prenyl group added to the pterocarpan ring (**Appendix P).**

An individual analysis of the relative abundance data of RTs, in terms of XICs, of some characterized phytoalexins was performed (**Figure 11**), summarized by pathway of biosynthesis (**Figure 12**) of phytoalexins derived from isoflavones, such as coumestans, pterocarpans and glyceollins, being able to relate the relative abundance of the compounds (**Appendix Q**) in terms of the HR-triggered by the non-compatible bacterium *P. syringae*. By individually analyzing the results of the phytoalexin biosynthesis pathway map (**Figure 12**), some compounds were grouped into similar patterns. Three compounds formed the first grouping: Formononetin-9.2, Glyceollin I and Glyceollin II, which showed high concentrations for both infected genotypes, but higher in C9 plants. One compound, Formononetin-7.6, showed high relative abundance to infected WT plants. Finally, five compounds, Medicarpin-7.2 and 8.6, Coumestrol-8.6 and 9.2 and Glyceollin III, form the

third cluster, which showed higher levels of relative abundance in both inoculated genotypes (**Figure 12**).

Figure 12 – Schematic overview of phytoalexins biosynthesis pathway reconstructed using the characterized compounds from soybean leaves. Each quadrant follows same pattern form the heat map obtain to MetaboAnalyst according to the caption in the upper right corner, been an indicative of the correlation analysis and express the levels of increase or decrease of relative levels for each genotype in response to inoculation of *P. syringae* pv. tomato.

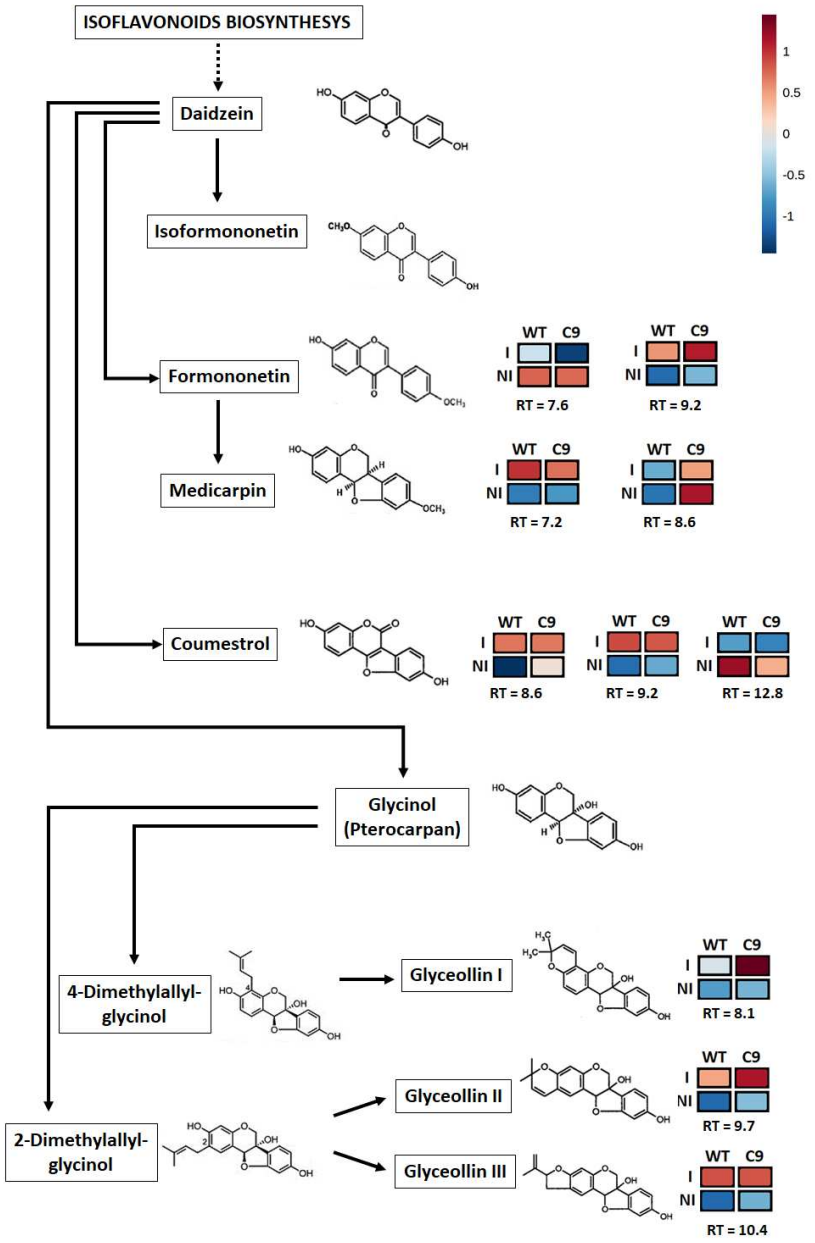

Source: Survey's data.

4 DISCUSSION

Previous studies have proven that BiP overexpression confers drought tolerance in soybeans and that this mechanism involves delaying the expression of senescence-inducing genes in leaves (Valente et al. 2009). This occurs through the modulation of the misfolded protein pathway (UPR) by the overexpressed protein BiP, also involving the transduction of programmed cell death (PCD) signals related to NRPs proteins. It also involved the attenuation of PCD caused by ER and osmotic stress (Reis et al. 2011; Carvalho et al. 2014a,b; Reis et al. 2016).

As also verified by Rodrigues et al. (2021), the hypersensitive response occurred after the infiltration of non-compatible bacterium of *P. syringae* pv. tomato in leaves, being visible 36 hours after infection (**Figure 1**). There was the formation of halos of dead brown cells, like a belt around the site of infection that limit pathogen spread (Coll et al 2011). The brown necrosis halos spots occurred in greater number in BiP-overexpressing plants indicated enhanced, as observed by Carvalho et al. (2014), indicating a greater effect of accelerated PCD induced by HR. This is accordance with previous studies that have linked BiP protein overexpression with PCD mechanisms in response to various stresses involving NRP (Alvim et al. 2001; Valente et al. 2009; Reis et al. 2011; Reis et al. 2016).

The HR-triggered by bacterial non-host injures the leaf tissue and significantly disturbs the activity of enzymes responsible for energy production, such as the photosynthetic apparatus, the Calvin Benson cycle and respiration. In fact, an HR-associated PCD in soybean to *P. syringae* pv. glycinea caused the down-regulation of photosynthesis-related proteins (**Figure 3, 4 and 5**), as reported by Zou et al. (2005). According, we observed several photosynthesis-related enzymes responsive to bacterial infection.

However, some showed different regulation such as carbonic anhydrase 2 (CA2), being up-regulated in the WT and down-regulated in C9 genotype. CA2 is an enzyme present in most intracellular compartments, being essential in photosynthesis and in the regulation of internal CO_2 levels, Studies in tobacco show the implication between CA isoforms and salicylic acid-binding proteins and their role in combating the oxidative stress caused by HR (Slaymaker et al. 2002). Decreased differential expression of photosynthesis enzymes and CO_2 fixation may be associated with leaf senescence and PCD triggered in order to contain bacterial proliferation in soybean leaf tissues.

In addition to these being used for protein translation and protection of plant cells against abiotic stresses, many enzymes related to amino acids participate in the plant defense system (Rojas 2014; Batista-Silva et al. 2019). Coutinho (2019) observed that amino acids showed an increase in relative abundance in BiP-overexpressing plants under drought, while Rojas observed an accumulation of aminocacids as a result of HR caused by pathogenic or non-pathogenic organisms (Rojas et al. 2014) which indicates that changes in amino acid levels constitute an adaptive response to various environmental stresses. We observed that the relative concentration of chloroplast cysteine synthase [O-acetylserine (thiol) lyase B (OAS-B)], which acts by catalyzing the incorporation of a sulfide group (S^{2-}) to O-acetylserine and cysteine synthesis, increased in transgenic plants after infection. Alvarez et al. (2012) report that cytosolic cysteine accumulation plays an active role in the onset of pathogenic HR. Furthermore, cysteine is a key amino acid in the synthesis of ethylene, glucosinolates, glutathione and polyamines, compounds related to pathways of development and plant responses to biotic stress (Romero et al. 2014). Aspartate aminotransferase (AAT), a key enzyme for primary metabolism and energy production, increased in WT and decreased in C9 after infection. Despite this, AAT remained at higher levels for the transgenic genotype. This may relate to both better metabolic nitrogen recycling and the synthesis of small stress-responsive molecules such as proline, GABA, PABA and polyamines (Walters 2003; Fabro et al. 2004; Rodrigues et al. 2021), and specialized metabolites (Brauc et al. 2011).

On the other hand, some proteins responsive to infection in the WT genotype were down-regulated, such as some proteins related to stress response: Chloroplastic drought-induced stress protein of 32 kDa, which acts by preserving chloroplastic structures against oxidative damage caused by drought (Broin et al. 2000); and Esponsive to dehydration 21B (spot 97), a probable cysteine protease that interacts with bacterial responsive proteins (Zhang et al. 2014). Studies have indicated that these proteins may contribute in the plant defence responses against biotic stresses (Nisa et al. 2019; De Souza Cândido et al. 2011; Kuo et al. 2013).

As a primary response to stress, plants can also invest in external barriers. Studies indicate how one of the activities of the GDSL protein is associated with cutin deposition in the cell wall as protection against non-stomatic water loss in leaves (Chao et al. 2017). Arabidopsis mutants with less cutin were more susceptible to virulent *P. syringae*, and compounds derived from cutin act as signalers, repressing the expression of bacterial type III

genes (Xiao et al. 2004). The increased expression of GDSL-lipase in C9 may, therefore, be related to a greater investment in the primary barrier to bacterial resistance.

Another front line in plant resistance to invading organisms is the recognition by receptors present in the plant cell membrane of PAMPs or elicitors (De Wit 2007; Kim et al. 2008), and in the transduction of signals that increase the expression of genes encoding pathogen-responsive proteins (PR-proteins), mostly peptidases, proteases, hydrolases, phosphatases, nucleases and ribonucleases (Van Loon 1985; Van Loon et al. 2006; Sinha et al. 2014). Such proteins play an important role in recognizing and HR-triggered by microorganisms. Studies show that Bet v 1-like proteins can alter the permeability of cell membranes (Morgensen et al. 2007) favoring the transport of secreted compounds in the intra- and intercellular compartment, in addition to differentially binding to various compounds, such as phenylpropanoids and flavonoids, regulating the activity of enzymes in the pathway (Morris et al. 2020).

On the other hand, the plant-bacterium interaction results in changes in the level of ROS, originating from subcellular compartments through various metabolic pathways, resulting in increased expression and activity of antioxidative enzymes (Sharma et al. 2012). In infected plants, transient ROS production can act as a triggering factor for PCD associated with HR and as an activating factor for antioxidant defense mechanisms and production of antimicrobial agents (Huang et al. 2019). The C9 genotype had a higher number of dysregulated enzymes which activities may be involved in antioxidant metabolism. There was an expressive up-regulation of SOD enzymes after infection in WT plants and especially in C9, in addition to other enzymes such as AKR and AOR.

Among the proteins involved in oxidative stress and responsive to bacterial infection, enzymes related to the detoxification of carbohydrate-derived reactive carbonyls arising from alterations in primary metabolism were found. 2-Oxoaldehydes are compounds involved in protein glycation, a non-enzymatic MPT observed in many organisms (McLellan and Thornalley 1989; Suttisansanee et al. 2011). Such compounds in plants can serve as molecular markers for proteins destined for degradation or as molecular markers for plant senescence (Rabbani et al. 2020; Shumilina et al. 2019), the excess being controlled by the glyoxalase pathway (Thornalley 2003). Two isoforms of glyoxalase I were observed, both up-regulated at C9 after infection, whereas AKR was down-regulated at C9. Thus, glyoxalase I is the first enzyme in an oxidative pathway that prevents glycation reactions mediated by 2-oxoaldehydes, and its increase in the transgenic genotype under biotic stress may indicate that

this is one of the mechanisms of neutralization and recycling of HR-derived reactive metabolites caused by the incompatible bacteria.

Studies have showed increase in the expression of aldo-keto reductase (AKR), which acts in the reduction of potential aldehyde groups in the formation of toxic compounds, in response to various stresses such as drought (Jin et al. 2007; Yu et al. 2020). However, AKR showed lower levels in C9 under normal conditions, and was down-regulated under biotic stress. In turn, there was a significant increase after bacterial inoculation in the C9 genotype of NADPH-dependent alkenal/one oxidoreductase (AOR), which acts mainly in the reduction of double bonds of unsaturated lipid peroxide-derived reactive carbonyls (Yamauch et al. 2011). Thus, AOR may collaborate in the elimination of reactive carbonyl compounds in chloroplasts produced by ROS related to HR caused by *P. syringae* by reinserting them into primary metabolic pathways. There is a regulation of reductases and up-regulation of oxidases in the elimination pathway of reactive carbonyls in response to bacterial attack.

Finally, one of the main detoxifying proteins is glutathione S transferases (GSTs), enzymes capable of catalyzing the conjugation reaction of several cytotoxic molecules (lipid peroxides, alkenals, unsaturated aldehydes, etc.) with the tripeptide glutathione. Under conditions of abiotic and biotic stresses, these enzymes tend to be up-regulated in plants in a cross-tolerance (Gullner et al. 2018; Labudda and Safiul Azam 2014; Ji et al. 2010), given their role in redox homeostasis, however, we observed that, for proteome of the C9 transgenic genotype, two classes of GSTs were down-regulated (GST lambda 1 was detected only in the control, while GST tau 11 decreased 1.3-fold). The C9 genotype phosphoproteome showed down-regulation of GST lambda 1 (-3.4-fold). Thus, the BiP overexpressing genotype seems to use different response mechanisms to oxidative stress caused by HR related to incompatible bacteria.

In general, among the most relevant recurrent MPTs in proteins is reversible phosphorylation, which participates in the regulation of wide diversity of cellular processes. In fact, phosphorylation can act in the activation or deactivation of enzymes and transcription factors, transport of proteins to other subcellular compartments, regulation and signal transduction (García-Mauriño et al. 2009; Fang et al. 2007; Park et al. 2012). Although proteins have several phosphorylation sites, the role of transient phosphorylation in response to environmental stresses, in addition to the kinases and phosphatases involved in the process, remains to be elucidated. The phosphoproteome analysis showed that proteins related to photosynthesis were affected in response to inoculation with *P. syringae*, especially proteins

from photosystem II and the Calvin-Benson cycle, with a transient increase in C9 phosphorylated proteins being observed, whereas in C9 and WT was observed up- and down-regulated isoforms of the same phosphoprotein (**Figure 6, 7 and 8**). With the imposition of stress, antioxidant metabolism enzymes also underwent alterations in the phosphoprotein profile, with changes in the expression of SODs and GSTs being observed in both genotypes. However, changes in the phosphoproteome can be useful to understand how proteins from different soybean varieties respond to the imposition of different forms of stresses.

A successful plant defense system needs to contain the advance of bacterial colonization effectively and with the lowest possible energy cost. Therefore, structural barriers are used, such as the reinforcement of the cell wall, and molecular barriers, such as the production of phytoalexins. In both cases, a fundamental step is the methylation of phenylpropanoids and flavonoids promoted by methyl transferases. In a previous study Carvalho et al. 2014a have been observed up-regulation of OMTs in these BiP-overepressing transgenic soybean plants. OMTs are a large family of transferases that are related to the methylation of phenolic compounds, such as benzoic acid derivatives, phenylpropanoids and flavonoids, and have been linked to antimicrobial activity and plant pathogen and microbial resistance (Lam et al. 2007; Ozçelik et al. 2011). The metabolism and accumulation of flavonoids at 36 hours after bacterial inoculation was confirmed by LC/MS (**Figure 9 and 10**), where methylated forms of flavones (diosmetin), flavonols (kaempferide, isoramnetin) and isoflavones (formononetin, afrormosin, glycitein; 4',7-dimethoxygenistein) and coumestrol, compounds with antimicrobial and phytoestrogenic effects (Nchancho et al. 2009). The methylation of flavonoid hydroxyl groups contributes to their biological activity by increasing the hydrophobicity and molecular stabilization, in addition to favoring the transport of flavonoids and their biological activity in interaction with the cytoplasmic membrane of microorganisms (Xie et al. 2014; Berim et al. 2016). In vitro studies with the fruit peel of Citrus reticulate (Liu et al. 2020) indicate that methylated flavonoids have greater cytotoxicity, and other studies have indicated the same with several prenylated flavonoids (Sohn et al. 2004; Xie et al. 2014). Methylated compounds can thus interact more actively against invading agents. Finally, flavonoid methylation and/or prenylation is essential for the biosynthesis of phytoalexins, such as formononetin, medicarpin and glyceollins. Thus, the greater presence of methylated flavonoids indicates that the increase in OMT protein activity observed in plant cells under HR may be related to leaf senescence and PCD triggered by invasive agents that reduce damage caused by biotic and oxidative stress. In fact, we found

that, for the infected WT genotype, glucoside- or malonyl-glucoside-conjugated methylated flavonoids (isorhamnetin-3-O-glucoside; 6"-O-malonylglycitin and afrormosin-7-O-glucoside-6"-O-malonate), showed higher levels (**Figure 10**). Studies show that most flavonoids are present as glycosylated forms under natural conditions, and under stress conditions they can release aglycones as biologically active forms (Boué et al. 2003; Mierziak et al. 2014). Collectively, these results suggest that methylated flavonoid aglycones are responsive to infected treatments and play an important role in bacterial non host colonization, and higher levels of expression of malonyl and glycoconjugates, forms of some flavonoids, with lower biological activity, were observed in WT genotype.

Nucleotide sugars are the key precursors for all glycosylation reactions. Several recent studies have also suggested UDP-Glc as a signaling molecule, in addition to its precursor function. The primary synthesis of UDP-sugars is catalyzed by specific pyrophosphorylases and other important role for UDP-Glc is to serve as a substrate for glycosylation of a plethora of specialized metabolites such flavonoids (Decker and Kleczkowski 2019). Protein profiles by 2DE-MS reveled that UDP-pyrophosphorylase were responsive to bacterial infection in the BiP-overexpressing C9 genotype. Therefore, the activation of these enzymes may be acting to supply UDP-sugars maintaining the heights levels of the biosynthesis of flavonols glycoconjugates

Caffeoyl coenzyme A (CoA) O-methyltransferase (OMT) (CCoAOMT) is an S-adenosyl-L-methionine (SAM)-dependent O-methyltransferase related within lignin biosynthesis, but also acts in the methylation of flavanones, dihydrofavonols, flavones and flavonols (Marita et al. 2003; Do et al. 2007). Proteome results show differential expression of OMTs: CCoAOMT was down-regulated in WT genotype, whereas Caffeic acid/5-hydroxyferulic acid O-methyltransferase isoforms were up-regulated in C9 or found only infected genotype (**Figure 4**). Studies show that CCoAOMT in maize CCoAOMT homologues associate with leucine-rich repeat proteins NLR Rp1 to modulate the defense response involving HR, suppressing the response in the absence of pathogen (Wang et al. 2016). Thus, OMTs acts on the phenolic and flavonoids methylation under the cross-effect of drought and biotic stress, in order to activate defense pathways of lignin and phytoalexins biosynthesis.

Another difference between soybean genotypes was the detection of 9-oxo-10E,12Z,15Z-octadecatrienoic acid (9-OxoOTrE) at higher levels in C9 I plants than observed in the WT I genotype (**Figure 10**). In the previous study, HR in soybeans activated by non-

pathogenic bacterium was related to an increased expression of compounds in the salicylic acid-dependent sphingolipid pathway (Rodrigues et al. 2021). Furthermore, the increase in JA in infected soybean genotypes was related to the hemibiotrophic capacity of *P. syringae* pv. tomato (Robert-Seilaniantz et al. 2011). MYC3, which encodes a MYC-related transcriptional activator related to the repression of JAZ and jasmonic acid ZIM-domain proteins, was detected as a down-regulated isoform only in C9 NI (**Figure 4**). Thus, it may be involved in the cascades of oxidation in the lipoxygenase pathway of linolenic acid (C18:3), precursor of oxylipins and jasmonates, with damage to cell membranes and activation of lipid-related plant defense pathways. As a compound resulting from LOX activity, 9-OxoOTrE is an indirect indicator of lipid oxidation. In the signaling pathways after the entry of non-pathogenic bacteria, the ROS burst and the peroxidation of fatty acids (FA) in the membranes can be estimated by the action of lipoxygenases (LOX) in the production of phytooxylipins, products of oxidation of unsaturated FA. Studies with tobacco and Arabidopsis leaves showed that accumulation of LOX-dependent phytooxylipin metabolites can be considered a marker of HR cell death triggered by incompatible interactions (Montillet et al. 2002). Thus, the detection in C9 of higher levels of 9-OxoOTrE, an oxylipin of the LOX-derived molecules pathway, in addition to the increased expression of proteins related to oxidative stress such as SOD, AOR, are indicative of the occurrence of cell damage caused by ROS burst and FA peroxidation of membranes, in addition to cell wall reinforcement by increasing GDSL-lipase in C9 infected plants.

Upregulation was also observed in C9 plants, 2-keto3-deoxyarabinoheptusonolate-7-phospate sinthase (2KDAH7PS) and chalcone-flavanone isomerase (CFI), related to the synthesis of phenolic compounds and implicated in the biosynthesis of a large class of specialized plant metabolites. Under drought stress conditions, the accumulation of misfolded proteins can activate a stress-induced stress response in the endoplasmic (ER) and osmotic reticulum, involving an HR-indued programmed cell death (PCD) (Reis and Fontes 2012). These mechanisms also attested for the interaction soybean-*P. syringae* pv. tomato and enhanced regulation of some flavonoid-related genes (Carvalho et al. 2014). Thus, phenolic compounds content (**Figure 11**) may be related to a performance in cell protection against oxidative stress in C9 leaves.

The presence of Brassinosteroid-6-oxidase 2 (BR6OX2) was higher in C9-infected plants. BR6OX2 encodes the cytochrome P450 enzyme that catalyzes the synthesis reaction of brassinosteroids (BRs), steroidal phytohormones that are essential for plant growth and

development. Cytochromes P450 are ubiquitous proteins among living beings, and plants use them in monooxygenation and hydroxylation reactions of several compounds, especially from specialized metabolism such as steroids, lignins, alkaloids and glyceollins (Mizutani and Sato 2011).

From the peak area data of the phytoalexin chromatograms (**Appendix Q**), the relative abundance was interpreted in terms of a map of the phytoalexin biosynthetic pathway and defined by the colors of the caption (**Figure 12**), making it possible to analyze the relationship between the levels of compounds and the impact on plant metabolism of genotypes as a function of the treatments. There was an increase in the synthesis of phytoalexin glyceollins in response to bacterial attack, and there were higher levels of some compounds for the transgenic genotype. As we can see in the biosynthetic pathway of isoflavonoids, daidzein and formononetin are precursor compounds of important phytoalexins, such as cumestans (coumestrol), pterocarpans (medicarpins and glyceollins). Studies show the accumulation of coumestrol due to stress factors (Tripathi et al. 2016; Silva et al. 2018; Ha et al. 2019) and the antibacterial action of glycinol (Weinstein and Albersheim 1983), a pterocarpan precursor of glyceollins, formed by prenylation and cyclization of the prenyl group with the hydroxyl of the pterocarpan nucleus. The antimicrobial properties of glyceollins are known for pathogenic fungi (Darvill and Albersheim 1984). However, the participation of these compounds as part of the mechanisms of a HR and in the containment of non-compatible avirulent bacterial infection is poorly studied. Alterations in the biosynthesis pathways of isoflavonoids phytoalexins observed in BiP-overexpressing and plant-bacterial interactions support the hypothesis of linking the antibacterial action of these compounds. In fact, the action of isoflavone O-methyltransferases (IOMTs) form formononetin and, from this, medicarpin, a phytoalexin that accumulates in alfalfa, as attested by He and Dixon (2000). Indeed, we observed in a previous study induction of transcription of the gmI4'OMT gene in transgenic plants, and increased levels of prenylated isoflavonoids (Rodrigues et al. 2021).

5 CONCLUSION

Furthermore, HR-related plant defense mechanisms in BiP overexpressing plants may play a key role in an increased presence of flavonoids and isoflavonoids methylated, a fact corroborated by the increased expression of O-methyltransferases in transgenic plants, resulting from the increased expression of proteins related to the phenylpropanoid and

isoflavonoids pathway. Elevated levels of phytoalexins such as coumestrol, pterocarpans and glyceollins were also observed in infected genotypes. In addition to observing a negative regulation of photosynthetic and upregulation of antioxidative metabolism as a form of resistance to the colonization of plant tissue by *P. syringae*.

REFERENCES

AGRAWAL, G. K.; THELEN, J. J. (2009) A high-resolution two dimensional Gel-and Pro-Q DPS-based proteomics workflow for phosphoprotein identification and quantitative profiling. In Phospho-Proteomics Humana Press: 3-19. https://doi.org/10.1007/978-1-60327-834-8_1

AHANGER, M. A.; AKRAM, N. A.; ASHRAF, M.; ALYEMENI, M. N.; WIJAYA, L.; AHMAD, P. (2017) Plant responses to environmental stresses-from gene to biotechnology. AoB Plants, 9(4), plx025. https://doi.org/10.1093/aobpla/plx025

AHUJA, I.; KISSEN, R.; BONES, A. M. (2012) Phytoalexins in defense against pathogens. Trends in Plant Science, 17(2), 73-90. https://https://doi.org/10.1016/j.tplants.2011.11.002

ALVAREZ, C.; BERMÚDEZ, M. A.; ROMERO, L. C.; GOTOR, C.; GARCIA, I. (2012) Cysteine homeostasis plays an essential role in plant immunity. New Phytol. 193, 165-177.

ALVIM, F. C.; CAROLINO, S. M. B.; CASCARDO, J. C. M.; NUNES, C. C.; MARTINEZ, C. A.; OTONI, W. C.; FONTES, E. P. B. (2001) Enhanced accumulation of BiP in transgenic plants confers tolerance to water stress. Plant Physiol. 126, 1042-1054. https://doi.org/10.1104/pp.126.3.1042.

ARYAL, U. K.; KROCHKO, J. E.; ROSS, A. R. (2012) Identification of phosphoproteins in *Arabidopsis thaliana* leaves using polyethylene glycol fractionation, immobilized metal-ion affinity chromatography, two-dimensional gel electrophoresis and mass spectrometry. J Proteome Res. 1;11(1):425-37. https://https://https://doi.org/10.1021/pr200917t

BATISTA-SILVA, W.; HEINEMANN, B.; RUGEN, N.; NUNES-NESI, A.; ARAÚJO, W. L.; BRAUN, H. -P.; HILDEBRANDT, T. M. (2019) The role of amino acid metabolism during abiotic stress release. Plant, Cell & Environment. https://https://https://doi.org/10.1111/pce.13518

BERGER, S.; PAPADOPOULOS, M.; SCHREIBER, U.; KAISER, W.; ROITSCH, T. (2004) Complex regulation of gene expression, photosynthesis and sugar levels by pathogen infection in tomato. Physiologia Plantarum, 122(4), 419-428. https://https://doi.org/10.1111/j.1399-3054.2004.00433.x

BERIM, A.; GANG, D. R. (2016) Methoxylated flavones: Occurrence, importance, biosynthesis. Phytochem. Rev. 15, 363-390

BILGIN, D. D.; ZAVALA, J. A.; ZHU, J.; CLOUGH, S. J.; ORT, D. R.; DELUCIA, E. H. (2010) Biotic stress globally downregulates photosynthesis genes. Plant Cell Environ. 2010 Oct;33(10):1597-613. https://https://doi.org/10.1111/j.1365-3040.2010.02167.x

BOUÉ, S. M.; CARTER-WIENTJES, C. H.; SHIH, B. Y.; CLEVELAND, T. E. (2003) Identification of flavone aglycones and glycosides in soybean pods by liquid chromatography-tandem mass spectrometry. J Chromatogr A. 991:61-8

BRADFORD, M. M. (1976) A rapid and sensitive method for the quantitation of microgram quantities of protein utilizing the principle of protein-dye binding. Anal Biochem. 7; 72:248-54. https://https://doi.org/10.1006/abio.1976.9999

BRAUC, S.; DE VOOGHT, E.; CLAEYS, M.; HÖFTE, M.; ANGENON, G. (2011) Influence of over-expression of cytosolic aspartate aminotransferase on amino acid metabolism and defence responses against Botrytis cinerea infection in *Arabidopsis thaliana*. J Plant Physiol. 15;168(15):1813-9. https://https://doi.org/10.1016/j.jplph.2011.05.012

BROIN, M.; CUINÉ, S.; PELTIER, G.; REY, P. (2000) Involvement of CDSP 32, a drought-induced thioredoxin, in the response to oxidative stress in potato plants. FEBS Lett. 11;467(2-3):245-8. https://https://doi.org/10.1016/s0014-5793(00)01165-0

CARVALHO, H. H.; BRUSTOLINI, O. J.; PIMENTA, M. R.; MENDES, G. C.; GOUVEIA, B. C.; SILVA, P. A.; SILVA, J. C.; MOTA, C. S.; RAMOS, J. R. L.; S.; FONTES, E. P. B. (2014) The molecular chaperone binding protein BiP prevents leaf dehydration-induced cellular homeostasis disruption. PLoS One. 2014 Jan; 9(1):e86661. https://https://doi.org/10.1371/journal.pone.0086661

CARVALHO, H. H.; SILVA, P. A.; MENDES, G. C.; BRUSTOLINI, O. J.; PIMENTA, M. R.; GOUVEIA, B. C. VALENTE, M. A.; RAMOS, H. J. O.; RAMOS, J. R. L.; S.; FONTES, E. P. (2014) The endoplasmic reticulum binding protein BiP displays dual function in modulating cell death events. Plant Physiol. 164(2):654-70. https://https://doi.org/10.1104/pp.113.231928

CHIN, S.; BEHM, C.; MATHESIUS, U. (2018) Functions of Flavonoids in Plant-Nematode Interactions. Plants 7(4):85. https://https://doi.org/10.3390/plants7040085

CHIVASA, S.; TOMÉ, D. F.; SLABAS, A. R. (2013) UDP-glucose pyrophosphorylase is a novel plant cell death regulator. J Proteome Res. 12(4):1743-53. https://https://doi.org/10.1021/pr3010887

COLL, N. S.; EPPLE, P.; DANGL, J. L. (2011) Programmed cell death in the plant immune system. Cell Death Differ 18:1247-1256. https://https://doi.org/10.1038/cdd.2011.37

COUTINHO, F. S.; SANTOS, D. S.; LIMA, L. L.; VITAL, C. E.; SANTOS, L. A.; PIMENTA, M. R.; SILVA, J. C.; RAMOS, J. R. L.; S.; METHA, A.; FONTES, E. P. B.; RAMOS, H. J. O. (2019) Mechanism of the drought tolerance of a transgenic soybean overexpressing the molecular chaperone. BiP Physiol. Mol. Biol. Plants. 1, 1-16. https://doi.org/10.1007/s12298-019-00643-x.

DE CAMARGOS, L. F.; FRAGA, O. T.; OLIVEIRA, C. C.; SILVA, J. C. F.; FONTES, E. P. B.; REIS, P. A. B. (2018) Development and cell death domain-containing asparagine-rich protein (DCD/ NRP): an essential protein in plant development and stress responses. Theor. Exp. Plant Physiol. 31, 59-70. https://doi.org/10.1007/s40626-018-0128-z.

DE SOUZA CÂNDIDO, E.; PINTO, M. F. S.; PELEGRINI, P. B.; LIMA, T. B.; SILVA, O. N.; POGUE, R.; GROSSI-DE-SÁ, M.; F. FRANCO, O. L. (2011) Plant storage proteins with antimicrobial activity: novel insights into plant defense mechanisms. FASEB J. 25, 3290-3305. https://https://doi.org/10.1096/fj.11-184291

DE WIT, P. J. (2007) How plants recognize pathogens and defend themselves. Cell Mol Life Sci. 64(21):2726-32. https://https://doi.org/10.1007/s00018-007-7284-7

DECKER, D; KLECZKOWSKI, L. A. (2019) UDP-Sugar Producing Pyrophosphorylases: Distinct and Essential Enzymes with Overlapping Substrate Specificities, Providing de novo Precursors for Glycosylation Reactions. Front Plant Sci. 4; 9:1822. https://https://doi.org/10.3389/fpls.2018.01822

DO, C. T.; POLLET, B.; THÉVENIN, J.; SIBOUT, R.; DENOUE, D.; BARRIÈRE, Y.; LAPIERRE, C.; JOUANIN, L. (2007) Both caffeoyl Coenzyme A 3-O-methyltransferase 1 and caffeic acid O-methyltransferase 1 are involved in redundant functions for lignin, flavonoids and sinapoyl malate biosynthesis in Arabidopsis. Planta. 226(5):1117-29. https://https://doi.org/10.1007/s00425-007-0558-3

FABRO, G.; KOVÁCS, I.; PAVET, V.; SZABADOS, L.; ALVAREZ, M. E. (2004) Proline Accumulation andAtP5CS2Gene Activation Are Induced by Plant-Pathogen Incompatible Interactions inArabidopsis. Molecular Plant-Microbe Interactions, 17(4), 343-350. https://https://doi.org/10.1094/mpmi.2004.17.4.343

FANG, Y.; SATHYANARAYANAN, S.; SEHGAL, A. (2007) Post-translational regulation of the Drosophila circadian clock requires protein phosphatase 1 (PP1). Genes & Development 21: 1506 - 1518.

FERREIRA, C. C. A.; OLIVEIRA, M. G. A.; BRUMANO, M. H. N.; GUEDES, R. N. C.; SILVA, C. H. O.; MOREIRA, M. A. (2005) Lack of seed lipoxigenases does not affect soybean defense by reproductive tissue removal. Biosci. J. 21, 49-55.

FEUSSNER, I.; WASTERNACK, C. (2002) The lipoxygenase pathway. Annu Rev Plant Biol. 53:275-97. https://https://doi.org/10.1146/annurev.arplant.53.100301.135248

GAO, J.; AGRAWAL, G. K.; THELEN, J. J.; XU, D. (2009) P3DB: a plant protein phosphorylation database. Nucleic Acids Res. 37(Database issue):D960-2. https://https://doi.org/10.1093/nar/gkn733

GAO, J; THELEN, J. J.; DUNKER, A. K.; XU, D. (2010) Musite, a tool for global prediction of general and kinase-specific phosphorylation sites. Mol Cell Proteomics. 9(12):2586-600. https://https://doi.org/10.1074/mcp.M110.001388

GARCÍA-MAURIÑO, S.; MONREAL, J. A.; ÁLVAREZ, R.; VIDAL, J. Y.; ECHEVARRÍA, C. (2009) Characterization of a salt stressenhanced phosphoenolpyruvate

carboxylase kinase activity in leaves of Sorghum vulgare: independence of osmotic stress, involvement of ion toxycity and significance of dark phosphorylation. Planta 216: 648 - 655

GARDAN, L.; SHAFIK, H.; BELOUIN, S.; BROCH, R.; GRIMONT, F.; GRIMONT, P. A. D. (1999) DNA relatedness among the pathovars of *Pseudomonas syringae* and description of *Pseudomonas tremae* sp. nov. and *Pseudomonas cannabina* sp. nov (ex Sutic and Dowson 1959). Int. J. Syst. Evol. Microbiol. 49, 469-478. https://doi.org/10.1099/00207713-49-2-469.

GOMEZ, J. D.; VITAL, C. E.; OLIVEIRA, M. G. A.; RAMOS, H. J. O. (2018) Broad range flavonoid profiling by LC/MS of soybean genotypes contrasting for resistance to Anticarsia gemmatalis (Lepidoptera: Noctuidae). PloS One 13 (10), e0205010. https://doi.org/101371/journalpone0205010

GÓMEZ, J. D.; PINHEIRO, V. J. M.; SILVA, J. C.; ROMERO, J. V.; MERIÑO-CABRERA, Y.; COUTINHO, F. S.; LOURENÇÃO, A. L.; SERRÃO, J. E.; VITAL, C. E.; FONTES E. P. B.; OLIVEIRA, M. G. A.; RAMOS, H. J. O. (2020) Leaf metabolic profiles of two soybean genotypes differentially affect the survival and the digestibility of Anticarsia gemmatalis caterpillars. Plant Physiology and Biochemistry. https://https://doi.org/10.1016/j.plaphy.2020.07.010

GOODSTEIN, D. M.; SHU, S.; HOWSON, R.; NEUPANE, R.; HAYES, R. D.; FAZO, J.; MITROS, T.; DIRKS, W.; HELLSTEN, U.; PUTNAM, N.; ROKHSAR, D. S. (2012) Phytozome: a comparative platform for green plant genomics. Nucleic Acids Res. 40 (Database issue): D1178-86. https://https://doi.org/10.1093/nar/gkr944

GOUVEIA, F.; BICKER, J.; GONÇALVES, J.; ALVES, G.; FALCÃO, A.; FORTUNA, A. (2019) Liquid chromatographic methods for the determination of direct oral anticoagulant drugs in biological samples: a critical review. Anal. Chim. Acta 1076, 18-31. https://doi.org/10.1016/j.aca.2019.03.061. Epub 2019 Apr 8. Review.

GOUVEIA, A. S.; LIMA, L. L.; COUTINHO, F. S.; RODRIGUES, J. M.; PINHEIRO, V. J. M.; RAMOS, M. E. S.; VITAL, C. E.; PONTES, C. S. L.; PINHEIRO, D. P.; VIDIGAL, P. M.; BARROS, E.; RAMOS, H. J. O. (2019) Metabolic pathway analysis by liquid chromatography (UHPLC) coupled to high resolution mass spectrometry (LC/MS).

GRAHAM, T. L. (1998) Flavonoid and flavonol glycoside metabolism in Arabidopsis. Plant Physiol. Biochem. 36 (1-2), 135-144. https://doi.org/10.1016/s0981-9428(98)80098-3.

GULLNER, G.; KOMIVES, T.; KIRÁLY, L.; SCHRÖDER, P. (2018) Glutathione S-Transferase Enzymes in Plant-Pathogen Interactions. Front. Plant Sci. 9:1836. https://https://doi.org/10.3389/fpls.2018.01836

HA, J.; KANG, Y. G.; LEE, T.; KIM, M.; YOON, M. Y.; LEE, E.; YANG, X.; KIM, D.; KIM, Y-J.; LEE, T. R.; KIM, M. Y.; LEE, S-H. (2019) Comprehensive RNA sequencing and co-expression network analysis to complete the biosynthetic pathway of coumestrol, a phytoestrogen. Sci Rep 9, 1934. https://doi.org/10.1038/s41598-018-38219-6

HAHN, A.; KILIAN, J.; MOHRHOLZ, A.; LADWIG, F.; PESCHKE, F.; DAUTEL, R.; HARTER, K.; BERENDZEN, K. W.; WANKE, D. (2013) Plant core environmental stress

response genes are systemically coordinated during abiotic stresses. Int J Mol Sci.14(4):7617-7641. https://https://doi.org/10.3390/ijms14047617

HE, X. Z.; DIXON, R. A. (2000) Genetic manipulation of isoflavone 7-O-methyltransferase enhances biosynthesis of 4'-O-methylated isoflavonoid phytoalexins and disease resistance in alfalfa. Plant Cell. 12(9):1689-702. https://https://doi.org/10.1105/tpc.12.9.1689

HUANG, H.; ULLAH, F.; ZHOU, D. -X.; YI, M.; ZHAO, Y. (2019) Mechanisms of ROS Regulation of Plant Development and Stress Responses. Frontiers in Plant Science, 10. https://https://doi.org/10.3389/fpls.2019.00800

JI, W.; ZHU, Y.; LI, Y.; YANG, L.; ZHAO, X.; CAI, H.; BAI, X. (2010) Over-expression of a glutathione S-transferase gene, GsGST, from wild soybean (Glycine soja) enhances drought and salt tolerance in transgenic tobacco. Biotechnol Lett. 32(8):1173-9. https://https://doi.org/10.1007/s10529-010-0269-x

JIN, Y.; PENNING, T. M. (2007) Aldo-keto reductases and bioactivation/detoxication. Annu. Rev. Pharmacol. Toxicol. 47, 263-292.

KIM, M. G.; KIM, S. Y.; KIM, W. Y.; MACKEY, D.; LEE, S. Y. (2008) Responses of *Arabidopsis thaliana* to challenge by *Pseudomonas syringae*. Mol Cells. 25(3):323-31.

KUO, W. Y.; HUANG, C. H.; LIU, A. C.; CHENG, C. P.; LI, S. H.; CHANG, W. C.; WEISS, C.; AZEM, A.; JINN, T.L. (2013) CHAPERONIN 20 mediates iron superoxide dismutase (FeSOD) activity independent of its co-chaperonin role in Arabidopsis chloroplasts. New Phytol. 197(1):99-110. https://https://doi.org/10.1111/j.1469-8137.2012.04369.x

LABUDDA, M.; SAFIUL AZAM, F. M. (2014) Glutathione-dependent responses of plants to drought: a review. Acta Societatis Botanicorum Poloniae, 83(1), 3-12. https://https://doi.org/10.5586/asbp.2014.003

LAM, K. C.; IBRAHIM, R. K.; BEHDAD, B.; DAYANANDAN, S. (2007) Structure, function, and evolution of plant O-methyltransferases. Genome 50(11), 1001-1013. https://doi.org/10.1139/g07-077

LI, C.; CHEN, G.; MISHINA, K.; YAMAJI, N.; MA, JF.; YUKUHIRO, F.; TAGIRI, A.; LIU, C.; POURKHEIRANDISH, M.; ANWAR, N.; OHTA, M.; ZHAO, P.; LUNDQVIST, U.; LI, X.; KOMATSUDA, T. A (2017) GDSL-motif esterase/acyltransferase/lipase is responsible for leaf water retention in barley. Plant Direct. 1(5): e00025. https://https://doi.org/10.1002/pld3.25

LIMA, L. L.; BALBI, B. P.; MESQUITA, R. O.; SILVA, J. C. F.; COUTINHO, F. S.; CARMO, F. M. S.; VITAL, C. E.; MEHTA, A.; FONTES, E. P. B.; BARROS, E. G.; RAMOS, H. J. O. (2019) Proteomic and metabolomic analysis of a drought tolerant soybean genotype from Brazilian Savanna. Crop Breed. Genet. Genom. e190022-32, 2019

LIU, X.; WANG, Y.; CHEN, Y.; XU, S.; GONG, Q.; ZHAO, C.; CAO, J.; SUN, C. (2020) Characterization of a Flavonoid 3′/5′/7-O-Methyltransferase from Citrus reticulata and Evaluation of the In Vitro Cytotoxicity of Its Methylated Products. Molecules. 15;25(4):858. https://https://doi.org/10.3390/molecules25040858

MA, B.; ZHANG, K.; HENDRIE, C.; LIANG, C.; LI, M.; DOHERTY-KIRBY, A.; LAJOIE, G. (2003) PEAKS: powerful software for peptide de novo sequencing by tandem mass spectrometry. Rapid Commun Mass Spectrom. 17(20):2337-42. https://doi.org/10.1002/rcm.1196

MARITA, J. M.; RALPH, J.; HATFIELD, R. D.; GUO, D.; CHEN, F.; DIXON, R. A. (2003) Structural and compositional modifications in lignin of transgenic alfalfa down-regulated in caffeic acid 3-O-methyltransferase and caffeoyl coenzyme A 3-O-methyltransferase. Phytochemistry. 62(1):53-65. https://https://doi.org/10.1016/s0031-9422(02)00434-x

MCLELLAN, A. C.; THORNALLEY, P. J. (1989) Glyoxalase activity in human red blood cells fractioned by age. Mechanisms of Ageing and Development, 48(1), 63-71. https://https://doi.org/10.1016/0047-6374(89)90026-2

MELO, B. P.; FRAGA, O. T.; SILVA, J. C. F.; FERREIRA, D. O.; BRUSTOLINI, O. J. B.; CARPINETTI, P. A.; MACHADO, J. P. B.; REIS, P. A. B.; FONTES, E. B. P. (2018) Revisiting the soybean GmNAC superfamily. Front. Plant Sci. 9, 1864. https://doi.org/10.3389/fpls.2018.01864.

MIERZIAK, J.; KOSTYN, K.; KULMA, A. (2014) Flavonoids as important molecules of plant interactions with the environment. Molecules 19 (10), 16240-16265. https://doi.org/10.3390/molecules191016240.

MIZUTANI, M.; SATO, F. (2011) Unusual P450 reactions in plant secondary metabolism. Archives of Biochemistry and Biophysics, 507(1), 194-203. https://https://doi.org/10.1016/j.abb.2010.09.026

MOGENSEN, J. E.; FERRERAS, M.; WIMMER, R.; PETERSEN, S. V.; ENGHILD, J. J.; OTZEN, D. E. (2007) The major allergen from birch tree pollen, Bet v 1, binds and permeabilizes membranes. Biochemistry. 20;46(11):3356-65. https://https://doi.org/10.1021/bi062058h

MONTILLET, J. -L.; AGNEL, J. -P.; PONCHET, M.; VAILLEAU, F.; ROBY, D.; TRIANTAPHYLIDÈS, C. (2002) Lipoxygenase-mediated production of fatty acid hydroperoxides is a specific signature of the hypersensitive reaction in plants. Plant Physiology and Biochemistry, 40(6-8), 633-639. https://https://doi.org/10.1016/s0981-9428(02)01402-x

MORRIS, J. S.; CALDO, K. M.; LIANG, S.; FACCHINI, P. (2020) PR10/Bet v 1-like proteins as novel contributors to plant biochemical diversity. ChemBioChem. https://https://doi.org/10.1002/cbic.202000354

MÜLLER, M.; MUNNÉ-BOSCH, S. (2011) Rapid and sensitive hormonal profiling of complex plant samples by liquid chromatography coupled to electrospray ionization tandem mass spectrometry. Plant methods 7(1): 37. https://doi.org/10.1186/1746-4811-7-37

NCHANCHO, K.; KOUAM, J.; TANE, P.; KUETE, V.; WATCHUENG, J.; FOMUM, Z. T. (2009) Coumestan glycosides from the stem bark of Cylicodiscus gabunensis. Nat Prod Commun. 4(7):931-4. https://https://doi.org/10.1177/1934578x0900400711

NEUHOFF, V.; STAMM, R.; EIBL, H. (1985) Clear background and highly sensitive protein staining with Coomassie Blue dyes in polyacrylamide gels: A systematic analysis. Electrophoresis, 6(9), 427-448. https://https://doi.org/10.1002/elps.1150060905

NISA, M. -U.; HUANG, Y.; BENHAMED, M.; RAYNAUD, C. (2019) The Plant DNA Damage Response: Signaling Pathways Leading to Growth Inhibition and Putative Role in Response to Stress Conditions. Frontiers in Plant Science, 10. https://https://doi.org/10.3389/fpls.2019.00653

OLIVEROS, J. C. (2007-2015) Venny. An interactive tool for comparing lists with Venn's diagrams. https://bioinfogp.cnb.csic.es/tools/venny/index.html

OZÇELIK, B.; KARTAL, M.; ORHAN, I. (Apr 2011) Cytotoxicity, antiviral and antimicrobial activities of alkaloids, flavonoids, and phenolic acids. Pharm Biol. 49(4):396-402. https://https://doi.org/10.3109/13880209.2010.519390.

PARK, C. -J.; CADDELL, D. F.; RONALD, P. C. (2012) Protein phosphorylation in plant immunity: insights into the regulation of pattern recognition receptor-mediated signaling. Frontiers in Plant Science, 3. https://https://doi.org/10.3389/fpls.2012.00177

PRESTON, G. M. (2000) *Pseudomonas syringae* pv. tomato: the right pathogen, of the right plant, at the right time. Mol. Plant Pathol. 1 (5), 263-275. https://doi.org/10.1046/j.1364-3703.2000.00036.x.

RABBANI, N.; AL-MOTAWA, M.; THORNALLEY, P. J. (2020) Protein Glycation in Plants - um campo pouco pesquisado com muito ainda a descobrir. Int. J. Mol. Sci. 21, 3942. https://doi.org/10.3390/ijms21113942

REIS, P. A. B.; CARPINETTI, P. A.; FREITAS, P. P. J.; SANTOS, E. G. D.; DE CAMARGOS, L. F.; OLIVEIRA, I. H. T.; SILVA, J. C. F.; CARVALHO, H. H.; COSTA, M. D. L.; RAMOS, J. L. R. S.; FONTES, E. P. B. (2016) Functional and regulatory conservation of the soybean ER stress-induced DCD/NRP-mediated cell death signaling in plants. BMC Plant Biol. 16, 156. https://doi.org/10.1186/s12870-016-0843-z.

REIS, P. A. B.; ROSADO, G. L.; SILVA, L. A.; OLIVEIRA, L. C.; OLIVEIRA, L. B.; COSTA, M. D.; ALVIM, F. C.; FONTES, E. P. B. (2011) The binding protein BiP attenuates stress-induced cell death in soybean via modulation of the N-rich protein-mediated signaling pathway. Plant Physiol. 157, 1853-1865.

REIS, P. A.; FONTES, E. P. (2012) N-rich protein (NRP)-mediated cell death signaling: a new branch of the ER stress response with implications for plant biotechnology. Plant Signaling & Behavior, 7(6), 628-632. https://doi.org/10.4161/psb.20111

ROBERT-SEILANIANTZ, A.; GRANT, M.; JONES, J. D. (2011) Hormone crosstalk in plant disease and defense: more than just jasmonate-salicylate antagonism. Annu Rev Phytopathol. 49:317-43. https://https://doi.org/10.1146/annurev-phyto-073009-114447

RODRIGUES, J. M.; COUTINHO, F. S.; SANTOS, D. S.; VITAL, C. E.; RAMOS, J. R. L. S.; REIS, P. B.; OLIVEIRA, M. G. A.; MEHTA, A.; FONTES, E. P. B.; RAMOS, H. J. O.

(2021) BiP-overexpressing soybean plants display accelerated hypersensitivity response (HR) affecting the SA-dependent sphingolipid and flavonoid pathways. Phytochemistry. 185:112704. https://https://doi.org/10.1016/j.phytochem.2021.112704

ROGACHEV, I.; AHARONI, A. (2012) UPLC-MS-based metabolite analysis in tomato. Methods Mol. Biol. 860, 129-144. https://doi.org/10.1007/978-1-61779-594-7_9

ROJAS, C. M.; SENTHIL-KUMAR, M.; TZIN, V.; MYSORE, K. S. (2014) Regulation of primary plant metabolism during plant-pathogen interactions and its contribution to plant defense. Front. Plant Sci. 5, 17. https://doi.org/10.3389/fpls.2014.00017.

ROMERO, L. C.; AROCA, M. Á.; LAUREANO-MARÍN, A. M.; MORENO, I.; GARCÍA, I.; GOTOR, C. (2014) Cysteine and Cysteine-Related Signaling Pathways in *Arabidopsis thaliana*. Molecular Plant, 7(2), 264-276. https://https://doi.org/10.1093/mp/sst168

SALVO, V. A.; BOUE, S. M.; FONSECA, J. P.; ELLIOTT, S.; CORBITT, C.; COLLINS-BUROW, B. M.; CURIEL T. J.; SRIVASTAV S. K.; SHIH B. Y.; CARTER-WIENTJES C.; WOOD C. E.; ERHARDT P. W,; BECKMAN B. S.; MCLACHLAN J. A.; CLEVELAND T. E.; BUROW, M. E. (2006) Antiestrogenic Glyceollins Suppress Human Breast and Ovarian Carcinoma Tumorigenesis. Clinical Cancer Research, 12(23), 7159-7164. https://https://doi.org/10.1158/1078-0432.ccr-06-1426

SHARMA, P.; JHA, A. B.; DUBEY, R. S.; PESSARAKLI, M. (2012) Reactive Oxygen Species, Oxidative Damage, and Antioxidative Defense Mechanism in Plants under Stressful Conditions. Journal of Botany, 2012, 1-26. https://https://doi.org/10.1155/2012/217037

SHEVCHENKO, A.; TOMAS, H.; HAVLĬSOLSEN, J. V.; MANN, M. (2007) In-gel digestion for mass spectrometric characterization of proteins and proteomes. Nat Protoc 1:2856-2860

SHUMILINA, J.; KUSNETSOVA, A.; TSAREV, A.; JANSE VAN RENSBURG, H. C.; MEDVEDEV, S.; DEMIDCHIK, V.; VAN DEN ENDE, W.; FROLOV, A. (2019) Glycation of Plant Proteins: Regulatory Roles and Interplay with Sugar Signalling? International Journal of Molecular Sciences, 20(9), 2366. https://https://doi.org/10.3390/ijms20092366

SIEBERS, M.; BRANDS, M.; WEWER, V.; DUAN, Y.; HÖLZL, G.; DÖRMANN, P. (2016) Lipids in plant-microbe interactions. Biochimica et Biophysica Acta (BBA) - Molecular and Cell Biology of Lipids, 1861(9), 1379-1395. https://https://doi.org/10.1016/j.bbalip.2016.02.021

SILVA, E. C.; ABHAYAWARDHANA, P. L.; LYGIN, A. V.; ROBERTSON, C. L.; LIU, M.; LIU, Z.; SCHNEIDER, R. W. (2018) Coumestrol Confers Partial Resistance in Soybean Plants Against Cercospora Leaf Blight. Phytopathology, 108(8), 935-947. https://https://doi.org/10.1094/phyto-05-17-0189-r

SILVA, P. A.; SILVA, J. C. F.; CAETANO, H. A. D. N.; MACHADO, J. P. B.; MENDES, G. C.; REIS, P. A. B.; BRUSTOLINI, O. J. B.; DAL-BIANCO, M.; FONTES, E. P. B. (2015) Comprehensive analysis of the endoplasmic reticulum stress response in the soybean genome: conserved and plant specific features. BCM Genomics 16, 783. https://doi.org/10.1186/s12864-015-1952-z

SINHA, M.; SINGH, R. P.; KUSHWAHA, G. S.; IQBAL, N.; SINGH, A.; KAUSHIK, S.; KAUR, P.; SHARMA, S.; SINGH, T. P. (2014) Current overview of allergens of plant pathogenesis related protein families. The Scientific World Journal, 543195. https://doi.org/10.1155/2014/543195

SLAYMAKER, D. H.; NAVARRE, D. A.; CLARK, D.; DEL POZO, O.; MARTIN, G. B.; KLESSIG, D. F. (2002) The tobacco salicylic acid-binding protein 3 (SABP3) is the chloroplast carbonic anhydrase, which exhibits antioxidant activity and plays a role in the hypersensitive defense response. Proc. Natl. Acad. Sci. USA 99:11640-11645

SOHN, H. -Y.; SON, K. H.; KWON, C. -S.; KWON, G. -S.; KANG, S. S. (2004) Antimicrobial and cytotoxic activity of 18 prenylated flavonoids isolated from medicinal plants: *Morus alba* L. *Morus mongolica* Schneider, *Broussnetia papyrifera* (L.) Vent, *Sophora flavescens* Ait and *Echinosophora koreensis* Nakai. Phytomedicine, 11(7-8), 666-672. https://https://doi.org/10.1016/j.phymed.2003.09.005

SUTTISANSANEE, U.; HONEK, J. F. (2011) Bacterial glyoxalase enzymes. Seminars in Cell & Developmental Biology, 22(3), 285-292. https://https://doi.org/10.1016/j.semcdb.2011.02.004

TAKAHASHI, Y.; BERBERICH, T.; KANZAKI, H.; MATSUMURA, H.; SAITOH, H.; KUSANO, T.; TERAUCHI, R (2009) Serine palmitoyl transferase, the first step enzyme in sphingolipid biosynthesis, is involved in non host resistance. Mol. Plant Microbe Interact. 22, 31-38. https://https://doi.org/10.1094/MPMI-22-1-0031

TAUTENHAHN, R.; PATTI, G. J.; RINEHART, D.; SIUZDAK, G. (2012) XCMS Online: a web-based platform to process untargeted metabolomic data. Anal. Chem. 84, 5035-5039. Epub 2012 May 10. https:// https://https://doi.org/10.1021/ac300698c

THORNALLEY, P. J. (2003) Glyoxalase I - structure, function and a critical role in the enzymatic defence against glycation. Biochem. Soc. Trans. 31 (Pt 6): 1343-8. https://https://doi.org/10.1042/BST0311343

TRIPATHI, P.; RABARA, R. C.; REESE, R. N.; MILLER, M. A.; ROHILA, J. S.; SUBRAMANIAN, S.; SHEN, Q. J.; MORANDI, D.; BÜCKING, H.; SHULAEV, V.; RUSHTON, P. J. (2016) A toolbox of genes, proteins, metabolites and promoters for improving drought tolerance in soybean includes the metabolite coumestrol and stomatal development genes. BMC Genomics. 9;17:102. https://https://doi.org/10.1186/s12864-016-2420-0.

UPCHURCH, R. G. (2008) Fatty acid unsaturation, mobilization, and regulation in the response of plants to stress. Biotechnology Letters, 30(6), 967-977. https://https://doi.org/10.1007/s10529-008-9639-z

VALENTE, M. A. S.; FARIA, J. Q. A.; RAMOS, J. R. L. S.; REIS, P. A. B.; PINHEIRO, G. L.; PIOVESAN, N. D.; MORAIS, A. T.; MENEZES, C. C.; CANO, M. A. O.; FIETTO, L. G.; LOUREIRO, M. E.; ARAGAO, F. J. L.; FONTES, E. B. P. (2009) The ER luminal binding protein (BiP) mediates an increase in drought tolerance in soybean and delays

drought-induced leaf senescence in soybean and tobacco. J. Exp. Bot. 60, 533-546. https://doi.org/10.1093/jxb/ern296

VAN LOON, L. C. (1985) Pathogenesis-related proteins. Plant Molecular Biology, 4(2-3), 111-116. https://https://doi.org/10.1007/bf02418757

VAN LOON, L. C.; REP, M.; PIETERSE, C. M. J. (2006) Significance of Inducible Defense-related Proteins in Infected Plants. Annual Review of Phytopathology, 44(1), 135-162. https://https://doi.org/10.1146/annurev.phyto. 44.070505.143425

VIERLING, E.; KIMPEL, J. A. (1992) Plant responses to environmental stress. Current Opinion in Biotechnology, 3(2), 164-170. https://https://doi.org/10.1016/0958-1669(92)90147-b

VITAL, C. E.; GÓMEZ, J. D.; VIDIGAL, P. M.; BARROS, E.; PONTES, C. S. L.; VIEIRA, N. M.; RAMOS, H. J. O. (2019) Phytohormone profiling by liquid chromatography coupled to mass spectrometry (LC/MS). Protocols. io. https://doi.org/10.17504/protocols.io.zgff3tn

VITAL, C. E.; GÓMEZ, J. D.; VIDIGAL, P. M.; BARROS, E. G.; PONTES, C. S. L.; VIEIRA, N. M.; OLIVEIRA, M. G. A.; RAMOS, H. J. O. (2019) Flavonoid profiling by liquid chromatography coupled to mass spectrometry (LC/MS). Protocols. io. https://doi.org/10.17504/protocols.io.zggf3tw

WALLEY, J. W.; KLIEBENSTEIN, D. J.; BOSTOCK, R. M.; DEHESH, K. (2013) Fatty acids and early detection of pathogens. Curr Opin Plant Biol. 16(4):520-6. https://https://doi.org/10.1016/j.pbi.2013.06.011

WALTERS, D. R. (2003) Polyamines and plant disease. Phytochemistry, 64(1), 97-107. https://https://doi.org/10.1016/s0031-9422(03)00329-7

WANG, G. -F.; BALINT-KURTI, P. J. (2016) Maize Homologs of CCoAOMT and HCT, Two Key Enzymes in Lignin Biosynthesis, Form Complexes with the NLR Rp1 Protein to Modulate the Defense Response. Plant Physiology, 171(3), 2166-2177. https://https://doi.org/10.1104/pp.16.00224

WANG, X. M. (2004) Lipid signaling. Curr. Opin. Plant Biol. 7, 329-336. https://https://doi.org/10.1016/j.pbi.2004.03.012

WEINSTEIN, L. I.; ALBERSHEIM, P. (1983) Host-pathogens interactions: XXIII. The mechanism of the antibacterial action of glycinol, a pterocarpan phytoalexin synthesized by soybeans. Plant Physiology, 72, 557-563

WELTI, R.; SHAH, J.; LI, W.; LI, M.; CHEN, J.; BURKE, J. J.; FAUCONNIER, M. L.; CHAPMAN, K.; CHYE, M. L.; WANG, X. (2007) Plant lipidomics: discerning biological function by profiling plant complex lipids using mass spectrometry. Front. Biosci. 12:2494-2506. https://https://doi.org/10.2741/2250

XIAO, F.; MARK GOODWIN, S.; XIAO, Y.; SUN, Z.; BAKER, D.; TANG, X.; JENKS, M. A.; ZHOU, J. -M. (2004) Arabidopsis CYP86A2 represses *Pseudomonas syringae* type III

genes and is required for cuticle development. The EMBO Journal, 23(14), 2903-2913. https://https://doi.org/10.1038/sj.emboj.7600290

XIE, Y.; YANG, W.; TANG, F.; CHEN, X.; REN, L. (2014) Antibacterial Activities of Flavonoids: Structure-Activity Relationship and Mechanism. Current Medicinal Chemistry, 22(1), 132-149. https://https://doi.org/10.2174/09298673216661409161134443

YAMAUCHI, Y.; HASEGAWA, A.; TANINAKA, A.; MIZUTANI, M.; SUGIMOTO, Y. (2011) NADPH-dependent reductases involved in the detoxification of reactive carbonyls in plants. J. Biol. Chem. 286, 6999-7009

YAO, Q.; BOLLINGER, C.; GAO, J.; XU, D.; THELEN, J. J. (2012) P(3)DB: An Integrated Database for Plant Protein Phosphorylation. Frontiers in plant science, 3: 206. https://doi.org/10.3389/fpls.2012.00206

YU, J.; SUN, H.; ZHANG, J.; HOU, Y.; ZHANG, T.; KANG, J.; WANG, Z.; YANG, Q.; LONG, R. (2020) Analysis of Aldo-Keto Reductase Gene Family and Their Responses to Salt, Drought, and Abscisic Acid Stresses in *Medicago truncatula*. International Journal of Molecular Sciences, 21(3), 754. https://https://doi.org/10.3390/ijms21030754

ZHANG, Q.; XIAO, S. (2015) Lipids in salicylic acid-mediated defense in plants: focusing on the roles of phosphatidic acid and phosphatidylinositol 4-phosphate. Frontiers in Plant Science, 6. https://https://doi.org/10.3389/fpls.2015.00387

ZHAO, J.; DEVAIAH, S. P.; WANG, C.; LI, M.; WELTI, R.; WANG, X. (2013) Arabidopsis phospholipase Dbeta1 modulates defense responses to bacterial and fungal pathogens. New Phytol. 199, 228-240. https://https://doi.org/10.1111/nph.12256

ZOU, J.; RODRIGUEZ-ZAS, S.; ALDEA, M.; LI, M.; ZHU, J.; GONZALEZ, D. O.; VODKIN, L. O.; DELUCIA, E.; CLOUGH, S. J. (2005) Expression profiling soybean response to *Pseudomonas syringae* reveals new defense-related genes and rapid hr-specific downregulation of photosynthesis. Mol Plant-Microbe Interact 18(11):1161-1174

APPENDIX

Appendix A – Protein profile in 2-DE/SDS-PAGE gel of soybean leaf extract in WT genotype in response to inoculation with *P. syringae* pv. tomato. (A) Infected WT and (B) mock infected WT. Arrows indicate differential spots identified by LC-MS. Gels were stained with Coomassie Blue and differential expression was analyzed in ImageMaster 2D Platinum software.

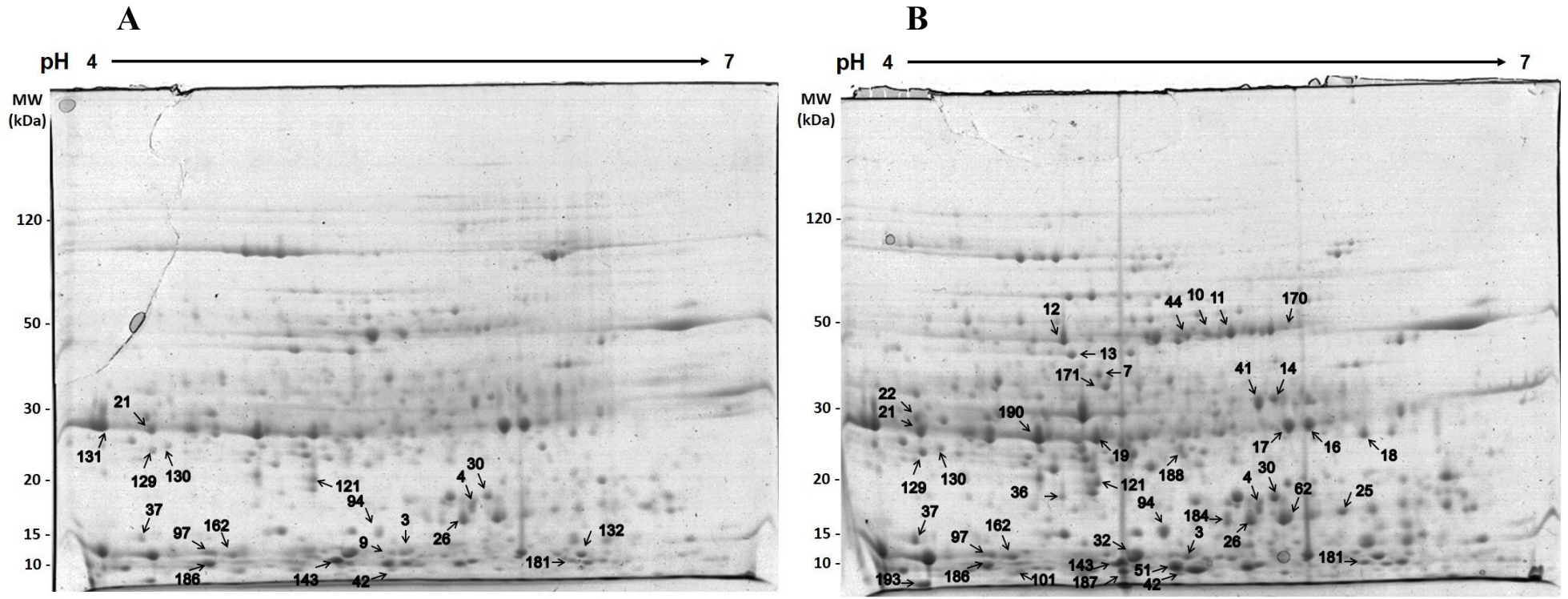

Source: Survey's data.

Appendix B – Protein profile in 2-DE/SDS-PAGE gel of soybean leaf extract in C9 genotype in response to inoculation with *P. syringae* pv. tomato. (A) Infected C9 and (B) mock infected C9. Arrows indicate differential spots identified by LC-MS. Gels were stained with Coomassie Blue and differential expression was analyzed in ImageMaster 2D Platinum software.

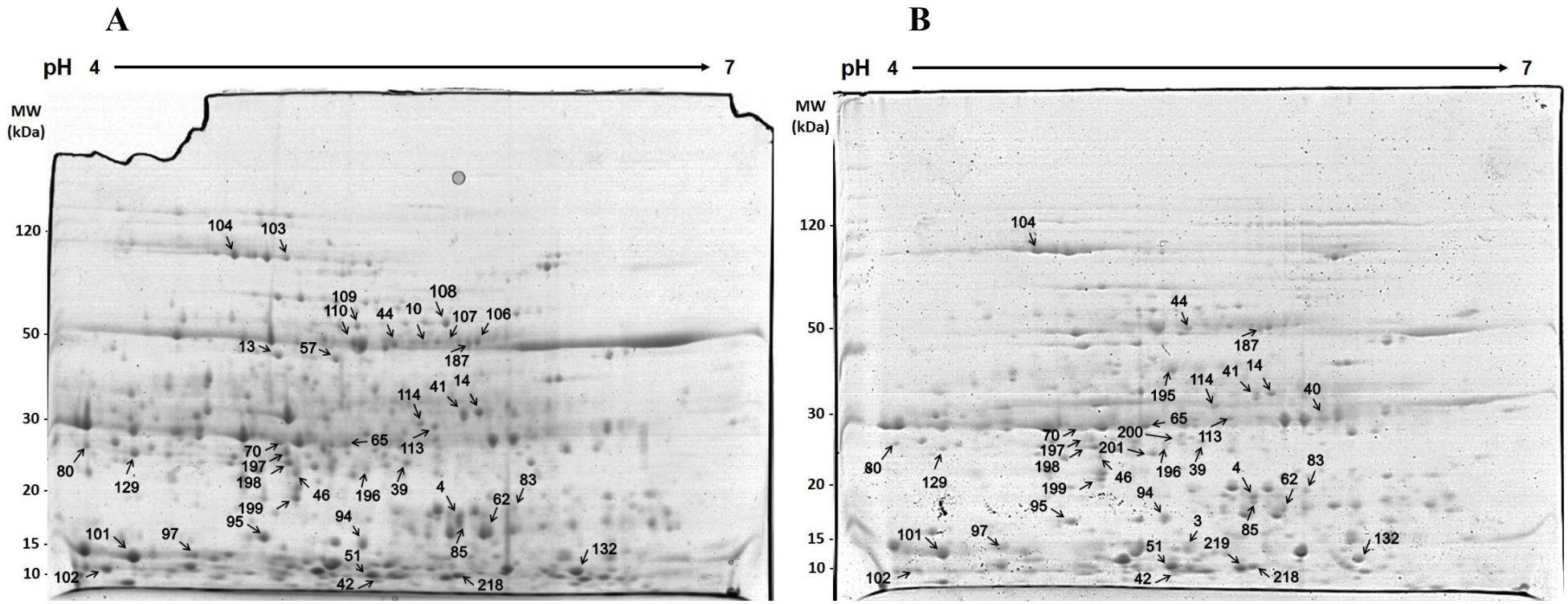

Source: Survey's data.

Appendix C – Protein profile in 2-DE/SDS-PAGE gel of soybean leaf extract in the mock infection by *P. syringae* pv. tomato (NI). (A) C9 genotype (B) WT genotype. Arrows indicate differential spots identified by LC-MS. Gels were stained with Coomassie Blue and differential expression was analyzed in ImageMaster 2D Platinum software.

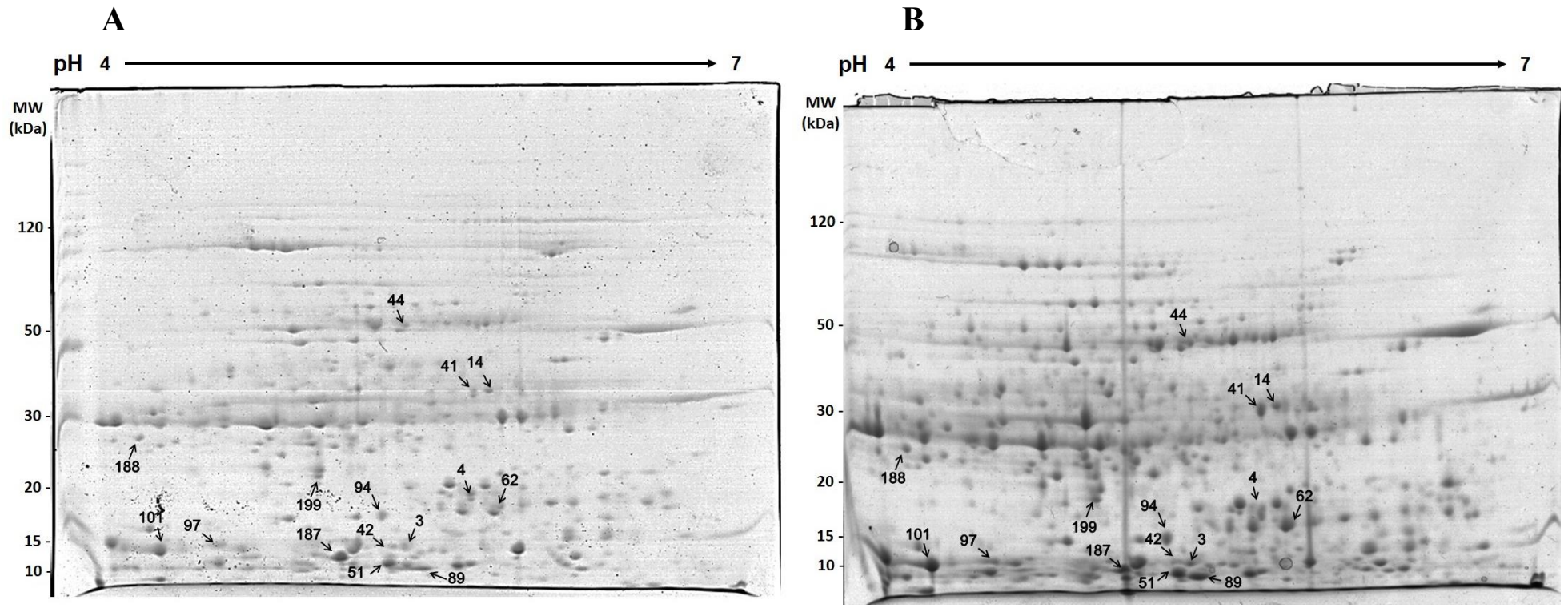

Source: Survey's data.

Appendix D – Differences in the protein abundances of each protein spot of the leaves from wild-type genotype (WT) under infection (I) or mock inoculation (NI) by *P. syringae* pv. tomato. Positive and negative expression level values indicate up- and down-regulation, respectively. Values of fold change for protein spots when present only in a genotype or treatment are shown as 10.00 or -10.00, respectively.

Spot ID	Protein name	ABREV	Glyma code	TAIR code	-10lgP	Coverage (%)	Peptide Number	Media WT NI	SD WT NI	Media WT I	SD WT I	Expression level
	PHOTOSYNTHESIS											
25	Carbonic anhydrase 2, chloroplastic-related	CA2	Glyma.19g007700.7.p	AT5G14740.1	67.84	14	3	0.344	± 0.022			-10
101	Carbonic anhydrase 2, chloroplastic-related	CA2	Glyma.05g007100.4.p	AT5G14740.1	64.54	13	3	0.667	± 0.05			-10
17	Fructose-1,6-bisphosphatase, cytosolic	FBPase	Glyma.11g226900.1.p	AT1G43670.1	163.03	44	18	0.772	± 0.075			-10
131	Fructose-bisphosphate aldolase 1	ALDO1	Glyma.11g111400.1.p	AT2G21330.2	157.66	22	9			0.214	± 0.029	10
19	Fructose-bisphosphate aldolase 1	ALDO1	Glyma.12g037400.1.p	AT2G21330.2	222.71	36	15	1.252	± 0.092			-10
181	Light-harvesting complex II chlorophyll a/b binding protein 3	LHCB3	Glyma.13g282000.1.p	AT5G54270.1	117.68	14	4	0.27	± 0.029	0.124	± 0.001	-2.177
62	Phosphoglycerate kinase 1, chloroplastic-related	PGK2	Glyma.08g165500.1.p	AT1G56190.1	100.47	9	4	0.953	± 0.068			-10
14	Phosphoribulokinase	PRK	Glyma.01g010200.1.p	AT1G32060.1	103.62	14	5	0.742	± 0.062			-10
181	Photosystem I reaction center PsbP-domain protein 1	PSI_PSBP	Glyma.03g230300.1.p	AT4G15510.1	125.18	15	4	0.27	± 0.029			-10
30	Photosystem II subunit O	PSII_PSBO	Glyma.01g180800.1.p	AT5G66570.1	34.93	2	2	0.321	± 0.023	0.125	± 0.001	-2.568

Spot ID	Protein name	ABREV	Glyma code	TAIR code	-10lgP	Coverage (%)	Peptide Number	Media WT NI	SD WT NI	Media WT I	SD WT I	Expression level
94	Photosystem II subunit O	PSII_PSBO	Glyma.01g180800.1.p	AT5G66570.1	124.47	12	2	0.248	± 0.041	0.146	± 0.011	-1.699
51	Photosystem II subunit P-1	PSII_PSBP1	Glyma.18g114900.1.p	AT1G06680.1	196.23	51	14	0.543	± 0.212			-10
42	Photosystem II subunit P-1	PSII_PSBP1	Glyma.18g114900.1.p	AT1G06680.1	88.79	18	4	1.252	± 0.107	0.449	± 0.124	-2.788
187	Photosystem II subunit P-1	PSII_PSBP1	Glyma.14g031800.1.p	AT1G06680.1	130.47	16	5	1.501	± 0.325			-10
143	Photosystem II subunit P-1	PSII_PSBP1	Glyma.02g282500.1.p	AT1G06680.2	142.97	25	5	0.672	± 0.079	0.392	± 0.02	-1.714
132	Ribose 5-phosphate isomerase A	RPIA	Glyma.03g246300.1.p	AT3G04790.1	93.21	15	5			0.338	± 0.007	10
36	(Ribulose / Xilulose)-5-phosphate 3-epimerase	RPE / XPE	Glyma.17g101700.5.p	AT5G61410.1	164.07	43	11	0.667	± 0.05			-10
162	(Ribulose / Xilulose)-5-phosphate 3-epimerase	RPE / XPE	Glyma.05g025300.1.p	AT5G61410.1	60.4	8	3	0.467	± 0.042	0.186	± 0.034	-2.511
16	Sedoheptulose-1,7-bisphosphatase	SBPase	Glyma.18g030400.1.p	AT3G55800.1	163.03	44	18	0.772	± 0.075			-10
32	Triosephosphate isomerase, plastid isoform	TPI	Glyma.10g059500.1.p	AT2G21170.1	212.19	57	15	1.641	± 0.106			-10
143	Triosephosphate isomerase, plastid isoform	TPI	Glyma.19g186000.1.p	AT2G21170.1	160.31	35	6	0.344	± 0.022	0.672	± 0.672	1.953
	PRIMARY METABOLISM											

Spot ID	Protein name	ABREV	Glyma code	TAIR code	-10lgP	Coverage (%)	Peptide Number	Media WT NI	SD WT NI	Media WT I	SD WT I	Expression level
170	Beta-amylase	BETA-AMY	Glyma.06g301500.1.p	AT4G15210.1	99.68	16	5	1.039	± 0.09			-10
21	Cytosolic NAD-dependent malate dehydrogenase 1	cMDH1	Glyma.10g006500.1.p	AT1G04410.1	168.97	27	7	2.61	± 0.196	0.495		-5.273
190	Cytosolic NAD-dependent malate dehydrogenase 1	cMDH1	Glyma.10g006500.1.p	AT1G04410.1	94.94	8	4	1.252	± 0.092			-10
10	Enolase	ENO2	Glyma.19g190900.1.p	AT2G36530.1	114.79	17	5	0.452	± 0.038			-10
11	Enolase	ENO2	Glyma.19g190900.1.p	AT2G36530.1	119.29	15	6	0.997	± 0.066			-10
184	Haloacid dehalogenase-like hydrolase superfamily protein	HAD	Glyma.04g191700.1.p	AT3G48420.1	128.98	16	6	0.953	± 0.068			-10
129	Lactate/malate dehydrogenase family protein (Mitochondrial)	mMDH2	Glyma.06g231500.1.p	AT3G15020.1	137.03	19	4	0.929	± 0.062	0.22	± 0.126	-4.223
44	Mitochondrial ATP synthase beta-subunit	ATPeF1B	Glyma.10g267200.1.p	AT5G08690.1	111.65	10	4	0.997	± 0.066			-10
10	UDP-glucose pyrophosphorylase 2	UGP2	Glyma.14g210700.1.p	AT5G17310.2	127.36	20	5	0.452	± 0.038			-10
	SPECIALIZED METABOLISM											
171	1-Deoxy-D-xylulose-5-phosphate	DXR	Glyma.16g089000.2.p	AT5G62790.2	133.99	22	7	0.537	± 0.062			-10

Spot ID	Protein name	ABREV	Glyma code	TAIR code	-10lgP	Coverage (%)	Peptide Number	Media WT NI	SD WT NI	Media WT I	SD WT I	Expression level
	reductoisomerase											
94	Caffeoyl coenzime A O-methyltransferase 1	CCoAOMT1	Glyma.07g214700.1.p	AT4G34050.3	107.68	26	5	0.248	± 0.041	0.146	± 0.011	-1.699
188	L-galactose 1-dehydrogenase	GALDH	Glyma.08g064100.1.p	AT4G33670.1	114.19	16	9	0.538	± 0.069			-10
	AMINOACID METABOLISM											
4	Aspartate aminotransferase, chloroplastic	AspAT	Glyma.17g216000.2.p	AT5G19550.1	109.43	11	4	0.156	± 0.031	0.543	± 0.057	3.481
	PHOTORESPIRATION											
7	Glutamate:glyoxylate aminotransferase 2	GGT2	Glyma.01g026700.1.p	AT1G70580.1	80.18	9	3	0.997	± 0.066			-10
13	Glutamate:glyoxylate aminotransferase 2	GGT2	Glyma.01g026700.3.p	AT1G70580.1	126.03	24	10	0.289	± 0.019			-10
	ANTIOXIDATIVE METABOLISM											
22	Aldo-keto reductase family 4 member c10	AKR4C10	Glyma.03g066800.1.p	AT2G37760.3	149.19	31	9	0.504	± 0.049			-10
9	Fe superoxide dismutase 1	SOD1	Glyma.10g193500.1.p	AT4G25100.2	161.68	32	6			0.226	± 0.018	10
3	Fe superoxide dismutase 1	SOD1	Glyma.10g193500.1.p	AT4G25100.2	150.09	30	6	0.389	± 0.065	0.775	± 0.068	1.992
32	Fe superoxide dismutase	SOD2	Glyma.20g	AT5G5	142.66	27	5	1.641	± 0.106	2.338		1.425

Spot ID	Protein name	ABREV	Glyma code	TAIR code	-10lgP	Coverage (%)	Peptide Number	Media WT NI	SD WT NI	Media WT I	SD WT I	Expression level
	2		196900.1.p	1100.1								
121	Leaf ferredoxin-NADP(+)-oxidoreductase 1	LFNR1	Glyma.16g127300.1.p	AT5G66190.1	45.4	4	2	0.489	± 0.102	0.371	± 0.099	-1.318
	RESPONSE TO STRESS											
186	Chaperonin 20 kDa, chloroplastic	CPN20	Glyma.13g112500.2.p	AT5G20720.2	82.73	18	3	0.667	± 0.05	1.388	± 0.175	2.081
26	Chloroplastic drought-induced stress protein of 32 kDa	CDSP32	Glyma.14g222500.1.p	AT1G76080.1	135.17	22	8	0.66	± 0.045	0.367	± 0.025	-1.798
97	Esponsive to dehydration 21B	RD21B	Glyma.14g085600.1.p	AT5G43060.1	132.04	15	6	0.44	± 0.052	0.328	± 0.133	-1.341
41	GDSL-like esterase/acyltransferase/lipase superfamily protein	GDSL1	Glyma.15g089000.1.p	AT5G45670.1	105.14	9	3	0.742	± 0.062			-10
193	Matrixin family protein	MMP	Glyma.02g215700.1.p	AT2G45040.1	180.63	28	11	0.629	± 0.105			-10
37	Vegetative storage protein 1	VSP1	Glyma.08g200100.1.p	AT5G24780.1	132.37	28	8	0.49	± 0.044	0.794	± 0.002	1.62
	REGULATION											
12	Adenosylhomocysteinase	SAHH1	Glyma.08g108800.1.p	AT4G13940.1	160.49	19	8	0.539	± 0.053			-10
18	Adenosylhomocysteine nucleosidase	SAHN	Glyma.06g084200.1.p	AT1G52190.1	95.5	18	5	0.365	± 0.034			-10

Spot ID	Protein name	ABREV	Glyma code	TAIR code	-10lgP	Coverage (%)	Peptide Number	Media WT NI		SD WT NI	Media WT I		SD WT I	Expression level
130	DNA mismatch repair protein MSH3	MSH3	Glyma.20g157600.4.p	AT4G25540.1	35.68	3	2	0.307	±	0.071	0.404	±	0.043	1.316
32	N-acetylglucosaminyltransferase SPINDLY-related	SPY	Glyma.19g196000.1.p	AT3G11540.1	206.34	47	18	1.641	±	0.106				-10

Source: Survey's data.

Appendix E – Differences in the protein abundances of each protein spot of the leaves from overexpressing BiP genotype C9 under infection (I) or mock inoculation (NI) by *P. syringae* pv. tomato. Positive and negative expression level values indicate up- and down-regulation, respectively. Values of fold change for protein spots when present only in a genotype or treatment are shown as 10.00 or -10.00, respectively.

Spot ID	Protein name	ABREV	Glyma Code	TAIR Code	-10lgP	Coverage (%)	Peptide Number	Media C9 NI		SD C9 NI	Media C9 I		SD C9 I	Expression level
	PHOTOSYNTHESIS													
101	Carbonic anhydrase 2, chloroplastic-related	CA2	Glyma.05g007100.4.p	AT5G14740.1	91.73	20	3	0.233			0.311	±	0.089	1.335
197	Coproporphyrinogen III oxidase	CPOX	Glyma.14g003200.2.p	AT1G03475.1	105.65	18	5	0.543	±	0.212	0.249	±	0.114	-2.181
39	Fructokinase 4 / Fructokinase 7	FRK 4 / FRK 7	Glyma.13g344500.1.p	AT3G59480.1	107.29	11	3	0.333			0.25	±	0.076	-1.332
195	Fructose-bisphosphate aldolase 1	ALDO1	Glyma.12g037400.1.p	AT2G21330.2	135.43	13	6	0.472	±	0.236				-10
62	Phosphoglycerate kinase 1, chloroplastic-related	PGK2	Glyma.08g165500.1.p	AT1G56190.1	66.88	4	2	1.89			1.246	±	0.063	-1.517
70	Phosphoglycerate kinase	PGK2	Glyma.15g	AT1G5	252.59	51	21	0.44			0.328	±	0.133	-1.341

Spot ID	Protein name	ABREV	Glyma Code	TAIR Code	-10lgP	Coverage (%)	Peptide Number	Media C9 NI	SD C9 NI	Media C9 I	SD C9 I	Expression level
	1, chloroplastic-related		261900.1.p	6190.1								
62	Phosphoglycerate kinase 1, chloroplastic-related	PGK2	Glyma.15g 261900.1.p	AT1G5 6190.1	118.82	10	3	1.89		1.246	± 0.063	-1.517
40	Phosphoglycerate kinase 1, chloroplastic-related	PGK2	Glyma.15g 261900.2.p	AT1G5 6190.1	88.14	13	3	0.628	± 0.121			-10
14	Phosphoribulokinase	PRK	Glyma.01g 010200.1.p	AT1G3 2060.1	66.14	9	4	0.835		0.318	± 0.051	-2.626
113	Phosphoribulokinase	PRK	Glyma.09g 210900.1.p	AT1G3 2060.1	115.62	13	4	0.354		0.184	± 0.053	-1.924
83	Photosystem II subunit O	PSII_PS BO	Glyma.11g 061300.1.p	AT3G5 0820.1	97.36	21	5	1.074	± 0.462	0.668	± 0.096	-1.608
187	Photosystem II subunit P-1	PSII_PS BP1	Glyma.14g 031800.1.p	AT1G0 6680.1	161.41	21	8	0.397		0.301	± 0.089	-1.319
51	Photosystem II subunit P-1	PSII_PS BP1	Glyma.18g 114900.1.p	AT1G0 6680.1	203.78	44	12	0.547		0.206	± 0.028	-2.655
42	Photosystem II subunit P-1	PSII_PS BP1	Glyma.18g 114900.1.p	AT1G0 6680.1	174.51	54	12	0.734	± 0.154	0.456	± 0.054	-1.61
132	Ribose 5-phosphate isomerase A	RPIA	Glyma.03g 246300.1.p	AT3G0 4790.1	164.54	37	7	0.798		0.208	± 0.038	-3.837
	PRIMARY METABOLISM											
10	Enolase	ENO2	Glyma.03g 190500.1.p	AT2G3 6530.1	95.86	14	4			0.32	± 0.036	10
129	Lactate/malate dehydrogenase family protein (Mitochondrial)	mMDH2	Glyma.06g 231500.1.p	AT3G1 5020.1	116.66	18	6	0.138222	± 0.0051 29	0.228077	± 0.126 846	-1.65

Spot ID	Protein name	ABREV	Glyma Code	TAIR Code	-10lgP	Coverage (%)	Peptide Number	Media C9 NI	SD C9 NI	Media C9 I	SD C9 I	Expression level
44	Mitochondrial ATP synthase beta-subunit	ATPeF1B	Glyma.10g267200.1.p	AT5G08690.1	142.27	16	6	0.73	± 0.202	0.19	± 0.095	-3.842
109	Phosphoglycerate mutase (cofactor-independent)	iPGM	Glyma.18g279400.3.p	AT4G09520.1	22.13	1	2			0.232		10
85	Pyrophosphorylase 6	PPa6	Glyma.13g253600.1.p	AT5G09650.1	89.28	17	6	0.369	± 0.069	0.253	± 0.064	-1.458
10	UDP-glucose pyrophosphorylase 2	UGP2	Glyma.14g210700.1.p	AT5G17310.2	172.18	30	9			0.19	± 0.095	10
	SPECIALIZED METABOLISM											
114	Caffeic acid/5-hydroxyferulic acid O-methyltransferase	COMT1	Glyma.12g109800.1.p	AT5G54160.1	20.09	1	2	0.512		0.668	± 0.056	1.305
108	Caffeic acid/5-hydroxyferulic acid O-methyltransferase	COMT1	Glyma.12g109800.1.p	AT5G54160.1	24.47	2	2			0.289	± 0.069	10
94	Caffeoyl coenzime A ester O-methyltransferase 7	CCoAOMT7	Glyma.01g004200.1.p	AT4G26220.1	155.15	18	4	0.328	± 0.004	0.55	± 0.055	1.677
102	Chalcone-flavanone isomerase	CFI	Glyma.20g241500.1.p	AT3G55120.1	184.48	45	9	0.393	± 0.162	0.511	± 0.109	1.3
198	Phenylcoumaran benzylic ether reductase 1	PCBER1	Glyma.04g012300.1.p	AT4G39230.1	72.09	14	3	0.603	± 0.212	0.449	± 0.02	-1.343
	AMINOACID											

Spot ID	Protein name	ABREV	Glyma Code	TAIR Code	-10lgP	Coverage (%)	Peptide Number	Media C9 NI	SD C9 NI	Media C9 I	SD C9 I	Expression level
	METABOLISM											
104	2-Keto-3-deoxyarabinoheptulosonate-7-phosphate syntase	DAHPS 1	Glyma.14g 176600.1.p	AT1G2 2410.1	26.92	1	2	0.594	± 0.143	0.798	± 0.19	1.343
4	Aspartate aminotransferase, chloroplastic	AspAT	Glyma.17g 216000.2.p	AT5G1 9550.1	158.72	20	7	0.369	± 0.069	0.253	± 0.064	-1.458
196	Cysteine synthase B / O-acetylserine (thiol) lyase B	Csase B / OASB	Glyma.02g 138400.1.p	AT2G4 3750.1	154.02	18	6	0.339		0.544	± 0.124	1.605
	PHOTORESPIRATION											
13	Glutamate:glyoxylate aminotransferase 2	GGT2	Glyma.01g 026700.3.p	AT1G7 0580.1	84.88	7	3			0.293	± 0.018	10
57	Glutamate:glyoxylate aminotransferase 2	GGT2	Glyma.02g 038100.2.p	AT1G7 0580.1	98.13	16	6			0.364	± 0.013	10
	ANTIOXIDATIVE METABOLISM											
129	Aldo-keto reductase family 4 member c10	AKR4C1 0	Glyma.03g 066800.1.p	AT2G3 7760.3	117.12	18	6	0.228	± 0.127	0.138	± 0.005	-1.652
108	Brassinosteroid-6-oxidase 2	BR6OX2	Glyma.13g 052900.4.p	AT3G3 0180.1	155.15	18	4	0.328	± 0.004	0.55	± 0.055	1.677
3	Fe superoxide dismutase 1	SOD1	Glyma.10g 193500.1.p	AT4G2 5100.2	136.2	24	5	0.236	± 0.012	1.332	± 0.174	5.644
107	Ferredoxin-NADP(+) oxidoreductase -like	FNLR	Glyma.10g 267000.2.p	AT1G1 5140.1	79.07	12	2			0.208	± 0.023	10

Spot ID	Protein name	ABREV	Glyma Code	TAIR Code	-10lgP	Coverage (%)	Peptide Number	Media C9 NI	SD C9 NI	Media C9 I	SD C9 I	Expression level
219	Glutathione S-transferase lambda 1	GSTL1	Glyma.13g135500.1.p	AT5G02780.2	96.03	21	3	0.499	± 0.123	0	0	-10
218	Glutathione S-transferase tau 11	GSTU11	Glyma.01g040200.1.p	AT1G69930.1	138.53	19	5	0.208	± 0.038	0.16	± 0.034	-1.3
46	Glyoxalase I homolog	GLX1	Glyma.07g261400.3.p	AT1G11840.1	74.28	16	3	0.385	± 0.047	0.655	± 0.057	1.701
199	Glyoxalase I homolog	GLX1	Glyma.07g261400.5.p	AT1G11840.1	99.48	20	6	0.472	± 0.236	0.949	± 0.036	2.011
80	NADPH-dependent alkenal/one oxidoreductase	AOR	Glyma.16g073600.1.p	AT1G23740.1	174.64	39	12	0.157	± 0.1	0.948	± 0.346	6.038
103	Peroxisome 1	PEX1	Glyma.07g224000.2.p	AT5G08470.2	22.89	1	2			0.125	± 0.001	10
	RESPONSE TO STRESS											
201	Aldose 1-epimerase family protein	GALM	Glyma.01g173300.1.p	AT5G66530.3	74.79	13	4	0.255	± 0.189			-10
97	Esponsive to dehydration 21B	RD21B	Glyma.14g085600.1.p	AT5G43060.1	112.37	13	3	2.264	± 0.857	1.521	± 0.214	-1.488
41	GDSL-like esterase/acyltransferase/lipase superfamily protein	GDSL1	Glyma.15g089000.1.p	AT5G45670.1	186.59	20	8	0.428	± 0.121	0.663	± 0.098	1.549
200	MYC3 transcription factor	MYC3	Glyma.06g295100.1.p	AT5G46760.1	70.17	12	3	0.339	± 0.212			-10
65	PR-protein Bet v I family / PR-10	BET_V_1 / PR-10	Glyma.15g146400.1.p	AT2G02410.1	91.52	11	3	0.35		0.23	± 0.021	-1.522

Spot ID	Protein name	ABREV	Glyma Code	TAIR Code	-10lgP	Coverage (%)	Peptide Number	Media C9 NI	SD C9 NI	Media C9 I	SD C9 I	Expression level
	REGULATION											
62	ATP citrate lyase	ACL	Glyma.10g039000.1.p	AT2G20420.1	116.66	18	6	0.313	± 0.049			-10
110	Class II aminoacyl-tRNA and biotin synthetases superfamily protein / Aspartate-tRNA ligase / Aspartyl-tRNA synthetase	aaRS	Glyma.14g101500.1.p	AT4G26870.1	24.88	2	2			0.343	± 0.101	10
106	Guanyl-nucleotide exchange factor SPIKE 1	GEF-SPI1	Glyma.15g212800.4.p	AT4G16340.1	28.75	1	2			0.289	± 0.069	10
	UNKNOWN PROTEIN											
95	Uncharacterized protein AT2G37660, chloroplastic		Glyma.07g133200.2.p	AT2G37660.1	152.96	30	11	0.351		0.493	± 0.067	1.405

Source: Survey's data.

Appendix F – Differences in protein abundances of each protein spot of the leaves from both genotypes in absence of bacterial infection (**C9NI x WTNI**). Positive and negative expression level values indicate up- and down-regulation, respectively.

Spot ID	Protein name	ABREV	Glyma Code	TAIR Code	Media C9 NI	SD C9 NI	Media WT NI	SD WT NI	Expression level
	PHOTOSYNTHESIS								
101	Carbonic anhydrase 2, chloroplastic-related	CA2	Glyma.05g00	AT5G14	0.233	± 0.002	0.667	± 0.05	-2.863

Spot ID	Protein name	ABREV	Glyma Code	TAIR Code	Media C9 NI	SD C9 NI	Media WT NI	SD WT NI	Expression level
			7100.4.p	740.1					
199	Fructose-bisphosphate aldolase 1	ALDO1	Glyma.12g037400.1.p	AT2G21330.2	0.472	± 0.236	1.252	± 0.092	-2.653
62	Phosphoglycerate kinase 1, chloroplastic-related	PGK2	Glyma.15g261900.1.p	AT1G56190.1	1.89	± 0.003	0.953	± 0.068	1.983
14	Phosphoribulokinase	PRK	Glyma.01g010200.1.p	AT1G32060.1	0.354	± 0.001	0.742	± 0.062	-2.096
51	Photosystem II subunit P-1	PSII_PSBP1	Glyma.18g114900.1.p	AT1G06680.1	0.547	± 0.001	1.252	± 0.107	-2.289
42	Photosystem II subunit P-1	PSII_PSBP1	Glyma.18g114900.1.p	AT1G06680.1	0.734	± 0.154	0.543	± 0.212	1.352
187	Photosystem II subunit P-1	PSII_PSBP1	Glyma.14g031800.1.p	AT1G06680.1	0.397	± 0.001	1.501	± 0.325	-3.781
89	Photosystem II subunit P-2	PSII_PSBP2	Glyma.08g304200.1.p	AT2G30790.1	1.7	± 0.631	0.672	± 0.079	2.53
	PRIMARY METABOLISM								
44	Mitochondrial ATP synthase beta-subunit	ATPeF1B	Glyma.10g267200.1.p	AT5G08690.1	0.73	± 0.202	0.997	± 0.066	-1.366
	SPECIALIZED METABOLISM								
94	Caffeoyl coenzime A ester O-methyltransferase 7	CCoAOMT7	Glyma.01g004200.1.p	AT4G26220.1	0.328	± 0.004	0.248	± 0.041	1.323
	AMINOACID METABOLISM								
4	Aspartate aminotransferase, chloroplastic	AspAT	Glyma.17g216000.2.p	AT5G19550.1	0.369	± 0.069	0.156	± 0.031	2.365

Spot ID	Protein name	ABREV	Glyma Code	TAIR Code	Media C9 NI	SD C9 NI	Media WT NI	SD WT NI	Expression level
	ANTIOXIDATIVE METABOLISM								
188	Aldo-keto reductase family 4 member c10	AKR4C10	Glyma.03g066800.1.p	AT2G37760.3	0.228	± 0.127	0.504	± 0.049	-2.211
3	Fe superoxide dismutase 1	SOD1	Glyma.10g193500.1.p	AT4G25100.2	0.236	± 0.012	0.389	± 0.065	-1.648
	RESPONSE TO STRESS								
97	Esponsive to dehydration 21B	RD21B	Glyma.14g085600.1.p	AT5G43060.1	2.264	± 0.857	0.44	± 0.052	5.145
41	GDSL-like esterase/acyltransferase/lipase superfamily protein	GDSL1	Glyma.15g089000.1.p	AT5G45670.1	0.428	± 0.121	0.742	± 0.062	-1.734

Source: Survey's data.

Appendix G – Phosphoprotein profile in 2-DE/SDS-PAGE gel of soybean leaf extract in WT genotype in response to inoculation with *P. syringae* pv. tomato. (A) Infected WT and (B) mock infected WT. Arrows indicate differentially phosphorylated spots identified by LC-MS. Gels were stained with Pro-Q® DPS kit and differential expression was analyzed in ImageMaster 2D Platinum software.

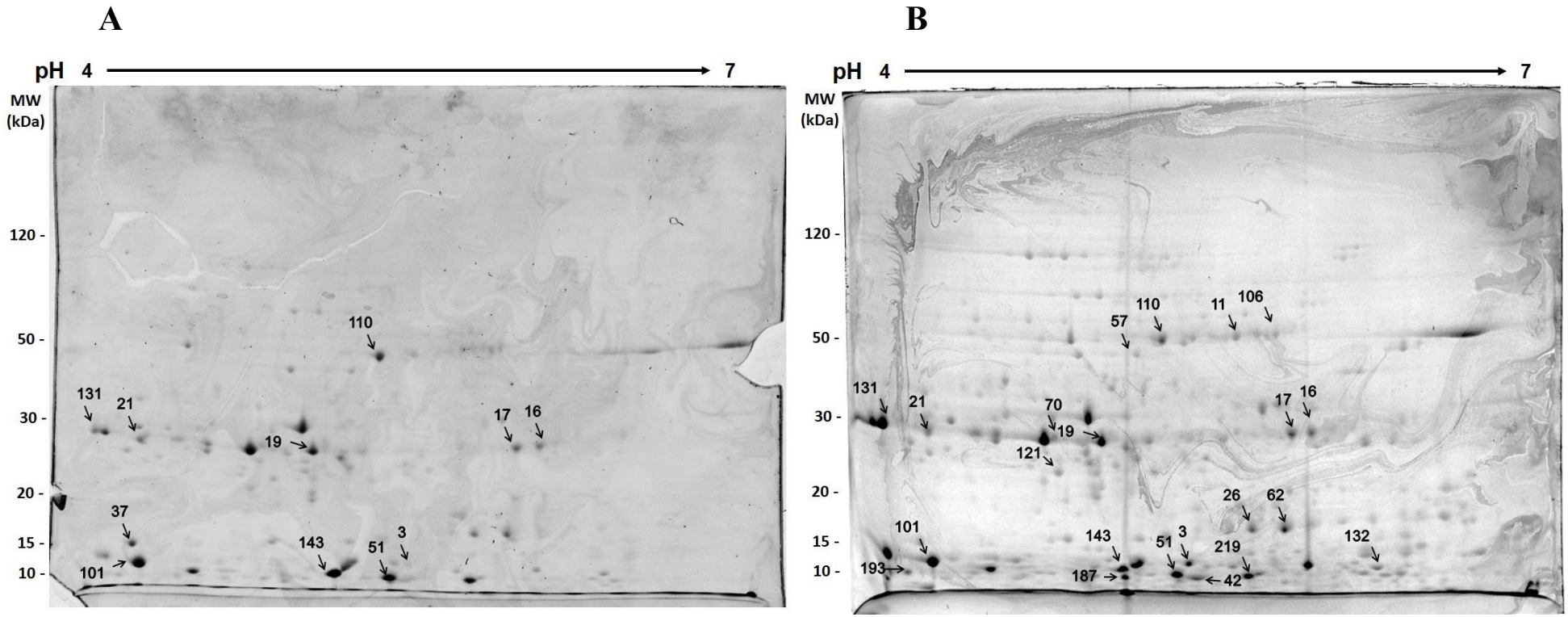

Source: Survey's data.

Appendix H – Phosphoprotein profile in 2-DE/SDS-PAGE gel of soybean leaf extract in C9 genotype in response to inoculation with *P. syringae* pv. tomato. (A) Infected C9 and (B) mock infected C9. Arrows indicate differentially phosphorylated spots identified by LC-MS. Gels were stained with Pro-Q® DPS kit and differential expression was analyzed in ImageMaster 2D Platinum software.

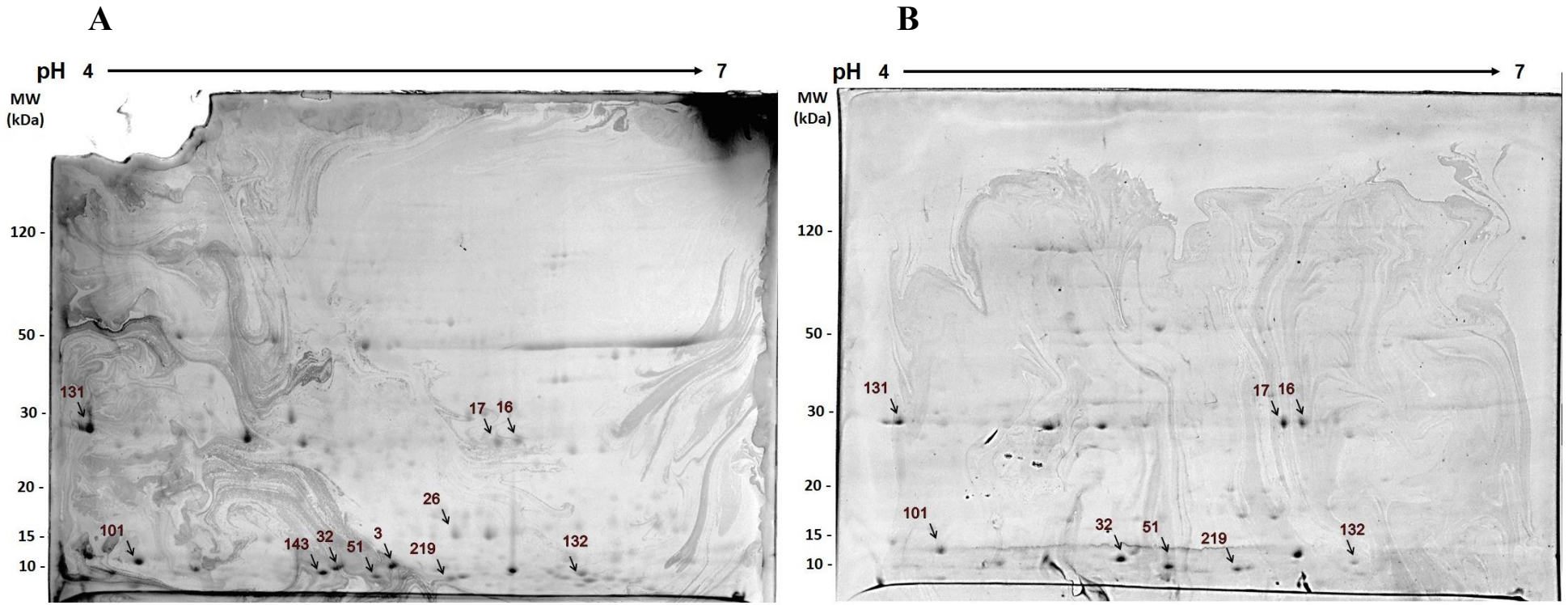

Source: Survey's data.

Appendix I – Phosphoprotein profile in 2-DE/SDS-PAGE gel of soybean leaf extract in the mock infection by *P. syringae* pv. tomato (NI). (A) C9 genotype (B) WT genotype. Arrows indicate differentially phosphorylated spots identified by LC-MS. Gels were stained with Pro-Q® DPS kit and differential expression was analyzed in ImageMaster 2D Platinum software.

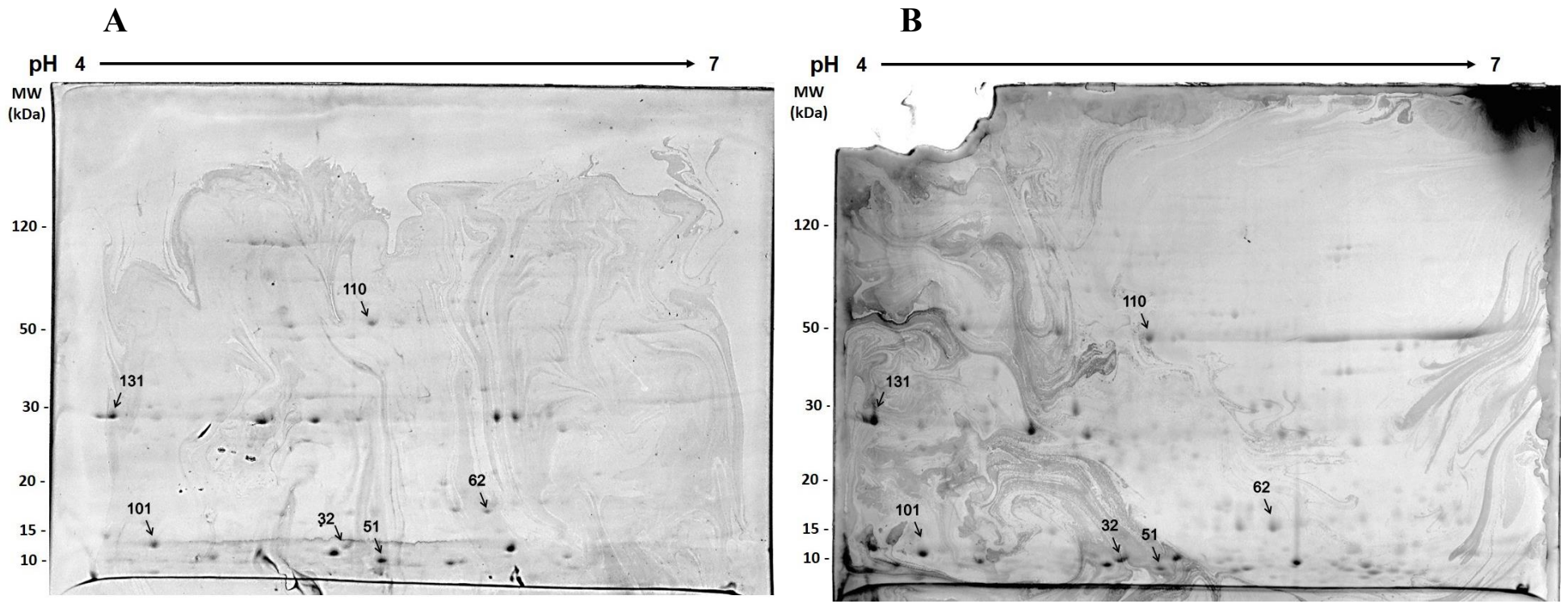

Source: Survey's data.

Appendix J – In **(A)** Venn Diagram showing the comparison of the number of phosphoproteinas differentially expressed. In **(B)** percentual of up-regulated or down-regulated proteins in response to bacterial infection in the leaves from WT and C9 genotypes. In **(C)** and **(D)** functional categorizations of diferentially expressed phosphoproteins responsive to infection.

A

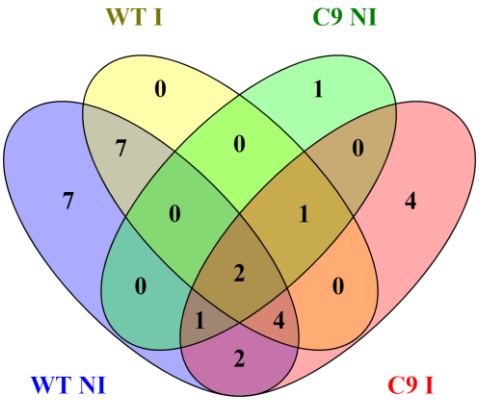

B

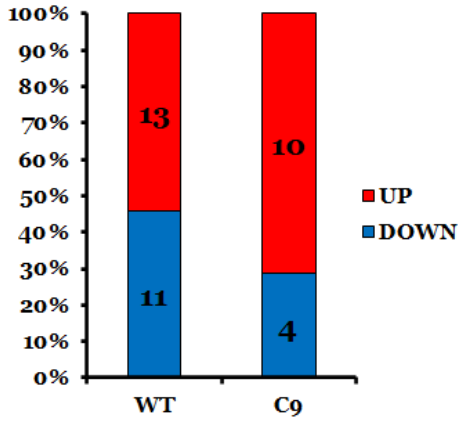

C

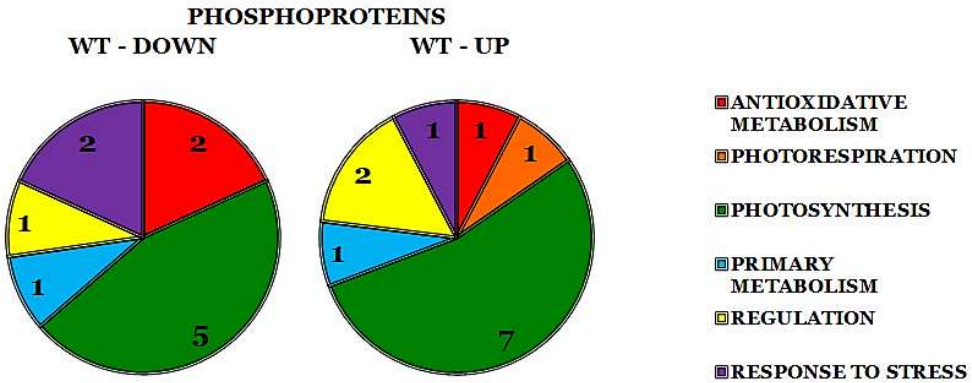

D

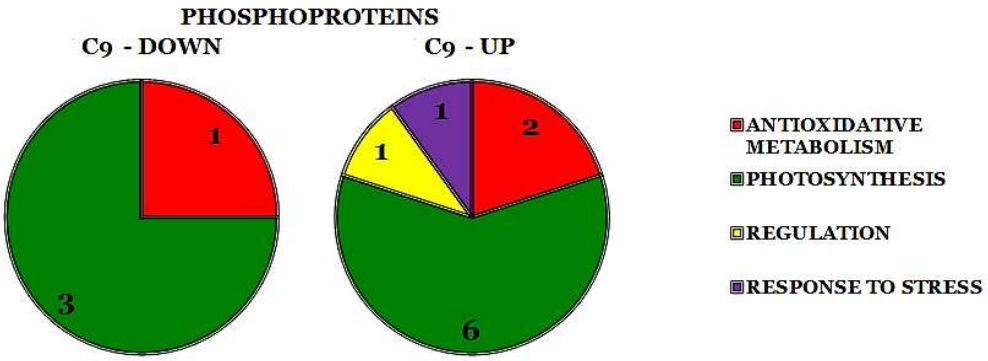

Appendix K – Differences in the protein abundances of each phosphoprotein spot stained by Pro-Q® Diamond of the leaves from overexpressing BiP genotype WT under infection (**WTI x WTNI**). Positive and negative expression level values indicate up- and down-regulation, respectively. Values of fold change for protein spots when present only in a genotype or treatment are shown as 10.00 or -10.00, respectively.

Spot ID	Phosphoprotein name	ABREV	Glyma code	TAIR code	Media WT NI	SD WT NI	Media WT I	SD WT I	Expression Level
	PHOTOSYNTHESIS								
101	Carbonic anhydrase 2, chloroplastic-related	CA2	Glyma.05g007100.4.p	AT5G14740.1			6.628	± 1.041	10
17	Fructose-1,6-bisphosphatase, cytosolic	FBPase	Glyma.11g226900.1.p	AT1G43670.1	2.075	± 0.06	5.381	± 1.039	2.593
19	Fructose-bisphosphate aldolase 1	ALDO1	Glyma.12g037400.1.p	AT2G21330.2	3.827	± 0.181	5.258	± 0.265	1.374
131	Fructose-bisphosphate aldolase 1	ALDO1	Glyma.11g111400.1.p	AT2G21330.2	8.478	± 0.128			-10
70	Phosphoglycerate kinase 1, chloroplastic-related	PGK2	Glyma.15g261900.1.p	AT1G56190.1	1.071	± 0.016			-10
62	Phosphoglycerate kinase 1, chloroplastic-related	PGK2	Glyma.08g165500.1.p	AT1G56190.1	2.872	± 0.043	5.451	± 1.434	1.898
187	Photosystem II subunit P-1	PSII_PSBP1	Glyma.14g031800.1.p	AT1G06680.1	1.303	± 0.02			-10
42	Photosystem II subunit P-1	PSII_PSBP1	Glyma.18g114900.1.p	AT1G06680.1	1.853	± 0.028			-10
143	Photosystem II subunit P-1	PSII_PSBP1	Glyma.02g282500.1.p	AT1G06680.2	2.579	± 0.039	6.019	± 1.08	2.334
51	Photosystem II subunit P-1	PSII_PSBP1	Glyma.18g114900.1.p	AT1G06680.1	3.854	± 0.692	5.109	± 0.726	1.326
132	Ribose 5-phosphate isomerase A	RPIA	Glyma.03g246300.1.p	AT3G04790.1	0.914	± 0.014			-10

Spot ID	Phosphoprotein name	ABREV	Glyma code	TAIR code	Media WT NI	SD WT NI	Media WT I	SD WT I	Expression Level
16	Sedoheptulose-1,7-bisphosphatase	SBPase	Glyma.18g030400.1.p	AT3G55800.1	1.211	± 0.018	5.223		4.313
	PRIMARY METABOLISM								
21	Cytosolic NAD-dependent malate dehydrogenase 1	cMDH1	Glyma.10g006500.1.p	AT1G04410.1	3.072	± 0.798	5.72	± 0.93	1.862
11	Enolase	ENO2	Glyma.19g190900.1.p	AT2G36530.1	0.946	± 0.014			-10
	PHOTORESPIRATION								
57	Glutamate:glyoxylate aminotransferase 2	GGT2	Glyma.02g038100.2.p	AT1G70580.1	1.1	± 0.017	5.414	± 2.051	4.922
	ANTIOXIDATIVE METABOLISM								
3	Fe superoxide dismutase 1	SOD1	Glyma.10g193500.1.p	AT4G25100.2	1.862	± 0.028	4.406	± 0.595	2.366
219	Glutathione S-transferase lambda 1	GSTL1	Glyma.13g135500.1.p	AT5G02780.2	1.915	± 0.029			-10
121	Leaf ferredoxin-NADP(+)-oxidoreductase 1	LFNR1	Glyma.16g127300.1.p	AT5G66190.1	0.694	± 0.01			-10
	RESPONSE TO STRESS								
26	Chloroplastic drought-induced stress protein of 32 kDa	CDSP32	Glyma.14g222500.1.p	AT1G76080.1	5.455	± 0.185	8.604	± 0.367	1.577
193	Matrixin family protein	MMP	Glyma.02g215700.1.p	AT2G45040.1	0.943	± 0.014			-10
37	Vegetative storage protein 1	VSP1	Glyma.08g200100.1.p	AT5G24780.1	5.479	± 0.113	2.498	± 0.057	-2.193

Spot ID	Phosphoprotein name	ABREV	Glyma code	TAIR code	Media WT NI	SD WT NI	Media WT I	SD WT I	Expression Level
	REGULATION								
62	ATP citrate lyase	ACL	Glyma.10g039000.1.p	AT2G20420.1	2.872	± 0.043	5.451	± 1.434	1.898
110	Class II aminoacyl-tRNA and biotin synthetases superfamily protein	aaRS	Glyma.14g101500.1.p	AT4G26870.1	2.47	± 0.509	3.848	± 0.347	1.558
106	Guanyl-nucleotide exchange factor SPIKE 1 (GTPase and GTP binding)	GEF-SPY1	Glyma.15g212800.4.p	AT4G16340.1	0.996	± 0.015			-10

Source: Survey's data.

Appendix L – Differences in the protein abundances of each phosphoprotein spot stained by Pro-Q® Diamond of the leaves from overexpressing BiP genotype C9 under infection (**C9I x C9NI**). Positive and negative expression level values indicate up- and down-regulation, respectively. Values of fold change for protein spots when present only in a genotype or treatment are shown as 10.00 or -10.00, respectively.

Spot ID	Phosphoprotein name	ABREV	Glyma code	TAIR code	Media C9 I	SD C9 I	Media WT I	SD WT I	Expression Level
	PHOTOSYNTHESIS								
101	Carbonic anhydrase 2, chloroplastic-related	CA2	Glyma.05g007100.4.p	AT5G14740.1	6.704	± 0.788	4.043	± 0.299	-1.658
17	Fructose-1,6-bisphosphatase, cytosolic	FBPase	Glyma.11g226900.1.p	AT1G43670.1	2.974	± 1.031	5.596	± 1.19	1.882
131	Fructose-bisphosphate aldolase 1	ALDO1	Glyma.11g111400.1.p	AT2G21330.2	4.957	± 0.59	9.437	± 0.632	1.904
181	Photosystem I reaction center PsbP-domain protein 1	PSI_PSBP	Glyma.03g230300.1.p	AT4G15510.1	2.663	± 0.099	4.458		1.674
143	Photosystem II subunit P-1	PSII_PSBP1	Glyma.02g282500.1.p	AT1G06680.2	5.597	± 0.153	3.354	± 0.489	-1.669

Spot ID	Phosphoprotein name	ABREV	Glyma code	TAIR code	Media C9 I	SD C9 I	Media WT I	SD WT I	Expression Level
51	Photosystem II subunit P-1	PSII_PSBP1	Glyma.18g114900.1.p	AT1G06680.1	6.569		2.529	± 0.201	-2.597
132	Ribose 5-phosphate isomerase A	RPIA	Glyma.03g246300.1.p	AT3G04790.1			3.748	± 0.906	10
16	Sedoheptulose-1,7-bisphosphatase	SBPase	Glyma.18g030400.1.p	AT3G55800.1	2.533	± 0.807	4.352	± 0.924	1.718
32	Triosephosphate isomerase, plastid isoform	TPI	Glyma.10g059500.1.p	AT2G21170.1			4.709	± 0.041	10
	ANTIOXIDATIVE METABOLISM								
3	Fe superoxide dismutase 1	SOD1	Glyma.10g193500.1.p	AT4G25100.2			3.642	± 0.465	10
32	Fe superoxide dismutase 2	SOD2	Glyma.20g196900.1.p	AT5G51100.1			4.709	± 0.041	10
219	Glutathione S-transferase lambda 1	GSTL1	Glyma.13g135500.1.p	AT5G02780.2	5.833	± 0.563	1.721	± 0.017	-3.389
	RESPONSE TO STRESS								
26	Chloroplastic drought-induced stress protein of 32 kDa	CDSP32	Glyma.14g222500.1.p	AT1G76080.1			2.29	± 0.298	10
	REGULATION								
32	N-acetylglucosaminyltransferase SPINDLY-related	SPY	Glyma.19g196000.1.p	AT3G11540.1			4.709	± 0.041	10

Source: Survey's data.

Appendix M – Differences in protein abundances of each phosphoprotein spot stained by Pro-Q® Diamond of the leaves from both genotypes in absence of bacterial infection (**C9NI x WTNI**). Positive and negative expression level values indicate up- and down-regulation, respectively.

Spot ID	Phosphoprotein name	ABREV	Glyma code	TAIR code	Media WT NI	SD WT NI	Media C9 NI	SD C9 NI	Expression Level
	PHOTOSYNTHESIS								
101	Carbonic anhydrase 2, chloroplastic-related	CA2	Glyma.05g007100.4.p	AT5G14740.1	0.943	± 0.043	6.704	± 2.364	7.109
62	Phosphoglycerate kinase 1, chloroplastic-related	PGK2	Glyma.08g165500.1.p	AT1G56190.1	1.781	± 0.459	2.919	± 0.954	1.639
51	Photosystem II subunit P-1	PSII_PSBP1	Glyma.18g114900.1.p	AT1G06680.1	3.854	± 0.692	6.569	±	1.704
131	Fructose-bisphosphate aldolase 1	ALDO1	Glyma.11g111400.1.p	AT2G21330.2	8.478	± 0.385	4.957	± 1.771	-1.71
	REGULATION								
62	ATP citrate lyase	ACL	Glyma.10g039000.1.p	AT2G20420.1	1.781	± 0.459	2.919	± 0.954	1.639
110	Class II aminoacyl-tRNA and biotin synthetases superfamily protein	aaRS	Glyma.14g101500.1.p	AT4G26870.1	1.474	± 0.602	3.877	± 1.118	2.63

Source: Survey's data.

Appendix N – Clustering analysis by Heat Map method of the characterized metabolites by LC/MS Q-TOF in soybean leaves from the WT and C9 genotypes under infection (I) or mock infection (NI) by *P. syringae* pv. tomato 36 hours after inoculation. The ions from LC/MS were exported from XCMS package as features where M designed the nominal mass and T the retention time.

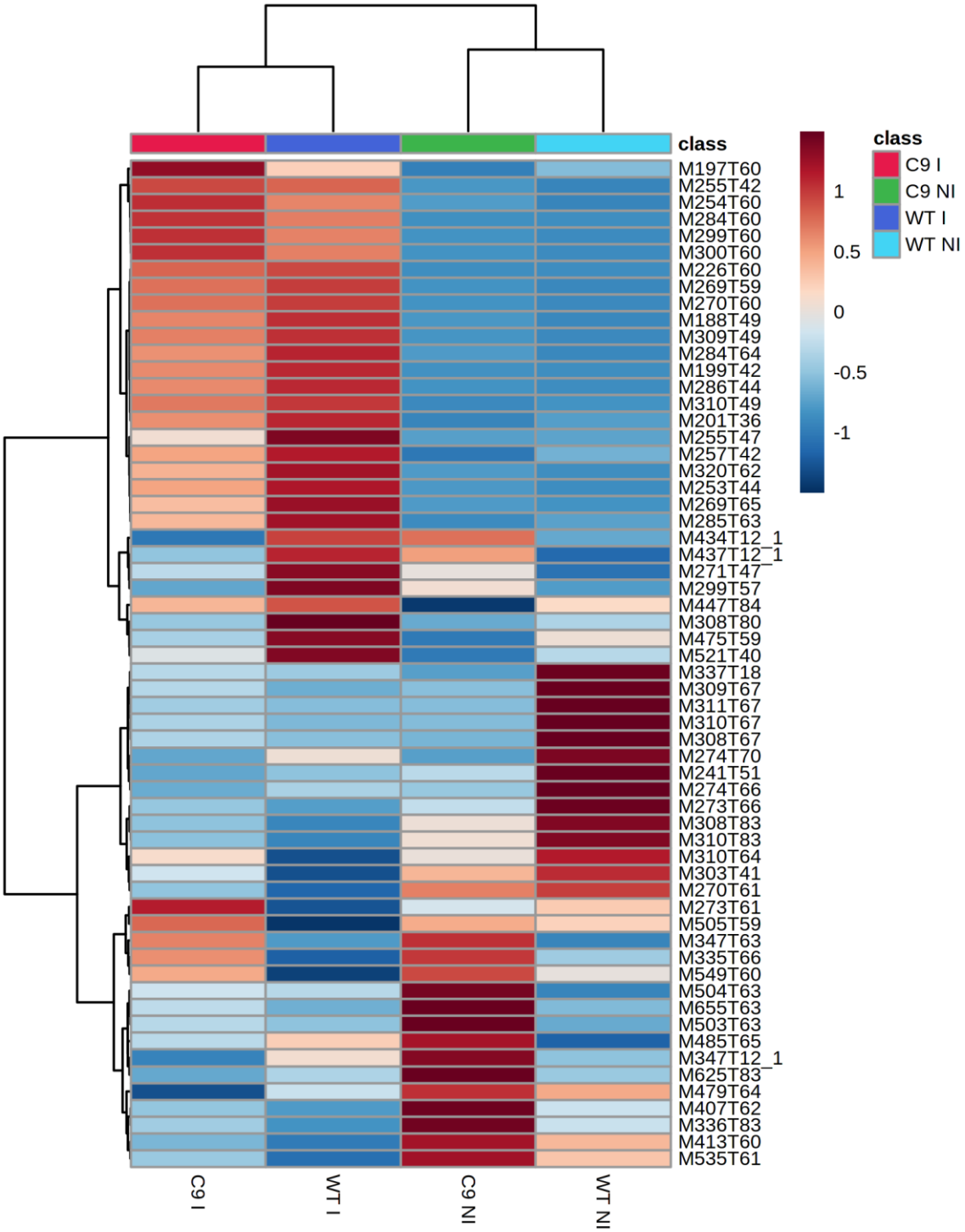

Source: Survey's data.

Appendix O – Major metabolites characterized by LC/MS Q-TOF responsible for discrimination between inoculated and mock inoculated soybean groups identified by VIP score. The ions from LC/MS were exported from XCMS package as features where M designed the nominal mass and T the retention time.

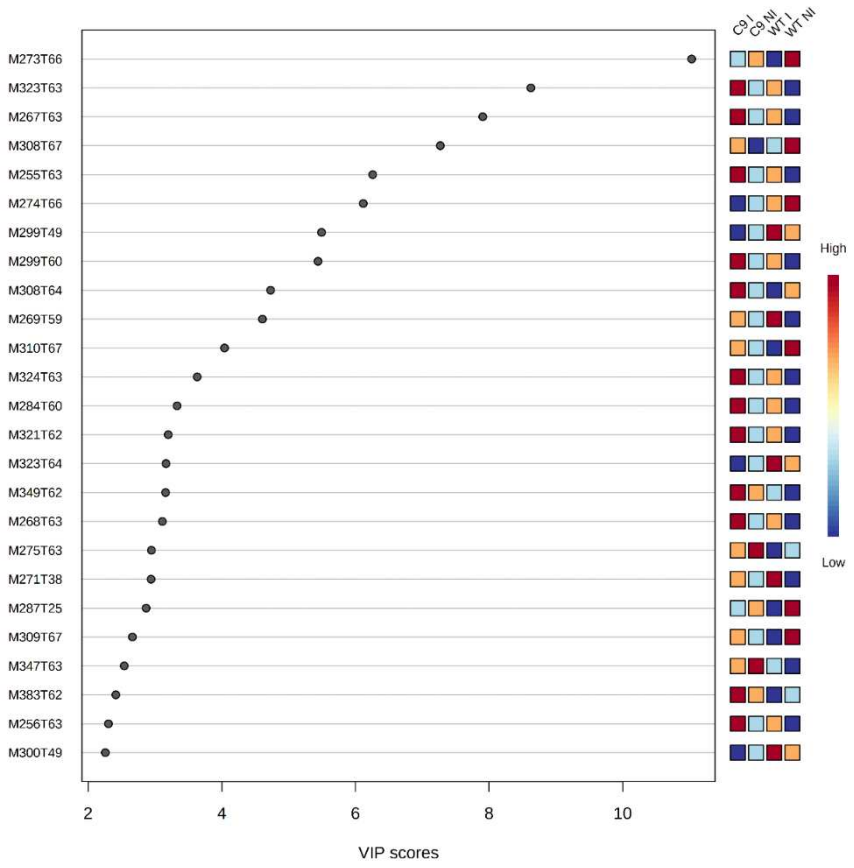

Source: Survey's data.

Appendix P – Nontarget analysis method of putative phytoalexins compounds in soybean leaves from the WT and C9 genotypes in response to infection by *P. syringae* pv. tomato. Compounds detected for each genotype, the retention times (RT) observed and their RFI% calculated. The compounds that share the same RFI% patterns were considered as belonging to a phytoalexins for those classes.

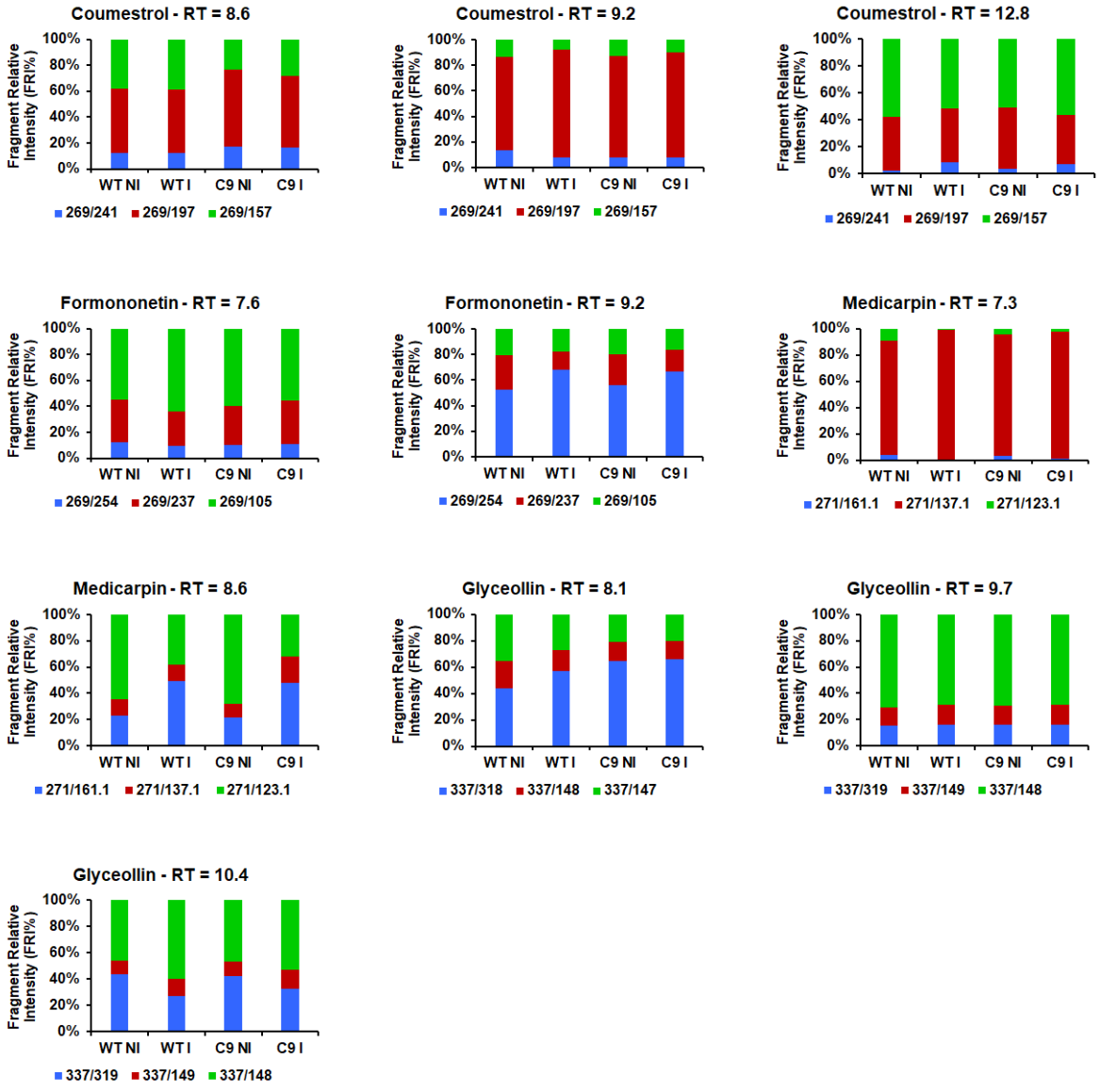

Source: Survey's data.

Appendix Q – Input data for phytoalexins analysis, obtained by LC-MS, in MetaboAnalyst 5.0. The values correspond to the intensity peaks areas exported from Skyline software

name	**WT I_R1**	**WT I_R2**	**WT I_R3**	**WT I_R4**	**WT NI_R1**	**WT NI_R2**	**WT NI_R3**	**WT NI_R4**	**C9 I_R1**	**C9 I_R2**	**C9 I_R3**	**C9 I_R4**	**C9 NI_R1**	**C9 NI_R2**	**C9 NI_R3**	**C9 NI_R4**
sample	**WT I**	**WT I**	**WT I**	**WT I**	**WT NI**	**WT NI**	**WT NI**	**WT NI**	**C9 I**	**C9 I**	**C9 I**	**C9 I**	**C9 NI**	**C9 NI**	**C9 NI**	**C9 NI**
label	**1**	**2**	**3**	**4**	**1**	**2**	**3**	**4**	**1**	**2**	**3**	**4**	**1**	**2**	**3**	**4**
Coumestrol-8.6	6055	4575	8167	5423	1634	3149	2508	1727	10627	5050	4538	3837	4224	4916	3294	1419
Coumestrol-9.2	13085	36537	26700	24823	2748	4601	3001	2009	18729	25059	11355	43965	16690	3319	3893	3000
Coumestrol-12.8	135	175	177	117	205	270	264	170	122	129	130	128	204	136	127	221
Formononetin-7.6	1250	1040	1048	1068	866	853	962	846	970	570	997	602	879	911	878	785
Formononetin-9.2	5860	16502	11455	9807	1680	1964	3231	1340	16017	10625	9942	18374	7105	3023	3159	2205
Medicarpin-7.2	4362	8228	3488	1369	124	1106	561	207	7200	2357	1419	5601	1133	493	335	735
Medicarpin-8.6	159	524	756	846	114	407	392	688	606	554	610	567	679	524	307	239
Glyceollin-9.7	3845	13565	11410	11042	1897	1209	2365	1127	12205	13100	8320	18037	8074	2620	2939	1755
Glyceollin-8.1	53	157	169	150	79	70	74	61	176	209	163	175	103	63	70	72
Glyceollin-10.4	438	977	893	1063	247	97	162	103	556	927	697	938	581	207	227	136

Source: Survey's data.

CAPÍTULO III

Pochonia chlamidosporia PROMOTES WATER DEFICIT TOLERANCE IN SOYBEAN PLANTS

CAPÍTULO III – *Pochonia chlamidosporia* PROMOTES WATER DEFICIT TOLERANCE IN SOYBEAN PLANTS

ABSTRACT

Due to the growing demand for food in the world, as the world population expands and extreme changes in rainfall and drought regimes become more frequent, new technologies are being studied to improve productivity, such as the development of products that promote more plants tolerance to drought. *Pochonia chlamydosporia* is more known for its nematicide capability and to be an endophytic fungus that makes beneficial associations with the plants, promoting the growth of several crops. In this work, the cross tolerance of soybean plants in response to drought and fungus was evaluated for the first time. Morphophysiological and metabolic changes in soybean roots and leaves with the presence of the fungus in the roots were analyzed. Under drought conditions, the plants under fungal interaction delayed one day, in average, to reach the same water potential comparing to the non-inoculated plants. The morphological parameters indicated that the hydraulic properties of the drought-tolerant genotype Embrapa48 are responsible for drought tolerance, while in the drought-sensitive genotype BR16 the fungus promoted greater efficiency in the use of water. Furthermore, the presence of the fungus positively impacted both genotypes, contributing to the maintenance of leaf turgor, reducing leaf relative water content drop and changing the caliber of root xylem vessels. Lastly, changes in phytohormones and polyamine levels and higher results for flavonoids and phytoalexins in Embrapa48 may indicate that BR16 responds differently from Embrapa48.

1 INTRODUCTION

In the environment, plants are subjected to events that can limit their survival. Therefore, they present cellular and structural defense mechanisms against biotic (such as pathogen attacks) and abiotic (such as drought) stresses, thus minimizing the effects of stress and restoring homeostasis (Cramer et al. 2011). At the same time, they interact with fungi, bacteria, viruses and other members of the ecosystem, establishing relationships of competition, parasitism, commensalism and mutualism, generically called symbiosis (Moran 2006).

Plants react unequally to different environmental factors, modifying their metabolism dynamics and ensuring homeostasis. The final phenotype of an organism is obtained from the interaction between the initial genome, mechanisms of epigenetic modification (important in polyploid organisms) and environmental conditions (Taiz and Zeiger 2013). Furthermore, within the same species, each genotype has a way of responding to planting conditions and there are inherent response mechanisms in response to environmental factors that reflect on the phenome (differences in phenotypic characteristics in a given situation).

In recent years, losses in soybean production have been reported in regions of Brazil that have experienced periods of drought, one of the main factors restricting Brazilian agriculture (Cunha et al. 2019). In water deficit stress, there is loss of water through evaporation and/or transpiration due to low atmospheric moisture conditions and soil water availability (Jaleel et al. 2007). The adverse effects of drought on plant growth and development affect agricultural productivity.

Plants show different responses to drought stress at different stages of development and event intensity. These mechanisms involve several genes that are activated, including transcription factors as well as of post-translational modifications that are regulated in order to protect cell functions (Wang et al. 2003). Physiological response culminates in the accumulation of osmoprotective compounds such as sugars and amino acids (Stewart and Larher, 1980), alterations in the rates of photosynthesis, photorespiration and cellular respiration and the metabolism of reactive oxygen species (ROS), responsible for stress and oxidative damage (Noctor et al. 2002).

The nematophagous fungus *Pochonia chlamydosporia* (Goddard) Zare & Gams (2001) is known and studied for having a predatory action on nematode eggs, especially of the

genus *Meloidogyne* (Arevalo et al. 2009). This pathogen causes damage to the roots of several cultivated plants (Bontempo et al. 2014). This fungus, in the absence of nematodes, can survive in soil as a saprophyte and form spores (chlamydospores) resistant to drought conditions (Arevalo et al. 2009; Siddiqui et al. 2009). In studies with tomato and lettuce, colonization of the rhizosphere by hyphae of *P. chlamydosporia* also promotes plant growth (Dallemole-Giaretta et al. 2015). This can occur due to the translocation of nutrients from the fungus to the plant. The fungus-plant system can also helps to increase the region of water availability, especially in regions of the soil not reached by the root, for the plant in periods of drought, cooperating for its survival. Thus, the symbiotic association of the soybean rhizosphere with the hyphae of *P. chlamydosporia* can bring potential benefits to the physiology of the plant under water stress conditions.

Ascomycetes and basidiomycetes fungi associate with the roots of most plants, especially those with a great impact on agriculture, such as from the Fabaceae family, to obtain advantages under unfavorable conditions (Bordallo et al. 2002). However, from an ecological point of view, fungi are ubiquitous organisms and can survive in the soil and establish facultative symbiotic relationships with plants, act as saprophytes or even as predators, with *P. chlamydosporia* being a nematophagous fungus (Zare et al. 2001; Hidalgo-Díaz et al. 2017). Studies show that *P. chlamydosporia* has the capacity to colonize epiphytically and endophytically the roots of food crops of great agricultural importance, such as carrot, lettuce, tomato and soybean (Podestá et al. 2013; Bontempon et al. 2014; Monteiro et al. 2018), guaranteeing the plant an increase in the acquisition of nutrients. However, there are few studies on the impact of the plant-fungus association in environments where water supply is restricted. Thus, in this study we evaluate if the soybean roots under *P. chlamydosporia* colonization show better water use, as well as determine the molecular and physiological responses to fungal interaction. In general, the presence of the fungus increased the drought tolerance of the evaluated soybean genotypes, although the physiological overall responses were genotype-dependent.

2 EXPERIMENTAL

2.1 EXPERIMENTAL CONDITION, PLANT GROWTH AND BIOTIC AND ABIOTIC STRESS ASSAYS

Soybean seeds of Embrapa48 and BR16 genotypes were used, which were characterized as tolerant and sensitive to drought, respectively, based on previous studies (Oya et al 2004; Carvalho et al 2015; Mesquita et al. 2020). The fungus *P. chlamydosporia* (isolate Pc10) was obtained from the nematophagous fungi collection of the Laboratory of Biological Control of Phytonematodes (Department of Plant pathology/Bioagro/UFV). Soybean seeds were first disinfested with 70% ethanol (v/v) and then 0.5% NaCℓO (v/v) for 15 min. After drying, they were placed in sterilized tubes and 1 mL of 0.5% sucrose solution (v/v) and 1 g of Rizotec® (a commercial product based on the fungus *P. chlamydosporia*) powder were added, which adhered to the seeds. Seeds were sown in 2 L pots with a mixture of soil, sand and cow manure (2:1:1, v/v/v) each. The plants were kept under natural light, photoperiod, relative humidity (75 ± 10%) and temperature (25 ± 10°C).

The experimental design was completely randomized, in a 2×2×2 factorial design, with two different genotypes (first factor), two abiotic treatments corresponding to plants' water potential status (second factor) and two biotic treatments (third factor), corresponding to presence (F) or absence (NF) of fungal interaction. Four repetitions were performed, in a total of 32 pots.

The plants were grown under normal water conditions until reaching the development stage V3 (when the third trifoliate was fully expanded and the fourth trifoliate was emerging). The water restriction procedure began on the 30th day after planting. The control plants assigned as I (irrigated) were watered daily with approximately 300 mL water per plant. The genotypes plants NI (non-irrigated) were exposed to slow drying soil treatment, which consisted of a reduction in irrigation to 40% of the normal daily (Valente et al. 2009), decreasing 5% with each irrigation.

The leaf water potential (Ψ) was measured in the third emerging trifoliate at dawn by using a Scholander pressure pump (Scholander et al. 1965) during the stress abiotic period. We measure the water potential of the plants until it exceeds -1.5 MPa, monitored before dawn and in the leaf from the apical meristem of each plant and set the different treatments and the results plotted on a graph $\Psi = f(t)$. Leaf and root samples were collected in liquid nitrogen when the tolerant and with fungal plants (Embrapa48 F NI) had a water potential -1.0 MPa and then stored at -80ºC.

Mathematical modeling of Ψ kinetics was performed using Excel software. Temporal rate of drop in leaf water potential ($d\Psi/dt$) was obtained by derivation. The quality of the modeling adjustments was inferred by the coefficient of determination (DC, equivalent to the

R2 of linear regression), calculated based on the sum of the squared errors (SSE) and the variance of the observed data (σ_{obs}): DC = 1 - (SSE/σ_{obs}).

2.2 MEASUREMENT OF GAS EXCHANGES

Measurements of gas exchange parameters were performed in the morning when the plants reached Ψ = -1.0 MPa, with the aid of an infrared gas analyzer (infrared gas analyzer, IRGA, portable model LI-6400XT, LI-COR Biosciences Inc. Lincon, Nebraska, USA). The net rate of CO_2 or photosynthetic assimilation (A), the stomatal conductance to water vapor (gs), the leaf transpiration rate (E) and the intercellular concentration of CO_2 (Ci) were measured from the central leaflet of the third trefoil. With these data, the following were calculated: internal and external carbon ratio (A/Ci); water use efficiency (A/E); intrinsic efficiency of water use (A/gs). All measurements were taken in the morning, under ambient conditions of temperature and steam pressure.

2.3 MEASUREMENT OF THE RELATIVE WATER CONTENT (RWC) AND LEAF HYDRAULIC CONDUCTIVITY (KF) OF LEAVES AND ROOTS

Leaf hydraulic conductivity (Kf) determination was performed using the evaporative flow method (EFM), according to the methodology described by Sack et al. (2002) and Brodribb and Holbrook (2003; 2006), with modifications. The water restriction experiment started when the third trefoil was fully expanded. The leaf water potentials (Ψ) were determined before dawn using a Scholander pressure pump and when the leaves reached Ψ of approximately -1.0 MPa, the gas exchange parameters were determined. The measurement of leaf transpiration rate (E) was carried out between 8:00 and 10:00h in the morning of the same day using an infrared gas analyzer (IRGA, portable model LI-6400xt, LI-COR Biosciences Inc. Lincon, Nebraska, USA). *Kf* was calculated using the equation: Kf = -E/Ψ.

To verify whether the presence of *P. chlamydosporia* in the rhizosphere influences plant growth under both irrigated and dry conditions, plant heights were collected in two stages (plant age in days after sowing): h_1 and h_2, at the beginning (t_1) and at the end (t_2) of the water restriction. Plant growth was calculated in terms of absolute growth in the presence of the fungus (g_F) and in the deficit imposition period (g_{NI}) and relative growth in the deficit imposition period (r_{NI}), according to the equations:

$$g_F = \frac{h_2}{t_2} \qquad g_{NI} = \frac{h_2 - h_1}{t_2 - t_1} \qquad r_{NI} = \frac{g_{NI}}{h_2} = \frac{1}{h_2} \cdot \frac{h_2 - h_1}{t_2 - t_1}$$

Stem diameter (Øs) was measured at the height of the cotyledons using a caliper.

Measurements of the morphological parameters of soybean roots

In order to measure the impact of environmental factors on the roots, the fresh volume of the root, the length of the main root and the dry weight of the roots were also measured, measured after incubation at 85°C until the sample reached a constant weight in the oven.

Leaves and roots relative water content (RWC) were calculated according to Silva and collaborators (2007). Three leaf discs from the same area and root material were collected and immediately weighed (Wf), immersed in deionized water in a dark environment for 12 hours and weighed (Wt). Finally, it was measured after incubation at 85 °C until the sample reached the constant weight in the oven and weighed (Wd). The data were applied in the following equation: RWC= 100·(Wf-Wd)/(Wt-Wd).

Moisture content in soil [h (%)] was measured by removing moisture from a soil sample by oven-drying until the mass remains constant. The values of h(%) were calculated from the sample mass before (Wf) and after drying (Wd), using the equation: h(%) = 100 · (Wf - Wd)/Wf.

2.4 ANALYSIS OF FUNGAL POPULATION IN THE SOIL

To determine if there was colonization of the rhizosphere by the fungus *P. chlamydosporia*, 1 g of soil was collected near the roots of plants with fungus. Three dilutions [10% (w/v), 1% (w/v) and 0.1% (w/v)] in ultrapure water were performed. For the isolation and counting of colony forming units (CFU), a semi-selective agar medium with rose bengal was prepared in Petri dishes. 100 µL of the solutions with dilutions of 1% and 0.1% were plated and stored at room temperature. After seven days, the number of formed CFUs were counted and the presence of the fungus was quantified, according to the equation: CFU/g soil = (C. F)/D, where C: number of colonies; D: dilution and F: dilution factor (=100).

2.5 ANATOMICAL ANALYSIS BY LIGHT MICROSCOPY

Samples from the middle-branched region of roots, stem and leaves were collected in FAA solution [formaldehyde, glacial acetic and acid ethanol 50% (v/v) at 1:1:18 (v/v/v)]. The samples were dehydrated in an ethanol series, included in methacrylate resin (Historesin Leica Microsystems Nussloch GmbH, Heidelberg, Germany) and transversally sectioned to 5 μm thickness using an automatic rotary microtome (model RM2155, Leica Microsystems Inc. Deerfield, USA). The sections were stained with toluidine blue pH 4.0 (O'Brien et al. 1964) and mounted in Permount®. After the anatomical analysis, the images that most represented the results of the treatments were selected to illustrate the data. Observations and photographic documentation were performed with a light microscope (AX70TRF, Olympus Optical, Japan) equipped with an image capture system (Ax Cam, Zeiss, Germany). Roots' xylem vessels lumen number, diameter and total area were measured using the ImageJ software for qualitative data analysis.

2.6 UNTARGETED METABOLITE PROFILING BY LC/MS

In order to investigate which metabolites were responsive to the interaction of the fungus with the plant and if this association was beneficial under water restriction, metabolites were extracted by grinding 200 mg of fresh root material in liquid nitrogen and adding 500 μl of extraction solvent [methanol 75% (v/v) and formic acid 0.1% (v/v)] to each sample according to Rogachev and Aharoni (2007) with modifications (Gomez et al. 2020). The extracts were centrifuged and filtered and analyzed as described by Gomez et al. (2020), using the nanoACQUITY UPLC system (Waters, Milford, MA, USA), containing a 3.0 μm – 300 μm × 150 mm trap column and a ProteCol GHQ303 C18 capillary column and capillary column, operating at a flow rate of 5.0 μl. min-1. The details of LC/MS analyze were described by Gomez et al. (2020). A detailed description of all the steps of the LC/MS profile analyzes is described in Gouveia et al. (2019). The peak lists were also generated in the generic mascot format (mgf) by the Data Analysis software program, and the putative metabolites were identified using the NIST library, containing the MS2 spectra for standard compounds downloaded from MassBank of North America, and converted to the NIST format.

The raw data converted into mzXML were also used to compare the LC/MS metabolite profiles from leaf extracts by XCMS platform (https://xcmsonline. scripps. edu).

The alignments were performed using the default parameters for the UPLC/Q-tof system, with 20 ppm accuracy for MS1 and a metabolite database for *Arabidopsis thaliana*.

A metabolite table containing the intensity of all ions detected in the runs was exported from the XCMS platform and used as an input for statistical analysis which was carried out by the MetaboAnalyst web-based platform (http://www.metaboanalyst.ca/). The quality filters based on standard deviation methods were used to automatically remove low-quality data. The intensity values were then normalized by the median and the data were converted using the Pareto Scaling method. Box-plot graphic based on One-way analysis of variance (ANOVA) and Heatmaps were used to visualize the compounds with differential abundance. Another table, containing the median values of the m/z from four replicates and the intensities, was used for a pathway inference against the metabolite database from *A. thaliana* using the MetaboAnalyst platform.

2.7 TARGETED METABOLITE PROFILING BY LC/MS: PHYTOHORMONES, PROLINE, POLYAMINES, PHENOLICS AND PHYTOALEXINS

The content of various compounds, classified as phytohormones, proline, polyamines and phenolic compounds (derived from benzoic acid, phenylpropanoids, flavonoids, isoflavonoids and phytoalexins) were extracted from soybean leaves and roots according to the methodology described by Müller and Munné-Bosch (2011) with modifications (Lima et al. 2019; Coutinho et al. 2019; Vital et al. 2019). Leaves and roots extract were prepared by powdering approximately 110 mg fresh weight in liquid nitrogen and 400 µL of extractive solution [methanol, isopropanol and acetic acid at 20:79:1 (v/v/v)] were added. The extract was shaken in vortex by four times for 20 s (on ice), subjected to ultrasound treatment for 5 min, placed on ice for 30 min and then centrifuged at 14000 × g for 30 min at 4ºC. Then the supernatant was removed and transferred to a new tube, with a new extraction cycle being performed with the resulting pellet from the previous extraction in order to increase the extraction efficiency and then the supernatants were pooled. Finally, the total supernatant was filtered through 0.45 mm filters, and about 400 µL of the extracts were placed in vials and 5.0 µL were injected into the LC/MS system (Agilent Eclipse Plus, RRHD, 1.8 µm, 2.1 × 50 mm), with continuous flow (Φ = 0.3 mL/min), joined online with a QQQ triple quadrupole mass spectrometer (Agilent) as described by Gomez et al. (2020). Three biological replications were performed for LC/MS analyses. The data were processed using the Skyline

package (MacCoss Lab; University of Washington) as described by Vital et al. (2018). The standard curve obtained for some compounds, in a concentration range of 0.1 to 1000 ng /mL, was used to convert the area values from XIC in ng/g of plant tissue. The abundance of each characterized phenolic compound and phytoalexin in terms of XIC area was combined in a table and analyzed in the MetaboAnalyst platform (http://www.metaboanalyst.ca), where quality filters based on the standard deviation method were used to remove low-quality data, the intensity values were normalized by median and the data were converted using the Pareto Scaling method. MetaboAnalyst platform were used to obtention of Heatmap to visualize the compounds with differential abundance in leaves and roots.

3 RESULTS

3.1 DROUGHT-SENSITIVE PLANTS UNDER FUNGAL INTERACTION BEHAVED AS THE DROUGHT-TOLERANT PLANTS IN THE ABSENCE OF THE FUNGUS DURING DROUGHT AND SOIL WATER CONTENT ASSAYS

The response of the soybean under interaction by the ascomycete fungus *P. chlamydosporia* to moderate drought was investigated by means of a water restriction assay (**Figure 1** and **Appendix A**). Control plants (irrigated) remained with leaf water potential (Ψ) above -0.2 Mpa throughout all assay. The values of Ψ in stressed plants progressively reduced from the sixth day of imposition of the water deficit, and plants with *P. chlamydosporia* presented differences of potentials of approx. +0.2 Mpa in relation to plants without fungus (**Figure 1**). On the 13th day, BR16 F NI (represented by the indigo curve) reached Ψ = -1.5 MPa while BR16 NF NI (green curve) reached Ψ = -1.7 MPa. On the 14th day, Embrapa48 F NI (blue curve) reached Ψ = -1.4 MPa, while Embrapa48 NF NI (red curve) presented Ψ = -1.6 MPa, indicating the tolerance of Embrapa48 to water deficit. Thus, the results indicate that the presence of the fungus *P. chlamydosporia* contributed, for both varieties, to a reduction in the effects of water deficit on the drop in Ψ. In general, the plants under fungal interaction delayed one day to reach the same potential than non-inoculated plants.

As water restriction continued over time, the difference between the saturated pot weight and the observed pot weight (ΔW) increased. Indeed, the volume of water to be irrigated ΔV (to which the value is indexed to ΔW) would tend to increase if not for a percentage reduction made at each observation. In fact, during the water restriction treatment,

the percentage of added water (initially 40% of that used in the irrigated condition) was reduced by 5% with each irrigation. Thus, the volume of irrigated water in each evaluation can be described mathematically as $\Delta V = (Ws - Wn) \cdot [40 - 5 \cdot (n - 1)]\%$, where Ws is the weight of the saturated vessel and Wn is the weight of the vessel in the n-th rating. The difference between the pot weight and the pot weight in the nth evaluation (ΔW) corresponds to the liquid phase of the soil, that is, the variation in the amount of water present in the soil. In order to understand the dynamics of soil water loss, directly related to plant response, variation in soil water weight and volume of irrigated water, we plotted the graph of the two y axes ΔV and ΔW (**Figure 2**) as a function of the evaluation time (t). There was a gradual increase in soil water loss in non-irrigated plants with the course of water restriction due to plant absorption and plant evaporation. In turn, the variation between the weight of the saturated vessels and the weight of each observation (ΔW) tends to increase, while there is an increase in the water added to the pots during the water deficit test (ΔV) (**Figure 2**). The graph of water loss in the system as a function of time (two-axis graph) showed that there was a gradual and progressive decrease in ΔV and indicated that Embrapa48 without fungus showed greater loss of water in the soil than the other treatments, while BR16 with fungus had greater loss than BR16 without fungus. Thus, the presence of the fungus interacting the roots promoted a better capability of water uptake of the soybean plants. These results may justify a higher water potential in the inoculated plants (**Figure 1**).

The mathematical modeling applied to the data obtained from for dynamic of temporal profile of leaf water potential (**Figure 1**), allows us to infer that the drop in water potential over time followed an exponential model (**Figure 3** and **Table 1 and 2**). From the coefficient of determination (DC), we can infer that the modeling is able to explain more than 95% of the variance of the experimental data obtained within the observed intervals of t and Ψ and the equations are valid in explaining the results. This is important because it allows us to deduce that, under the stress conditions imposed in the experiment, the variation of Ψ over time is exponentially proportional to the negative Ψ. While Ψ has a high value, it decays slowly; however, it reaches a limit where it decays quickly. As seen in **Table 1**, the exponential coefficient b is smaller for Embrapa48 than BR16, indicating that this is the drought-tolerant genotype. The value of *b* is also lower in plants under fungal interaction (F) plants than under non-interaction (NF), for both genotypes. This may indicate that the fungus increases the drought tolerance, mainly for the drought-sensitive genotype BR16 (**Figure 3A**).

Figure 1 – Temporal profile of leaf water potentials in the morning (Ψ; MPa) in two soybean genotypes, one drought-sensitive (BR16), and drought-tolerant (Embrapa48) in relation to the water deficit. Under irrigated (**I**) and non-irrigated (**NI**) conditions; under presence (**F**) or absence of fungus (**NF**). Each point represents the mean + standard error (n = 3, where n represents the number of plants). Asterisk is indicative of significance by test ($p<0.05$).

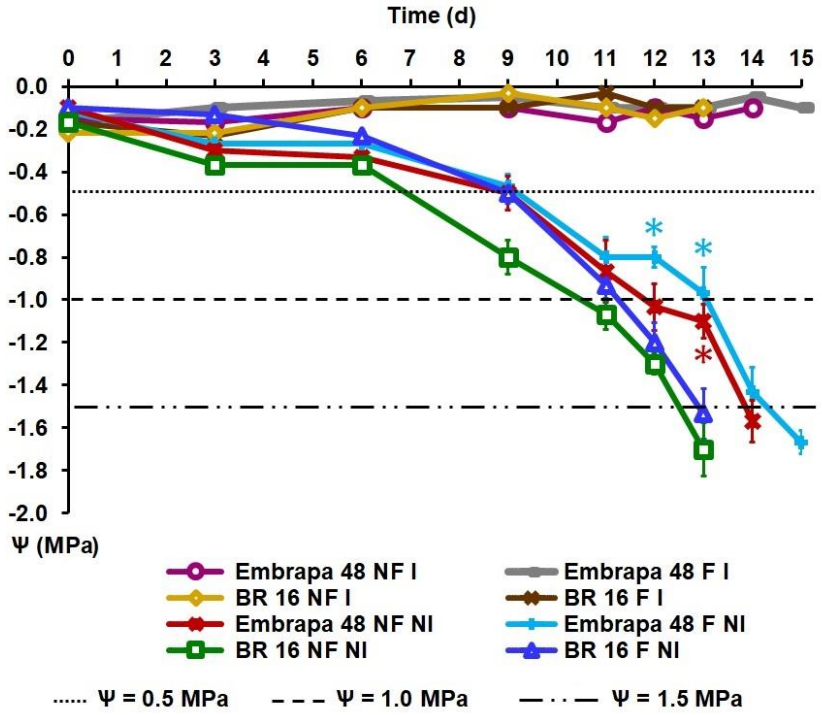

Source: Survey's data.

Figure 2 – Dynamics of the irrigation and the evolution of soil water loss through water restriction assay. Irrigated water volume (**ΔV**) and difference in vessel weights (ΔW) observed over time in the non-irrigated treatment (**NI**) are indicate. Under irrigated (**I**) and non-irrigated (**NI**) conditions; under presence (**F**) or absence of fungus (**NF**). Each point represents the mean + standard error (n = 4).

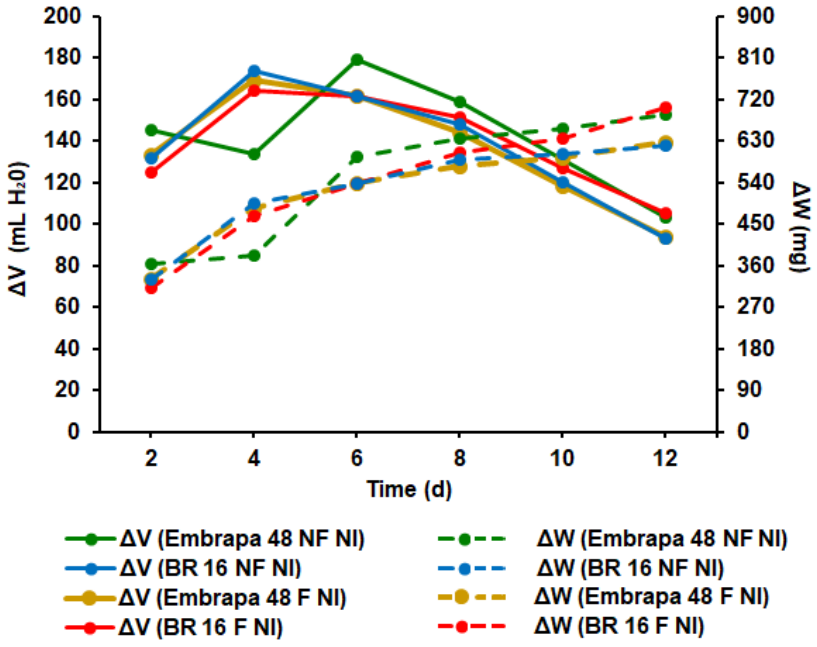

Source: Survey's data.

Figure 3 – Mathematic modeling of the dynamics of the irrigation and soil water loss during drought assay. In **(A)** Plot of the water potentials (Ψ) observed and those after modeling by regression, as a function of time [Ψ = f(t)] in non-irrigated plants (NI). In **(B)** Temporal rate of drop in leaf water potential (dΨ/dt) in plants under water deficit (NI) at long the drought treatment. Curves obtained by deriving the exponential equations as indicated in the Table 1.

(A)

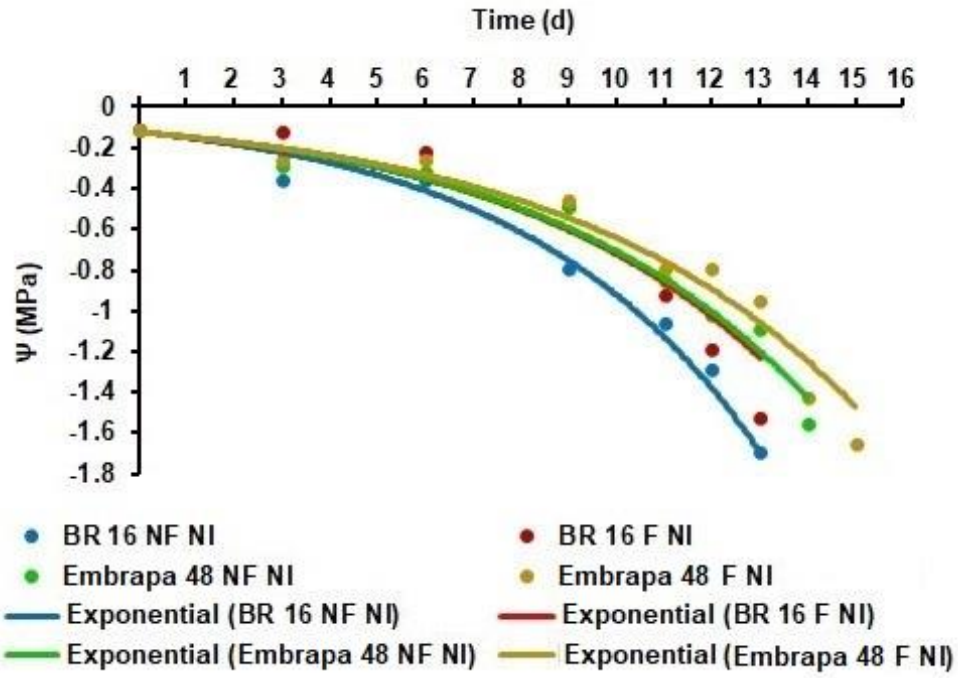

(B)

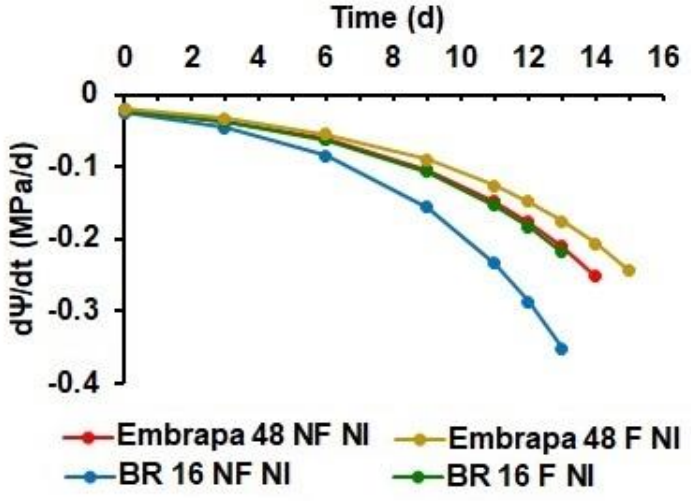

Source: Survey's data.

Table 1 – Exponential equations and determinative coefficient (DC) obtained by regression analysis on leaf water potential drop (Ψ) data of plants under water deficit (NI) over time **t.**

	$\Psi = ae^{bt}$	
Treatment	**Equation**	**DC**
BR16 NF NI	$\Psi = -0.1224e^{0.2020t}$	0.977
BR16 F NI	$\Psi = -0.1224e^{0.1775t}$	0.976
Embrapa48 NF NI	$\Psi = -0.1224e^{0.1756t}$	0.971
Embrapa48 F NI	$\Psi = -0.1224e^{0.1659t}$	0.966

Source: Survey's data.

Table 2 – Equations of variation in leaf water potential fall with respect to time (dΨ/dt) in plants under water deficit (NI) over time of abiotic treatment, obtained by deriving the exponential equations in Table 1.

Treatment	**Equation**
BR16 NF NI	$d\Psi/dt = -0.0248e^{0\ 2040t}$
BR16 F NI	$d\Psi/dt = -0.0217e^{0.1775t}$
Embrapa48 NF NI	$d\Psi/dt = -0.0215e^{0.1756t}$
Embrapa48 F NI	$d\Psi/dt = -0.0203e^{0.1659t}$

Source: Survey's data.

The rate of water potential over time dΨ/dt, was also obtained by deriving the exponential equations (**Figure 3B** and **Table 1**). This could be done because, if the water potential Ψ is related to time *t,* by means of an equation, dΨ/dt can be obtained by deriving both sides of the equation. Thus, dΨ/dt offers an interpretation of the downward trend of Ψ in the plants at the time analyzed. The BR16 genotype showed a faster drop in water potential (dΨ/dt) (more asymptotic curve), indicating that it is more sensitive to water shortage than Embrapa48 (**Figure 3B**). Plants with fungus had lower dΨ/dt, that is, the water potential decreased more slowly than in NF plants, with a greater retreat for BR16. We can also highlight that drought-sensitive BR16 plants under fungal interaction behaved as the drought tolerant plants in absence of infection, in terms of water potential in the leaves.

3.2 WATER USE EFFICIENCY WAS INCREASED IN THE DROUGHT-SENSITIVE BR16 PLANTS UNDER FUNGAL INTERACTION

Parameters related to gas exchanges (*A*, *E* and *gs*) have used to measure photosynthetic activity in the leaves and their relationship with energy metabolism and it were

significantly decreased in plants under drought (**Figure 4**). However, Embrapa48 showed higher levels than BR16 under drought. Differential photosynthetic rates (*A*) were observed in the BR16 genotype due to the presence of the fungus. It was also possible to observe a trend to increase the water use efficiency (A/E; mmol CO_2. mol^{-1} H_2O) and intrinsic water use efficiency (A/gs; μmol CO_2. mol^{-1} H_2O) (**Figure 4**). While the carboxylation rate (*A/Ci*) decreased in treatments under drought conditions, except for BR16 with fungus, where no significant difference was observed with the values presented by irrigated plants (**Figure 4**). The A/E kept its rates close to those of irrigated genotypes in plants under abiotic stress and with fungus, while the levels for plants without the fungus in the rhizosphere fell, with the drop being significantly greater for the drought genotype -sensitive BR16. The intrinsic efficiency of water use (A/gs) under water deficit was higher for this treatment while it remained low for the others.

3.3 FUNGAL INTERACTION IMPROVES RELATIVE WATER CONTENT (RWC) IN THE SOYBEAN ROOTS AND LEAVES

Plants with fungal interaction showed under irrigation conditions increase in the leaf hydraulic conductivity (Kf) for the BR16 genotype compared to the genotype without fungus (**Figure 5**). Under drought conditions, Kf dropped drastically, and the presence of the fungus does not appear to have significant effects on BR16, but it did lead to a slight increase in Kf in Embrapa48 when compared to BR16. As expected, Leaf RWC values decreased as a result of the imposition of water deficit, this drop was greater for the tolerant variety sensitive BR16 than for the Embrapa48 (Coutinho et al. 2021). Furthermore, the presence of the fungus positively impacted both genotypes, allowing maintenance of leaf turgor and reducing leaf RWC drop (**Figure 5**). Thus, the fungal interaction improves water uptake and relative water content (RWC) in the leaves, promoting a concomitant increase in photosynthetic parameters (**Figure 4**). In our conditions, the fungus presence had a tendency to increase plant growth, despite of did not statistically significant, specially in drought conditions (**Figure 4**). The growth relative to the period of water restriction (r_{NI}; d^{-1}) were increase for genotypes Embrapa48.

Figure 4 – Effect of water deficit on the gas exchanges: photosynthetic rate (A), stomatal conductance (gs), transpiratory rate (E), water use efficiency (A/E), carboxylation rate (A/Ci) and intrinsic water use efficiency (A/gs) in soybean cultivars. The different groups correspond to the treatments. Each bar represents the mean ± standard error (n = 4, where n represents the number of plants) (Tukey, p <05). Data represent mean ± standard error (n = 4). Means followed by the same letters do not differ significantly from each other (Tukey's test, p < 0.05).

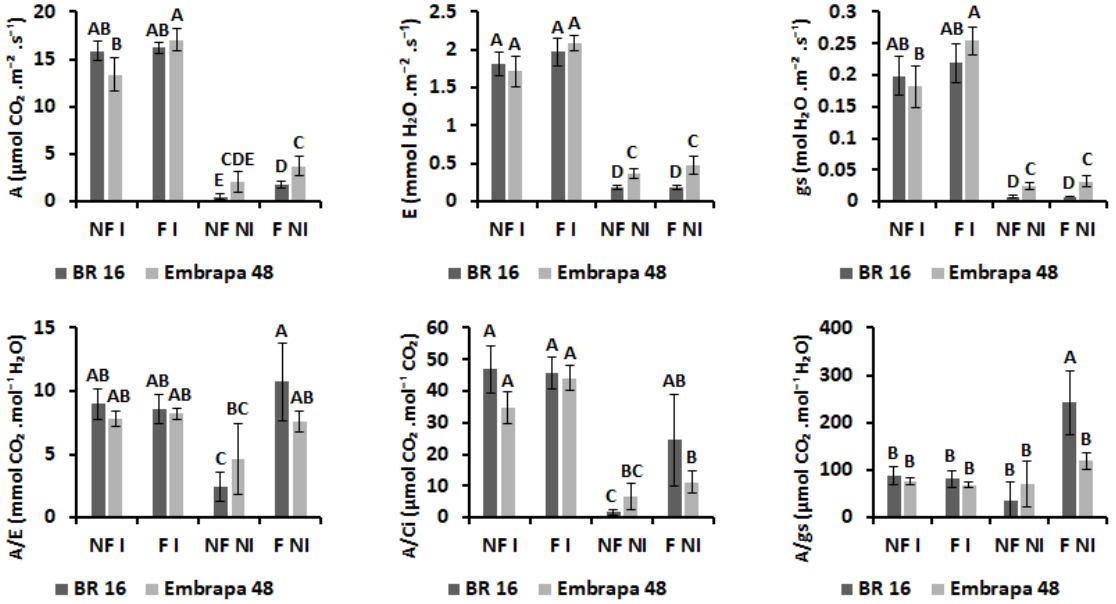

Source: Survey's data.

Figure 5 – Leaf hydraulic conductance (Kf); stem diameter (Øs), leaf rate water content (leaf RWC); absolute growth rate in the period of the presence of the fungus (g_F) and the imposition of water stress (g_{NI}); and relative growth rate in the period of imposition of water stress (r_{NI}) in Embrapa48 and BR16 genotypes under irrigated (I) and non-irrigated (NI) conditions, under presence (F) or absence (NF) of fungus. Data represent mean ± standard error (n = 4). Means followed by the same letters do not differ significantly from each other (Tukey's test, p < 0.05).

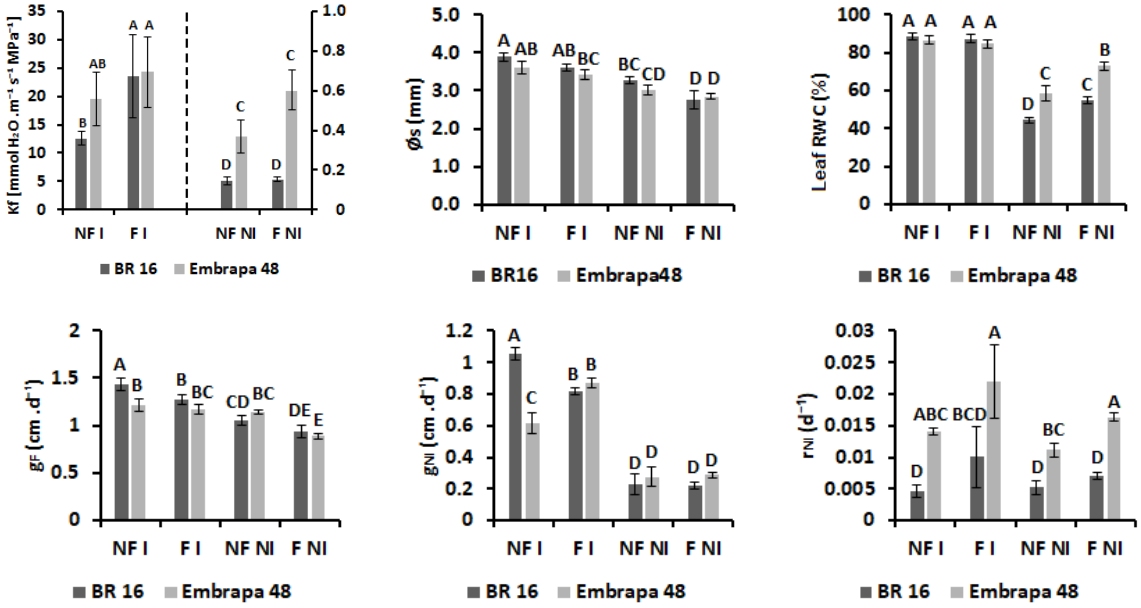

Source: Survey's data.

Some morphological parameters of the soybean roots were also affected by fungal interaction (**Figure 6 and 7**). Under full irrigation, Embrapa48 and BR16 genotypes showed greater root volume in the presence of the fungus (**Figure 6**), with the largest volume for the tolerant cultivar Embrapa48. Under water deficit, both genotypes were perceptible to lack of water, reducing the development of root volume. In its turn. plants under water deficit and in the presence of the fungus showed less lateral development and greater development of the taproot, with greater growth in depth for the cultivar Embrapa48.

Figure 6 – Soybean root phenotype Embrapa48 and BR16 genotypes under irrigated (I) and non-irrigated (NI) conditions, under presence (F) or absence (NF) of fungus, with emphasis on the length of the main root.

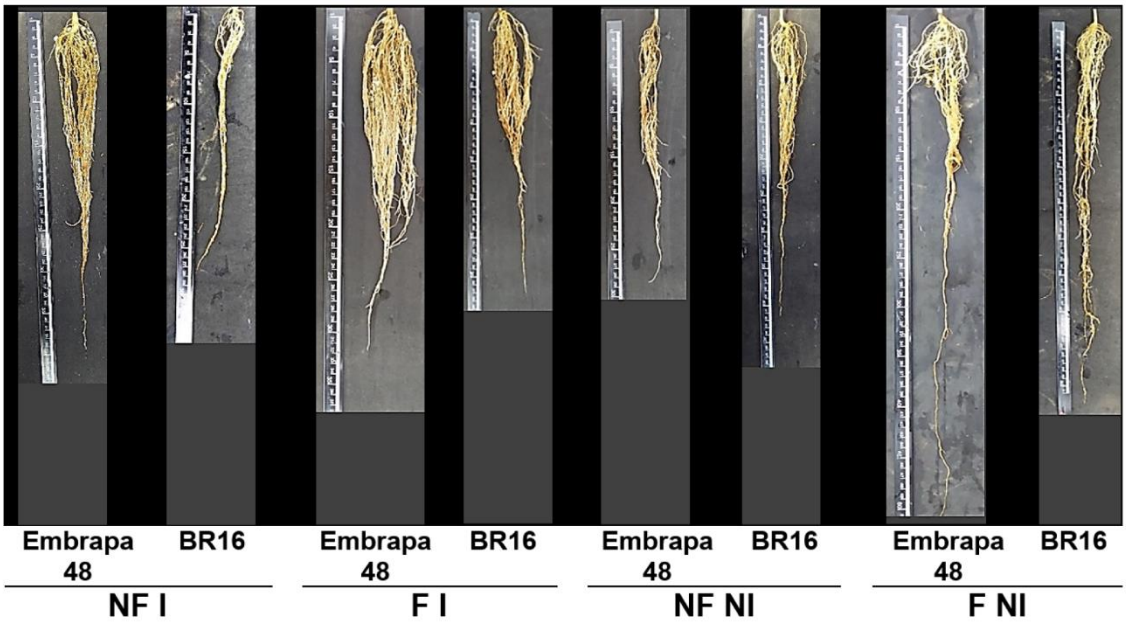

Source: Survey's data.

Root length and volume were affected only for Embrapa48 genotype, being increased under drought and in the presence of the fungus. One another way, the RWC% was increased only in the roots of the drought-sensitive BR16 genotype (**Figure 7**). Thus, under drought conditions of relative water contents (RWC) of the roots were similar in both genotypes when in the presence of the fungal interaction, while that for the leaves the levels of RWC were also increased, however being higher for Embrapa48 (**Figure 5**). As expected, soil moisture *h* (%) were lower for treatments under drought while the presence of the fungus did not contribute to a significant change in the soil moisture content (**Figure 7**).

Anatomical analysis of the soybean roots by light microscopy showed differences between genotypes (**Figure 8, 9, 10 and 11**). The thickness of the central region of the vessel lumen is greater for Embrapa48, while BR16 interacted by fungus and under drought

conditions has less thickness than in the absence of the fungus. Furthermore, light microscopy images for cross-sections of the stem showed that Embrapa48 presented more organized cells in the pith than BR16 under abiotic stress conditions. it was not possible to visualize the compartmentalization of the cells in the central region of the pith. This organization was greater for the Embrapa48 genotype than for BR16 and for irrigated plants than for non-irrigated plants. The presence of the fungus apparently favored stem cells in irrigated cultivars, especially BR16, whereas in plants under water restriction, no significant changes in cell structures were observed. (**Figure 8**).

Figure 7 – Root dry weight, main root length, root volume, root rate water content (root RWC) and soil moisture in Embrapa48 and BR16 genotypes under irrigated (I) and non-irrigated (NI) conditions, under presence (F) or absence (NF) of fungus. Data represent mean ± standard error (n = 4). Means followed by the same letters do not differ significantly from each other (Tukey's test, $p < 0.05$).

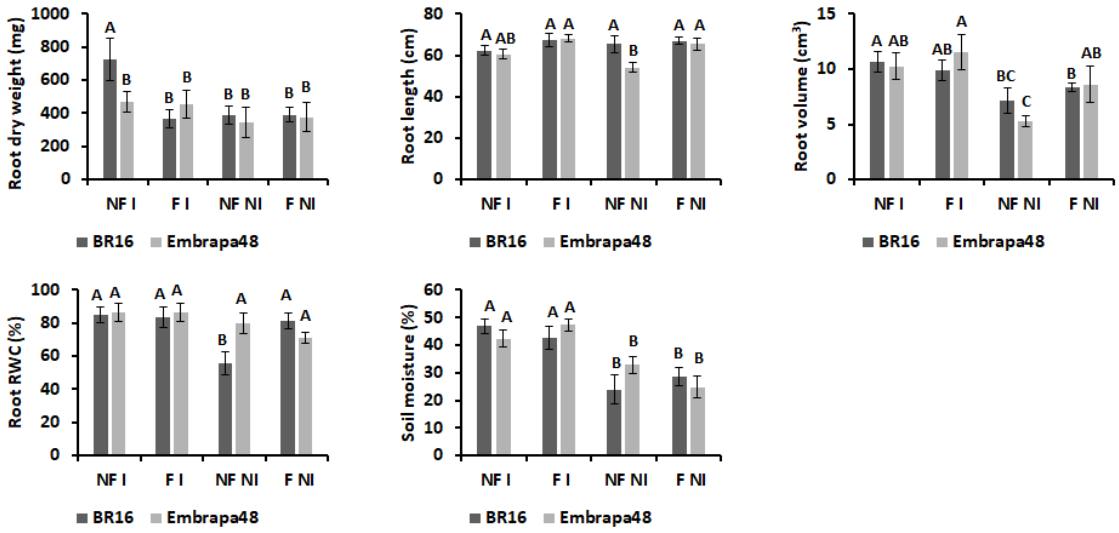

Source: Survey's data.

Figure 8 – Root cross sections of soybean cultivars in different treatments by light microscopy of the Embrapa48 and drought-sensitive BR16 under normal irrigation and drought conditions (-1.0 MPa), in presence or absence of fungus. Structures enhanced with toluidine blue. i: epidermis; ii: cortex; iii: phloem; iv: vascular cambium; v: endodermis; vi: vessel lumen. Bars correspond to 15 µm.

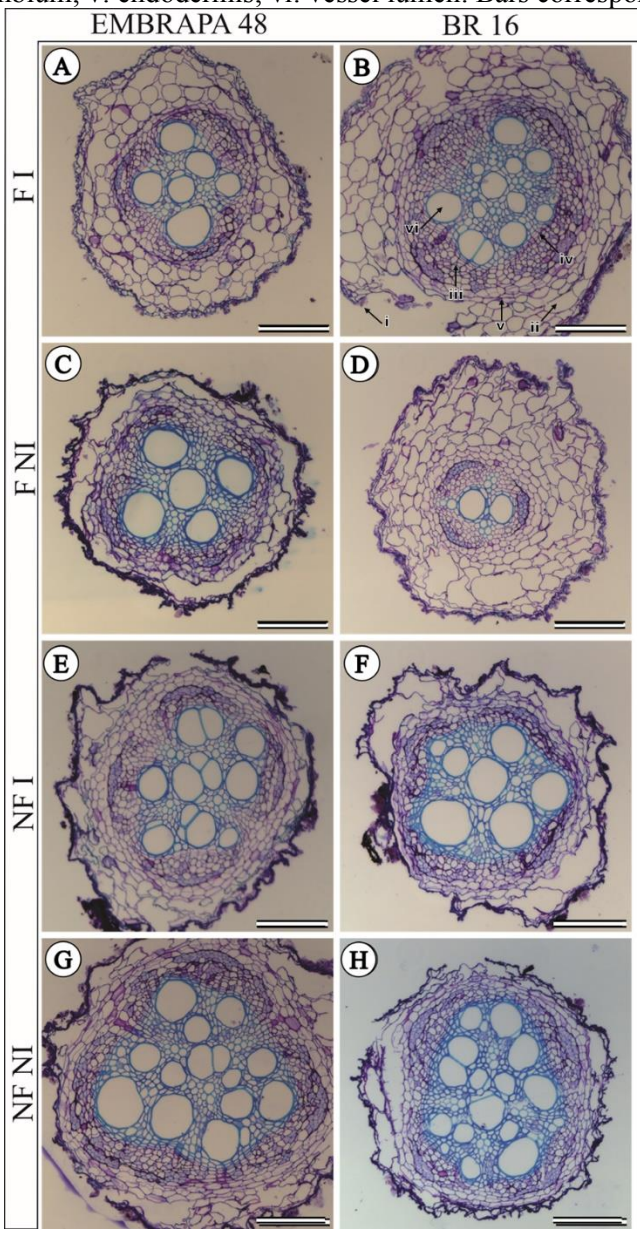

Source: Survey's data.

Figure 9 – Quantifications of the vessels lumens number, of the diameter of the vessel lumen and the vessel lumen total area in from the root xylem.

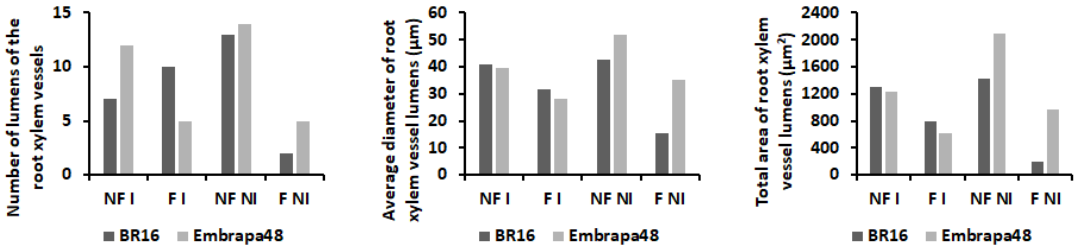

Source: Survey's data.

Figure 10 – Longitudinal root sections of soybean cultivars in different treatments under light microscopy of the Embrapa48 and drought-sensitive BR16 under normal irrigation and drought conditions (-1.0 MPa), in presence or absence of fungus. Structures enhanced with toluidine blue. i: epidermis; ii: cortex; iii: phloem; iv: vessel lumen. Bars correspond to 30 µm.

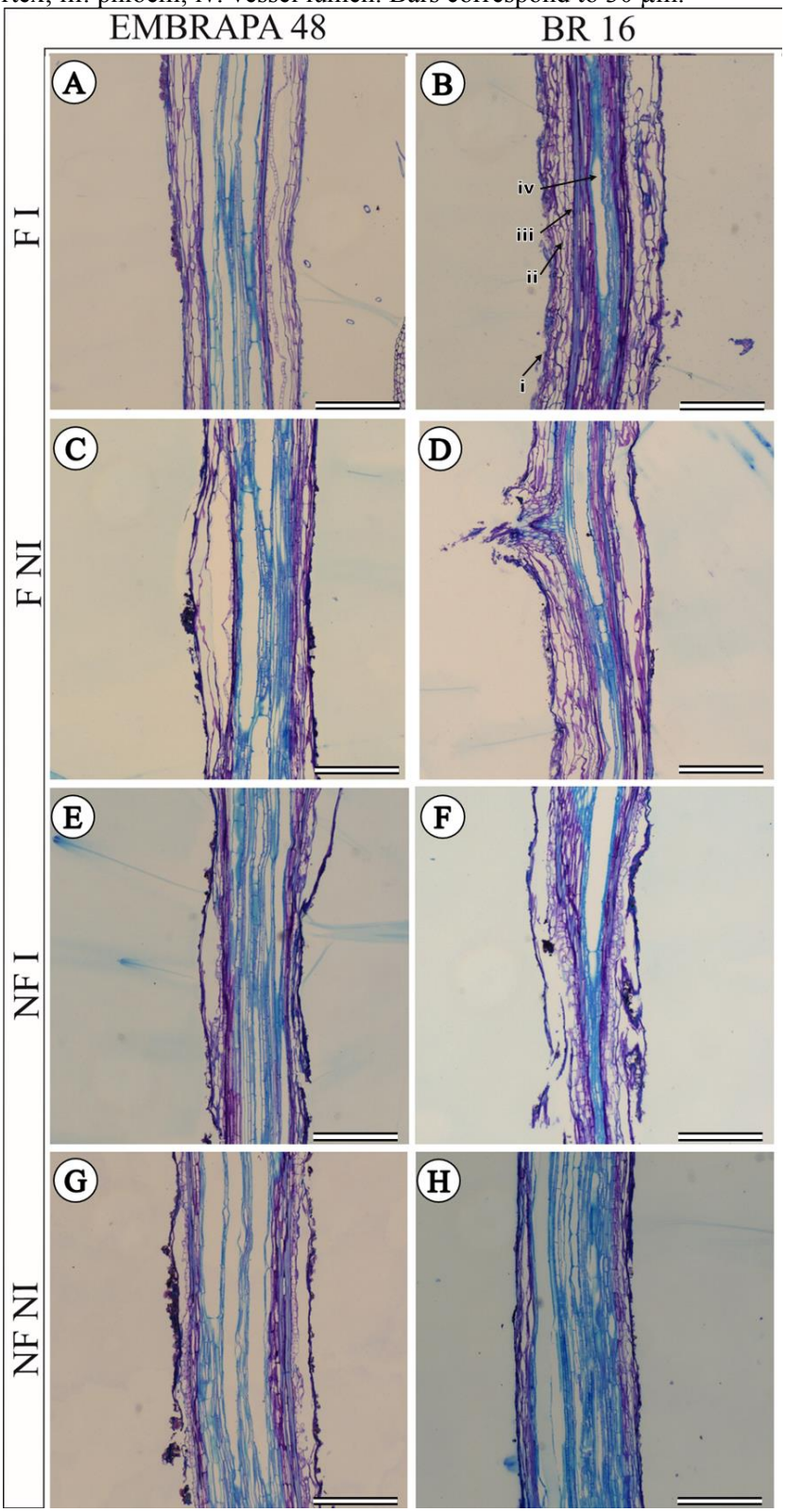

Source: Survey's data.

Figure 11 – Stem cross sections of soybean cultivars in different treatments under light microscopy of the Embrapa48 and drought-sensitive BR16 under normal irrigation and drought conditions (-1.0 MPa), in or absence of fungus. Structures enhanced with toluidine blue. i: epidermis; ii: phloem; iii: xylem; iv: vascular cambium; v: pith. Bars correspond to 15 µm.

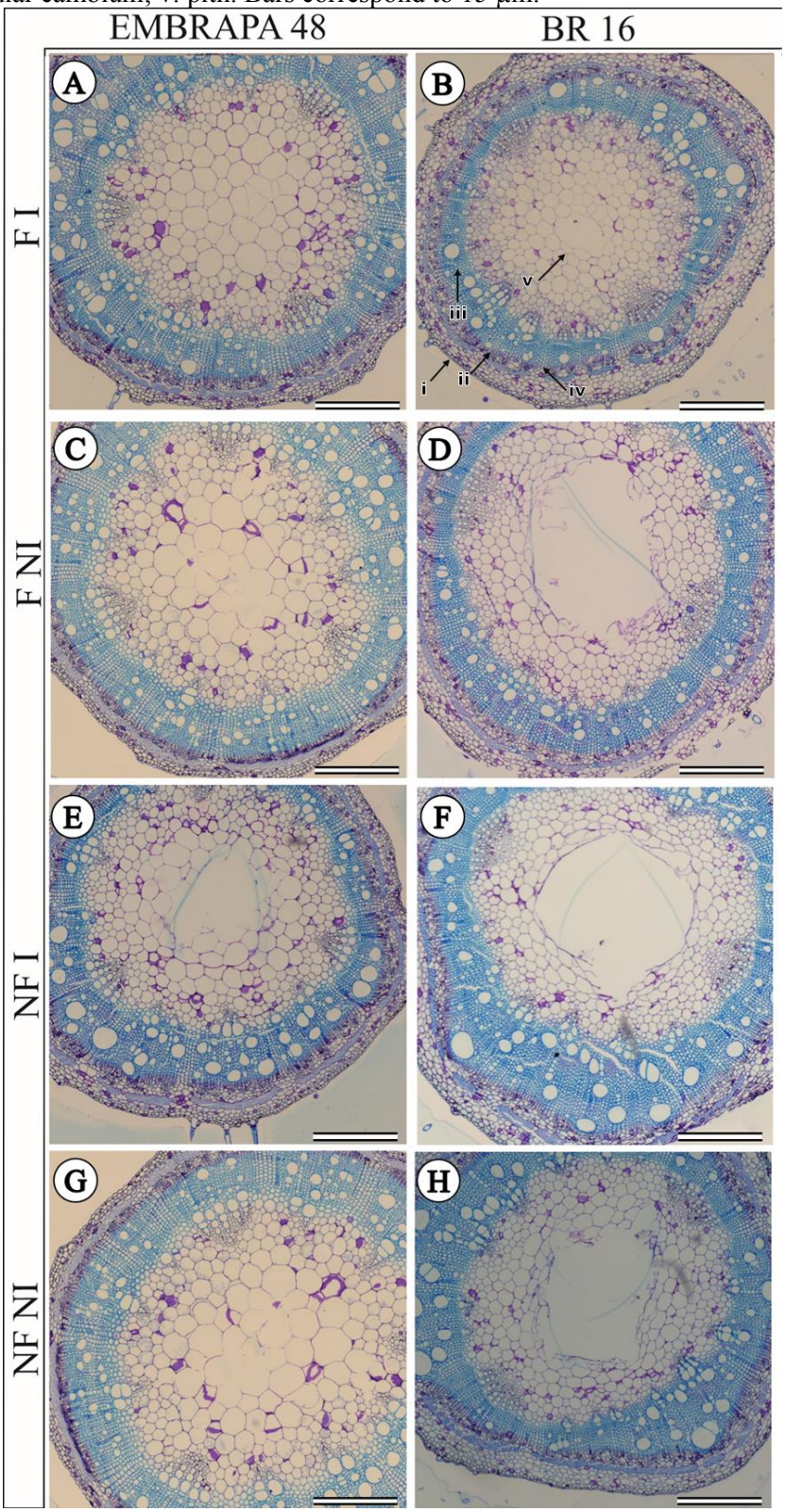

Source: Survey's data.

3.4 FUNGAL INTERACTION CHANGES METABOLITE PROFILES IN THE ROOT SOYBEAN

The presence of *P. chlamydosporia* in the soil was confirmed in the interacted treatments (F). Levels of some phytohormones were evaluated in the leaves and roots from both genotypes in response to drought and fungal interaction (**Figure 12**). As expected, the concentrations of abscisic acid (ABA) in the leaves and roots of both genotypes increased in response to water deficit. Also, the levels of jasmonic acid (JA) and 1-aminocyclopropane-1-carboxylic acid (ACC), the precursor to the plant hormone ethylene, were responsive to drought treatment. In general, the phytohormonal profiles of the soybean plants were less responsive to fungal interaction, only a significative decrease of ABA levels in the roots from BR16 genotype under drought conditions (**Figure 12**).

Given their multiple functions in cell structure and being compounds known for differential responses to various stresses, we analyzed the relative abundance of the amino acid proline and polyamines in soybean leaves and roots. It was observed that proline levels increased drastically under water restriction both in leaves and roots. In the presence of the fungus, the proline levels were significatively reduced under drought in the roots of the tolerant genotype Embrapa48. Others stress responsive metabolites were change under fungal interaction, such as spermine and spermidine which the levels were increased in soybean roots under drought and interaction conditions. Although of difference between genotypes under drought conditions, no changes were observed in levels of these metabolites in the leaves under fungal presence (**Figure 12**).

Figure 12 – The concentration (in terms of ng/g) or relative abundances (in terms of XIC area) of phytohormones, proline and polyamines without roots and leaves of Embrapa48 and BR16 under hydric restriction and in presence or absence of fungus. ABA: abscisic acid; JA: jasmonic acid; SA: salicylic acid; ACC: 1-aminocyclopropane-1-carboxylic acid (compound precursor to the ethylene); IAA: indoleacetic acid; BR: brassinosteroid; Each bar represents the mean ± SE (n = 4, where n represents the number of plants, t test $p<0.05$). Averages followed by the same letters do not differ significantly from each other.

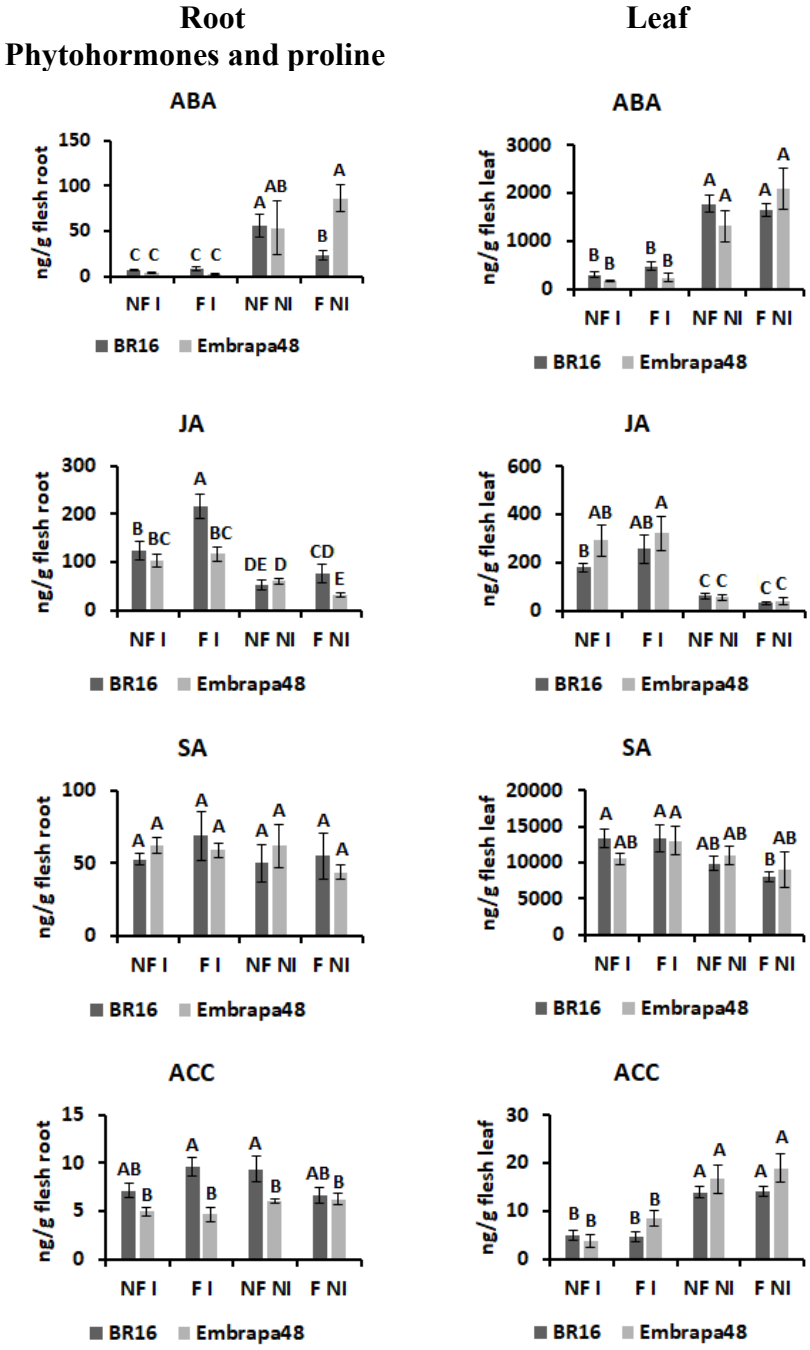

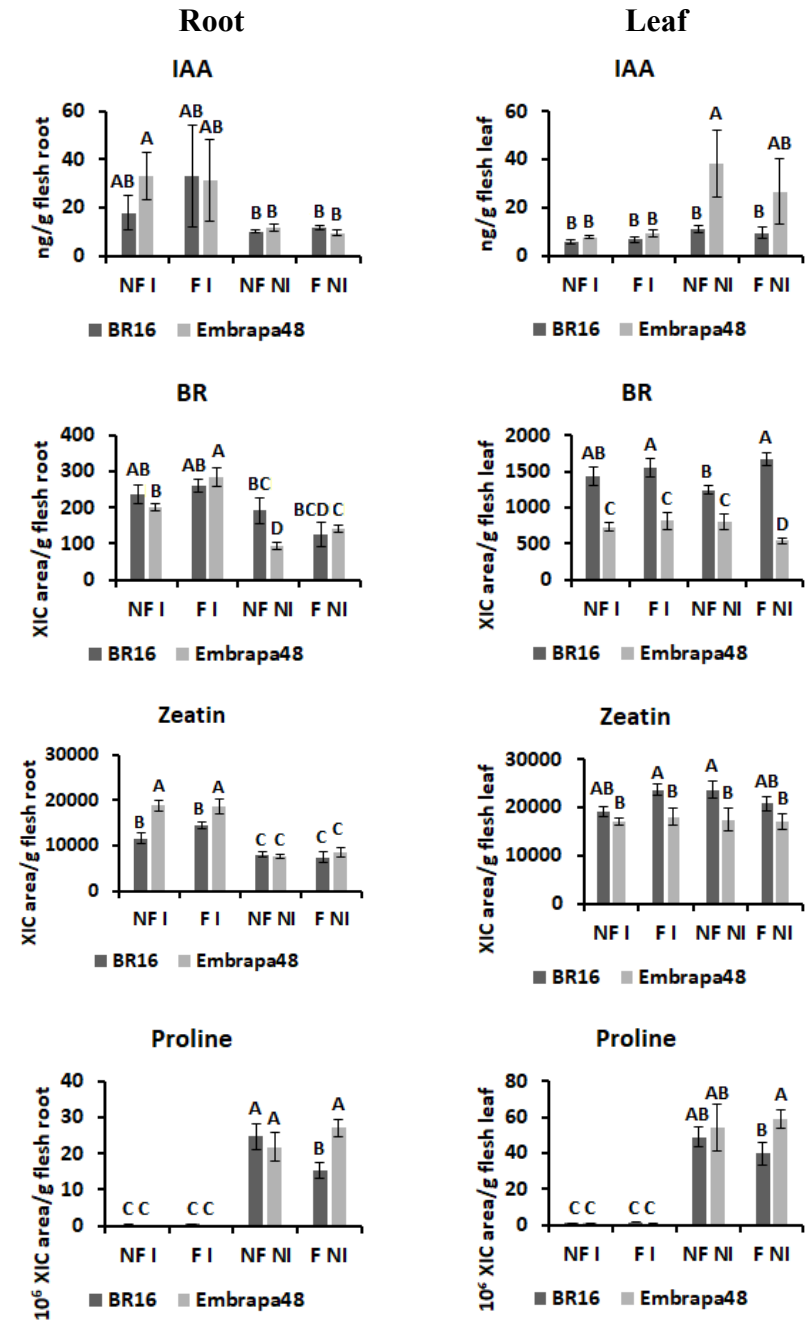
Root
Leaf
IAA
ng/g flesh root
ng/g flesh leaf
BR
XIC area/g flesh root
XIC area/g flesh leaf
Zeatin
Proline
10⁶ XIC area/g flesh root
10⁶ XIC area/g flesh leaf
NF I
F I
NF NI
F NI
BR16
Embrapa48

Polyamines

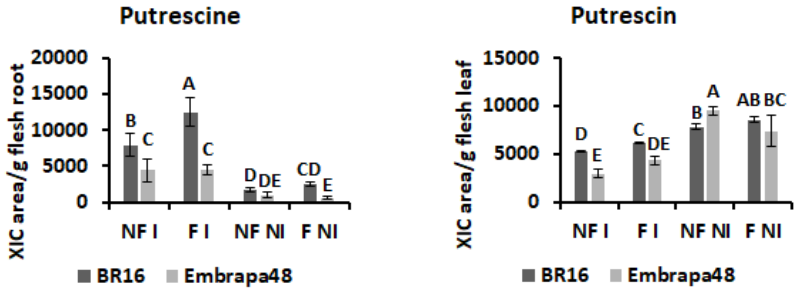
Putrescine
Putrescin
XIC area/g flesh root
XIC area/g flesh leaf
NF I
F I
NF NI
F NI
BR16
Embrapa48

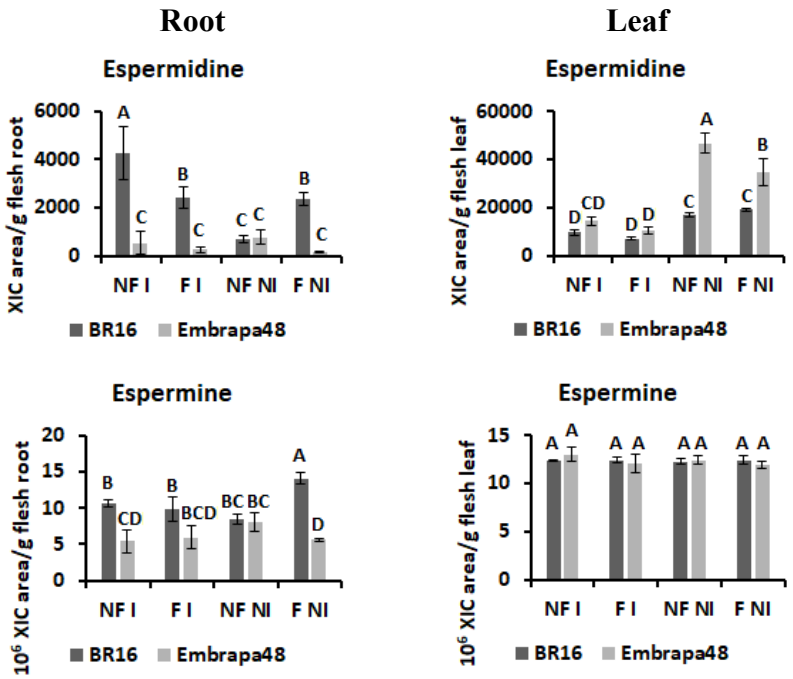

Source: Survey's data.

3.5 METABOLITE PROFILING OF UNTARGETED COMPOUNDS BY LC/MS

Analysis of the metabolic profile in soybean roots by a LC/MS-based untargeted method was also performed (**Figure 13** and **Figure 14**). Alignment of the chromatograms (**Figure 13C** and **14C**) allowed to identify the major pathways and compounds significantly altered in response to drought and fungal interaction, using the most intense ions against an *Arabidopsis thaliana* metabolite library (KEGG). Major of the dysregulated compounds belonging the pathways of phenolic compounds in both genotypes (**Figure 13B** and **14B**), with higher numbers of responsive ions related to flavonoid biosynthesis (marked as red boxes in Embrapa48 and in BR16, showing 35 and 29 responsive ions, respectively), flavone and flavonol biosynthesis (green boxes in Embrapa48 and BR16, with 5 and 6 responsive ions, respectively) and aromatic amino acid metabolism (indigo boxes in Embrapa48 and orange in BR16, with 8 and 7 responsive ions, respectively).

These compounds are involved with several functions of specialized metabolism, with protective action against damage from UV radiation energy and oxidative stress, maintenance of redox homeostasis and antimicrobial action. The analysis of PSL-DA for Embrapa48 (**Appendix C**) showed greater separation of components (biotic and abiotic treatments) than PSL-DA for BR16, with greater separation for the irrigated and fungus treatments. Interestingly, the PLS-DA of BR16 F NI (green) and BR16 NF NI (blue) showed a greater

separation of components than the same treatments of Embrapa48, indicating that there is a more intense metabolic response in the root of the drought-sensitive genotype when under deficit water and in the presence of the fungus than for the tolerant genotype (**Appendix B**). For tolerant genotype, differential response in the presence of the fungus was greater for the irrigated treatment.

The dysregulated ions in response to drought and fungal interaction showing high intensity were grouped using clustering analysis by heatmap (**Appendix C and D**) and their fragmentation partners were used to identification against NIST libraries (**Figure 14 and 15**).

Normalized relative abundance generated from MetaboAnalyst platform as box-plot are indicated (**Figure 15 and 16**). The following metabolites were identified for Embrapa48: M214T45: 4'-Acetoxy-7-hydroxy-6-methoxyisoflavone or Glycitein (derivative); M25543: Daidzein; M255T62: 6.2'-Dihydroxyflavone; M269T32: Coumestrol; M417T20: Daidzin; M27154: 2,3',4,6-Tetrahydroxybenzophenone (similarity); M503T24: 6"-O-Malonyldaidzin; M503T25: 6"-O-Malonyldaidzin; M517T32: Coumestrol (Derivative); M555T32: Coumestrol (Similarity, same retention time and similar fragment profile) (**Figure 15**).

While, for BR16, the following were identified: M229T47: Resveratrol; M255T50: Daidzein; M303T57: Neobavaisoflavone (similarity); M306T57: Neobavaisoflavone (similarity); M321T57: Neobavaisoflavone; M39764: Beta-Sitosterol, a phytosterol related to membrane stability and brasinolide synthesis (Similarity, same mass with 18 Da neutral loss); M417T18_2: Daidzin; M503T23: 6"-O-Malonyldaidzin; M519T28: 6"-O-Malonylgenistin. The ten putative metabolites identified by the NIST software for Embrapa48 and seven of the eight metabolites for BR16 had higher metabolite levels in FI, followed by NF I and finally NI plants. M39764 (similarity to Beta-Sitosterol), levels were higher for BR16 F NI (**Figure 16**).

Figure 13 – Analysis of the metabolite profiles from the Embrapa48 genotype leaves by LC/MS Q-TOF. All runs were aligned using XCMS algorithm in **(C)** and the intensities of the fifty principal ions were compared in **(A)** and the metabolic pathway analysis were performed using MetaboAnalyst platform in **(B)**. Colored boxes by red, indigo, green and yellow in **(A)** correspond to the ions belongings to the pathways assigned in the (B). The m/z of the ions showed in (B) are the medium values of 4 replicates.

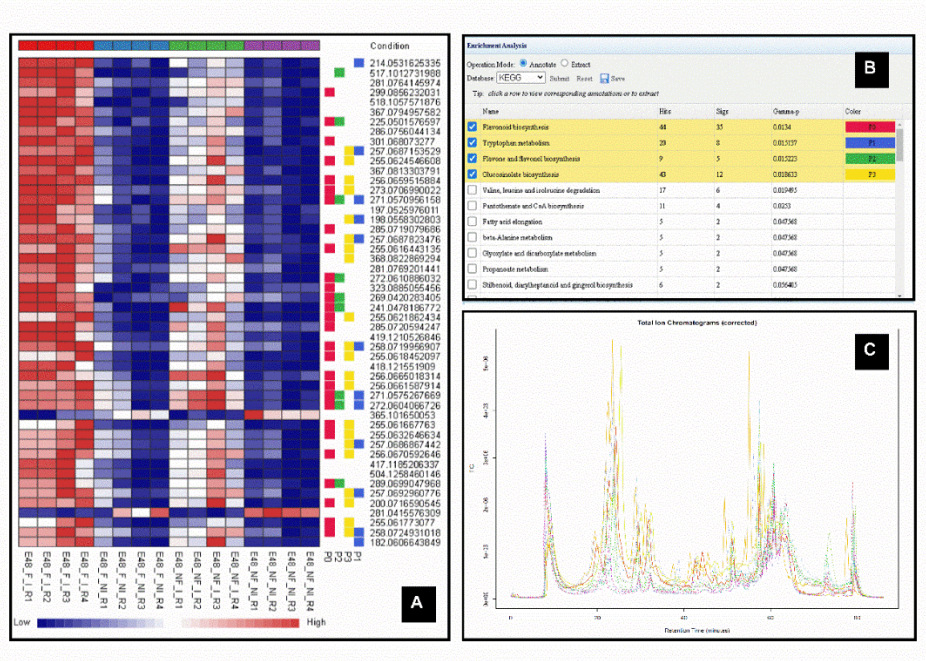

Source: Survey's data.

Figure 14 – Analysis of the metabolite profiles from the **BR16 genotype** leaves by LC/MS Q-TOF. All runs were aligned using XCMS algorithm in **(C)** and the intensities of the fifty principal ions were compared in **(A)** and the metabolic pathway analysis were performed using MetaboAnalyst platform in **(B)**. Colored boxes by red, green, purple, orange and indigo in **(A)** correspond to the ions belongings to the pathways assigned in the (B). The m/z of the ions showed in (B) are the medium values of 4 replicates.

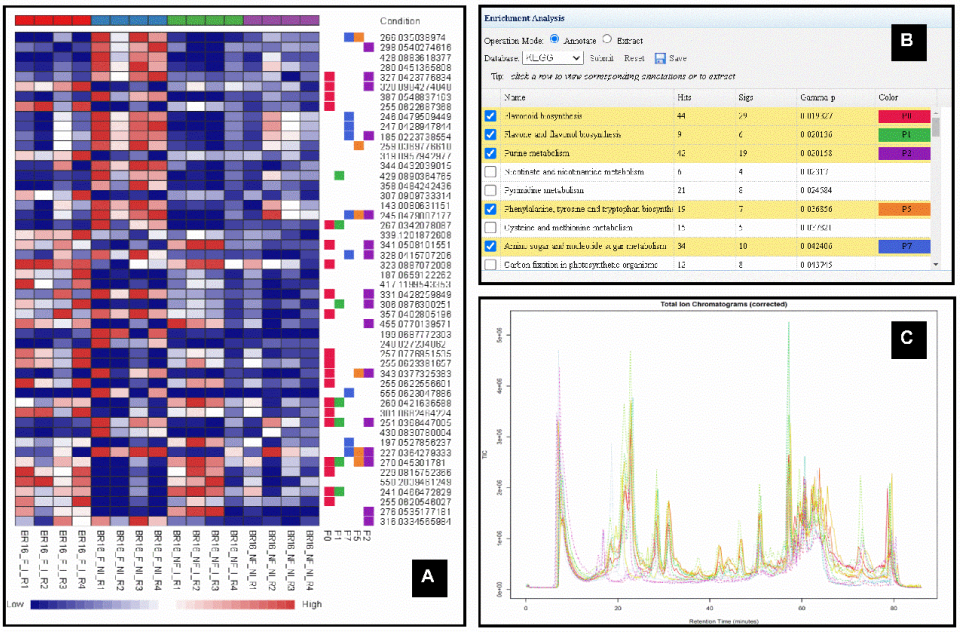

Source: Survey's data.

Figure 15 – Normalized relative abundances of some ions showing alterations in the Embrapa48 (E48) genotype under normal irrigation (I) and water restriction (NI) and in the presence (I) or absence (NF) of *P. chlamydosporia* in rhizosphere. Putative identifications were obtained for the metabolites listed below. M214T45: 4'-Acetoxy-7-hydroxy-6-methoxyisoflavone or Glycitein (derivative); M25543: Daidzein; M255T62: 6,2'-Dihydroxyflavone; M269T32: Coumestrol; M417T20: Daidzin; M27154: 2,3',4,6-Tetrahydroxybenzophenone (similarity); M503T24: 6"-O-Malonyldaidzin; M503T25: 6"-O-Malonyldaidzin; M517T32: Coumestrol (Derivative); M555T32: Coumestrol (Similarity, same retention time and similar fragment profile).

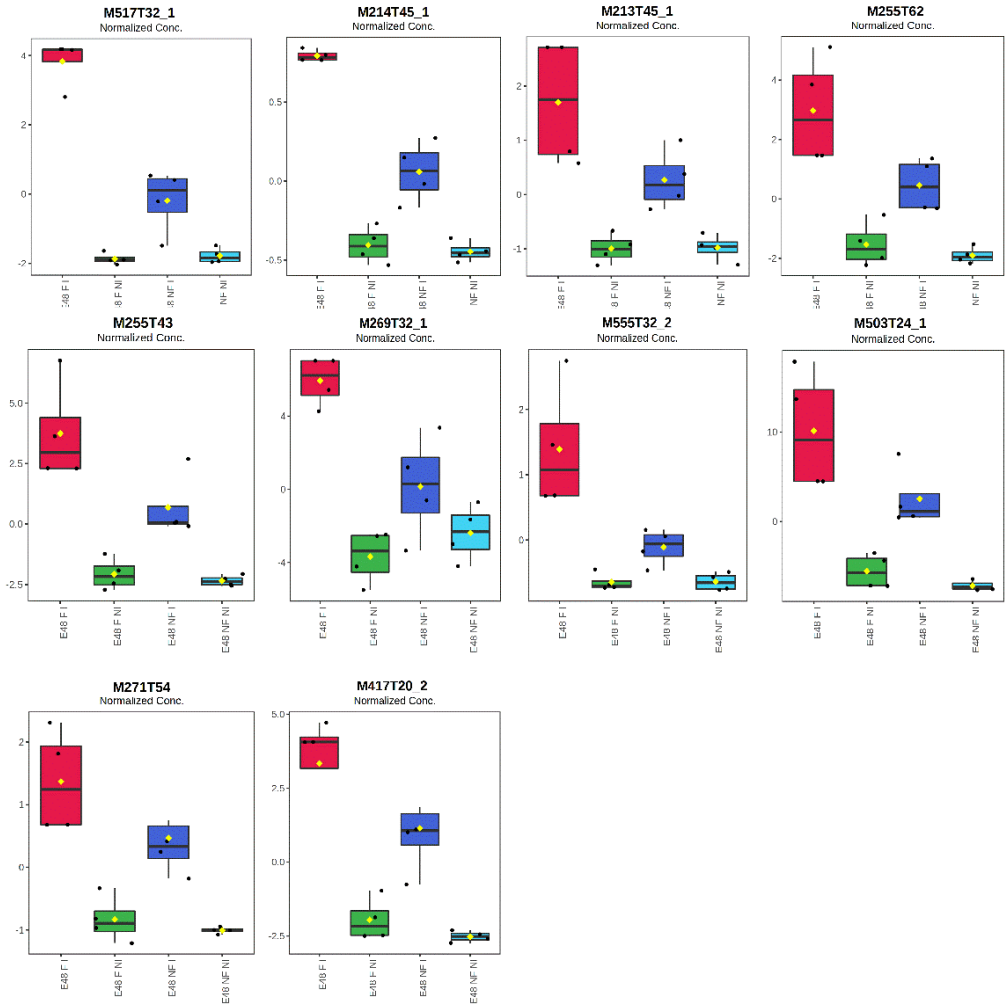

Source: Survey's data.

Figure 16 – Normalized relative abundances of some ions showing in the BR16 genotype under normal irrigation (I) and water restriction (NI) and in the presence (I) or absence (NF) of *P. chlamydosporia* in rhizosphere. Putative identifications were obtained for the metabolites listed below. M229T47: Resveratrol; M255T50: Daidzein; M303T57: Neobavaisoflavone (similarity); M306T57: Neobavaisoflavone (similarity); M321T57: Neobavaisoflavone; M39764: Beta-Sitosterol (Similarity, same mass with 18 Da neutral loss); M417T18_2: Daidzin; M503T23: 6"-O-Malonyldaidzin; M519T28: 6"-O-Malonylgenistin.

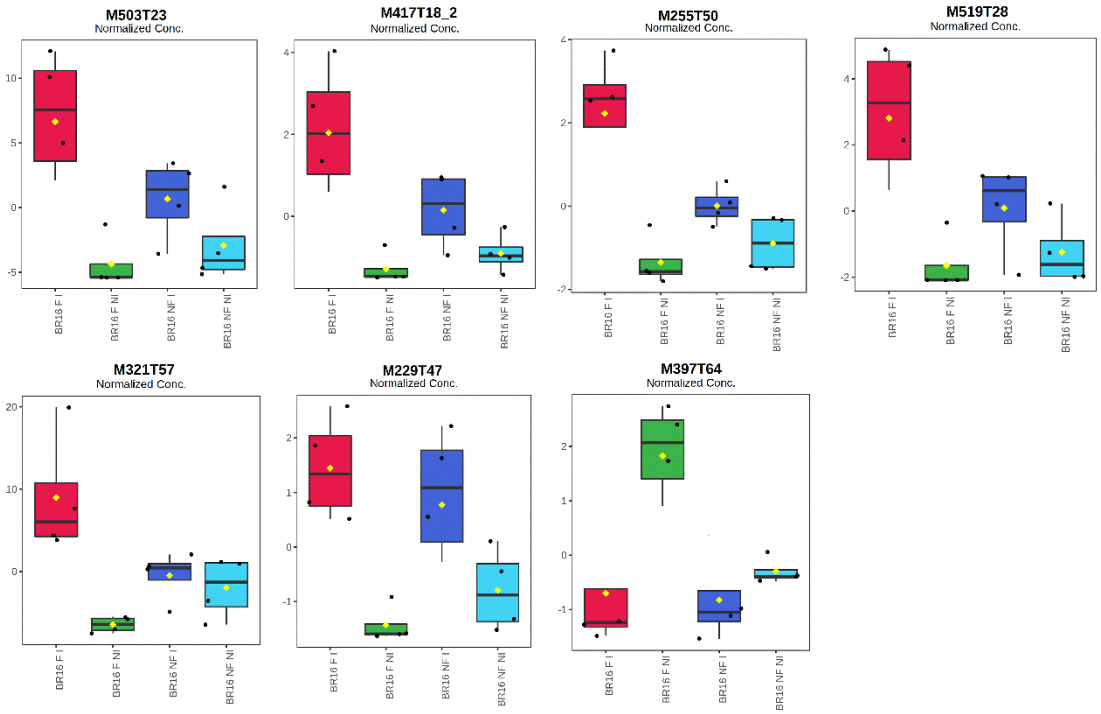

Source: Survey's data.

As the LC/MS profiles indicated dysregulated metabolites from phenylpropanoid pathway, some phenolic compounds were analyzed by a target LC/MS and Heatmap method by Metaboanalyst platform (**Figure 17 and 18**). Responsive to presence fungus, we can highlight some compounds (**Figure 14**). Methylated BA derivatives showed different profiles depending on the presence of the fungus. Syringic acid levels in roots of plants irrigated with fungus were higher in plants without the fungus. Under drought and with fungus, syringic acid was significantly increased in BR16 than in Embrapa48. In turn, vanillic aldehyde (vanillin) showed higher levels in both genotypes in the presence of the fungus and after water restriction.

Abundance of some compounds belonging the phenylpropanoid pathway were also changed in the roots during drought in response to fungal presence, such as neochlorogenic acid sinapic acid, synapil alcohol and coumarin. In general, there are differences of response between genotypes and these metabolites did not change in the leaves (**Figure 17 and 18**).

The levels of some aglycone flavonoids naringenin, daidzein, genistein and gossypin were reduced in roots in response to drought treatment, however did not change under fungal interaction. In the leaves these compounds did not show alteration in response to fungus, except daidzein levels were decreased.

Phytoalexins observed in soybean roots (Coumestrol-8.6 and -9.2, Formononetin-8.6, Medicarpin-6.0, -7.2 and -8.6, Glyceollin-8.6 and -9.8) suffered a decrease in their relative abundance after drought induction (**Figure 18**). The levels of coumestrol (Coumestrol-8.6) were slightly greater in the presence of the fungus in roots of the genotype Embrapa48 compared to BR16. Drought-tolerant plants Embrapa48 in treatments with the presence of the fungus showed higher values of formononetin (Formononetin-8.6) than drought-sensitive BR16. Medicarpin and glyceollin did not show significant changes due to the presence of the fungus.

Figure 17 – Analysis by Heatmap method in terms of XIC area of some phenolic compounds (Benzoic acid derivatives, Phenylpropanoids, Flavonoids, Isoflavonoids and Phytoalexins) characterized by leaves of Embrapa48 and BR16 under hydric restriction and in presence or absence of fungus. 4-HBA: 4-Hydroxybenzoic acid; CHL AC: Chlorogenic acid; FER AC: Ferulic acid; ISOFER AC: Isoferulic acid; NEOCHL AC: Neochlorogenic acid; trans-CIN AC: trans-Cinnamic acid; 3,5-DHBA: 3,5-Dihydroxy benzoic acid; CMS: Coumestrol; FMNT: Formononetin; MED: Medicarpin; GLYC: Glyceollin; RT: Retention time.

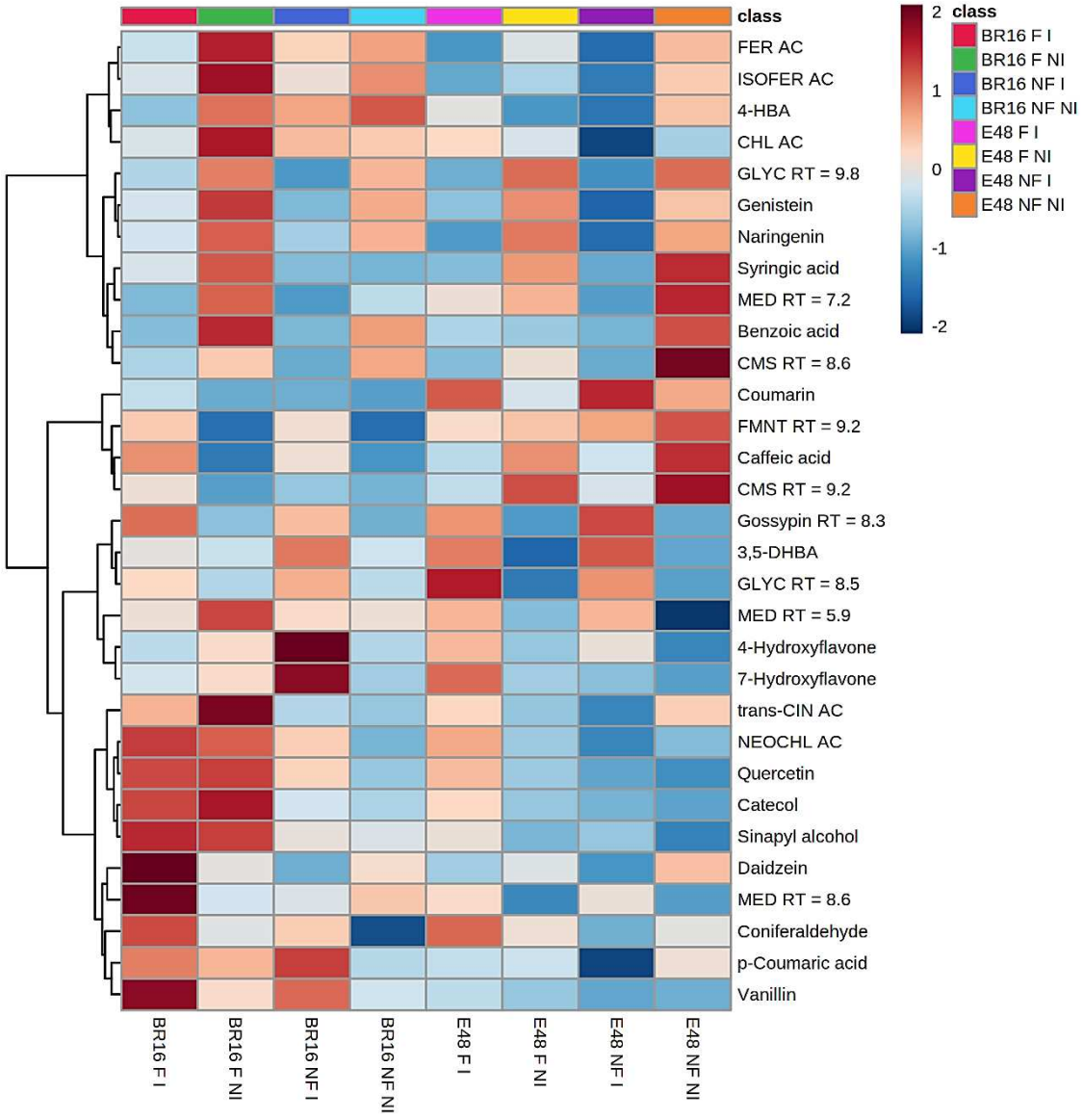

Source: Survey's data.

Figure 18 – Analysis by Heatmap method in terms of XIC area of some phenolic compounds (Benzoic acid derivatives, Phenylpropanoids, Flavonoids, Isoflavonoids and Phytoalexins) characterized by roots of Embrapa48 and BR16 under hydric restriction and in presence or absence of fungus. 4-HBA: 4-Hydroxybenzoic acid; CHL AC: Chlorogenic acid; FER AC: Ferulic acid; ISOFER AC: Isoferulic acid; NEOCHL AC: Neochlorogenic acid; trans-CIN AC: trans-Cinnamic acid; 3,5-DHBA: 3,5-Dihydroxy benzoic acid; CMS: Coumestrol; FMNT: Formononetin; MED: Medicarpin; GLYC: Glyceollin; RT: Retention time.

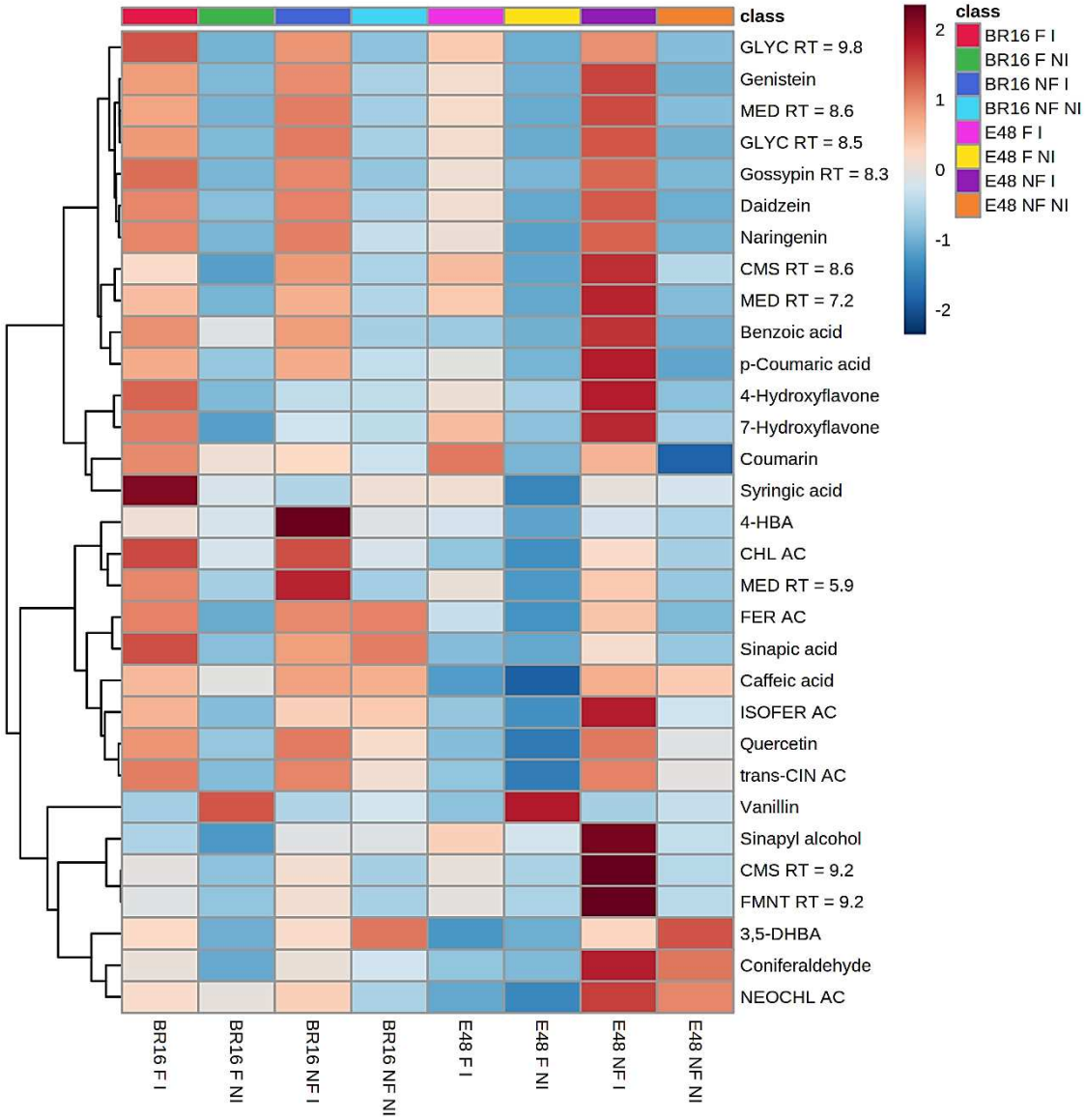

Source: Survey's data.

4 DISCUSSION

Under drought stress conditions, plants tend to promote associations with fungi, bacteria or both. Mycorrhizal fungi, especially ascomycetes and basidiomycetes, form extensive networks in the soil, are able to hydrolyze and move phosphorus and other micronutrients present in soil organic matter, facilitating root absorption (Bulgarelli et al.

2017). The fungus *Pochonia chlamydosporia* has been observed as root endophytic and has high efficiency in the control of plant parasitic nematode, as well as the ability to promote plant growth of several crops of agricultural importance because it is able to hydrolyze and move phosphorus and other micronutrients present in soil organic matter, facilitating root absorption and produces AIA (Escudero and Lopez-Llorca, 2012; Bontempon et al. 2014; Larriba et al. 2015; Hidalgo-Díaz et al. 2017; Monteiro et al. 2018; Gouveia et al. 2019). Thus, in this work we evaluated the capability of the *P. chlamydosporia* to improve the drought tolerance in soybean plants.

Here, the results of the water deficit assay showed that there is an interaction between soybean and *P. chlamydosporia* that favored the plant under water stress. The dehydration curve showed that, under water deficit, the Embrapa48 genotype required a longer time to reach the same leaf water potential (Ψ) levels as BR16. From the images taken from the plants on the same day, it can be seen that Embrapa48 has greater leaf strength and turgor than BR16. Under moderate and severe water deficit, plants of both genotypes with roots interactingwith *P. chlamydosporia* presented a lag in leaf water potential of approximately +0.2 MPa compared to plants without the fungus. Under drought conditions, the plants under fungal interaction delayed in average one day, to reach the same water potential than non-inoculated plants. Thus, leaf water potential and relative water content data (**Figure 1**) indicate the existence of an interaction of the fungus with the soybean root that contributes to the maintenance of leaf turgor and plant water balance.

The results of irrigation dynamics and soil water loss (two-axis plot; **Figure 2**) may indicate that the sensitive genotype BR16 is able to retain a greater amount of soil water under water deficit conditions with the help of the fungus, while the tolerant genotype Embrapa48 with the fungus removes a greater amount of water from the soil under abiotic stress.

The higher values of difference in vessel weights (ΔW) presented by the Embrapa48 NF (830 mg) relative to BR16 NF (650 mg) may indicate a better efficiency of use of the water by the drought tolerant genotype. In turn, the values of Embrapa48 F (650 mg) and BR16 F (755 mg) indicate that the fungus increased the preservation of soil water content for BR16 while it decreased for Embrapa48. This may be due to the phenotype of the genotypes and the differences between the symbiotic interactions between plant and fungus. The results may also indicate a behavior of the tolerant genotype Embrapa48 in retaining a greater amount of soil water under water deficit conditions in the absence of the fungus, as

demonstrated in root RWC, and increased uptake by the roots of the sensitive genotype BR16 in the presence of fungus.

Mathematical modeling analysis of the cin-fall kinetic data over time (**Figure 3**) indicates that both genotypes may respond better to water restriction in the presence of the fungus, but the difference between the exponents is greater for the sensitive genotype. Thus, the graphic modeling reinforces the hypothesis of the existence of mechanisms correlated with the presence of the fungus in the roots that act together with intrinsic characteristics of the plant genotype to maintain the water potential and cellular turgor and that the drought-sensitive genotype seems to respond better to the presence of the fungus under unfavorable water conditions.

As observed in previous studies (Mesquita et al. 2020; Coutinho et al. 2021), photosynthetic assimilation (A), the leaf transpiration rate (E) and stomatal conductance to water vapor (*gs*) suffered a strong decrease with the imposition of the water deficit. The lack of water stimulates the ABA-induced stomatal closure, decreasing the loss of water by the cells through transpiration (E) and decreasing the absorption of atmospheric CO_2 (A).

A possible explanation could be related to the conduction of water and photosynthates by the root-shoot system. Therefore, the morphology of cross sections of the root and stem was investigated.

In fact, there were significant changes in the carboxylation rate (A/Ci) and efficient water use (A/E and A/gs) for BR16 with fungus compared to plants without fungus, but not for Embrapa48. Leaf hydraulic conductivity values, estimated in terms of leaf water potential (Ψ) and leaf transpiration rate (E), showed a smaller reduction in Embrapa48 genotypes under drought, and didn't change to BR16 under drought due to the fungus.

Furthermore, root and leaf RWC, Kf and gas exchange data, in addition to root and stem microscopy results, together with the results observed for proline and polyamines may indicate that the presence of the fungus makes the use of water through the cell that does not appear to be related to the control of stomatal opening, but to the maintenance of water conduction through the vessel elements and the conservation of cellular turgor throughout the root-shoot system.

In the presence of the fungus, we observed an increase in the vascular cambium region, the region responsible for the activation and formation of vascular bundles in plants, for both genotypes under drought (**Figure 8 and 10**). Under normal conditions, the

Embrapa48 genotype appears to show a thicker cambium than BR16, which reflects a better water and nutrient distribution system to other parts of the plant.

Under drought conditions, genes encoding aquaporins are regulated, a response dependent on several factors such as ionic potential, phytohormonal changes and generation of reactive species during abiotic stresses (Porcel, et al. 2006) that reduce root hydraulic conductivity and stimulate the expression of genes related to the cell wall, leading to an increase in the root area/volume ratio. In addition, the route of water absorption by the roots occurs through the apex regions, which are younger and with less suberin accumulation, which may explain greater growth and formation of root structures in plants under water deficit.

Under abiotic stress, it is observed in roots and stem a narrowing in the thickness of the conducting vessels, a reduction in the area of the xylem lumen, in the number of elements of the vascular system. Such adaptation allows the maintenance of the root-shoot conduction and prevents cavitation and consequent embolisms. The genotypes had smaller stem diameter and absolute growth rates than in the irrigated treatments, and plants with the fungus had a slightly smaller diameter. During the period of water restriction, the absolute growth did not change significantly due to the presence of the fungus. In turn, the relative growth rate of the aerial part of irrigated and dry plants shows a better use of Embrapa48 than for BR16, regardless of the presence of the fungus. the differential increase in leaf hydraulic conductivity observed in Embrapa48 may explain the ability to maintain leaf turgor longer than the sensitive genotype BR16, resulting in higher photosynthetic (A), transpiration (E), stomatal conductance (gs) and carboxylation rates (A/Ci). The greater stress felt, in turn, in the sensitive BR16 genotype, can trigger an interactive response with symbiotic fungi in the soil, leading to beneficial associations that result in a better efficient use of water, presenting better efficiency values in the use of water (A/ E) and efficiency in the internal use of water (A/gs).

The hydraulic conductivity of shoots decreases in dry conditions because of the reduction in caliber and the total luminal area of the xylem vessels, according to Lovisolo and Schubert (1998). These characteristics can vary according to the varieties, with higher yielding strains having higher conductance values due to the differential increase in the xylem parameters, which increases the efficiency of absorption, maintenance and use of water. The presence of the fungus in the roots may influence the better water use efficiency observed in the drought-sensitive genotype, while the changes observed in the conducting vessels of the

root and stem of Embrapa48 and BR16 (**Figure 11**) may be involved with higher levels of leaf hydraulic conductance and root and leaf relative water content (RWC) shown in the drought tolerant genotype.

Changes in the root-shoot system conductive vessel bundles and the efficient use of water may indicate a better mutualistic association of the symbiotic fungus with the sensitive genotype, while mathematical modeling associated with high levels of specialized metabolites, especially phytoalexins, show a lower response to the symbiotic association of the drought-tolerant genotype, possibly because of the hydraulic properties of the vascular bundles, which attenuate the effects of water stress and make the genotype less in need of biotic interaction.

The absolute growth rates g (**Figure 5**) and shoot development (**Appendix A**) were higher in irrigated plants, while the relative growth rate r was higher for the cultivar Embrapa48 under water stress. The presence of the fungus increased the r value for Embrapa48 under drought, confirming that it is drought tolerant. Water constitutes a large part of plant aerial weight and participates in carbon fixation in plant tissues. The explanation may exist for a possible efficient use of water in plant biomass formation. In previous studies, it was shown that BR16 presents higher values for shoot growth and Embrapa48 presents greater volume and development of the root part to the detriment of the shoot part (Mesquita et al. 2020). There is, therefore, a morphophysiological mechanism of tolerance to the water deficit adapted by the genotype Embrapa48. The mechanisms of action of the soybean-fungus interaction in a water deficit regime cause morphological changes in plant roots, but they do not seem to significantly alter the morphology of the leaf part (**Figure 6 and Appendix A**).

Plants under irrigated conditions and with the fungus presented a more volumes root system than plants without fungus, indicating a possible role of the fungus in promoting root growth and development (Monteiro et al. 2018; Gouveia et al. 2019). Visual results of shoots and soybean roots under water deficit conditions indicate a compromised shoot development and an increase in shoot/root share ratio. There were no visible morphological differences between plants with and without fungus (although there is a tendency to higher values in plants with fungus and under water deficit.

According to the images of roots and shoots and the results of relative growth and stem diameter (**Figure 5**), the fungus promoted the growth and accumulation of biomass in the irrigated varieties. Root branching is related to an increase in the plant's capacity to

explore the rhizosphere in search of water, as it increases the root exposure surface with the soil and decreases the volume/area ratio.

Abiotic stress and the presence of the fungus can induce the vascular cambium to stimulate the formation of secondary vascular tissues such as xylem and phloem in order to maintain the tightness of the conducting vessels and prevent disruption of the conduction of root-shoot solutes. The greater structural integrity of the pith and the decrease in the number and caliber of conducting vessels under conditions of abiotic stress and in the presence of the fungus may be an adaptation to avoid cavitation of the liquid solution in the vessels.

Root and stem light microscopy results again indicate that Embrapa48 tolerates drought conditions. Plants with the presence of the fungus had a smaller number of conducting vessels in the roots, with a smaller total lumen area and, therefore, less need for conduction of solutes. For cultivar BR16, however, the presence of the fungus seemed to have more effect on increasing tolerance, as fewer lumens and smaller diameters were noted, indicating less need for conduction of solutes, in addition to higher values of A. This may indicate that the tolerance shown by Embrapa48 may be related to the hydraulic properties inherent to the genotype, and that there is an internal regulation of photosynthetic parameters to prevent water loss in response to the presence of the fungus in the rhizosphere that benefits both genotypes, but BR16 in greater intensity. Increasing the caliber of vessels increases conduction efficiency and avoids problems arising from lack of water, such as cavitation and embolism, in addition to maintaining the exchange of water and solutes/photosynthesized between the root and the aerial part of the plant. In Embrapa48 under drought and with fungus, the size of the pots was similar to that of irrigated plants, corroborating the hypothesis that drought tolerance is related to the hydraulic properties presented by the genotype.

The presence of the fungus did not cause significant changes in the gas exchange parameters in the drought-tolerant cultivar Embrapa48. Studies reinforce that Embrapa48 genotype has a greater efficiency in the absorption and conduction of water and maintenance of water balance (Lima et al. 2019; Mesquita et al. 2020; Coutinho et al. 2021), confirmed by leaf and roots relative water contents. The internal mechanisms of adaptation, such as activation of dehydration-responsive genes, osmolyte relocation, showed lower values in the gas exchange variables.

Finally, internal mechanisms of drought adaptation can act in the synthesis of lignin, which can act in the reinforcement of the secondary wall, in the formation of hydrophobic fibers in the root and stem in order to provide mechanical support to the plant. Pectin, in turn,

is a heterogeneous polysaccharide polymer that acts as a rigid gel matrix, filling the apoplastic space and giving it resilience and permeability. Coutinho (2021) observed that genes that encode proteins involved in pectin metabolism were up-regulated in the Embrapa48, which may indicate that one of the mechanisms of tolerance to water shortage in the drought-tolerant genotype involves the metabolism of pectin. The uptake of nutrients such as nitrogen and phosphorus, induced by the fungus *Pochonia chlamydosporia* isolate 10 (Monteiro et al. 2018; Gouveia et al. 2019), and the reuse of endogenous nutrients may be linked to the pectin content in the root apex (Zhu et al. 2016). In the formation of apical and subapical root segments that promote root branching, the synthesis of matrix polysaccharides during water stress may be linked to drought tolerance (Piro et al. 2003).

Thus, the metabolic profiles indicate that the metabolites detected by XCMS, such as phenolic compounds and flavonoids, especially phenolic compounds, were responsive to the presence of the fungus, especially in irrigated plants, showing low levels of relative abundance under the effect of water deficit under both biotic treatments. This may indicate that the effects of lack of water drastically modify plant metabolism, leading to a reduction in the presence of phenolic compounds.

Plants that are more tolerant to drought tend to adopt ways to adapt to water-restricted conditions, such as resistance mechanisms or tolerance to lack of water. Among the mechanisms adopted, the anatomical changes promoted in the plant vascular system, on the one hand, demand activation of genes that promote polymer synthesis reaction such as pectins, lignans and lignins and genes related to cell division and growth to the formation and reinforcement of vessel elements (McCann et al. 1991; Malavasi et al. 2016; Hu et al. 2009; Le Gall et al. 2015). On the other hand, several osmoprotective compounds are synthesized and stored in cell vacuoles in order to maintain cell turgor under osmotic stress conditions. Modifications in cell wall pectins can contribute to the maintenance of water balance and delay the activation of cell death pathways (Leucci et al. 2008). Finally, the presence of non-enzymatic antioxidant metabolism compounds such as flavonoids and isoflavonoids with antimicrobial activity can hinder the establishment of favorable ecological relationships.

An interesting point to highlight is the differences between the highest levels of plant hormones observed in roots and leaves. Indeed, ABA levels were 20 times higher in leaves than in roots, while JA and indoleacetic acid (IAA) levels were 1.5 times higher. ACC showed twice the root levels in leaves, and salicylic acid levels were 250 times higher in leaves than

in roots. Thus, the differences in the abundance of phytohormones in different parts of the plant are highlighted, linked to their mode of action and regulation of plant homeostasis.

Abscisic acid is possibly the hormone most related to the plant response to drought, presenting three intrinsic properties to abiotic stress. by closing the stomata and decreasing the transpiration rate (supported by gas exchange data) (Zhang and Davies, 1990), by decreasing the growth of shoot growth, by controlling root water uptake through root growth, stimulating the elongation of the primary root towards deeper regions of the soil (Sharp 2002), the relocation of the root to the shoot, leading to changes in the vascular system (Saab et al. 1990) or in the hydraulic conductivity of the root (Parent et al. 2009). The lowest levels of ABA observed in roots of BR16 plants when compared to Embrapa48, in the presence of the fungus, can be correlated with a higher assimilation of CO_2 (higher A value; **Figure 4**) in leaves. Despite this, no change in E and gs was observed due to the fungus, which indicates that the greater assimilation of CO_2 observed in BR16 F may be due to the efficient use of water inside the leaf. Higher ABA levels in Embrapa48 roots under drought may impact other mechanisms involved in drought tolerance, such as increased flavonoid levels and modulation of oxidative damage (Jiang et al. 2001) in roots and leaves.

Differences in root volume and length between plants with and without fungus (**Figure 7**) indicate the presence and possible interaction between the fungus and soybean roots. The presence of *P. chlamydosporia* stimulated the elongation of the taproot in plants under water deficit towards the depth of the soil in order to capture the scarce water. (**Figure 6**). Previous studies have indicated that the presence of *P. chlamydosporia* is related to the release of exogenous indoleacetic acid (IAA) (released by the fungus), acting in the control of symbiosis (Godoy 2018; Junior et al. 2021). This auxin is related to the promotion of growth, development and tropism. In turn, endogenous abscisic acid (ABA) (produced by the plant), which is related to the inhibition of shoot growth and the promotion of root growth.

Drought stimulates the induction of responsive genes and induces the accumulation of ABA in the root and the expression of signaling genes associated with morphological changes in the root, such as root meristem stimulation in soil depth exploration (leading to increased root length) and discouraging the formation of adventitious roots in drier regions close to the surface (leading to a decrease in root volume) (**Figure 7**), in addition to stimulating the interaction of the root with its adherence region with the soil and increasing the region of depletion of water resources (Karanja et al. 2021). Studies show the role of ABA and PAs in the regulation, in roots of plants under drought stress, of aquaporins, channel proteins that

allow the passage of water in cells (Mahdieh and Mostajeran, 2009) and also as the possible upregulation of aquaporins by root interaction with symbiotic fungi can help to alleviate drought stress (Sharma et al. 2021). Thus, the presence of the mycorrhizal fungus and the increased levels of PAs synergistically contribute to increasing the root's capacity to withstand stressful conditions (Zhang et al. 2019).

The study of the influence of ABA on the hydraulic properties of the root-shoot system in maize plants showed that root, leaf and total conductance is enhanced with ABA production (Parent et al. 2009). This may indicate an existing relationship between leaf (leaf RWC) and root (root RWC) water status (**Figure 5 and 7**) and increased ABA levels in leaves and roots (**Figure 12**) and at slightly higher values of conductivity leaf hydraulics (**Figure 5**) observed in Embrapa48 stressed by water restriction and in the presence of fungus.

The role of JA and ACC in plant roots in response to water restriction is still poorly understood. Several studies point to the role of JA in leaves as a modulator of oxidative stress and plant senescence. It also acts on gene expression and on transcription factors responsive to various environmental stresses. Jasmonic acid is also associated with senescence in synergy with ethylene (measurable from ACC, its immediate precursor (Plett et al. 2014). The drop in JA levels in both leaves and roots of genotypes under drought is in agreement with these studies (**Figure 12**).

At the same time, in irrigated plants we observed an increase in jasmonic acid (JA) on BR16 with fungus. Mycorrhizal fungi can increase resistance to pathogens as observed by Li et al. (2013), where arbuscular mycorrhizal fungi contributed to resistance in the pathosystem soybean - *Phytophthora soybeane*, showing that the defense was due to increased ROS production and JA accumulation. This process is possibly related to the synthesis of phenylpropanoids and the ROS-induced and jasmonate-dependent cell wall lignification (Denness et al. 2011). The observed alterations of sinapyl alcohol in roots and of caffeic acid, coniferyl aldehyde and sinapyl alcohol in leaves help to reinforce this interpretation.

In turn, jasmonic acid can also induce the metabolism of phenolic compounds (Gutjahr and Paszkowski 2009). JA data related to flavonoids, isoflavones and pterocarpans reinforce the idea that the role of phenolic compounds in roots is related to protective and control activity of the rhizosphere microbiome, while in leaves it may be related to a more effective antioxidative mechanism, given its increase even in the absence of the fungus.

In a study on the symbiosis of plants of the genus *Populus* and the fungus Basidiomycota *Laccaria bicolor* (Plett et al. 2014), it was found that the JA and ACC pathways are later activated in plants in response to interactions with symbiotic fungus. The increase in the levels of ACC and JA may be related to the attempt to limit the growth of the fungus within its roots, which could hinder plant development. Furthermore, because they have a common substrate (S-adenosyl methionine; SAM), polyamines and ethylene often have antagonistic functions, and this compound is decisive to define the predominant pathway. In fact, signs of senescence may be related to increased ethylene production (identified from its precursor in the pathway, ACC) and catabolism and decreased PAs synthesis (Pandey et al. 2002).

High levels of indole acetic acid (IAA) can act by hindering fungal symbiosis by decreasing the expression of genes related to microbial perception. Indeed, AM and *P. chlamydosporia* colonization induces levels of IAA in the roots, which possibly inhibits further colonization. The increase in the abundance of these hormones in leaves of plants stressed by drought may be related to the suppression of levels in the root, which can benefit or hinder colonization by fungus and other organisms (Denness et al. 2011; Gouveia et al. 2019).

Osmolytes such as proline, sugars, sugar alcohols and quaternary ammonium compounds are essential for the conservation of cellular turgor with a lower water potential. Proline levels in roots, as expected, were strongly increased in roots and leaves of plants under water restriction, and a significant reduction of proline was observed only in BR16 roots in the presence of the fungus. Studies show that there is less proline accumulation observed in plants colonized by mycorrhizal fungus (Ruiz-et al. 2010; Fan and Liu 2011). However, the degradation of excess proline can lead to the formation of compounds that are harmful to the normal functioning of cells.

Studies point out among several functions of polyamines in response to abiotic stresses such as drought, salinity and heavy metals are the stabilization of membranes and nucleic acids by the conjugation of amines that hold a pair of free electrons with the head of phospholipids and DNA phosphates and RNA (Sharma et al. 2021), but the biological function of the changes in polyamine levels due to environmental factors is only partly elucidated. One of the hypotheses suggested would be that the increase in polyamines can stimulate the accumulation of osmoregulators in leaf and root cells and regulate root cell expansion, increasing root plasticity, in addition to playing a role in the control of redox

homeostasis through the positive regulation of enzymatic antioxidant genes (Sharma et al. 2021). Another related function would be the maintenance of redox homeostasis (Hasan et al. 2021). Spermine, in fact, has been associated with increased tolerance to drought-induced oxidative stress either through osmoregulation or induction of antioxidant defense mechanisms (Hasan et al. 2021).

Polyamines (PAs) can act both free and conjugated in antimicrobial defense, but the mechanisms of action remain less clear. Diamine oxidase (DAO) and polyamine oxidase (PAO) mediate the catabolic oxidation of PAs in peroxisomes and apoplasts (Gill and Tuteja 2010), generating, among other by-products, H_2O_2, which acts on stomatal closure, lignin synthesis and cell wall reinforcement, and induction of HR-induced PDC. A crosstalk between phytohormone and polyamine induction pathways may help to explain behavior under conditions of biotic and abiotic stress. There is positive feedback between ABA and PAs, since putrescine triggers the 9-cis-epoxycarotenoid dioxygenase (NCED) gene, which triggers ABA accumulation and whose overexpression improves the tolerance of transgenic *A. thaliana* to dehydration stress (Iuchi et al. 2002), which in turn activates transcription factors related to the synthesis of PAs (Alcazar et al. 2010). Root ABA levels increased in plants under drought, except for BR16 with the fungus, which showed lower levels. The same occurred for ACC, which is in agreement with the levels of putrescine and spermidine, which decreased in plants under water restriction, especially in the drought-sensitive genotype.

The fact that the levels of certain PAs are lower in Embrapa48 roots compared to BR16, even under irrigated conditions, may indicate a greater tolerance of the genotype to water stress due to a lesser dependence on the increase of these compounds or a rapid catabolic response of them. The levels of PAs between genotypes were similar only in plants under water stress and in the absence of the fungus, and the presence of the fungus in water stress for the sensitive genotype stimulated the increase, above all, of spermine and spermidine. The endogenous or exogenous nature of these PAs (ie, whether they are of plant or fungal origin) remains to be clarified, as studies indicate that there is a similarity in the functions of PAs between plants and arbuscular mycorrhizae (Valdés-Santiago and Ruiz-Herrera 2014), and given the importance of these compounds in the restoration and maintenance of homeostasis and in the cell differentiation of the fungus (Gasch 2007; Valdés-Santiago and Ruiz-Herrera 2014), the increase in PAs in roots can stimulate mutualistic plant-fungus symbiosis in drought conditions, especially in the drought-sensitive BR16 genotype.

In plants, benzoic acid (BA) derivatives can be synthesized in two ways: from metabolic precursors via shikimate or degradation from phenylpropanoid substrates, mainly trans-cinnamic acid and p-coumaric acid, or via non- oxidative (dependent or independent of coenzyme-A) or beta-oxidation. These reactions can occur in several organelles such as chloroplasts, mitochondria and peroxisomes, indicating a high specialization of plants in the synthesis. The final products (acids, aldehydes or alcohols derived from BA) can undergo several modifications, such as glucosylation, methylation, hydroxylation and amination. Generally, methylation of BA-derived, phenylpropanoids and flavonoids increases lipophilicity and mobility across cellular membranes, in addition to, in some cases, their toxicity, while glycosylation acts to increase their solubility and storage in the vacuole (Widhalm and Dudareva 2015). The accumulation of these compounds in the root and rhizosphere are associated with the perception of surrounding microorganisms and the protection of the plant against attacks.

In response to drought, plants invest in secondary wall formation and reinforcement of the xylem vessels with lignin, a polymer formed from units of p-coumaryl alcohol, coniferyl alcohol and synapyl alcohol, monolignols formed in the phenylpropanoid pathway and which differ each other by the methylation of the 3- and 5-hydroxyl of the aromatic ring. Concentrations of hydroxycinnamic acid derivatives observed in biotic interactions may be transient with the state of stress. The different levels observed may be related to the fact that they are intermediate compounds of different pathways (derived from benzoic acid, flavonoids, pterocarpans and glyceollins, monolignols and lignins) (Widhalm and Dudareva. 2015; Valanciene et al. 2020; Yoneyama et al. 2016). In fact, in the presence of the fungus, the levels of sinapic acid and sinapyl alcohol were lower in BR16 roots under drought, while sinapyl alcohol was up-regulated in BR16 leaves under drought compared to Embrapa48. Strengthening the cell wall by lignification implies reducing the attack by pathogen hydrolases (Lee et al. 2019).

Several studies point to the intrinsic relationship between changes in the levels of isoflavones in roots, leaves and seeds, a response to drought (Tian et al. 2014; Akitha et al. 2015) and symbiotic associations. In fact, symbiotic fungi and bacteria can associate with soybean roots and isoflavonoids can act as molecular signals in the establishment and control of mutualistic relationships (Antunes et al. 2006). The results of daidzein in leaves of plants with fungus, associated with box-plot plots of isoflavonoids in roots observed by the LC/MS (**Figure 15 and 16**) are in agreement with Salloum et al. (2019), who observed lower levels of

isoflavonoids in soybean roots with arbuscular mycorrhizal fungus symbiosis. Glycoconjugate isoflavones have also been observed. Malonyl and glucosyl-malonate forms derivatives of isoflavones still exhibited considerable bioactivity, despite the lower intensity compared to free aglycones (Ahmad et al. 2017). The lower levels also observed in plants without fungus under drought may indicate that these compounds are being directed towards the biosynthesis of other compounds such as cumestanes, pterocarpans and glyceollins, or being conjugated to other compounds such as sugars and stored in vacuoles.

In general, phenolic compounds act as phytoalexins (antibacterial and/or antifungal) inhibiting, in the invading organism, nucleic acid synthesis or energy metabolism, or acting on the plasma membrane by changing its permeability, triggering an uncontrolled potential ionic and inhibiting the action of porins (Ozçelik et al. 2011; Xie et al. 2014). There was decrease in the levels of isoflavones, coumestrol, medicarpins and glyceollins during abiotic stress, which can occur through degradation, conjugation such as glycosylation or malonylglycosylation and sequestration to the vacuoles. The levels of formononetin and coumestrol were slightly higher in Embrapa48 roots under drought and in the presence of the fungus, compared to BR16, indicating that the drought tolerance mechanisms present in the drought-tolerant genotype reduce the fall of phytoalexins, which can act on the plant defense against attacks by soil microorganisms. On the other hand, the low levels of phytoalexins in the roots of the drought-sensitive genotype can stimulate symbiotic associations with the fungus *P. chlamydosporia*, benefiting the absorption of water from the soil.

Studies report the antifungal activity of prenylated isoflavones isolated from soybeans. Moreover, 3-dimetylallyldaidzein (neobavaisoflavone) was identified in BR16 **(Figure 14)**, presenting high levels for BR16 plants with fungus and normally irrigated, behavior similar to the other flavonoids identified by LC/MS Q-TOF. This is in agreement with the interpretation that, under ideal conditions of water and nutrients, plants prefer symbiotic associations. Prenilated pterocarpans, glyceollins in soybean show antifungal and antioxidant activity in soy root, leaves and stem against various fungi (Boué et al. 2000; Ebel et al. 1988). In vitro assays glyceollins obtained by the pathosystem soybean - *Aspergillus soybeane* exhibited potential antifungal activity, controlling the growth of several plant pathogenic fungi (Kim et al. 2010). On the other hand, coumestrol and glyceollins induced in the pathosystem soybean - *Aspergillus oryzae* showed antioxidant activity 5 to 30 times higher than daidzein and genistein (Jeon et al. 2012). Consequently, the production of glyceollins in soybean roots and leaves may be a defense mechanism in response to oxidative

and biotic stresses such as fungi (Darvill and Albersheim, 1984). Indeed, we observed a decrease in the heatmap data of Glyceollin-8.6 and -9.8 in roots **(Figure 17)**. The increase in coumestrol-9.2 and formononetin-9.2 levels in Embrapa48 leaves and in the levels of coumestrol-8.6 and glyceollin-9.8 in leaves of both genotypes stressed by lack of water may have a double role: action against oxidizing agents and protection against possible infections caused by pathogenic or non-pathogenic agents.

The cytotoxic properties of phytoalexins, however, can act on the plant cell itself, causing deleterious effects on cell homeostasis, being conjugated to molecules and stored in vacuoles (Dare et al. 2017). This may be the main reason why the levels of isoflavone-derived phytoalexins decrease under water stress conditions: to reduce greater damage to the integrity of cell metabolism under unfavorable conditions. The rapid fall in coumestrol, formononetin, medicarpins and glyceollins during abiotic stress **(Figure 17 and 18)** may also be an important component to facilitate plant-fungus symbiosis. Several points remain to be elucidated, such as the role of the symbiotic fungus in decreasing phytoalexins levels and whether this aided their ability to colonize soybean plants (Lygin et al. 2010).

Under irrigated conditions, the soil becomes a favorable environment for the reproduction and population growth of the soil microbiome such as fungi, oomycetes, bacteria and viruses, among others, and competition for space and nutrients becomes the limiting factor for growth. In this environment, plants can accumulate phytoalexins in their roots to protect themselves from pathogenic organisms, parasites or even competitors, allowing, however, beneficial associations. In the meantime, there are ectomycorrhizas, endomycorrhizae (arbuscular mycorrhizae), in addition to associations with bacteria such as rhizobia.

Under irrigated conditions, however, plants may fail to take advantage of symbiotic affinities, turning the ecological relationship from mutualistic to commensal or even parasitic, to the detriment of the vegetable. The inactivation of antimicrobial compounds under drought conditions, either by catabolism or by export to vacuoles or other parts of the plant, or by conjugation with sugars or other compounds, can be a mechanism to allow the plant to establish mutual ecological relationships with other organisms to ensure tolerance and survival under unfavorable conditions.

5 CONCLUSION

The morphophysiological and gas exchange, turgor and conductivity results indicate that the resistance presented by Embrapa48 and BR16 derives from hydraulic properties inherent to the genotype, which were increased by the presence of the fungus. The low levels of phenolic compounds may indicate a more favorable ecological relationship between the plant and the soil microbiome, to which *P. chlamydosporia* is inserted. The results of A, E and gs indicate that the greater efficiency in the use of water by plants containing the fungus are of non-stomatic origin. The results of light microscopy, in turn, show that the fungus can help the hydraulic conductivity of vessels under drought and in the root-shoot conduction system.

In turn, the higher results for flavonoids and phytoalexins in Embrapa48 may indicate that, in the presence of water deficit, BR16 seems to respond differently from Embrapa48, showing a drop in the levels of compounds acting against microorganisms and showing a possible receptivity to form associations with *P. chlamydosporia*.

Furthermore, the association of the fungus *P. chlamydosporia* with soybean roots indicates to promote morphological changes in the root system, changes in the system of conducting vessels of the root and stem in both genotypes, associated with a smaller drop in water potential and a greater maintenance of cellular turgor under water deficit conditions, changes observed in Embrapa48 and, to a lesser extent, in BR16.

REFERENCES

AHMAD, M. Z.; LI, P.; WANG, J.; REHMAN, N. U.; ZHAO, J. (2017) Isoflavone Malonyltransferases GmIMaT1 and GmIMaT3 Differently Modify Isoflavone Glucosides in Soybean (*Glycine max*) under Various Stresses. Frontiers in Plant Science, 8. https://doi.org/10.3389/fpls.2017.00735

AKITHA DEVI, M. K.; GIRIDHAR, P. (2015) Variations in Physiological Response, Lipid Peroxidation, Antioxidant Enzyme Activities, Proline and Isoflavones Content in Soybean Varieties Subjected to Drought Stress. Proc. Natl. Acad. Sci. India, Sect. B Biol. Sci. 85, 35-44. https://doi.org/10.1007/s40011-013-0244-0

ALCÁZAR, R.; ALTABELLA, T.; MARCO, F.; BORTOLOTTI, C.; REYMOND, M.; KONCZ, C.; CARRASCO, P.; TIBURCIO, A. F. (2010) Polyamines: molecules with regulatory functions in plant abiotic stress tolerance. Planta 231, 1237-1249. https://doi.org/10.1007/s00425-010-1130-0

ANTUNES, P. M.; RAJCAN, I.; GOSS, M. J. (2006) Specific flavonoids as interconnecting signals in the tripartite symbiosis formed by arbuscular mycorrhizal fungi, Bradyrhizobium japonicum (Kirchner) Jordan and soybean (*Glycine max* (L.) Merr.). Soil Biology and Biochemistry, 38(3), 533-543. https://doi.org/10.1016/j.soilbio.2005.06.008

AREVALO, J.; HIDALGO-DÍAZ, L.; MARTINS, I.; SOUZA, J. F.; CASTRO, J. M. C.; CARNEIRO, R. M. D. G.; TIGANO, M. S. (2009) Cultural and morphological characterization of *Pochonia chlamydosporia* and *Lecanicillium psalliotae* isolated from *Meloidogyne mayaguensis* eggs in Brazil. Tropical Plant Pathology 34 (3)

BONTEMPO, A. F.; FERNANDES, R. H.; LOPES, J.; FREITAS, L. G.; LOPES, E. A. (2014) *Pochonia chlamydosporia* controls *Meloidogyne incognita* on carrot. Australasian Plant Pathology, 43(4), 421-424. https://doi.org/10.1007/s13313-014-0283-x

BORDALLO, J. J.; LOPEZ-LLORCA, L. V.; JANSSON, H. B.; SALINAS, J.; PERSMARK, L.; ASENSIO, L. (2002) Colonization of plant roots by egg-parasitic and nematode-trapping fungi. New Phytologist, 154, 491-499.

BOUÉ, S. M.; CARTER, C.; EHRLICH, K. C.; CLEVELAND, T. E. (2000) Induction of the soybean phytoalexins coumestrol and glyceollin by Aspergillus. Journal of Agricultural and Food Chemistry, 48, 2167-2172.

BRODRIBB, T. J.; HOLBROOK, N. M. (2003) Changes in leaf hydraulic conductance during leaf shedding in seasonally dry tropical forest. New Phytologist 158:295-303.

BRODRIBB, T. J.; HOLBROOK, N. M. (2006) Declining hydraulic efficiency as transpiring leaves desiccate: two types of response. Plant, Cell & Environment, 29:2205-2215.

BULGARELLI, R. G.; MARCOS, F. C. C.; RIBEIRO, R. V.; DE ANDRADE, S. A. L. (2017) Mycorrhizae enhance nitrogen fixation and photosynthesis in phosphorus-starved soybean (*Glycine max* L. Merrill). Environmental and Experimental Botany, 140, 26-33. https://doi.org/10.1016/j.envexpbot.2017.05.015

CARVALHO, J. F. C.; CRUSIOL, L. G. T.; PERINI, L. J.; SIBALDELLI, R. N. L.; FERREIRA, L. C.; GUIMARÃES, F. C. M.; NEPOMUCENO, A. L.; NEUMAIER, N.; FARIAS, J. R. B. (2015) Phenotyping soybeans for drought responses using remote sensing techniques and non-destructive physiological analysis. Glob Sci Technol 8:1-16

COUTINHO, F. S.; SANTOS, D. S.; LIMA, L. L.; VITAL, C. E.; SANTOS, L. A.; PIMENTA, M. R.; SILVA, J. C.; RAMOS, J. R. L.; S.; METHA, A.; FONTES, E. P. B.; RAMOS, H. J. O. (2019) Mechanism of the drought tolerance of a transgenic soybean overexpressing the molecular chaperone. BiP Physiol. Mol. Biol. Plants. 1, 1-16. https://doi.org/10.1007/s12298-019-00643-x.

COUTINHO, F. S.; RODRIGUES, J. M.; LIMA, L. L.; MESQUITA, R. O.; CARPINETTI, P. A.; MACHADO, J. P. B.; VITAL, C. E.; VIDIGAL, P. M.; RAMOS, M. E. S.; MAXIMIANO, M. R.; MEHTA, A.; OLIVEIRA, M. G. A. O; FONTES, E. P. B.; RAMOS, H. J. O. (2021) Remodeling of the cell wall as a drought-tolerance mechanism of a soybean genotype revealed by global gene expression analysis. aBIOTECH, 2(1), 14-31. https://doi.org/10.1007/s42994-021-00043-4

CRAMER, G. R.; URANO, K.; DELROT, S.; PEZZOTTI, M.; SHINOZAKI, K. (2011) Effects of abiotic stress on plants: a systems biology perspective. BMC Plant Biology, 11, 163.

CUNHA, A. P. M. A.; ZERI, M.; LEAL, K. D.; COSTA, L.; CUARTAS, L. A.; MARENGO, A.; TOMASELLA, J.; VIEIRA, R. M.; BARBOSA, A. A.; CUNNINGHAM, C.; GARCIA, J. V. C.; BROEDEL, E.; ALVALÁ, R.; RIBEIRO-NETO, G. (2019) Extreme Drought Events over Brazil from 2011 to 2019. Atmosphere, 10(11), 642. https://doi.org/10.3390/atmos10110642

DALLEMOLE-GIARETTA, R.; FREITAS, L. G.; LOPES E. A.; SILVA, M. C. S.; KASUYA, M. C. M.; FERRAZ, S. (2015) *Pochonia chlamydosporia* promotes the growth of tomato and lettuce plants. Acta Scientiarum. Agronomy Maringá, 37(4):417-423. https://doi.org/10.4025/actasciagron.v37i4.25042

DARE, A. P. YAUK, Y. -K. TOMES, S. MCGHIE, T. K. REBSTOCK, R. S. COONEY, J. M.; ATKINSON, R. G. (2017) Silencing a phloretin-specific glycosyltransferase perturbs both general phenylpropanoid biosynthesis and plant development. Plant J. Cell Mol. Biol. 91, 237-250. https://doi.org/10.1111/tpj.13559

DARVILL, A. G.; ALBERSHEIM, P. (1984) Phytoalexins and their elicitors - A defense against microbial infection in plants. Annual Review of Plant Physiology, 35, 243-275.

DENNESS, L.; MCKENNA, J. F.; SEGONZAC, C.; WORMIT, A.; MADHOU, P.; BENNETT, M.; MANSFIELD, J.; ZIPFEL, C.; HAMANN, T. (2011) Cell Wall Damage-Induced Lignin Biosynthesis Is Regulated by a Reactive Oxygen Species- and Jasmonic Acid-Dependent Process in Arabidopsis. Plant Physiology, 156(3), 1364-1374. https://doi.org/10.1104/pp.111.175737

EBEL, J.; GRISEBACH, H. (1988) Defense strategies of soybean against the fungus Phytophthora megasperma f. sp. glycinea: A molecular analysis. Trends in Biochemical Sciences, 1, 23-27.

ESCUDERO, N.; LOPEZ-LLORCA, L. V. (2012) Effects on plant growth and root-knot nematode infection of an endophytic GFP transformant of the nematophagous fungus *Pochonia chlamydosporia*. Symbiosis, 57(1), 33-42.

FAN Q. J.; LIU J. H. (2011) Colonization with arbuscular mycorrhizal fungus affects growth, drought tolerance and expression of stress-responsive genes in Poncirus trifoliata. Acta Physiol. Plant. 33 1533-1542. 10. 1007/s11738-011-0789-6

GASCH, A. P. (2007) Comparative genomics of the environmental stress response in ascomycete fungi. Yeast 24, 961-976. https://doi.org/10.1002/yea.1512

GILL, S. S.; TUTEJA, N. (2010) Polyamines and abiotic stress tolerance in plants. Plant Signaling & Behavior, 5(1), 26-33. https://doi.org/10.4161/psb.5.1.10291

GÓMEZ, J. D.; PINHEIRO, V. J. M.; SILVA, J. C.; ROMERO, J. V.; MERIÑO-CABRERA, Y.; COUTINHO, F. S.; LOURENÇÃO, A. L.; SERRÃO, J. E.; VITAL, C. E.; FONTES E. P. B.; OLIVEIRA, M. G. A.; RAMOS, H. J. O. (2020) Leaf metabolic profiles of two soybean genotypes differentially affect the survival and the digestibility of Anticarsia gemmatalis caterpillars. Plant Physiology and Biochemistry. https://https://doi.org/10.1016/j.plaphy.2020.07.010

GOMEZ, J. D.; VITAL, C. E.; OLIVEIRA, M. G. A.; RAMOS, H. J. O. (2018) Broad range flavonoid profiling by LC/MS of soybean genotypes contrasting for resistance to Anticarsia gemmatalis (Lepidoptera: Noctuidae). PloS One 13 (10), e0205010. https://doi.org/101371/journalpone0205010

GODOY, V. H. S. *Pochonia* spp. como promotor de crescimento vegetal. 2018. 148f. Dissertação (Mestrado em Biotecnologia) - Universidade Federal do Tocantins, Programa de Pós-Graduação em Biotecnologia, Gurupi, 2018

GOUVEIA, F.; BICKER, J.; GONÇALVES, J.; ALVES, G.; FALCÃO, A.; FORTUNA, A. (2019) Liquid chromatographic methods for the determination of direct oral anticoagulant drugs in biological samples: a critical review. Anal. Chim. Acta 1076, 18-31. https://doi.org/10.1016/j.aca.2019.03.061. Epub 2019 Apr 8. Review.

GOUVEIA, A. S.; MONTEIRO, T. S. A.; VALADARES, S. V.; SUFIATE, B. L.; FREITAS, L. G.; RAMOS, H. J. O.; DE QUEIROZ, J. H. (2019) Understanding how *Pochonia chlamydosporia* increases Phosphorus availability. Geomicrobiology Journal, v. 1, p. 1-5.

GUTJAHR, C.; PASZKOWSKI, U. (2009) Weights in the Balance: Jasmonic Acid and Salicylic Acid Signaling in Root-Biotroph Interactions. Molecular Plant-Microbe Interactions, 22(7), 763-772. https://doi.org/10.1094/mpmi-22-7-0763

HASAN, M. M.; SKALICKY, M.; JAHAN, M. S.; HOSSAIN, M. N.; ANWAR, Z.; NIE, Z. F.; ALABDALLAH, N. M.; BRESTIC, M.; HEJNAK, V.; FANG, X. W. (2021) Spermine: Its Emerging Role in Regulating Drought Stress Responses in Plants. Cells. 28;10(2):261. https://doi.org/10.3390/cells10020261

HE, X. Z.; DIXON, R. A. (2000) Genetic manipulation of isoflavone 7-O-methyltransferase enhances biosynthesis of 4'-O-methylated isoflavonoid phytoalexins and disease resistance in alfalfa. Plant Cell. 12(9):1689-702. https://doi.org/10.1105/tpc.12.9.1689

HIDALGO-DÍAZ, L.; FRANCO-NAVARRO, F.; FREITAS, L. G. (2017) *Pochonia chlamydosporia* Microbial Products to Manage Plant-Parasitic Nematodes: Case Studies from Cuba, México and Brazil. In R. H. Manzanilla-López L. V. Lopez-Llorca (Ed. Springer). Sustainnability in Plant and Crop Protection: Perspectives in Sustainable Nematode Management Through *Pochonia chlamydosporia* Applications for Root and Rhizosphere Health.

HU, Y. LI, W. C. XU, Y. Q. LI, G. J. LIAO, Y. FU, F. -L. (2009) Differential expression of candidate genes for lignin biosynthesis under drought stress in maize leaves. Journal of Applied Genetics, 50(3), 213-223. https://doi.org/10.1007/bf03195675

IUCHI, S.; KOBAYASHI, M.; TAJI, T.; NARAMOTO, M.; SEKI, M.; KATO, T.; TABATA, S.; KAKUBARI, Y.; YAMAGUCHI-SHINOZAKI, K.; SHINOZAKI, K. (2001) Regulation of drought tolerance by gene manipulation of 9-cis-epoxycarotenoid dioxygenase, a key enzyme in abscisic acid biosynthesis in Arabidopsis. Plant J. 27(4):325-33. https://doi.org/10.1046/j.1365-313x.2001.01096.x. Erratum in: Plant J. 2002 Jun;30(5):611.

JALEEL, C. A.; MANIVANNAN, P.; KISHOREKUMAR, A.; SANKAR, B.; GOPI, R. SOMASUNDARAM, R.; PANNEERSELVAM, R. (2007) Alterations in osmoregulation, antioxidant enzymes and indole alkaloid levels in *Catharanthus roseus* exposed to water deficit. Colloids Surf B Biointerfaces. 1;59(2):150-7. https://doi.org/10.1016/j.colsurfb.2007.05.001

JEON, H. Y.; SEO, D. B.; SHIN, H. -J.; LEE, S. -J. (2012) Effect of Aspergillus oryzae-challenged germination on soybean isoflavone content and antioxidant activity. Journal of Agricultural and Food Chemistry, 60, 2807-2814.

JIANG, M.; ZHANG, J. (2001) Effect of abscisic acid on active oxygen species, antioxidative defence system and oxidative damage in leaves of maize seedlings. Plant Cell Physiol. 42(11):1265-73. https://doi.org/10.1093/pcp/pce162

JUNIOR, A. F. C.; CHAGAS, L. F. B.; MARTINS, A. L. L.; OLIVEIRA, R. S.; LUZ, L. L.; COLONIA, B. S. O.; GOMES, F. L.; SOUZA, M. C. (2021) Phosphate solubilization, synthesis of Indol Acetic Acid and effect on biomass soybean inoculated with *Pochonia*. Brazilian Journal of Development, Curitiba, 7(7): 72919-72934. https://doi.org/10.34117/bjdv7n7

KARANJA, J. K.; ASLAM, M. M.; QIAN, Z.; YANKEY, R.; DODD, I. C.; WEIFENG, X. (2021) Abscisic Acid Mediates Drought-Enhanced Rhizosheath Formation in Tomato. Front Plant Sci. 23;12:658787. https://doi.org/10.3389/fpls.2021.658787

KIM, H. J.; SUH, H. -J.; LEE, C. H.; KIM, J. H.; KANG, S. C.; PARK, S.; KIM, J. -S. (2010) Antifungal Activity of Glyceollins Isolated from Soybean Elicited with Aspergillus sojae. Journal of Agricultural and Food Chemistry, 58(17), 9483-9487. https://doi.org/10.1021/jf101694t

LARRIBA, E.; JAIME, M. D. L. A.; NISLOW, C.; MARTÍN-NIETO, J.; LOPEZ-LLORCA, L. V. (2015) Endophytic colonization of barley (*Hordeum vulgare*) roots by the nematophagous fungus *Pochonia chlamydosporia* reveals plant growth promotion and a general defense and stress transcriptomic response. Journal of Plant Research, 128(4), 665-678.

LE GALL, H.; PHILIPPE, F.; DOMON, J. -M.; GILLET, F.; PELLOUX, J.; RAYON, C. (2015) Cell Wall Metabolism in Response to Abiotic Stress. Plants, 4(1), 112-166. https://doi.org/10.3390/plants4010112

LEE, M. H.; JEON, H. S.; KIM, S. H.; CHUNG, J. H.; ROPPOLO, D.; LEE, H. J.; CHO, H. J.; TOBIMATSU, Y.; RALPH, J.; PARK, O. K. (2019) Lignin-based barrier restricts pathogens to the infection site and confers resistance in plants. EMBO J. 2;38(23):e101948. https://doi.org/10.15252/embj.2019101948

LEUCCI, M. R.; LENUCCI, M. S.; PIRO, G. DALESSANDRO, G. (2008) Water stress and cell wall polysaccharides in the apical root zone of wheat cultivars varying in drought tolerance. Journal of Plant Physiology, 165(11), 1168-1180. https://doi.org/10.1016/j.jplph.2007.09.006

LI, Y.; LIU, Z.; HOU, H.; LEI, H.; ZHU, X.; LI, X.; HE, X.; TIAN, C. (2013) Arbuscular mycorrhizal fungi-enhanced resistance against *Phytophthora sojae* infection on soybean leaves is mediated by a network involving hydrogen peroxide, jasmonic acid, and the metabolism of carbon and nitrogen. Acta Physiol Plant 35, 3465-3475. https://doi.org/10.1007/s11738-013-1382-y

LIMA, L. L.; BALBI, B. P.; MESQUITA, R. O.; SILVA, J. C. F.; COUTINHO, F. S.; CARMO, F. M. S.; VITAL, C. E.; MEHTA, A.; FONTES, E. P. B.; BARROS, E. G.; RAMOS, H. J. O. (2019) Proteomic and metabolomic analysis of a drought tolerant soybean genotype from Brazilian Savanna. Crop Breed. Genet. Genom. e190022-32, 2019

LOVISOLO, C.; SCHUBERT, A. (1998) Effects of water stress on vessel size and xylem hydraulic conductivity in *Vitis vinifera* L. Journal of Experimental Botany, 49(321), 693-700. https://doi.org/10.1093/jxb/49.321.693

LYGIN, A. V.; HILL, C. B.; ZERNOVA, O. V.; CRULL, L.; WIDHOLM, J. M.; HARTMAN, G. L.; LOZOVAYA, V. V. (2010) Response of soybean pathogens to glyceollin. Phytopathology 100:897-903.

MAHDIEH, M.; MOSTAJERAN, A. (2009) Abscisic acid regulates root hydraulic conductance via aquaporin expression modulation in *Nicotiana tabacum*. Journal of Plant Physiology, 166(18), 1993-2003. https://doi.org/10.1016/j.jplph.2009.06.001

MALAVASI, U. C.; DAVIS, A. S.; MALAVASI, M. M. (2016) Lignin in Woody Plants under Water Stress: A Review. Floresta e Ambiente, 23(4), 589-597. https://doi.org/10.1590/2179-8087.143715

MCCANN, M.; ROBERTS, K. (1991) Architecture of the primary cell wall. In The Cytoskeletal Basis of Plant Growth and Form; Lloyd, C. W. Ed.; Academic Press: London, UK, 109-129

MESQUITA, R. O.; COUTINHO, F. S.; VITAL, C. E.; NEPOMUCENO, A. L.; RHYS WILLIAMS, T. C.; RAMOS, H. J. O.; LOUREIRO, M. E. (2020) Physiological approach to decipher the drought tolerance of a soybean genotype from Brazilian savana. Plant Physiology and Biochemistry. https://doi.org/10.1016/j.plaphy.2020.03.004

MONTEIRO, T. S. A.; VALADARES, S. V.; DE MELLO, I. N. K.; MOREIRA, B. C.; KASUYA, M. C. M.; ARAÚJO, J. V.; FREITAS, L. G. (2018) Nematophagus fungi increasing phosphorus uptake and promoting plant growth. Biological control, 123:71-75

MORAN, N. A. (2006) Symbiosis. Current Biology 16 (20). R866

MÜLLER, M.; MUNNÉ-BOSCH, S. (2011) Rapid and sensitive hormonal profiling of complex plant samples by liquid chromatography coupled to electrospray ionization tandem mass spectrometry. Plant methods 7(1): 37. https://doi.org/10.1186/1746-4811-7-37

NOCTOR, G.; VELJOVIC-JOVANOVIC, S.; DRISCOLL, S.; NOVITSKAYA, L.; FOYER, C. H. (2002) Drought and oxidative load in the leaves of C3 plants: a predominant role for photorespiration? Annual Botany 89: 841 - 850.

O'BRIEN, T. P.; FEDER, N.; MCCULLY, M. E. (1964) Polychromatic staining of plant cell walls by toluidine blue O. Protoplasma 59, 368-373. https://doi.org/10.1007/BF01248568

OYA, T.; NEPOMUCENO, A. L.; NEUMAIER, N.; FARIAS, J. R. B.; TOBITA, S.; ITO, O. (2004) Drought tolerance characteristics of Brazilian soybean cultivars. Plant Production Science 7(2): 129-137. https://doi.org/10.1626/pps.7.129

OZÇELIK, B.; KARTAL, M.; ORHAN, I. (2011) Cytotoxicity, antiviral and antimicrobial activities of alkaloids, flavonoids, and phenolic acids. Pharm Biol.;49(4):396-402. https://doi.org/10.3109/13880209.2010.519390

PANDEY, S.; RANADE, S. A.; NAGAR, P. K.; KUMAR, N. (2000) Role of polyamines and ethylene as modulators of plant senescence. J. Biosci. 25 (3): 291-9. https://doi.org/10.1007/BF02703938

PARENT, B.; HACHEZ, C.; REDONDO, E.; SIMONNEAU, T.; CHAUMONT, F.; TARDIEU, F. (2009) Drought and abscisic acid effects on aquaporin content translate into changes in hydraulic conductivity and leaf growth rate: a trans-scale approach. Plant Physiol. 149(4):2000-2012. https://doi.org/10.1104/pp.108.130682

PIRO, G.; LEUCCI, M. R.; WALDRON, K.; DALESSANDRO, G. (2003) Exposure to water stress causes changes in the biosynthesis of cell wall polysaccharides in roots of wheat cultivars varying in drought tolerance. Plant Science, 165(3), 559-569. https://doi.org/10.1016/s0168-9452(03)00215-2

PLETT, J. M.; KHACHANE, A.; OUASSOU, M.; SUNDBERG, B.; KOHLER, A.; MARTIN, F. (2014) Ethylene and jasmonic acid act as negative modulators during mutualistic symbiosis between Laccaria bicolor and Populus roots. New Phytol. 202(1):270-286. https://doi.org/10.1111/nph.12655

PODESTÁ, G. S.; FREITAS, L. G.; DALLEMOLE-GIARETTA, R.; ZOOCA, R. J. F.; CAIXETA, L. B.; FERRAZ, S. (2013) *Meloidogyne javanica* control by *Pochonia chlamydosporia*, *Gracilibacillus dipsosauri* and soil conditioner in tomato. Summa Phytopathologica, 39(2), 122-125.

PORCEL, R.; AROCA, R.; AZCON, R.; RUIZ-LOZANO, J. M. (2006) PIP aquaporin gene expression in arbuscular mycorrhizal *Glycine max* and *Lactuca sativa* plants in relation to drought stress tolerance. Plant Mol. Biol. 60, 389-404. https://doi.org/10.1007/s11103-005-4210-y

ROGACHEV, I.; AHARONI, A. (2012) UPLC-MS-based metabolite analysis in tomato. Methods Mol Biol. 860:129-44. https://doi.org/10.1007/978-1-61779-594-7_9.

RUIZ-SÁNCHEZ, M.; AROCA, R.; MUÑOZ, Y.; POLÓN, R.; RUIZ-LOZANO, J. M. (2010) The arbuscular mycorrhizal symbiosis enhances the photosynthetic efficiency and the antioxidative response of rice plants subjected to drought stress. J Plant Physiol. 15; 167(11):862-9

SAAB, I. N.; SHARP, R. E.; PRITCHARD, J.; VOETBERG, G. S. (1990) Increased endogenous abscisic Acid maintains primary root growth and inhibits shoot growth of maize

seedlings at low water potentials. Plant physiology, 93(4), 1329-1336. https://doi.org/10.1104/pp.93.4.1329

SACK, L.; MELCHER, P.J.; ZWIENIECKI, M.A.; HOLBROOK, N. M. (2002) The hydraulic conductance of the angiosperm leaf lamina: a comparison of three measurement methods. Journal of Experimental Botany, 53:2177-2184.

SALLOUM, M. S.; INSANI, M.; MONTEOLIVA, M. I.; MENDUNI, M. F.; SILVENTE, S.; CARRARI, F.; LUNA, C. (2019) Metabolic responses to arbuscular mycorrhizal fungi are shifted in roots of contrasting soybean genotypes. Mycorrhiza. https://doi.org/10.1007/s00572-019-00909-y

SCHOLANDER, P. E.; HAMMEL, H. T.; BRADSTREET, E. D.; HEMMINGSEN, E. A. (1965) Sap pressure in vascular plants. Science 148:339-346

SHARMA, K.; GUPTA, S.; THOKCHOM, S. D.; JANGIR, P. KAPOOR, R. (2021) Arbuscular Mycorrhiza-Mediated Regulation of Polyamines and Aquaporins During Abiotic Stress: Deep Insights on the Recondite Players. Front. Plant Sci. 12:642101. https://doi.org/10.3389/fpls.2021.642101

SHARP, R. E. (2002) Interaction with ethylene: changing views on the role of abscisic acid in root and shoot growth responses to water stress. Plant Cell Environ. 25(2):211-222. https://doi.org/10.1046/j.1365-3040.2002.00798.x

SIDDIQUI, I. A.; SIDDIQUI, S. D.; ATKINS, B.R.; KERRY, B.R. (2009) Relationship between saprotrophic growth in soil of different biotypes of *Pochonia chlamydosporia* and the infection of nematode eggs Annals of Applied Biology Vol. 155(1): 131-141.

SILVA, M. A.; JIFON, J. L.; SILVA, J. A. G.; SHARMA, V. (2007) Use of physiological parameters as fast tools to screen for drought tolerance in sugarcane. Brazilian Journal of Plant Physiology, 19: 193-201.

STEWART, G. R.; LARHER, F. (1980) Accumulation of Amino Acids and Related Compounds in Relation to Environmental Stress. Amino Acids and Derivatives, 609-635. https://doi.org/10.1016/b978-0-12-675405-6.50023-1

TAIZ, L.; ZEIGER, E. Fisiologia vegetal. 5ª. ed. Porto Alegre: Artmed, 2013.

TIAN, F.; JIA, T.; YU, B. (2014) Physiological regulation of seed soaking with soybean isoflavones on drought tolerance of *Glycine max* and *Glycine soja*. Plant Growth Regul 74, 229-237. https://doi.org/10.1007/s10725-014-9914-z

VALANCIENE, E.; JONUSKIENE, I.; SYRPAS, M.; AUGUSTINIENE, E.; MATULIS, P.; SIMONAVICIUS, A.; MALYS, N. (2020) Advances and Prospects of Phenolic Acids Production, Biorefinery and Analysis. Biomolecules, 10(6), 874. https://doi.org/10.3390/biom10060874

VALDÉS-SANTIAGO, L.; RUIZ-HERRERA, J. (2014) Stress and polyamine metabolism in fungi. Frontiers in Chemistry, 1. https://doi.org/10.3389/fchem.2013.00042

VALENTE, M. A. S.; FARIA, J. Q. A.; RAMOS, J. R. L. S.; REIS, P. A. B.; PINHEIRO, G. L.; PIOVESAN, N. D.; MORAIS, A. T.; MENEZES, C. C.; CANO, M. A. O.; FIETTO, L. G.; LOUREIRO, M. E.; ARAGAO, F. J. L.; FONTES, E. B. P. (2009) The ER luminal binding protein (BiP) mediates an increase in drought tolerance in soybean and delays drought-induced leaf senescence in soybean and tobacco. J. Exp. Bot. 60, 533-546. https://doi.org/10.1093/jxb/ern296

VITAL, C. E.; GÓMEZ, J. D.; VIDIGAL, P. M.; BARROS, E.; PONTES, C. S. L.; VIEIRA, N. M.; RAMOS, H. J. O. (2019) Phytohormone profiling by liquid chromatography coupled to mass spectrometry (LC/MS). Protocols. io. https://doi.org/10.17504/protocols.io.zgff3tn

VITAL, C. E.; GÓMEZ, J. D.; VIDIGAL, P. M.; BARROS, E. G.; PONTES, C. S. L.; VIEIRA, N. M.; OLIVEIRA, M. G. A.; RAMOS, H. J. O. (2019) Flavonoid profiling by liquid chromatography coupled to mass spectrometry (LC/MS). Protocols. io. https://doi.org/10.17504/protocols.io.zggf3tw

WANG, W.; VINOCUR, B.; ALTMAN, A. (2003) Plant responses to drought, salinity and extreme temperatures: towards genetic engineering for stress tolerance. Planta, Berlin, v. 218, p. 1-14.

WIDHALM, J. R.; DUDAREVA, N. (2015) A Familiar Ring to It: Biosynthesis of Plant Benzoic Acids. Molecular Plant, 8(1), 83-97. https://doi.org/10.1016/j.molp.2014.12.001

XIE, Y.; YANG, W.; TANG, F.; CHEN, X.; REN, L. (2014) Antibacterial Activities of Flavonoids: Structure-Activity Relationship and Mechanism. Current Medicinal Chemistry, 22(1), 132-149. https://doi.org/10.2174/09298673216661409161134443

YONEYAMA, K.; AKASHI, T.; AOKI, T. (2016) Molecular Characterization of Soybean Pterocarpan 2-Dimethylallyltransferase in Glyceollin Biosynthesis: Local Gene and Whole-Genome Duplications of Prenyltransferase Genes Led to the Structural Diversity of Soybean Prenylated Isoflavonoids. Plant Cell Physiol 57(12):2497-2509

ZARE, R.; GAMS, W.; EVANS, H. C. (2001) A revision of VERTICILLIUM SECTION V. Prostrata. The genus *Pochonia*, with notes on Rotiferophthra. Nova Hedwigia, 73(1-2): 51-86.

ZHANG, J.; DAVIES, W. J. (1990) Changes in the concentration of ABA in xylem sap as a function of changing soil water status can account for changes in leaf conductance. Plant Cell Environ 13 277-285

ZHANG, F.; ZOU, Y. -N.; WU, Q. -S.; KUČA, K. (2019) Arbuscular mycorrhizas modulate root polyamine metabolism to enhance drought tolerance of trifoliate orange. Environmental and Experimental Botany, 103926. https://doi.org/10.1016/j.envexpbot.2019.103926

ZHU, C. Q.; ZHU, X. F.; HU, A. Y.; WANG, C.; WANG, B.; DONG, X. Y.; SHEN, R. F. (2016). Differential effects of nitrogen forms on cell wall phosphorus remobilization in rice (*Oryza sativa*) are mediated by nitric oxide, pectin content and the expression of the phosphate transporter OsPT2. Plant Physiology, pp. 00176. 2016. https://doi.org/10.1104/pp.16.00176

APPENDIX

Appendix A – Overview of the pants at the end of the experiment, showing the pots from the Embrapa48 and BR16 genotypes under irrigated (**I**) and non-irrigated (**NI**) conditions, under presence (**F**) or absence of fungus **(NF**). Plants under water deficit of Ψ = -1.0 MPa.

EMBRAPA48

F NI **NF NI** **F I** **NF I**

BR16

F NI **NF NI** **F I** **NF I**

Source: Survey's data.

Appendix B – Analysis of 2D Scores Plot by Partial Least Squares Discriminant Analysis (PLS-DA) of the metabolite profiles by LC/MS Q-TOF from genotypes soybean leaves in response to biotic and abiotic stresses. **A)** Embrapa48; **B)** BR16.

A

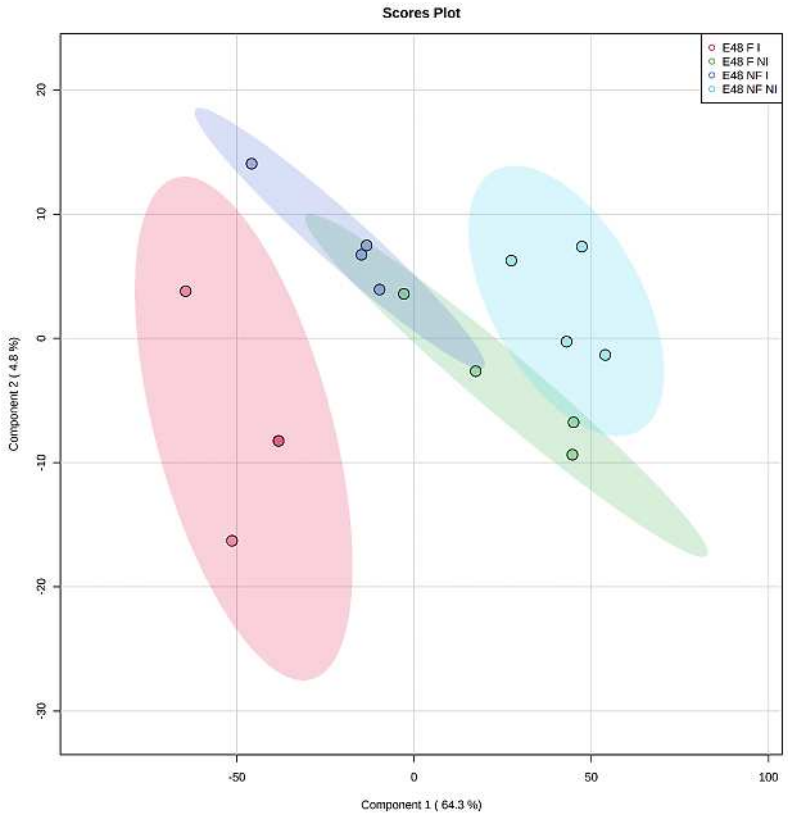

B

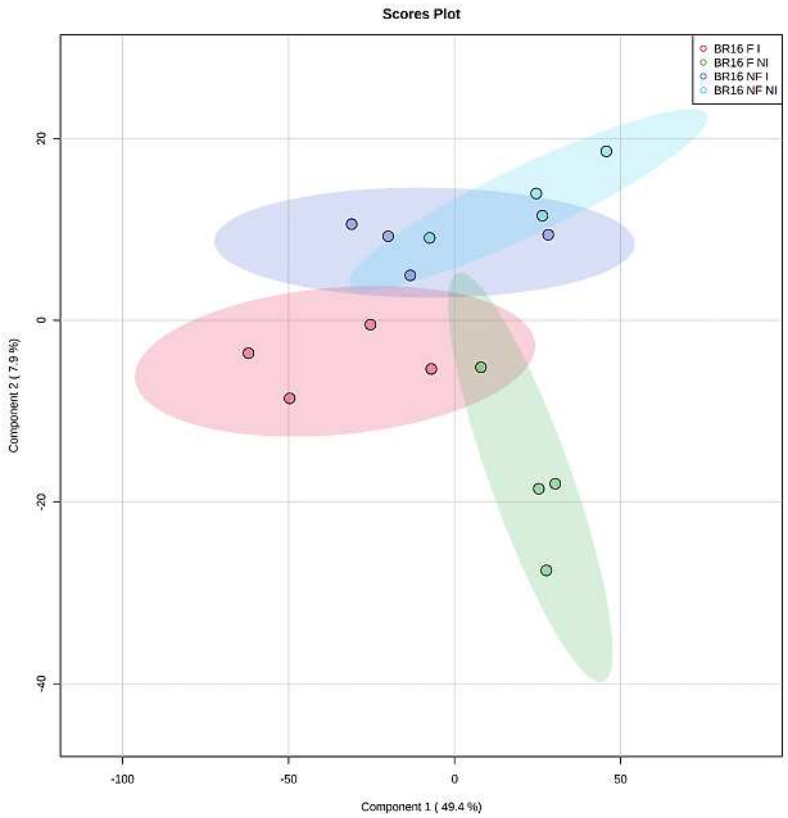

Source: Survey's data.

Appendix C – Analysis by Heatmap method of the characterized metabolites by LC/MS Q-TOF in soybean leaves from the Embrapa48 genotype under biotic and abiotic stresses. Differences in the abundance of the metabolites are indicate in response to treatments. The ions from LC/MS were exported from XCMS package as features where M designed the nominal mass and T the retention time.

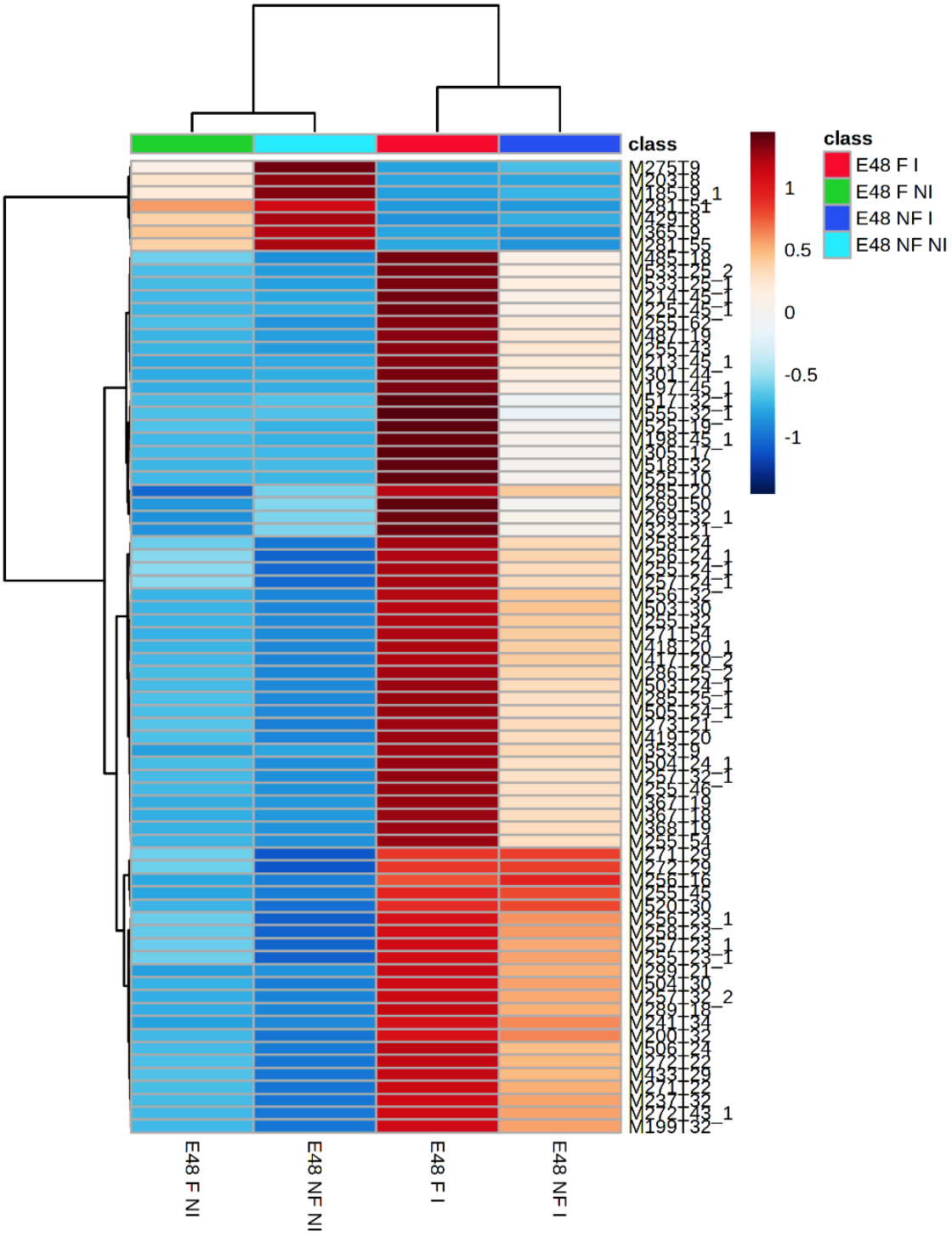

Source: Survey's data.

Appendix D – Analysis by Heatmap method of the characterized metabolites by LC/MS Q-TOF in soybean leaves from the BR16 genotype under biotic and abiotic stresses. Differences in the abundance of the metabolites are indicate in response to treatments. The ions from LC/MS were exported from XCMS package as features where M designed the nominal mass and T the retention time.

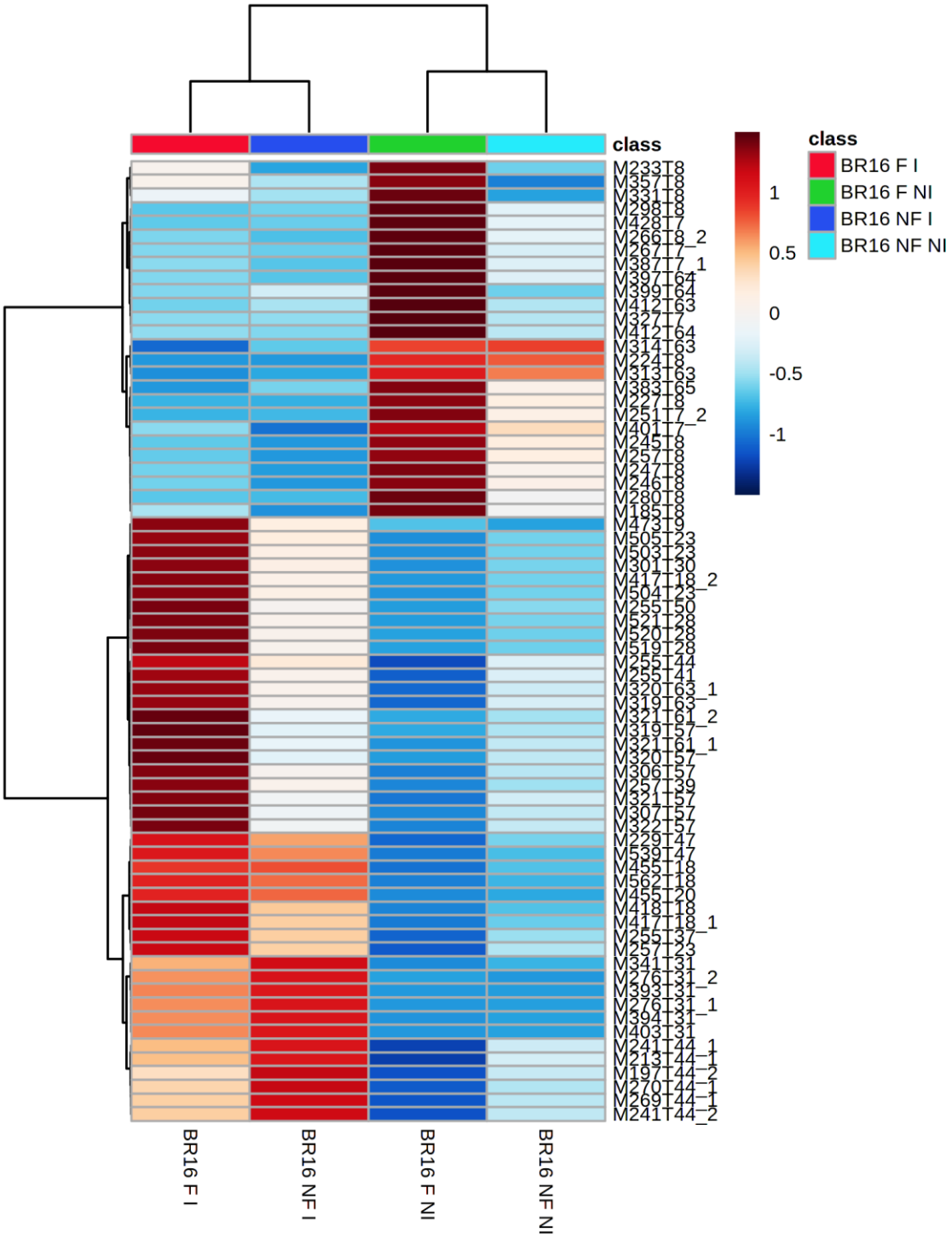

Source: Survey's data.

CONCLUSÃO GERAL

Devido a exposição simultânea a estresses abióticos e bióticos, plantas evoluíram para suportar estresses concomitantes por meio de uma série de respostas bioquímicas e fisiológicas. A tolerância cruzada a estresses ambientais permite a plantas responder com equilíbrio e o menor gasto metabólico possível às interações abióticas e bióticas.

A superexpressão do chaperona molecular BiP em plantas transgênicas de soja tem mostrado aumento na tolerância à seca e retardo da morte celular induzida pela reação de hipersensibilidade em resposta à infecção bacteriana. A infecção causada por bactéria não compatível *Pseudomonas syringae* pv. *tomato* provocou maior reação hipersensitiva no genótipo transgênico, assim como maior abundância de flavonoides. Por sua vez, não houve diferença significativa de proteínas do metabolismo flavonoides e especializado.

A percepção do vegetal da presença de PAMPs fúngicos e bacterianos, que desencadeia a expressão de genes responsivos ao estresse, pode ativar enzimas do metabolismo especializado de fenilpropanoides, flavonoides e isoflavonoides, além de O-metiltransferases e preniltransferases que atuam na síntese de isoflavonoides e fitoalexinas. Compostos antimicrobianos que atuam na resistência basal ou inata a patógenos em soja e na interação hospedeiro-simbionte podem sofrer queda nos níveis em raízes de plantas sob déficit hídrico, favorecendo a absorção de água e o possível estabelecimento de associações mutualísticas com o microbioma do solo.

A presença do fungo *Pochonia chlamydosporia* na raiz de soja garantiu um atraso na queda do potencial hídrico em genótipos contrastantes à seca, além de promover um alterações morfológicas no sistema radicular, na condutividade hidráulica e no eficiente uso da água em folhas. No que diz respeito ao contraste soja: fungo: seca, demonstrou-se que os mecanismos moleculares e biológicos respondem de modo diferenciado entre os diferentes genótipos de soja, de acordo com características definidas pela condição genética e fenotípica de cada variedade. Assim, o genótipo tolerante respondeu favoravelmente à presença do fungo com predominância nas alterações nas propriedades hidráulicas dos vasos condutores, ao passo que o genótipo sensível a seca apresentou alterações nos níveis de compostos com conhecida ação antimicrobiana, o que pode favorecer interações com organismos simbióticos presentes no solo.

O entendimento dos mecanismos que explicam a tolerância cruzada a estresses bióticos e abióticos podem, assim, ajudar na identificação de novos alvos para estudo aumentar a resiliência das culturas a estresses ambientais.